The Development of Cerebral Arteriovenous Malformations

A thesis submitted to the University of Manchester for the degree of
Doctor of Medicine
in the Faculty of Biology, Medicine and Health

2021

Suparna Das

School of Medical Sciences
Division of Cardiovascular Sciences

List of Contents

Word count: 36, 139

List of Figures

List of Tables

*Tables included in Appendices not listed here

List of Abbreviations

Abbreviation	Meaning
3DISCO	Three-dimensional imaging of solvent-cleared organs
ALK1 or ACVRL1	Activin-like kinase 1
ANG-1	Angiopoietin-1 protein
ANG-2	Angiopoietin-2 protein
ANGPT2	Angiopoietin-2 gene
AP	Anteroposterior
ATV	Atorvastatin
AVM	Arteriovenous malformation
AV	Arteriovenous
BA	Basilar artery
BMP	Bone morphogenetic protein
Cas	CRISPR-associated systems
cAVM	Cerebral arteriovenous malformation
CC	Craniocaudal
CI	Confidence interval
CRISPR	Clustered, regularly interspaced, short palindromic repeats
CT	Computed Tomography
CTA	CT Angiography
CVST	Cerebral Venous Sinus Thrombosis
DBE	Dibenzylether
DMSO	Dimethyl sulfoxide
dpf	Days post-fertilisation
DSA	Digital subtraction angiography
ECM	Extracellular matrix
ECs	Endothelial cells
ENG	Endoglin
ENU	N-ethyl-N-nitrosourea
FDISCO	Fluorescence three-dimensional imaging of solvent-cleared organs
FLT1	Fms Related Receptor Tyrosine Kinase 1
FPS	Frame rate per second
GFP	GFP
GM	Greater Manchester
GOS	Glasgow Outcome Scale
HHT	Hereditary Haemorrhagic Telangiectasia
HIFα or HIF-1α	Hypoxia inducible factor alpha
hpf	Hours post-fertilisation
ICA	Internal carotid artery
ICH	Intracerebral haemorrhage
IL-1β	Interleukin-1β
IL-6	Interleukin-6
IQR	Interquartile range
ITGAV	Integrin Subunit Alpha V

JWG	Joint Writing Group
kdrl	Kinase insert domain receptor-like
LL	Laterolateral
MCCN	Manchester Centre for Clinical Neurosciences
mib	Zebrafish *mindbomb* gene
MMP	Matrix metalloproteinases
MRA	MR Angiography
MRI	Magnetic resonance imaging
mRS	Modified Rankin Scale
MS222	Tricaine methanesulfonate
NaOH	Sodium hydroxide
nBCA	N-Butyl Cyanoacrylate
NOMASS	Northern Manhattan Stroke Study
Notch	Single-pass transmembrane receptor
*Notch4**	*Notch4* allele
OR	Odds Ratio
PBS	Phosphate-Buffered Saline
PBS-T	PBS containing 0.1% Triton-X
PCR	Polymerase Chain Reaction
PDGF	Platelet-Derived Growth Factor
PFA	Paraformaldehyde
PFG	Pollock-Flickinger grading
pH	Numerical scale to determine acidity or alkalinity of a solution
PHIL	Precipitating Hydrophobic Injectable Liquid
PlGF	Placental Growth Factor
poly (I:C)	Polyinosinic: polycytidylic acid
PRISMA	Preferred Reporting Items for Systematic Reviews and Meta-Analyses
PROSPERO	International Prospective Register of Systematic Reviews
PTU	Phenylthiourea
RASA1	RAS P21 Protein Activator 1
SIVMS	Scottish Intracranial Vascular Malformation Study
SMG	Spetzler-Martin Grade
SNP	Single Nucleotide Polymorphism
SPECT	Single-Photon Emission Computed Tomography
SRS	Stereotactic Radiosurgery
SSS	Superior Sagittal Sinus
TALEN	Transcription Activator-Like Effector Nucleases
TGF	Transforming Growth Factor
THF	Tetrahydrofuran
TIE2 or TEK	Tndothelial cell-specific tyrosine-protein kinase receptor
TNF-a	Tumour Necrosis Factor-alpha
uDISCO	Ultimate three-dimensional imaging of solvent-cleared organs
VEGF	Vascular Endothelial Growth Factor
VEGFR1	Vascular Endothelial Growth Factor Receptor-1
κ	Kappa
µl	Microlitre

µm	Micrometre
µM	Micromolar

Abstract

Cerebral arteriovenous malformations (cAVM) are a significant cause of morbidity and mortality, particularly in the young. They consist of a tangle of abnormal cerebral blood vessels with an artery feeding into a nidus, which drains into a vein, in the absence of capillaries. Angiogenesis refers to new vessel formation, which is detectable on an angiogram as a border of friable vessels immediately surrounding the nidus. The overall aim of this thesis is to understand the development of cAVMs by investigating angiogenesis through three projects.

Catheter angiography is the gold standard investigation to study and assess cAVMs. We reviewed 100 cAVM patient angiograms and recorded their angioarchitectural features, including angiogenesis. We tested for any association between the latter and all other features. Inter-observer agreement and intra-observer agreement were assessed using 10 cases. We detected angiogenesis in 39 cAVMs. There were statistically significant associations between angiogenesis and artery: vein ratio and arterial ectasia. Mostly, strong intra-observer agreement and moderate inter-observer agreement was noted. Specifically, for angiogenesis, there was fair to substantial inter-observer agreement and substantial intra-observer agreement.

We identified a lack of standardisation in cAVM reporting despite the publication of a consensus document in 2001. We predicted that few publications adhered to the recommendations. We conducted a systematic review to describe how cAVM angioarchitecture is reported in the literature, considering whether this consensus document was followed. Out of 4306 publications identified from the database search, 219 relevant articles were identified. Only 33 publications reported using the recommended terminology. Most authors only reported on size (78%), location (68%) and venous drainage (77%). The review confirmed our suspicions that few studies followed the guidelines.

A reliable in vivo animal model for human cAVMs does not exist. There are problems with existing rodent models: the most important being that they produce a fistula with no nidus, not truly representing a cAVM. We combined a zebrafish genetic risk factor model (*alk1* heterozygous mutant background, which causes vascular instability) with an environmental angiogenic stimulus (intracerebral haemorrhage) to produce an animal model to test for cAVM development in the future. We optimised an innovative protocol to visualise the neurovasculature in fixed and cleared whole adult *alk1* zebrafish.

We advanced our knowledge of cAVM development by reviewing angiograms, performing a systematic review on the reporting of cAVMs, and using the two-hit hypothesis to produce a zebrafish cAVM model as well as optimise a protocol for whole animal vascular imaging. Our studies have demonstrated that it is possible to reliably identify angiogenesis on cAVMs, there is a lack of uniformity when describing cAVMs, and that we have successfully developed a protocol to image the cerebral vasculature of an intact adult *alk1* zebrafish.

Declaration

No portion of the work referred to in the thesis has been submitted in support of an application for another degree or qualification of this or any other university or other institute of learning.

Copyright statement

i. The author of this thesis (including any appendices and/or schedules to this thesis) owns certain copyright or related rights in it (the "Copyright") and s/he has given The University of Manchester certain rights to use such Copyright, including for administrative purposes.

ii. Copies of this thesis, either in full or in extracts and whether in hard or electronic copy, may be made **only** in accordance with the Copyright, Designs and Patents Act 1988 (as amended) and regulations issued under it or, where appropriate, in accordance with licensing agreements which the University has from time to time. This page must form part of any such copies made.

iii. The ownership of certain Copyright, patents, designs, trademarks and other intellectual property (the "Intellectual Property") and any reproductions of copyright works in the thesis, for example graphs and tables ("Reproductions"), which may be described in this thesis, may not be owned by the author and may be owned by third parties. Such Intellectual Property and Reproductions cannot and must not be made available for use without the prior written permission of the owner(s) of the relevant Intellectual Property and/or Reproductions.

iv. Further information on the conditions under which disclosure, publication and commercialisation of this thesis, the Copyright and any Intellectual Property and/or Reproductions described in it may take place is available in the University IP Policy (see http://documents.manchester.ac.uk/DocuInfo.aspx?DocID=2442 0), in any relevant Thesis restriction declarations deposited in the University Library, The University Library's regulations (see http://www.library.manchester.ac.uk/about/regulations/) and in The University's policy on Presentation of Theses.

Acknowledgements

My utmost gratitude goes to my supervisors, Mr Hiren Patel, Dr Paul Kasher, and Dr Adrian Parry-Jones for their invaluable support, advice, and encouragement. I am very thankful to Dr Siobhan Crilly, James Cooper, and Sarah Withers for all their help and guidance in the lab. I am indebted to Dr Ingo Schiessl for his vital assistance with zebrafish clearing and imaging. I thank the Bioimaging facility for their training in image processing. Thanks goes to the Brain Inflame Group for all their support. I am obliged to my clinical colleagues Ms Helen Raffalli-Ebezant for her essential contribution to the angiogram study, and Mr Mueez Waqar for his help with the systematic review. I am grateful to Dr Katherine Watson for reviewing my thesis. And finally none of this work would have been possible without the boundless love and support of my mum, dad, and Uttam.

Dedication

I would like to dedicate my thesis to my beloved grandparents.

The Author

Dr Suparna Das MBBS MRCS MRes

I graduated from Newcastle University in 2010 with a MRes in Medical and Molecular Biosciences (Neuroscience), and, subsequently completed my medical degree at the same university in 2012. In the following years, I completed my membership examinations in surgery. During a two-month summer placement at Mater Dei Hospital, Malta, in 2009, I conducted educational research into anatomy training methods. During my MRes, I undertook a six-month period of psychology research at the Academic Psychiatry Unit at Newcastle General Hospital. I started my current MD programme at the University of Manchester in January 2019.

Chapter 1 – Introduction

1.1 What is an arteriovenous malformation?

An arteriovenous malformation (AVM) consists of a disruption of the blood vessels: there is an abnormal tangle of blood vessels, with an artery feeding into a nidus, which drains into a vein. Normal circulation involves blood being supplied through arteries, then circulating into a network of capillaries, followed by venous drainage. This disorder can occur all over the body, though this thesis specifically discusses those lesions occurring in the brain, known as cerebral arteriovenous malformations (cAVMs).

cAVMs are considered congenital lesions, which are secondary to a problem in the formation of blood vessels during embryogenesis. Anatomically, a cAVM comprises a nidus, that shunts blood directly from the arterial feeders to the draining veins, in the absence of capillaries (Figure 1.1.1).[1,2] This nidus is composed of "a complex tangle of arteries and veins" linked by fistulae.[3] The latter directly connect the arterial and venous circulations, enabling blood to quickly shunt from artery to vein.[3] Radiologically, the best description of a cAVM is using cerebral angiography, with the pathognomonic features being a nidus and early venous drainage (Figure 1.1.1).[4] Vascular tumours (angiomas) are distinguishable from AVMs, which do not have any neoplastic endothelial cell turnover.

It is useful to differentiate between brain AVMs, cerebral AVMs and pial AVMs. Strictly speaking, brain AVMs refer to AVMs anywhere in the brain, cerebral AVMs occur in the supratentorial region, and pial AVMs are cortical. These descriptive terms are important in AVM management as the location is key to planning the best management option. For example, a pial AVM would usually be more accessible for surgical treatment as will be discussed in Section 1.8.

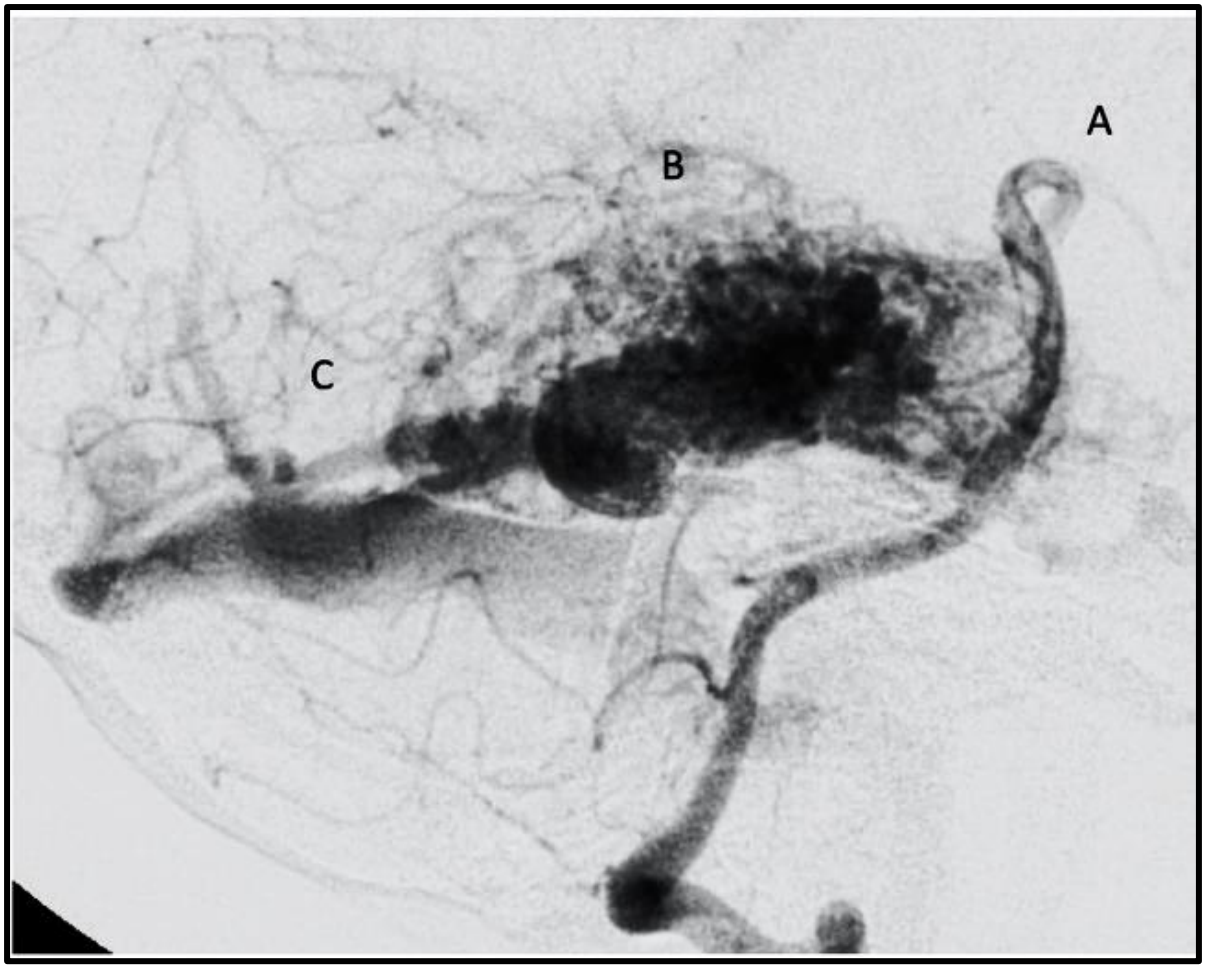

Figure 1.1.1: Cerebral arteriovenous malformation on digital subtraction angiography showing a branch of the basilar artery (A), a central nidus (B), and a superficial or cortical early draining vein (C)

1.2 Demographics

There are difficulties in precisely ascertaining the incidence and prevalence of cAVMs for three main reasons. As well as being asymptomatic, they can also result in sudden death, and are rare. Historically, angiography was the only diagnostic imaging resulting in over-representation of cases with haemorrhage.[5] cAVM detection has been boosted by the advent of non-invasive cerebral imaging: computed tomography (CT) in the 1970s and magnetic resonance imaging (MRI) in the 1990s.[5] Despite this, correct diagnosis is difficult: cAVMs can be angiographically occult (especially if there is an overlying haemorrhage, when just an early draining vein might be identifiable), the morphology can be indistinguishable from other vascular abnormalities, and sometimes it is inappropriate to image some patients (e.g. due to comorbidities).[6]

Several authors have attempted to comprehend cAVM epidemiology with variable success. Prior to non-invasive brain imaging, an autopsy study revealed a cAVM incidence of 4.3%: out of this, 12.2% were symptomatic. The majority of these symptomatic patients had haemorrhaged (88%).[7] A cAVM patient series (diagnosed by angiography) reported an 8.6% incidence of haemorrhagic cAVMs.[8] Retrospective population studies in the Dutch Antilles between 1980 and 1990, and Olmsted, Minnesota between 1965 and 1992 have disclosed an incidence of 1.1 – 1.84 per 100 000 person-years.[6,9] Linkoping University produced a study reporting 1.24 cAVMs per 100 000 person-years, with an incidence of haemorrhage of 0.876 per 100 000 person-years.[6] The Scottish Intracranial Vascular Malformation Study (SIVMS) reported a detection rate of 1.12 per 100 000 adults per year, and of 0.51 per 100 000 adults per year for first-time cAVM haemorrhage.[6] A similar incidence rate of first-time cAVM haemorrhage of 0.55 per 100 000 person-years was identified by the Northern Manhattan Stroke Study (NOMASS).[6]

The prevalence of cAVMs is 15-18 per 100 000.[4,10] Using MRI brains, cAVMs are incidentally identified in 0.05% of cases.[4] Nine per cent of all primary intracerebral haemorrhages (ICH) are caused by cAVMs, making up 1.4-2% of all strokes.[4] The most common age range for cAVM presentation is 32-39 years.[11] No specific gender predisposition exists.[11] The recorded cAVM mortality rate is 0.7-2.9%.[12]

Despite their importance, there are few good quality studies on cAVM frequency. Detection estimates ideally require the prospective study of well-defined stable populations.[10] The population size should be sufficiently large, as cAVMs are rare, to allow the detection rate to be precisely estimated. To confirm external validity and for comparing easily, these studies require standardised definitions and methods.[10] Both the population studies of SIVMS and NOMASS provide important data. Crucially they are not hospital-based studies, which would have been inadequate. There are multiple reasons for this: they depend on an institution's referral patterns, special interests, patterns of investigation, interventional treatment preferences, classification used, pathologist expertise, post-mortem frequency, and tendency to miss certain groups (sudden deaths, asymptomatic individuals, and those unsuitable for treatment, all of which would not be admitted).[10] When detecting cAVMs with non-haemorrhagic presentations (i.e. presenting with headache, seizure, or focal neurological

deficit amongst other symptoms), there are further hurdles. For example, the NOMASS cohort was unable to ascertain the incidence of unruptured cAVMs.[13]

1.3 Presentation

The most common presenting feature is haemorrhage, which is also the largest cause of cAVM morbidity and mortality.[11] Haemorrhage occurs in cAVMs in 38-71% of cases.[4] The annual ICH rate for cAVMs is 2-4%, with the greatest haemorrhage risk being in the first five years after diagnosis.[11,14] In unruptured cAVMs, the annual ICH rate is 1.3 – 2.2%.[15,16] Amongst the numerous ICH risk factors are previous cAVM rupture, young age, deep and infratentorial location, deep venous drainage, and large cAVM size.[14] In the majority of cases, mortality rates are associated with ruptured cAVMs causing haemorrhage, with rates varying between 10 to 40%.[4]

The second most common presentation is seizures, with 17-30% of cases presenting with this.[11] Risk factors include cortical location, temporal or frontal locations, absence of aneurysms, middle cerebral artery and cortical feeders, varices, male gender, and previous cAVM haemorrhage.[17–19] In those with haemorrhagic presentation, epilepsy develops in 22% within 20 years of diagnosis.[20]

In up to 14% of patients, non-haemorrhagic headache occurs, which is not limited to a specific location.[11]

The presenting features of 5-15% are focal neurological deficits.[11] A vascular steal phenomenon may explain the deficits, with a reduced vascular supply in the surrounding parenchyma caused by high shunting through the cAVM.[4] CT perfusion and single-photon emission computed tomography (SPECT) have revealed the encompassing cerebral parenchyma has reduced blood flow.[4] After cAVM excision, blood flow normalises: this correlates with recovery from deficits.[4] Others propose neurological deficits are actually due to compressive venous dilatation causing mass effect on vulnerable white matter pathways.[4] Risk factors for focal neurological deficits include female gender, older age, venous ectasia, and deep location.[21]

1.4 Investigations

cAVMs are diagnosed using numerous imaging modalities. These include non-invasive (e.g. CT, MRI) and invasive methods (e.g. angiography).

Angiography

The gold standard investigation is digital subtraction angiography (DSA) (Figure 1.4.1). DSA enables both anatomical and temporal investigation of the cAVM. Since it allows temporal resolution of the abnormality, all pathognomonic components of a cAVM (shunting, nidus, and an early draining vein) can be identified using one investigation. DSA also supplies us with the most precise description of cAVM haemodynamics and angioarchitecture.[22] After cAVM identification by CT or MRI, DSA further characterises the lesion, especially when considering treatment.[22] In the presence of haemorrhage, the cAVM nidus may be undetected by all imaging modalities as the haematoma compresses it. Hence, after haematoma resolution, follow-up vascular imaging ought to be completed to permit detection.[22] DSA risks include radiation exposure, a low risk of thromboembolic stroke, and retroperitoneal haemorrhage.[22]

CT and MR scan imaging

Initial diagnosis of most cAVMs occurs on non-invasive cross-sectional imaging, i.e. either on CT or MRI scans of the brain (Figure 1.4.1). Information on the surrounding brain parenchyma is also obtained using these techniques.

For acute subarachnoid haemorrhage or haemorrhagic stroke, a non-contrast CT scan has >90% sensitivity.[22] Although CT demonstrates several features indicating vascular abnormalities (e.g. enlarged vessels, regions of increased density correlating with the vascular nidus, calcification along haematoma edges), its cAVM detection ability is restricted.[22] CT Angiography (CTA) is the term used when a CT scan has contrast injected and images are obtained during the arterial phase. It permits visualisation of the arterial circulation, is minimally invasive, accessible, fast, and has excellent resolution.[23] Due to the presence of ionising radiation, metallic streak artefacts (e.g. aneurysm coils) degrade images. When detecting an underlying vascular anomaly with neighbouring haemorrhage, CTA has high sensitivity (83.6-100%) and specificity (77.2-100%).[22]

MR Angiography (MRA) uses magnetic resonance to display the arterial circulation. In the presence of ICH, MRA has a sensitivity of 0.98 and specificity of 0.99.[24] Despite using additional sequences (e.g. contrast-bolus and time-of-flight), MRA is deficient in the detection of venous outflow anatomy, small nidi, aneurysms, and smaller vessels.[22] In addition to these structures, information on the neighbouring parenchyma, is crucial in planning treatment. Subclinical microhaemorrhage in cAVMs without ICH can be detected with susceptibility-weighted MRI.

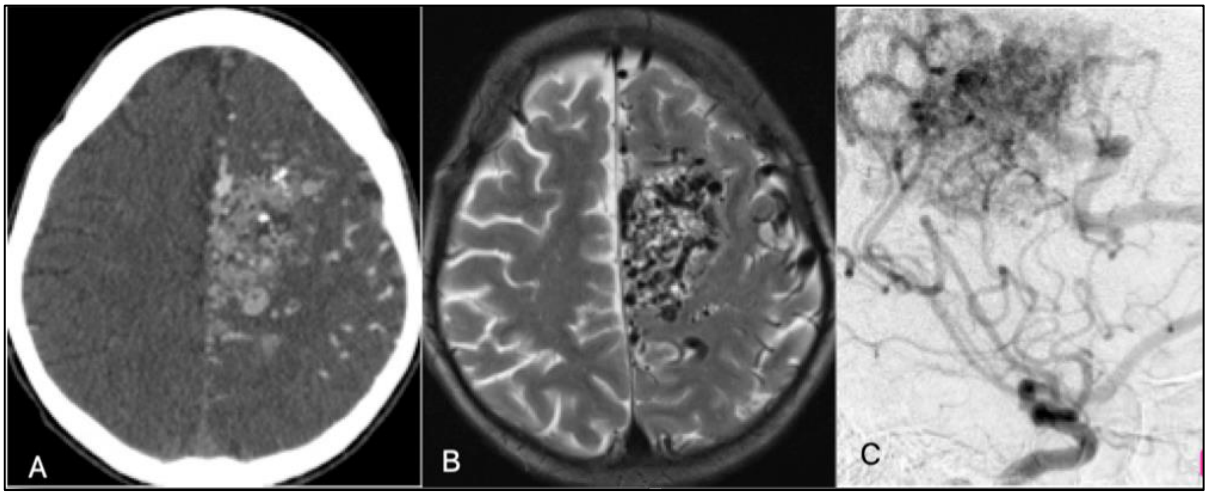

Figure 1.4.1: Different imaging modalities demonstrating cAVMs.
(A) Axial CTA showing an intensely enhancing nidus in the left frontoparietal lobe. (B) Axial T2-weighted MRI showing left frontoparietal nidus, with surrounding hyperintensity and a hypointense rim indicating haemorrhage. (C) Lateral left internal carotid angiogram showing a compact cortical nidus, with left anterior cerebral artery and middle cerebral artery supply and left parietal cortical early venous drainage.

The cAVM diagnostic criteria, reflecting the definition, are the presence of (a) a nidus, (b) dilated arterial feeders (both visible on DSA, CT or MR), and (c) early venous drainage (to appreciate timing, ideally viewed on DSA).[3] The latter is noted by visualising the veins in the arterial phase on DSA, but MRA or CTA may also demonstrate this if the vessels are large enough. Dynamic MRA and CTA use is becoming more common for cAVM diagnosis in the recognition of early venous drainage in smaller lesions.

1.5 Grading/ Classification

There are multiple methods by which cAVMs are graded or classified. They can be divided into anatomical grades (delivering details on topology and morphology) and into grades to ascertain the likelihood of the success and risks of treatment.

Spetzler-Martin Grade

The commonest cAVM classification system is the Spetzler-Martin Grade (SMG) (Table 1.5.1). Its creation facilitated management decisions based on the risks of mortality and morbidity.[25] The long-term risks of non-treatment are balanced against the immediate risks of surgery to decide to operate. A perfect grading system would specify how difficult safe surgical resection would be for a singular cAVM.[25] Despite being sufficiently simple to be applied universally, it would provide a sensible estimate of mortality and morbidity. Prior to the SMG, such a grading system did not exist.

Spetzler and Martin's experiences with cAVM management were used to identify the variables of the SMG.[25] Since many factors were interrelated, major elements involved in determining resection difficulty (number of feeding arteries, amount of blood flow through the cAVM, extent of arterial steal, size, location, eloquence of surrounding parenchyma, venous drainage pattern, and surgical accessibility) could be rationalised to venous drainage pattern, size, and eloquence.

To test the predictive value of the SMG, 100 consecutive completely excised cAVMs were retrospectively evaluated.[25] cAVM grading was based on their imaging and surgical complications (subdivided into minor and major deficits, and mortality). Neurological deficits lasting less than three days were excluded. There was good correlation between the incidence of neurological complications and cAVM grade, e.g. when Grade I lesions were resected, there was only minimal neurological deficit. One of the study authors and two neurosurgeons individually graded 25 cAVM angiograms to assess the reproducibility and reliability of the grading system.[25] Correlation between all observers was excellent.

The SMG score consists of eloquence of surrounding parenchyma (eloquent if in the hypothalamus, brainstem, thalamus, cerebellum, language, visual, sensory, or motor cortex),

deep or superficial venous drainage, and nidus size (<3 cm, 3-6cm, >6 cm).[1] Clinically important regions are eloquent. To facilitate treatment decision-making, the risk of surgical morbidity and mortality is established using the SMG.[25] The grading only applies to cAVMs.

Table 1.5.1: Spetzler-Martin Grade[25]

Size of AVM	**Score**
Small	1
Medium	2
Large	3
Eloquence of adjacent brain*	
Non-eloquent	0
Eloquent	1
Pattern of venous drainage†	
Superficial	0
Deep	1
Grade = Total of scores	

*Eloquent = sensorimotor, language and visual cortex; hypothalamus and thalamus; internal capsule; brainstem; cerebellar peduncles; deep cerebellar nuclei. †Superficial = cortical venous system & cerebellar hemispheric veins (which drain directly into the straight or transverse sinuses), the rest is deep

The supplementary SMG was created to improve our prediction of post-operative neurological outcomes.[26] It supplements the SMG with these additional variables: diffuseness of nidus, haemorrhagic presentation, and patient age. It stratifies the surgical risk more evenly, has a high accuracy for calculating the preoperative risk prediction, as well as improving patient selection.

Pollock-Flickinger Grade

The Pollock-Flickinger grading (PFG) system was devised to permit decision-making between radiosurgery and surgery and for anticipation of post-radiosurgery outcomes.[27] It consists of a formula computed from the cAVM location, patient age, and cAVM volume (Table 1.5.2). When predicting radiosurgery outcomes, the SMG is unreliable as it does not include radiation dose and location.

Table 1.5.2: Calculating the Pollock-Flickinger grade.

Characteristic	Coefficient
AVM volume (cm^3)	0.1
Patient age (years)	0.02
AVM location† Frontal or temporal = 0 Parietal, occipital, intraventricular, corpus callosum, or cerebellar = 1 Basal ganglia, thalamic, or brainstem = 2	0.3

AVM score = (0.1)(AVM volume) + (0.02)(patient age) + (0.3)(AVM location)
†When an AVM involves multiple sites, fractional values are used according to the number of sites (0.5 for two sites, 0.33 for three sites)

A multivariate analysis was performed to develop this grading system: data on 220 patients treated between 1987 and 1991 were obtained.[27] Excellent patient outcome was the dependent variable, i.e. complete cAVM obliteration after treatment with no new neurological deficit. A separate cohort of 136 cAVM patients (treated between 1990 and 1996 at a different unit) was used to test the PFG, thus demonstrating the scale could be used to predict patient outcomes after radiosurgery ($p<0.001$).[27] Whereas all patients with a PFG ≤1 had an excellent outcome, the latter only occurred in 39% of those with a score >2. Substantial correlation occurred between the PFG system and patient outcomes after single-session radiosurgery. Conversely, the SMG ($p=0.13$) did not correlate with excellent patient outcomes. Amongst the shortcomings of the PFG, are the fact that the system was developed at centres using the gamma knife (so it is unclear if it can be used with radiosurgery delivered by linear accelerator), it predicts patient outcomes after a single radiosurgery session (not after a complete course), and the system was developed and applied retrospectively.

Embolisation Prognostic Risk Score

The Embolisation Prognostic Risk Score was proposed to assess the severity, predictors of and frequency of neurologic deficits after adjuvant embolisation.[28] To create this, a multivariate analysis was performed on 202 patients treated using 377 embolisation procedures. For the development of immediate post-embolisation neurological deficits, risk factors noted were eloquent location, small and large size, complex vascular anatomy (requiring multiple embolisation procedures), and deep venous drainage. Nonetheless, a considerable fraction of patients developing post-treatment deficits recover over time. Therefore, the score's use is limited to a specific patient group.

A topographical classification was devised by Valavanis (Table 1.5.3) and is discussed further in the next section.

Table 1.5.3: Topographic classification system for AVMs[2]

A. Supratentorial arteriovenous malformations (86%)
1. Neopallial arteriovenous malformations (47%) (frontal, temporal, parietal, occipital and central lobes)
a) sulcal (pure sulcal, with subgyral, with paraventricular extension)
b) gyral (pure gyral, with subgyral, with paraventricular extension)
c) mixed sulcal-gyral (with subgyral, with paraventricular extension)
2. Archi- and paleopallial arteriovenous malformations (9%) (i.e. limbic and paralimbic system arteriovenous malformations: cingulum, amygdalo-hippo-parahippocampal, septal, insular arteriovenous malformations)
a) sulcal, fissural
b) gyral, parenchymal
c) mixed
3. Deep central arteriovenous malformations (27%) (strio-capsulo-thalamic, diencephalic, mesencephalic and intraventricular-plexal)
a) fissural, cisternal
b) parenchymal
c) mixed
d) plexal-intraventricular (lateral and/or IIIrd ventricle)
4. Vein of Galen aneurysmal malformations (3%)
B. Infratentorial arteriovenous malformations (14%)
1. Neocerebellar arteriovenous malformations (11%)
a) sulcal, fissural
b) folial
c) mixed
2. Paleo-Archicerebellar arteriovenous malformations (1%)
a) sulcal, fissural
b) folial
c) mixed
3. Deep-central arteriovenous malformations (2%) (cerebellar-nuclear, brainstem, intraventricular arteriovenous malformations)
a) fissural, cisternal
b) parenchymal
c) intraventricular (IVth ventricle and/ or aqueduct)

1.6 AVM topology

cAVMs are known to follow stereotypical patterns based on their locations. cAVM topology and exact localisation is believed to be the first basic step in cAVM understanding, leading in turn to an anatomical classification, which aids in management decisions (Table 1.5.3). Correlated with cAVM topography and location, are the arteries and veins, and the vascular and functional territories associated with each individual cAVM.[2] A topographic classification system for cAVMs is outlined (Table 1.5.3), which was derived using 3D-tractography, diffusion-tensor MR and high-resolution MR.[2] Surrounding functional cortical regions are identified by functional MRI: this reveals if the cAVM induces functional changes in these areas. A cAVM's vascular composition is defined using MRA.

1.7 cAVM angioarchitecture

Aside from cAVM topology, it is acknowledged that the morphology or 'angioarchitecture' is important: this refers to "the angiographically demonstrable vascular elements composing the brain AVM".[29] The term comprises the feeding arteries, nidus, draining veins, any secondary vascular changes occurring due to the high blood flow (referred to as high-flow angiopathy), and any associated abnormal vasculature. A mixture of radiological investigations is often necessary to suitably characterise a cAVM.

Although they have not been systematically studied, multiple angioarchitectural features have been described. An effort was made in 2001 to outline the key angiographical features with the intention being the development of a universal language for the description of cAVMs to aid in their understanding. The terminology for reporting AVM angioarchitecture features has been clearly defined by the Joint Writing Group (JWG) of the Technology Assessment Committee: these are considerably useful in clinical trials for standardising definitions.[30] More complex terminology is listed (Table 1.7.1). Since this publication, the demonstration of reliability in reporting between observers has been challenging (though the identical definitions have not consistently been employed).[31] There have been additional studies with further features describing abnormalities.

Table 1.7.1: Some of the more elaborate cAVM angioarchitecture feature definitions as described by the Joint Writing Group of the Technology Assessment Committee[30]

Angioarchitecture feature	Definition	Image
Venous stenosis/ occlusion	Narrowing of the outflow pathway of any draining vein (the diameter as the vein leaves the nidus is used if diameter is non-uniform). In this relative index, the venous outflow tract immediately proximal is the denominator.	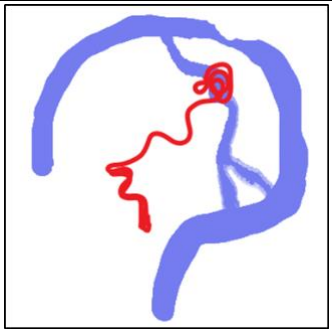
Venous ectasia/ dilatation	Any change in venous calibre in the venous drainage with a >2-fold calibre change in any draining venous channel	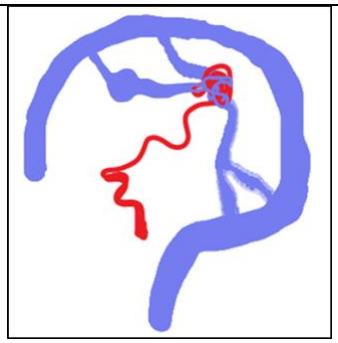
Venous reflux	Reversal of flow in any venous pathway in a direction other than the normal pathway (which is towards the closest venous sinus)	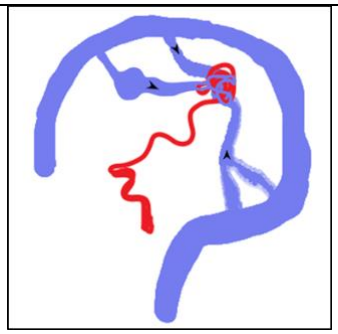
Nidal aneurysm	Aneurysm that is continuous with the nidus, but it can extend past the nidus boundary	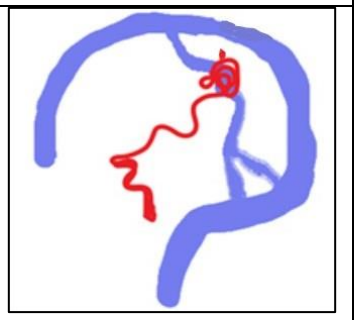

The angioarchitectural features that may be useful, when studying cAVMs are: (1) feeding artery types (dural, leptomeningeal, choroidal, perforating); (2) nidus composition (compact or diffuse, with or without perinidal angiogenesis, mono- or multicompartmental, pure plexiform or mixed plexiform and fistulous or pure fistulous); (3) forms of supply (mono- or multi- or pseudoterminal, indirect- antero or retrograde, dominant or supplementary); and

(4) venous drainage patterns (single or multiple, nidal veins joining or separate from compartmental veins).[2]

There are two nidus types: the more common is compact (abnormal vessels without intervening normal brain parenchyma), and the less typical one is diffuse (normal parenchyma is present amongst the abnormal vessels).[3]

Arterial feeders and venous drainage are contingent on nidus location.[3] If superficial, the pial vessels are the main arterial feeders (branches of the anterior, middle, and posterior cerebral arteries), and venous drainage is usually superficial. If ventricular, the feeders will be choroidal (anterior, medial, and lateral posterior choroidal arteries), and if deep, the feeders will be perforators (lenticulostriate and thalamoperforator), and, for both, the venous drainage will typically be deep.

When analysing cAVMs, there are particular angioarchitectural features that should be identified, and described in a radiology report, which are discussed below. No standardised reporting method exists, with there also being a lack of consensus on nomenclature. A group of agreed definitions would facilitate the comparison of research results. The creation of a uniform radiological assessment of cAVMs was pursued by a Scottish study. However, good interobserver agreement was not achieved, despite there being good intraobserver agreement.[31]

The definition of perinidal angiogenesis is “an angiogenetically-induced vascular network within the perinidal brain parenchyma interposed between the terminal segments of feeding arteries and nidus, without angiographic evidence of AV shunts” (Figure 1.7.1).[2] This occurs in 20-25% of AVM cases, usually together with high-flow intranidal AV shunts.[2] These shunts may result in mild hypoxia in the perinidal parenchyma: it has been suggested that this stimulates the expression of vascular endothelial growth factor (VEGF), triggering angiogenesis to offset the diminished arterial supply. Preventable morbidity is caused by interventional treatments targeting both angiogenesis and the nidus, while specifically focusing on the nidus can eliminate angiogenesis.[2,29] This emphasises the significance of recognising angiogenesis and distinguishing it from the nidus proper.

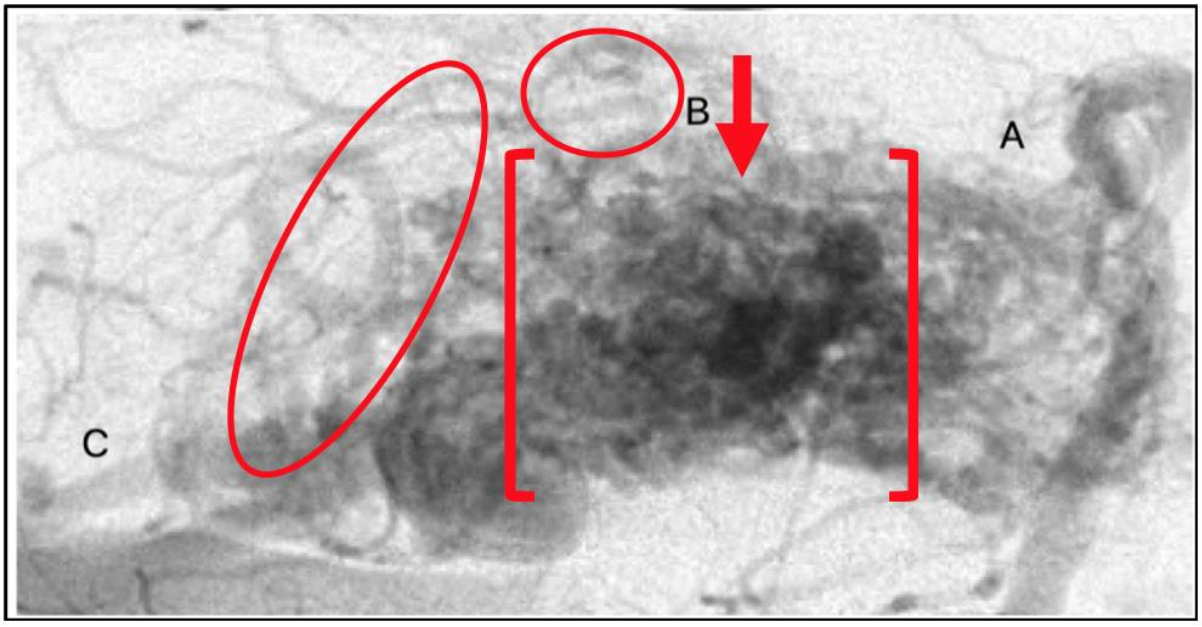

Figure 1.7.1: Perinidal angiogenesis on angiogram
An increased number of smaller calibre, perinidal vessels that do not supply the shunt, with the nidus at the centre. Oval and circle indicate the bordering angiogenesis. (A) feeding artery; (B) Thick arrow, with surrounding brackets, indicates nidus; (C) draining vein.

It can be difficult to radiologically distinguish between perinidal angiogenesis, Moya Moya-type changes and pial-to-pial collateralisation. All three have 'shaggy hair' appearances near the nidus due to less well-developed arteries.

Features of cAVMs can be employed in prognosticating the risks of complications (e.g. seizures), haemorrhage, and multiple treatments.[3] These features can be the targets of treatments to arrest or lessen the extent of the pertinent symptoms. The most common and serious presentation is that of ICH: accompanying features, known as 'weak points', are venous ectasia/pouches, venous stenosis, deep and single venous drainage, intranidal aneurysms, and posterior fossa location (Table 1.7.1).[3] A crucial and genuine predictor is prior haemorrhage, which, especially when asymptomatic, is best detected on gradient-echo T2-weighted MRI. Other likely associating factors are male gender and older age. Seizures could be associated with a long pial draining vein (visible on DSA) and venous congestion.[3] These features injure vast cerebral regions. Seizures as well as neurological deficits could result from mass effect from large venous abnormalities or the nidus (visible on cross-sectional imaging

such as CT). Often, temporary neurological deficits and headache are related to arterial steal, which can only be recognised using perfusion-weighted or functional MRI.

1.8 Treatment

The primary aim of definitive cAVM treatment is the total eradication of the nidus and arteriovenous (AV) shunt.[22] Options include conservative treatment, endovascular treatment (or embolisation), stereotactic radiosurgery (SRS), or surgical excision. The intention is to suppress new or recurrent haemorrhage.[29] Further goals are to treat intractable epilepsy, lessen the frequency and severity of chronic headache, and assist in recovery from neurological deficits.

Conservative treatment involves symptomatic treatment (e.g. analgesics, anti-epileptics) and clinical review at regular intervals in conjunction with imaging. This is more common in cases of small asymptomatic (or minimally symptomatic) cAVMs, where the risks of intervention outweigh the risks of non-occlusion.

Embolisation consists of superselective vascular catheterisation to distinctly illustrate the angioarchitecture of the distal arterial feeders of the cAVM.[32] Occlusive materials are injected via the catheter, such as coils (e.g. Guglielmi detachable coils), or liquid embolic agents (e.g. Onyx or cyanoacrylate).[2,33,34]

Embolic agents include N-Butyl Cyanoacrylate (nBCA), Onyx, Precipitating Hydrophobic Injectable Liquid (PHIL), and Squid.[35] nBCA benefits include that it has an additional colouring agent enabling clear identification of the embolic agent, and it has good safety and efficacy.[35,36] A disadvantage is that, in pure form, the microcatheter would immediately occlude due to instant polymerisation of the embolic agent so it requires admixture with iodised oil before use. Advantages of Onyx include multiple studies demonstrating its high efficacy and safety in endovascular embolisation of cAVMs.[35] Onyx limitations include the fact that the vial has to be kept on a shaker for at least 20 minutes prior to its use to ensure homogeneous suspension of the tantalum particles, and, during longer embolisation periods, the tantalum particles start sedimenting in the syringe and microcatheter which can occlude

the microcatheter or impair visibility. Also imaging artefacts in CT imaging occur, preventing detection of periprocedural haemorrhage and interfering with treatment planning for SRS. Additionally, there may be incomplete embolisation of certain structures due to Onyx precipitation occurring from the outside to the inside. Squid has the advantage of its tantalum powder having a smaller grain size resulting in slower particle sedimentation: this increases homogeneity with a slower drop in radiopacity and enhances visibility in the presence of longer injection times.[35] Squid's extra low viscosity versions permit quicker and longer antegrade flow of contrast during embolisation resulting in faster and more effective penetration. Disadvantages include severe artefacts during CT imaging, though this is reduced with low density versions. Similar to Onyx, there may be incomplete embolisation of certain structures due to the precipitation method. Unlike Onyx, there are limited studies investigating Squid. PHIL's benefits include the fact that it comes ready to use without any need for further preparations prior to use.[35] Also the lower viscosity version, similar to Squid, permits faster and more effective penetration of contrast. Unlike Onyx and Squid, there is constant radiopacity over time with PHIL. With CT imaging, only minor artefacts occur with PHIL (in contrast with Onyx and Squid) and none with MRI. One study has demonstrated that PHIL requires a lower volume for the same extent of embolisation as Onyx. Unfortunately, unlike Onyx, there are limited studies investigating PHIL. A disadvantage of all embolic agents is the vasotoxic and inflammatory effects caused by them.

The above properties influence the decision on which embolic agent to use, particularly in relation to the target lesion's morphology. Longer embolisation procedures would benefit from the use of PHIL as this does not sediment. Artefacts occurring with Onyx and Squid can prevent the detection of peri or postoperative haemorrhage, of which there is a higher risk with cAVM embolisation. During emergency procedures, PHIL may be preferable as it is ready to use.

SRS techniques include gamma knife, linear accelerator, or proton beam. Multiple radiation beams are directed at the nidus to induce thrombosis and injury. Thus, the surrounding brain parenchyma is minimally affected.[32] Using computer-imaging, isodose plans for multiple or single-treatment irradiation are calculated.[37] The ideal dose for cAVM obliteration is

calculated by balancing the complications expected from radiosurgery and/or incomplete treatment (causing subsequent rupture) against the anticipated obliteration rate for a dose.[38]

Surgery comprises identification of the cAVM borders, subsequent ligation of feeders, draining vein obliteration, and concluding with nidus resection.[32] Features indicating safer resection include a superficial location, supply from a single vascular territory, superficial venous drainage, and a less eloquent region. Multiple combinations of image guidance and neurosurgical navigation, functional magnetic resonance, intraoperative electrophysiological cortical mapping, and angiography are used to gather this information.[32]

Adjuvant use of embolisation is common, whether this is pre-SRS or pre-operative to reduce the nidus size, or post-SRS to eliminate residual cAVMs.[39] In small cAVMs in inaccessible locations, it is used as the only treatment.[39] However, in most cases, it is inadequate to solely eradicate cAVMs: this only occurs in 10-20% of cases.[3] To guide management, the SMG is frequently used. For SMG I and II, surgery is safer, but for IV and V, it is of higher risk.[40] Although excision permits instant obliteration, it introduces risks to neighbouring structures, including the parenchyma. SRS is considered safe for SMG III.[40] It is well-suited where there is higher risk in surgery for small to moderate size AVMs in eloquent or deep locations.[39] In prudently chosen patient groups, it achieves good eradication rates, although months or years may pass before obliteration is complete.[32,37] Typically, after multidisciplinary team (MDT) discussion, a mixture of approaches is employed, with decisions made based on each individual patient.

The ARUBA trial reported that medical treatment is superior to combined interventional and medical treatment for the prevention of stroke or death in cases of unruptured cAVM.[41] The study has multiple controversies, including small sample size, selection bias, overrepresentation of embolisation, prematurely shortened enrolment rates, short follow-up, and underrepresentation of surgical treatment.[39] Since the publication of ARUBA, multiple studies using ARUBA-eligible patients have been conducted, demonstrating a lower risk of death or stroke in the intervention group than the original study.[39]

1.9 Pathogenesis

It is not known for definite how cAVMs form. Several cAVMs occur at arterial territory borders: it is believed they may form during foetal development from persistent arterial connections, without going through remodelling.[4]

Cerebral blood vessel formation

Cerebral vascular development consists of two steps: vasculogenesis, then angiogenesis.[4] The first step refers to primordial endothelial cells forming, which, in turn, construct a primary vascular plexus.[4,16] The second step comprises plexus restructuring. This includes the formation of new branches, branch shortening, and the support of freshly developed vessels.[14] Blood vessel arborisation follows angiogenesis: there is further plexus remodelling into a coordinated system of veins and arteries, and ongoing branch adjustment. There are two parts to cerebral cortical vascular development: ventriculofugal and ventriculopetal.[14,15] Ventriculofugal branches travel in a radial pattern from the ventricle to the pial surface. Ventriculopetal branches traverse in the opposite direction. This vessel development occurs parallel to and in tandem with radial neurogenesis.

Vital to vascular development is the molecular environment (Table 1.9.1). In the early period of corticogenesis, within the ventricular zone, VEGF family cellular titres are high.[16] Migration of centripetally directed vessels relies on this. Signalling of molecules such as matrix metalloproteinases (MMP) and growth factors (e.g. VEGF) induces angiogenesis as further elaborated on in 'Genetic involvement' (Table 1.9.1, Fig 1.10.1).[16]

Classically, cAVMs are believed to be congenital lesions, which is the result of abnormal vascular development: supporting evidence arises from the association of cAVM with well-known genetic disorders, such as Sturge-Weber and Osler-Weber-Rendu syndromes, Hereditary Haemorrhagic Telangiectasia (HHT) as well as ataxia telangiectasia.[16] cAVMs are mostly sporadic, with a genetic mutation only occurring in 5% of cases. There is increasing evidence to suggest that cAVMs are dynamic with the ability to enlarge, spontaneously regress, and reappear even after treatment is completed & obliteration is noted.[16,19] A literature review has demonstrated 12 cases with recurrent cAVMs, where nine of the

patients were under the age of 20: this would suggest that instead of being congenital lesions, there is a tendency for recurrence, possibly requiring a 'primed' or immature neurovasculature.[19]

Table 1.9.1: Chemical and molecular factors critical to vasculogenesis and angiogenesis.[16]

Factor	Receptor	Actions
VEGF subtypes: A-E & placental growth factor	TKR: FLT1, KDR	Endothelial cell replication, migration, differentiation, survival
TGF	Type I/ II	Biphasic: in early development, TGFα is inhibitory to vascular endothelial proliferation; it later becomes stimulatory; activates migration & differentiation of surrounding mesenchymal cells in intercellular matrix to differentiate into pericytes & SMCs
TGFα	EGF	Stimulates pathways of cell growth
bFGF	TKR: FGFR-1 (highest affinity)	Stimulates a cascade of secondary messengers including MAPKs, triggering angiogenesis; acts on fibrocytes, myocytes, endothelial cells, & neuronal cells
ANG-1	TIE2 agonist	Regulates pericyte & smooth muscle precursor recruitment; stabilises vessels by promoting interactions between endothelial cells & support cells; like VEGF, heavily involved in angiogenesis
ANG-2	TIE2 antagonist	Regulates pericyte & smooth muscle precursor recruitment; vascular remodelling/ destabilisation is promoted by deconstructive signalling
Delta	Notch	Involved in arterial development; mutated delta/notch associated with CADASIL
Endoglin	Response to TGFα + SMADS	Endothelial proliferation is increased; mesenchymal cells are activated to differentiate within intercellular matrix to pericytes & SMCs; these migrate & encircle endothelial conduits due to TGFα influence
Neuropilin 1 & 2	Cofactor for KDR	Neuropilin-1 is linked to arterial development, while neuropilin-2 is linked to venous development
Ephrin B2	Ephrin B4	Eph/ephrin “repulsive” interactions regulate angiogenesis

VEGF: vascular endothelial growth factor, TGF: transforming growth factor, SMC: smooth muscle cell, EGF: epidermal growth factor, bFGF: basic fibroblast growth factor, TKR: tyrosine kinase receptor, FGFR-1: fibroblast growth factor receptor 1, MAPK: mitogen-activated protein kinase, ANG-1: angiopoietin 1, ANG-2: angiopoietin 2, CADASIL: cerebral autosomal dominant arteriopathy with subcortical infarcts and leukoencephalopathy, FLT1: or VEGFR-1, KDR: or FLK1 or VEGFR-2, TIE2: or TEK.

1.10 Genetic Involvement

While the vast majority of cAVMs are sporadic, inheritance of a genetic mutation occurs in 5% of cAVMs. A multitude of genes have been found to be linked with sporadic cAVMs: there are more than 900 genes, whose expression is altered, of which more than 300 are likely upregulated, and close to 560 are downregulated.[4,16] Proteins these genes code for include cell adhesion and extracellular matrix (ECM) factors, growth factors, MMPs, endocrine hormones, and inflammatory factors.[16]

Vascular endothelial growth factor (VEGF) is an important vascular growth factor. There are six VEGF subtypes (VEGF-A, VEGF-B, VEGF-C, VEGF-D, PlGF [placental growth factor], VEGF-E [Orf-VEGF]), and each of these has multiple splice variants.[16] VEGF-A is the main isoform: this is expressed in the astroglia surrounding AVMs. In cAVMs with larger niduses, there is a greater expression of VEGF-C and VEGF-D, which could lead to cAVM growth. Vascular endothelial tyrosine kinases (VEGFRs) are bounded by all VEGF subtypes.[16] Flt-1 (VEGFR-1) and KDR (Flk-1 or VEGFR-2) are examples of specific receptors. Ligand-binding leads to pathway activation, which, in turn, results in endothelial cell replication, migration, differentiation, and survival. VEGF is a soluble factor: it has a powerful mitogenic effect on endothelial cells in both small and large vessels, whether in vitro or in vivo.[16] During embryonic vascular development, VEGF is highly expressed, though, in adulthood, it is suppressed. In children with recurrent cAVMs, it is highly expressed. In the vessel media and endothelial layer of cAVMs, there is high VEGF expression. Typically, VEGFRs are solely expressed by vascular wall smooth muscle cells and vessel endothelial cells: they are likely to be essential to cAVM development.[16] Around cAVMs, there is increased expression of Flt-1, Flt-4, and Flk-1 receptor subtypes.[16] Also Flk-1 epitope expression is higher in the cAVM nidus endothelium. Embryological factors are expressed by cAVMs: this implies the process of formation is active, possible starting in utero, and advancing into childhood.[16]

Angiopoietins regulate pericyte and smooth muscle precursor recruitment and are implicated in angiogenesis and vascular stability.[16] An endothelial cell-specific tyrosine-protein kinase receptor (TIE2 or TEK) is used by angiopoietin-1 (ANG-1), whereas angiopoietin-2 (ANG-2) is a TIE2 antagonist. Vessels are stabilised by ANG-1 by the promotion of interactions between

support and endothelial cells. Vascular remodelling or destabilisation is promoted by ANG-2. There is upregulation of ANG-2 in cAVMs, but downregulation in normal vessels. The overexpression of ANG-2 leads to phenotypes similar to cAVM vessels, with abnormal dilation and lacking mature peri-extracellular support structures. In the systemic familial venous malformation syndrome, TIE2 is mutated: this closely resembles cAVMs. ANG-1 protein levels are 30% lower, ANG-2 protein levels are 600% higher, and ANG-2 mRNA levels are 40% higher than controls.[16]

Opposing forces inhibiting or supporting angiogenesis and vascular remodelling are thought to be involved in cAVM growth and regression.[16] If ANG-2 is present and VEGF is absent, vessels will undergo regression. Based on vessel size and their levels of concentration, there can be variation in the opposing actions of ANG-1 and ANG-2. At high concentrations, ANG-2 can switch from an antagonist to an agonist for the TIE2 receptor. The hypothesised pathway for pathogenesis is shown in Figure 1.10.1.

The cAVM's neighbouring environment is hypoxic and is thought to stimulate the activity and secretion of these described angiogenic factors.[16] VEGF secretion is stimulated by hypoxia and ischaemia: these two elements also trigger the release of VEGFRs and other growth factors. In a hypoxic environment, VEGF secretion has been noted to occur from astrocytes. AV shunting through the cAVM may lead to this hypoxia.

A promoter Single Nucleotide Polymorphism (SNP) in IL-6 was associated with a two-fold increased risk of cAVM in candidate gene studies in Hispanics.[1] Candidate gene studies have noted that in sporadic AVMs, there are SNPs in several genes associated with a higher likelihood of AVM and/ or ICH formation, including activin-like kinase 1 (*ACVRL1 or ALK1)*, interleukin-6 (*IL-6*), tumour necrosis factor-alpha (*TNF-α)*, and interleukin-*1β (IL-1β).*[42] A pro-inflammatory state, which contributes to AVM formation, may be maintained by genetic variation in cytokines.[43] Overexpression of inflammatory and angiogenesis-related genes has been detected by genome-wide expression profiling of cAVM tissue: these include *MMP9, VEGFA*, endoglin (*ENG)*, angiopoietin-2 (*ANGPT2)*, Integrin Subunit Alpha V (*ITGAV)*, and *VEGFR1* (*FLT1*).[44]

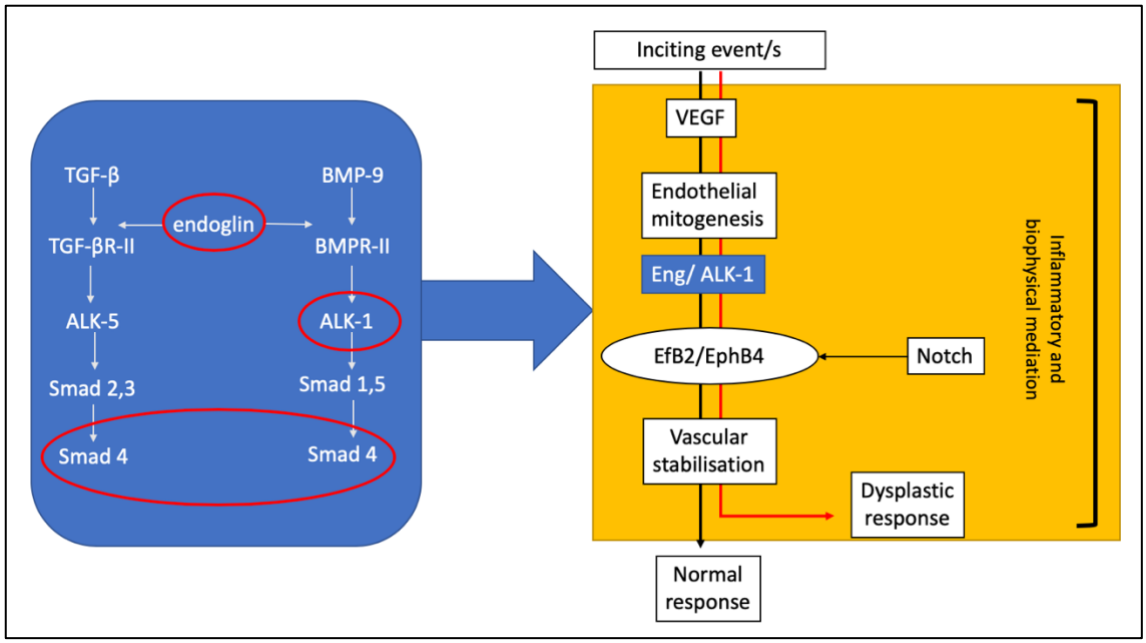

Figure 1.10.1: Adapted from Kim et al.[1] Proposed pathogenesis pathway.
TGFB: transforming growth factor beta, alk1: activin-like kinase 1, BMP9: bone morphogenic protein, BMPR-II: bone morphogenetic protein receptor type 2, Smad: Mothers Against Decapentaplegic Homolog 2 protein, a signal transducer/ transcriptional modulator, VEGF: vascular endothelial growth factor, ENG: endoglin, EfB2: ephrin B2. Yellow area shows (1) inciting events (unknown, but may include consequences of modest injury from trauma, infection, inflammation, irradiation, or mechanical stimulation like compression) upregulate angiogenic factor expression e.g. VEGF, causing endothelial cell (EC) mitogenesis. These new vessels will grow into a stable neovasculature; (2) this results in a vascular dysplastic response when signalling through abnormal *ALK1* or *ENG* or similar pathways; (3) ephrinB2 and EphrinB4 imbalance through Notch signalling; (4) possible influences from inflammation and circulating precursor cells. Blue area is a summary of possible EC *ALK1* and *ENG* signalling via TGF-β and BMP-9. Circled are the mutated genes in Hereditary Haemorrhagic Telangiectasia (HHT).

Studies have shown that for a cAVM to develop, the cerebral vasculature must have an inherent genetic susceptibility (first hit) and a secondary angiogenic clinically relevant environmental stimulus (second hit).[45,46] This is the basis of the two-hit hypothesis.

1.11 Experimental models

Three types of experimental AVM models exist, each having its benefits and faults: these include a fistula model, the carotid rete mirabile, and a genetically engineered model. The swine's carotid rete mirabile has been used as an experimental model: it consists of a tangle of arterioles and microarteries located at the end of the ascending pharyngeal artery at the

cranial base.[47] Even with modifications in the chronic model, changes of experimental AVM vessels observed were considered representative of realistic histopathologic features in human AVMs. The model is limited in that the abnormality rests outside the brain.

The earliest described models were those in which an anastomosis was created between the common carotid artery and the external jugular vein to induce cerebral hypoperfusion.[48] These models (cat and rat species) were created to mimic the brain environment (venous hypertension) of a cAVM and to study the response of the brain to surgical removal of a cAVM. The model lacks the basic characteristics of a cAVM in that there is no nidus, and there is no vascular abnormality in the brain. There are more severe models: an AV fistula is created by end-to-end and end-to-side anastomosis of the right common carotid artery with the posterior facial vein plus ligation of the contralateral external jugular vein.[49] This creation of high intracranial venous pressure induces VEGF and hypoxia inducible factor alpha (HIFα) expression, leading to angiogenesis with dural AV fistula formation. Pietilä et al. describe an intracranial anastomosis model in a dog with a bypass formation between the middle cerebral artery and the superior sagittal sinus.[48] This occurs with a superficial temporal artery interposition graft attached to a portion of the temporalis muscle. Postoperative angiography six months after the creation of the anastomosis demonstrated newly developed vessels surrounding the muscle implant. This suggests cAVM lesions in the adult brain could develop over the course of time, as a result of angiogenesis, on the condition of cerebral ischemia and/or venous hypertension. This model too has no nidus.

A number of mouse models have used sophisticated genetic engineering techniques**,** exploiting genetic defects associated with HHT. HHT is a clinical condition that is characterised by the presence of AVMs in multiple organs, including the brain.[1] HHT is caused by defects in the genes expressed primarily by endothelial cells: *ENG* (occurring in HHT1) or *ALK1* (occurring in HHT2) genes. Experimental mouse models engineered to study the effects of gene deletions in the *Eng* and *Alk1* genes have been used to develop a brain AVM model.

Global knockout of mouse *Eng* and *Alk1* is incompatible with life, thus limiting their use as a cAVM model. They exhibit embryonic vascular defects, including dilated and fused artery–vein pairs, dying in utero.[50,51]

Eng+/− or *Alk1+/−* heterozygous mice are viable and have been observed to develop peripheral AVMs during adulthood.[52,53] Although cerebrovascular abnormalities occur (niduses of dilated vessels, AV shunts, and rounded, misaligned endothelial cell nuclei), they are rare. Only one (out of ten) mice, were noted to have features consistent with a cAVM.[53]

The injection of VEGF into the brain of adult (8-10-week-old) *Eng+/−* mice increased the frequency of the development of abnormal vessels 2-4 weeks post-injection.[45] The vessels were twisted, large, clustered, and spiralled: they were localised at the site of adenoviral vector injection of VEGF. Hao et al similarly observed that focal adenoviral VEGF delivery into the brains of *Eng+/−* and *Alk1+/−* adult mice induced microvessel dysplasia (increased capillary density and abnormally large capillaries) six weeks following injection.[54] In addition, contrary to what is seen in the brain, endothelial deletion of *Alk1* or *Eng*, in combination with an angiogenic stimulus, readily results in features of non-brain AVM in mice suggesting that the adult brain does not readily support angiogenesis and, consequently, new vessel formation.[55,56]

Although vascular defects were more profound in *Eng+/−* mice than in the *Alk1+/−* mice, these observations suggest that an additional angiogenic stimulus, in conjunction with an inherent vessel vulnerability, may be necessary to induce cAVMs in heterozygote *Eng* or *Alk1* adult mice.[54]

Using more sophisticated genetic tools to delete both alleles of *Alk1* or *Eng* in a tissue-specific (endothelial cell) and temporal manner, homozygous *Alk1* or *Eng* knockouts are created in the late gestation or postnatal phase. Deletion of both alleles of *Alk1* from embryos results in late gestational or postnatal lethality from haemorrhagic complications associated with brain, lung or intestinal vascular dysplasia.[50] Gene deletion in adult mice results in lung and intestinal AVMs, but is insufficient to induce cAVMs.[52] This suggests that angiogenic potential is present during infancy, though it is lost in the brain in adulthood.

As with tissue-specific *Alk1* knockouts, homozygous endothelial and smooth muscle cell deletion of *Eng* post-natally leads to greatly enlarged and tortuous blood vessels consistent

with an AVM phenotype in 90% of mice at five weeks.[51] The mortality at six weeks is high, and although morphologically the abnormalities observed resemble human AVMs, the model is inconsistent, with variable AVMs because of shifting levels of gene deletion.

The observation that angiogenic potential is blunted in the brain in adulthood is supported by studies of *Notch* expression and the use of genetic engineering of the *Notch* gene.[57] Notch, which is a single peptide, is a single-pass transmembrane receptor.[58] Endothelial expression of a constitutively active *Notch4* allele (*Notch4**) in adult mice results in AVM features in the liver, skin, and uterus, but not in the brain, whilst endothelial expression of *Notch4** in immature mice leads to hallmarks of cAVM.[55] Vascular lesions in the brain were observed when *Notch4** was turned on from birth, causing lethality by post-natal day 36. Thus, unlike in adult brains, *Notch4** is able to induce AVMs in immature brains, suggesting that immature cerebral vasculature is susceptible to the process that controls angiogenesis, contrary to the adult state.

Walcott et al reviewed zebrafish (*Danio rerio*) models of cerebrovascular disease, including cAVMs.[59] Zebrafish constitute a useful animal model as the transgenic expression of fluorescent proteins coupled with larval translucency allows easy visualisation of their endothelium using live imaging techniques, so that the vasculature can be studied in intact animals in vivo.[59] Zebrafish are vertebrates and have significant molecular conservation to mammals, making the results of zebrafish studies relevant to human disease. It is possible to use genetic manipulation to recreate a phenotype resembling the preliminary stages of human AVM formation in zebrafish cranial circulation.[60,61] Due to their high fecundity, small size, amenability for live imaging, and ease of drug administration, zebrafish are highly suitable for high-throughput screening, lending them well to the discovery of effective medical treatment in the form of gene therapies or vascular targeted therapies.[59]

To model cAVMs and other cerebrovascular diseases in zebrafish, a reverse genetics approach has been used.[59,62] There is precise manipulation of the gene of interest to observe the phenotype.[59] Methods include zinc-finger nucleases, transcription activator-like effector nucleases (TALEN), the clustered, regularly interspaced, short palindromic repeats (CRISPR), CRISPR-associated (Cas) systems, and morpholino oligonucleotide knockdowns.[59]

A transient gene knockdown approach using antisense morpholino oligonucleotides has been applied to study the loss of *alk1* function in zebrafish larvae.[62] As per the mammalian orthologue, *alk1* encodes a transforming growth factor (TGF)-beta family type I receptor which has been found to be involved in a group of human cAVMs: mutations cause HHT.[62] There is a range of morphological, functional and molecular defects in *alk1* morphants, resembling defects seen in patients with cAVM. By 24 hours post-fertilisation (hpf), Walcott noted abnormal shunting of circulation, despite a normal vascular architecture developing: a prominent cranial circulation was noted, with a reduced circulation caudal to the heart. By 3 to 4 days post-fertilisation (dpf), zebrafish developed cerebral oedema, pericardial oedema, and oedema around the remaining yolk sac: these are all sequelae of high-output heart failure. A modest attenuation of the phenotype is produced by treatment with the antihypertensive, losartan, possibly by restoring bone morphogenetic protein (BMP) signalling.[62]

Roman et al identified a zebrafish mutant by performing an ENU mutagenesis screen: they used a phenotypic screen of larvae obtained from the breeding of randomly mutagenised zebrafish. They noticed abnormal circulation, where most blood cells failed to perfuse the trunk or tail at 2 dpf, and flowed through a limited number of dilated cranial vessels.[61] This comes from an increase in the number of endothelial cells in specific cranial vessels.[61] The authors show that *alk1*, a TGF-beta type 1 receptor, is predominantly expressed in the endothelium in dilated vessels.[61] Homozygous mutants become progressively oedematous, as also described by Walcott.[61,62] They die between 7 and 10 dpf.[61] Prior to genetic mapping to *alk1,* Roman et al have called this zebrafish mutant phenotype *violet beauregarde*.

However, it is worth noting that the phenotype produced that is being described as mimicking the human cAVM does not have the abnormal vascular pattern described earlier in this report. There is shunting and rapid circulation, but importantly the normal vascular architecture is preserved.

A mutation in RAS P21 Protein Activator 1 (*RASA1)* causes the syndrome of capillary malformation-arteriovenous malformation, another syndrome of cAVM development.[59] This

gene has been fully sequenced in zebrafish, and provides another model for further study. Zebrafish *rasa1* morphants demonstrate an enlarged caudal vascular deformity reducing posterior blood flow.[63,59] TALENs were used to produce zebrafish *eng* mutants. They demonstrate cerebral vessel dilatation, worsening pre-existing AV shunting, reminiscent of cAVMs.

All of the above models are limited for multiple reasons. Animal models that rely on genetic manipulation account for a small proportion of the human disease. They are not widely available as they require significant gene modification knowledge and skill. The phenotype created also does not accurately represent the human condition in that most of the abnormalities described are arterio-venous dysplasia, and the key characteristic (i.e. the nidus) is absent. The gene defects that the models exploit and engineer are so essential to normal life and development that even with sophisticated engineering, the models are fragile and it has not been possible to conduct any long-term studies. Despite this, adaptive responses of knockout animal models are underestimated, so it is not possible to interpret our findings as though there is a single gene deficit.[64] Models that exploit genetic defects are also limited as genetic conditions only account for 5% of all AVMs, with most occurring sporadically: therefore, this may not represent the true human AVM phenotype. Stressed animals (e.g. through maintenance in breeding cages/tanks, transportation) can confound experiment results.[64] Interpreting experimental results is generally an oversimplification of actual events as animals are significantly complex.[64] Finally, human cAVMs commonly occur in a classifiable anatomical and topological manner, which is not considered in genetic AVM models.

Zebrafish are remarkably well-suited for relatively short experiments, when balanced against more sentient vertebrates (as described earlier in this section).[59] Their transparency at the larval stage facilitates live imaging. On the other hand, in adulthood, a combination of whole zebrafish fixation, immunohistochemistry and clearing can permit intact tissue imaging.[65] Zebrafish that are genetically manipulated on a mutant *alk1* background, could be subjected to an additional stimulus to form a cAVM.[61] The endothelial cells form vessels, which are susceptible to dilation.[61] Stimuli have been applied to genetically susceptible mice so far.[66] This is not the case with zebrafish, where genetically manipulated specimens have been

studied alone, without exposure to stimuli.[60,61] This will be further discussed in Chapter 4. The primary challenge is that a genuine cAVM is not produced when a mutant mouse is exposed to an angiogenic stimulus. The major reasons for this failure are: (a) to date, animal models created developed a fistula (not a nidus, which is a critical cAVM feature), (b) for a primarily sporadic disease, genetic models are not a true representation, and (c) specialist expertise with limited availability is required for genetic models.

1.12 Hypoxia, venous occlusion, and angiogenesis

Through in vivo and in vitro studies, angiogenesis is induced by hypoxia via VEGF upregulation.[67–69] When the tissue is made anoxic, VEGF-A is upregulated.[70] Cells deprived of oxygen release HIFα: included in its multiple roles in controlling a diversity of angiogenic gene expression, this transcription factor also stimulates VEGF-A production.[69,71] Interestingly, de novo cAVM development has been detected in later life, in the presence of cerebral ischaemia or infarction, secondary to iatrogenic insult or ischaemic stroke.[72,73]

Cerebral Venous Sinus Thrombosis (CVST) leading to venous occlusion, is a disease process which results in cerebral ischaemia. Angiogenesis is induced by the ensuing hypoxia. Although it is rare for CVST to occur in childhood, such timing could induce angiogenesis and consequent formation of cAVMs. No investigations have occurred to assess how frequently children with CVST develop cAVMs. There are numerous risk factors for childhood CVST, namely, dehydration, head/ brain injury, fever, and infection.[74] Neonatal CVST is similarly associated with infection, and severe dehydration, but also hypoxia, during early life.[74] Hypothetically, these risk factors could precipitate CVST, inducing a hypoxic cerebral climate, which consequently triggers angiogenesis, leading to cAVM development. Additionally, on angiograms, features indicating venous occlusion could be correlated with more frequent angiogenesis.

1.13. The overall objective

A vital necessity exists to improve present cAVM management. Our comprehension of cAVM pathophysiology is lacking. Bridging the gap is critical to advance our diagnostic methods and

locate conceivable therapeutic targets. This project's overarching aim is to further consider the hypothesis that angiogenesis plays a critical role in cAVM development. Venous occlusion is thought to contribute to angiogenesis through the occurrence of cerebral hypoxia. This has not previously been shown on patient angiograms. The association of angioarchitectural features with angiogenesis has also not been investigated before. Understanding the predictors of angiogenesis could enable us to devise new treatments targeting these predictors before the cAVM develops. There is a lack of uniformity when describing the angioarchitecture of cAVMs, with the presence or absence of angiogenesis not being mentioned. Having a universal shared terminology would facilitate research on cAVMs and clinical discussions on management. To develop new treatments, a cAVM animal model would be highly beneficial: to our knowledge, such a model does not exist yet. Angiogenesis has not been studied in zebrafish using the two-hit hypothesis previously. Applying a clinically relevant stimulus to a genetically susceptible zebrafish could induce the development of a cAVM. To achieve our aim, the project will be broken down into three key objectives:

1. to evaluate the agreement on the presence of angiogenesis on angiograms,
2. to determine what proportion of the current literature uses the JWG terminology when reporting the angioarchitecture of cAVMs, and
3. to optimise a protocol for visualisation of the neurovasculature in intact, fixed adult zebrafish to assist in developing a cAVM animal model.

The aims and objectives will be listed in detail in each of the three chapters: angiogenesis in angiograms, systematic review, and the zebrafish model. To assess whether a relationship between CVST triggers and cAVMs exists, a study was proposed which is further discussed in Chapter 5. To improve on angiogenesis detection, parametric imaging was also discussed in Chapters 2 and 5.

Chapter 2 – Can angiogenesis be reliably determined on Digital Subtraction Angiography in cerebral arteriovenous malformations?

2.1 Introduction

Digital subtraction angiography (DSA) is the optimal technique for imaging cerebral arteriovenous malformations (cAVMs). A clear view of all the pathognomonic components of a cAVM altogether is only possible using DSA as an imaging modality: these components are the nidus, shunting, and early draining vein.[22] The vascular constituents that make up a cAVM demonstrated on a DSA are unique to each cAVM and these component features are known or described as being the angioarchitecture of a cAVM.[2] This term incorporates the feeding arteries, nidus, draining veins, any associated abnormal vasculature, and any vascular changes occurring subsequent to high blood flow (high-flow angiopathy).[29]

cAVM angioarchitectural features are thought to be useful in predicting the clinical course of the disease, including the risk of haemorrhage and other symptoms (e.g. seizures), and potential complications of treatments.[75] For example, angioarchitectural features associated with haemorrhage are venous ectasia, venous stenosis, single and deep venous drainage, and intranidal aneurysms, whilst cAVMs with a long pial draining vein and venous congestion have been associated with a presentation with seizures.[75] These features may be used to define targets for treatment to dampen symptom severity or overcome symptoms altogether.

Though several angioarchitectural features have been detailed, there was no endeavour to systematically classify and provide a standardised description of these features until 2001. The Joint Writing Group (JWG) of the Technology Assessment Committee tried to create a universal language for describing cAVMs to expand our knowledge of them.[30] The definitions they have produced were designed to assist in clinical research and simplify discussions about patient management.

In general, the JWG advocated that a description of cAVMs should include angioarchitectural features which can be divided into three general groups as described in Section 1.7: (a) nidus composition, (b) types of feeding arteries, and (c) patterns of venous drainage. A nidus commonly has a compact border, but occasionally a diffuse border can be present.[75] The qualities of the feeding arteries and draining veins vary with nidus location (see Section 1.7).[75]

New vessel formation or angiogenesis has been depicted or characterised in relation to cAVMs by Valavanis, who described angiogenesis as a network of vessels in the brain parenchyma bounded by the terminations of arterial feeders and the nidus (in the absence of AV shunts) (Figure 2.3.3).[2] This is often referred to as the classical definition. The JWG did not mention or describe angiogenesis, which is an oversight as will be explained below.

There is radiological and anatomical evidence (from surgical experience, which has also been published by Kozyrev et al) that there is a network of small vessels immediately adjacent to the nidus which are surgically recognised as narrow, friable vessels that lack an intima and are difficult to coagulate.[76] Throughout this thesis, we describe angiogenesis or perinidal angiogenesis as this network of friable vessels closely surrounding the nidus. This is distinguishable from a diffuse nidus where there is normal parenchyma present amongst the abnormal vessels.

Angiogenesis is new vessel formation and understanding this may increase our comprehension of cAVMs. It is observed in 20-25% of cAVMs.[2] As described in Section 1.9, there are numerous factors implicated in the process of angiogenesis, including Vascular Endothelial Growth Factor (VEGF), Transforming Growth Factor (TGF), and angiopoietin 1 (ANG-1). Angiogenesis mostly occurs in conjunction with high flow intranidal AV shunts according to Valavanis.[2] These shunts can result in minor hypoxia in the perinidal parenchyma, which is thought to trigger angiogenesis. The latter has not been regularly reported in the cAVM angiography publications so far, other than a handful of exceptions.[3,77]

As a critical contributor to the development of blood vessels, it is essential that we improve our understanding of the role of angiogenesis in the context of cAVM formation. If we comprehend the frequency and diagnosis of angiogenesis, there could be timely and targeted

treatment. Earlier in Section 1.12 ‘Hypoxia, venous occlusion, and angiogenesis’, we have outlined how cerebral venous occlusion may induce hypoxia, and lead to VEGF expression. In this study, using our definition of angiogenesis, we aim to assess if there is a correlation between features of venous hypertension and angiogenesis in cAVM presentation.

Objectives

The aims of the study were:

1. To determine the frequency of angiogenesis in patients who have had a DSA for a cAVM.
2. To evaluate the intra- and inter-observer agreement of a diagnosis of angiogenesis.
3. To determine if angiogenesis is seen more frequently in cAVMs with features of venous occlusion.

2.2 Methods

Study participants

The Neurovascular service at the Manchester Centre for Clinical Neurosciences (MCCN) maintains a database of all patients with cAVMs referred to the service. This was the source of our study participants. The MCCN covers the Greater Manchester (GM) area with a population of 3.2 million. General Practitioners and various specialties across the GM area make the referrals. All the database cases are consecutive. The patients were not prospectively consented for the use of their data. Ethical approval was granted for this study in June 2018. This was provided by the Health Research Authority and Health and Care Research Wales (REC reference 18/LO/0856).

Both DSA and thin-sliced CTA or MRA was performed for all patients reviewed at the MCCN. cAVM angioarchitectural features were recognised by reviewing angiograms as described later in this section.

Study Inclusion Criteria:

- Age ≥ 18 years
- First time diagnosis of a pial cAVM (between 2009-2017)
- AVM imaging (angiograms and pre-treatment MRA/CTA, MR T2 sequences)

Study Exclusion Criteria:

- Any other vascular malformation that is not a pial cAVM (dural arteriovenous fistulae, developmental venous anomalies, cavernomas).
- Pial cAVM that has been submitted to previous treatment(s) in another neurosurgical centre.

DSA Imaging

For clinical purposes, all participants underwent a DSA at Salford Royal Hospital. The imaging was performed on a Canon Infinix-I Biplane (Toshiba, Japan, since 2010, and Philips, Netherlands, prior to this). For elective cases, a DSA was performed within 6 months from identification of a cAVM on CT or MRI. For emergency cases, this was usually performed within 24-48 hours from diagnosis.

Data Collection

One hundred patient angiograms were reviewed and the angioarchitectural features recorded in a standardised manner by one observer (Table 2.2.2). Definitions are provided, including that of perinidal angiogenesis as outlined below (Table 2.2.3, Fig 1.7.1). The nidus size was quantified on angiograms by measuring the maximum diameters in each of three axes (anteroposterior [AP], laterolateral [LL], craniocaudal [CC]) and calculating a final volume according to this formula: (AP x LL x CC)/ 2. This method has been used to measure elliptical volumes in previous studies and is known to produce a three-dimensional volume.[78,79] Diameters were arbitrarily divided into two groups for the observer agreement (as described later in this section): ≥30mm and <30mm. This cut-off was used as it has been described previously.[31,25] For anterior circulation cAVMs, the genu of the petrous portion of the internal carotid artery (ICA) was used for calibration. The genu's diameter was measured in pixels (the unit of measurement available on the Centricity imaging program), and converted into millimetres, by assuming that the genu is typically 5mm in diameter. This method has been adopted by previous studies.[31,80] For posterior circulation cAVMs, the basilar artery (BA) diameter was measured in pixels on Centricity and assumed to be 3.17mm. This is in the middle of the range of BA diameters reported in the literature: from 1.1 to 6.6 mm.[81,82,83] Angiogenesis was measured using the methods and formulae demonstrated (Figure 2.2.1). This involved measured multiple individual diameters, depending on where angiogenesis was located in relation to the nidus.

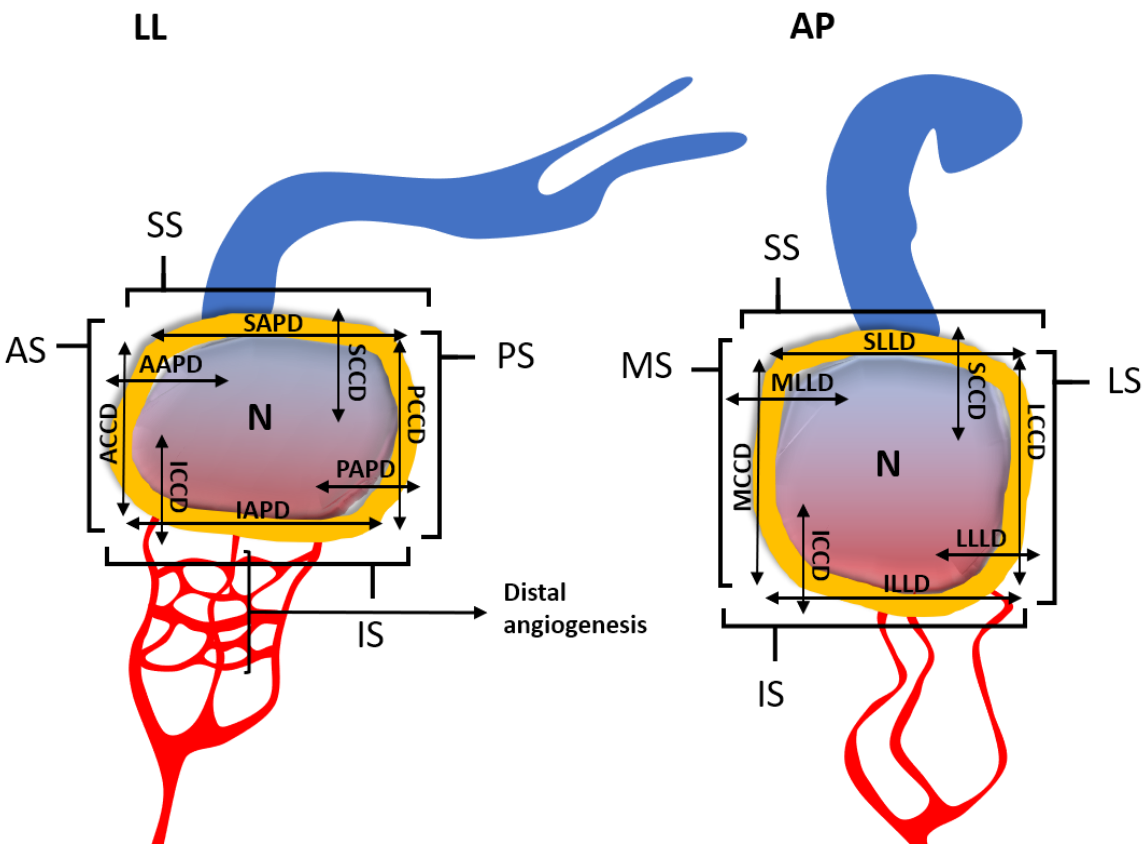

Perinidal angiogenesis
Draining vein
Feeding arteries
N Nidus
AP Antero-posterior view
LL Latero-lateral view

- *CALCULATIONS:*

1. $Vss = \frac{SAPD \times SCCD \times SLLD}{2}$
2. $Vis = \frac{IAPD \times ICCD \times ILLD}{2}$
3. $Vas = \frac{AAPD \times ACCD \times (I)SLLD}{2}$
4. $Vps = \frac{PAPD \times PCCD \times (I)SLLD}{2}$
5. $Vms = \frac{(A)PAPD \times MCCD \times MLLD}{2}$
6. $Vls = \frac{(A)PAPD \times LCCD \times LLLD}{2}$
7. $TV = \text{Vss} + Vis + Vas + Vps + Vms + Vls$

SAPD – superior surface antero-posterior diameter

SCCD – superior surface cranio-caudal diameter

SLLD – superior surface latero-lateral diameter

IAPD – inferior surface antero-posterior diameter

ICCD – inferior surface cranio-caudal diameter

ILLD – inferior surface latero-lateral diameter

PAPD – posterior surface antero-posterior diameter

PCCD – posterior surface cranio-caudal diameter

AAPD – anterior surface antero-posterior diameter

ACCD - anterior surface cranio-caudal diameter

MCCD - medial surface cranio-caudal diameter

MLLD - medial surface latero-lateral diameter

LLLD - lateral surface latero-lateral diameter

LCCD - lateral surface cranio-caudal diameter

Vss – superior surface volume; Vis – inferior surface volume; Vas – anterior surface volume; Vps – posterior surface volume; Vms – medial surface volume; Vls – lateral surface volume

Figure 2.2.1: Diagram describing the method of obtaining and calculating angiogenesis segmental volumes.
Adapted from study protocol. SS: superior surface, IS: inferior surface, AS: anterior surface, PS: posterior surface, MS: medial surface, LS: lateral surface.

Data were collected and stored as per the protocol submitted for ethics approval. Due to the pandemic, a large proportion of angiograms were reviewed via remote access.

Two other observers (Observers 2 and 3) were given ten patients' angiograms to review to assess inter-observer reliability, after some training was provided on the definitions. Training involved going through the definitions in Table 2.2.3 and explaining them on an angiogram. The observers were not blinded to patient demographics or clinical presentation. The same ten angiograms, and an additional ten, were reviewed by the author (Observer 1) after a six-month period to assess intra-observer reliability.

Table 2.2.1: Observers (all from the same specialty, neurosurgery) participating in reviewing cAVM angiograms and their level of experience

Observer	**Length of Experience**
Observer 1	third year neurosurgery registrar
Observer 2	consultant neurosurgeon with 6 years of interventional neuroradiology experience
Observer 3	neurosurgical vascular fellow, who was training in interventional neuroradiology for 6 months

Table 2.2.2: Descriptive data and angioarchitectural features collected and recorded for each cAVM.

Category	Variables
Demographics	• Age at diagnosis • Gender • NHS number
Diagnosis	Date of first DSA
Haemorrhage	Y/N
Seizures	Y/N
Other symptoms	Y/N
General	• Location • Depth – Lobar / Deep • Eloquence: Non-eloquent; Highly eloquent; Less eloquent • SMG – 1-5
Arterial	• Main supply - ICA, ECA, both • Feeders – arteries supplying the cAVM • High flow shunt (direct fistula) – Y/N • Angiopathy (Ectasia) – Y/N
Nidus	• Size – anteroposterior (AP), laterolateral (LL), craniocaudal (CC) • Border – compact / diffuse • Angiogenesis – Y/N • Angiogenesis – quantification in terms of location & subjective amount
Venous	• Number of draining veins • Drainage pattern – superficial / deep / both • Pial course length – not pial (deep), <3cm (short), >3cm (long) • Venous reflux – Y/N • Ectasia / Varix – Y/N • Stenosis – Y/N • Sinus Thrombosis – Y/N
Aneurysms	• Aneurysms – Y/N • Intranidal aneurysms – Y/N
Angiography	• Date • Quality – excellent, good, standard, poor, very poor • FPS [6 FPS/ 4 FPS/ high]

DSA – digital subtraction angiogram, ICA – internal carotid artery, ECA – external carotid artery, Y- yes, N – no, SMG - Spetzler-Martin Grade, AP – anteroposterior, LL – laterolateral, CC – craniocaudal, FPS – Frame rate per second.

Table 2.2.3: List of definitions of angioarchitectural features.

Feature	Definition/ Categorisation
Depth	• Lobar: cortical, subcortical, cortico-ventricular, insular, cortico-callosal • Deep: larger part of the nidus involving the thalamus, basal ganglia, internal capsule, choroidal, brain stem, cerebellar
Eloquence	• Non-eloquent • Highly eloquent: brainstem, basal ganglia, pre-central cortex • Less eloquent: cerebellar, post-central cortex, dominant temporal, visual cortex, corpus callosum
High flow shunt	Presence of a direct fistula as a direct transition of the artery into a vein without intervening nidus
Arterial Ectasia	Any change in calibre of an artery that is greater than 50% the normal diameter of the artery that does not supply the cAVM
Nidus	Vascular mass located in the brain parenchyma, supplied by arterial feeders, which ends at the emergence of draining veins
Intranidal Fistula	early contrast filling of the venous compartment which manifests before complete nidus visualisation
Angiogenesis	• Classical: "The presence of small calibre vessels observed around the cAVM nidus that are interposed between the terminal segments of feeding arteries and the nidus without AV shunts" • Non-classical (used by this study): "The presence of small calibre vessels in the immediate surround of an AVM"
Long venous drainage	Long pial course of draining veins (>3cm) (not applicable for deep venous drainage AVMs as only pial course)
Cortical venous drainage/ venous reflux	Retrograde drainage into cortical veins from draining veins of the AVM
Venous ectasia/Varix	Dilatation with a greater than 2-fold calibre change in any draining vein
Venous stenosis	Artery >/= 50% narrowing in the calibre of any draining vein
Venous hypertension	Pseudophlebitic appearance in the venous phase of the angiogram
Aneurysms	• Pre-nidal: arising from course of arteries eventually supplying the AVM; • Intranidal: Intranidal aneurysms in the nidus filling in the arterial phase of the angiography before venous filling contamination
Spetzler-Martin Grade	Combination of : • Size (1 if size < 3cm ; 2 if size 3-6 cm ; 3 if size >6cm) • Eloquence (0-1, with 1 if eloquent location) • Venous drainage (0-1, with 1 if deep venous drainage present)

cAVM – cerebral arteriovenous malformation, AV - arteriovenous

Four measures were used to assess angiogram quality: whether the frame rate per second (FPS) was recorded, at least five vessels were injected, at least three angiographic views were used, and the complete venous system was demonstrated. The quality was considered good if the following criteria were fulfilled:

1. an iodinated contrast agent was injected into bilateral internal and external carotid (or common carotid) and vertebral arteries,
2. at least anteroposterior, lateral, and a third (such as oblique) angiographic projection was used,
3. there was a high FPS (4 or 6 FPS) and this was noted in the radiology report, and
4. the contrast flowed through the entire cerebral venous system.

Statistical analysis

For each angioarchitectural characteristic, the χ^2 test was used to examine the association between the characteristic and angiogenesis. Multivariate analysis was restricted to the strongest predictors from univariate analysis to ensure an even per variable ratio of approximately 10 is maintained.[84] Multivariate logistic regression was performed after testing for multicollinearity among the selected independent variables (angiographical characteristics) by measuring the variance inflation factor. For all analyses, an association was considered statistically significant if a *P* value was < 0.05.

The Cohen's Kappa test was used to assess agreement between three different pairs of observers for 10 cAVMs, and to assess intra-observer agreement for the same 10 cAVMs. Observer agreement was quantified by the unweighted kappa (κ) statistic (for nominal data, e.g. presence or absence of angiogenesis) and the weighted kappa statistic (for ranked ordinal data, e.g. Spetzler-Martin Grade [SMG], and discrete interval data, e.g. number of feeders). For some variables, such as continuous data (e.g. measurements), the raw data was recoded to simplify the assessment of observer agreement using the kappa statistic. The kappa statistic ranges from -1 to 1, with 1 indicating perfect agreement.[85]

Statistical Package for the Social Sciences (SPSS) version 25 (IBM) was used for statistical analyses. GraphPad Prism 8 was used for the forest plots.

Role of the author in the project

My role consisted of data acquisition, analysis and writing the report. My primary supervisor, Mr Patel, ideated the project concept, and contributed data to the assessment of inter-observer agreement. Neurosurgical vascular fellow, Helen Raffalli-Ebezant, contributed data to the assessment of inter-observer agreement. Biomedical statistician, Calvin Heal, provided statistical advice.

2.3 Results

The population whose data was analysed was compared to the overall cAVM population in our local database, and no significant demographic differences were noted. Final analysis included 100 patients (male/female ratio, 58:42; median age, 40; range, 14-79) (Table 2.3.1). Two patients had two cAVMs so a total of a hundred-and-two cAVMs were reviewed and described. The most common presentation was with an intracerebral haemorrhage (53%). Stereotactic Radiosurgery (SRS) was the most commonly offered treatment overall (52%), regardless of the presence or absence of haemorrhage (37.7% vs 59.6%) (Table 2.3.2). SRS was used far more frequently for unruptured cAVMs. Excision was the second commonest treatment for cAVMs that present with haemorrhage (22.6%), whereas conservative management was the second commonest for non-haemorrhagic presentations (21.3%). The range of the follow-up period was from 1 month to 28 years (mean 4.24 years). On the whole, a good outcome (Glasgow Outcome Scale, GOS $\geq$4, modified Rankin Scale, mRS ≤ 1) was attained in 83 (81.4%) cases, with 56 (54.9%) achieving the best outcome (GOS 5, mRS 0).

Table 2.3.1: Baseline characteristics of patients with cAVMs.

Baseline characteristics	Overall population (N, %)	Analysed (N, %)
Number	159	100 (102 cAVMs)
Age (median (IQR))	41 (22)	40 (21)
M: F (N, %)	92 (57.9): 67 (42.1)	58 (58): 42 (42)
Presentation (N, %)		
Haemorrhage	75 (48.1)	53 (53)
Seizures	39 (25)	30 (30)
Other symptoms	34 (21.4)	48 (48)
Incidental	8 (5.1)	3 (3)
Treatment (N, %)		
Conservative	28 (17.6)	17 (17)
SRS	67 (42.1)	52 (52)
Embolisation	16 (10.1)	18 (18)
Excision	23 (14.4)	22 (22)
Combined	25 (15.7)	9 (9)
Location (N, %)		
Supratentorial	138 (86.8)	92 (90.2)
Superficial	90 (56.6)	65 (63.7)
Deep	48 (30.2)	27 (26.5)
Infratentorial	21 (13.2)	8 (7.84)
Cerebellum	17 (10.7)	7 (6.86)
Brainstem	4 (2.52)	1 (0.980)

IQR = interquartile range, M = male, F = female, N = number, SRS = stereotactic radiosurgery

Table 2.3.2: Treatment modality offered according to the presence or absence of haemorrhage

Treatment modality	Haemorrhage present (N, %)	Haemorrhage absent (N, %)
Conservative	8/53 (15.1)	10/47 (21.3)
SRS	20/53 (37.7)	28/47 (59.6)
Embolisation	7/53 (13.2)	2/47 (4.26)
Excision	12/53 (22.6)	4/47 (8.51)
Combined	6/53 (11.3)	3/47 (6.38)

Size

The cAVMs studied had a median nidus volume of 2.70 cm^3 (interquartile range, IQR: 0.91 to 6.83). The ranges of AP, LL, and CC diameters are displayed (Figure 2.3.1). The volume of angiogenesis, in comparison, was much smaller with a median volume of 0.31 cm^3 (IQR: 0.05 to 0.77).

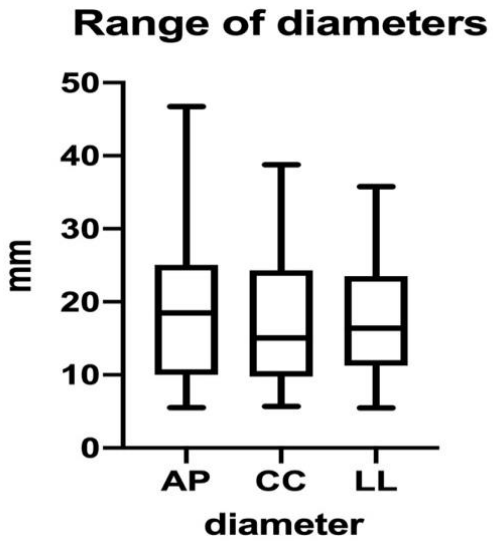

Figure 2.3.1 Box and whisker plot demonstrating the range of anteroposterior (AP), craniocaudal (CC) and laterolateral (LL) diameters of the cAVMs studied.
Lower quartile, median and upper quartile values are listed in millimetres for each as follows: AP – 10.8, 18.6, 25.2; CC – 11.4, 16.8, 25; LL – 11.4, 16.8, 23.8

Location

In this study group, 90.2% cAVMs were supratentorial, and most were located in the frontal lobe (36.3%), in non-eloquent regions of the brain (51%) and were superficial (cortical) (41.2%) (Table 2.3.3).

Table 2.3.3 Summary of anatomical features related to location in the brain, eloquence, and depth from the cortical surface listed with the associated number of cAVMs.

Images	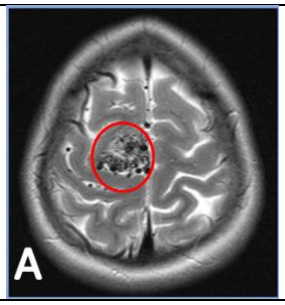	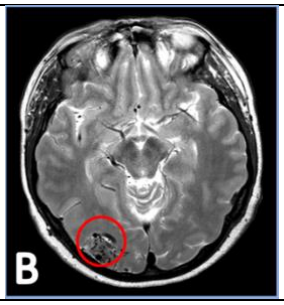	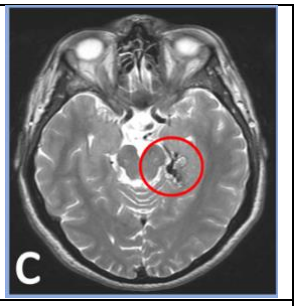
Location	Frontal	Occipital	Temporal
Frequency (N, %)	37 (36.3)	18 (17.6)	19 (18.6)
Images	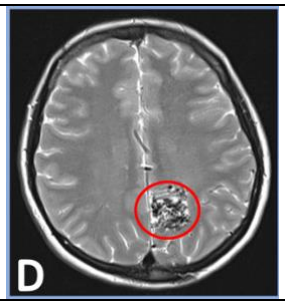		
Location	Parietal		
Frequency (N, %)	21 (20.6)		
Images	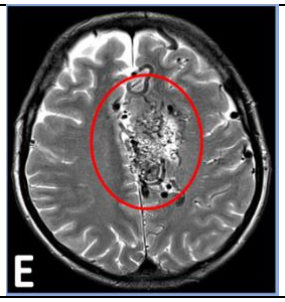	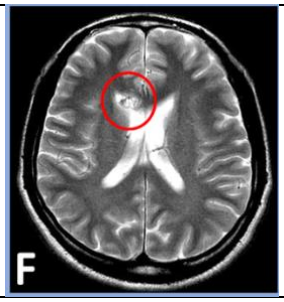	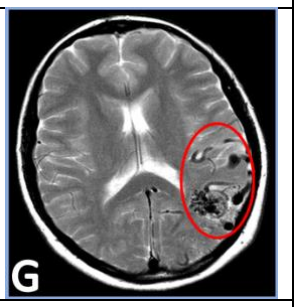
Eloquence	High (e.g. over left pre-central/ motor cortex)	None (e.g. in right frontal horn of lateral ventricle)	Less (e.g. over left post-central/ sensory cortex)
Frequency (N, %)	13 (12.7)	52 (51.0)	37 (36.3)
Images	As per B	As per G	As per F
Depth	Cortical	Cortico-subpial	Cortico-ventricular
Frequency (N, %)	42 (41.2)	24 (23.5)	10 (9.80)

Eloquence refers to a cerebral region associated with a neurological function. Examples are from T2-weighted MRI brain images. cAVMs are circled in red.

Arterial features

The most commonly observed arterial abnormality was arterial ectasia (41.2%) (Table 2.3.4). Despite most cAVMs being small and compact, they had numerous arterial feeders (Table 2.3.4). Twenty-four percent of cAVMs had an associated intracranial aneurysm (Table 2.3.4). The majority were flow aneurysms, located proximally on feeding vessels (13), with two occurring distal to the cAVM on the feeder. One aneurysm was proximal on a major artery

related to the cAVM, whereas three were located remotely on unrelated arteries. Five were intranidal.

Venous features

The most prevalent angioarchitectural features noted were venous abnormalities, with venous congestion and venous ectasia being the most frequent (85% and 81% respectively) (Table 2.3.4). Superficial venous drainage was the commonest drainage pattern (50%) (Table 2.3.4).

Table 2.3.4: Summary of angioarchitectural features listed with the associated number of cAVMs.

(A) Image	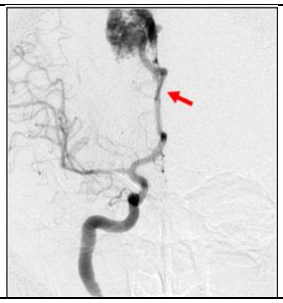	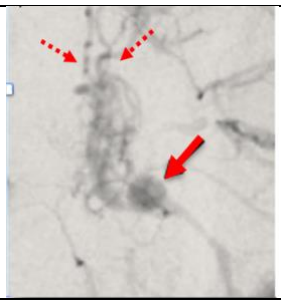	
(B) Angioarchitecture feature	**Arterial ectasia** (Any change in calibre of an artery that is irregular and greater than 50% normal diameter of the artery that does not supply the cAVM)	**Aneurysms** (e.g. Supply from distal pericallosal branch of right anterior cerebral artery & right lateral posterior choroidal artery [dotted arrows], and early filling of small intranidal aneurysm [solid arrow])	
(C) Frequency (%)	42 (41.2)	25 (24. 5)	
(A)	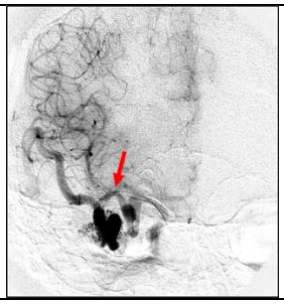	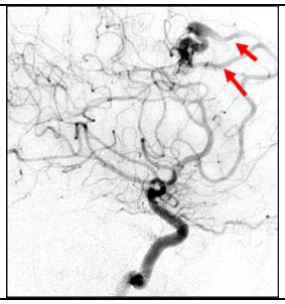	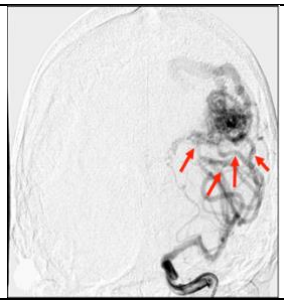

(B) number of arterial feeders	1	2	3	Multiple
(C)	9 (8.82)	12 (11.8)	8 (7.84)	73 (71.6)
(A)	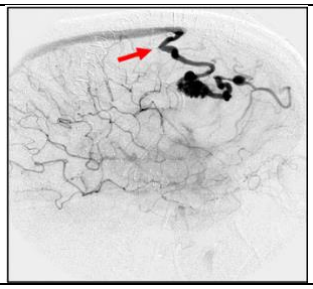	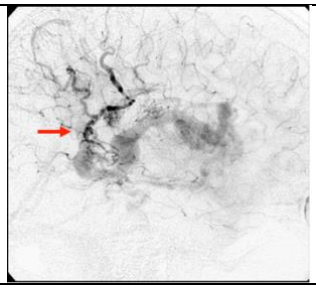	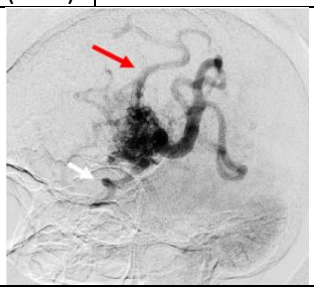	
(B) Venous drainage	Superficial	Deep	Both	
(C)	51 (50.0)	23 (22.5)	28 (27.5)	
(A)	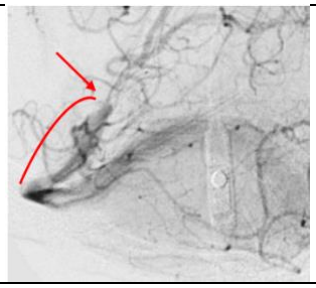	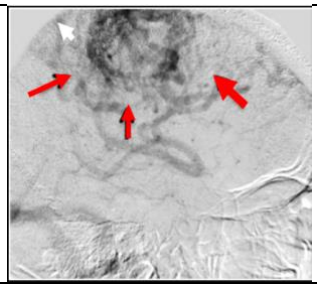	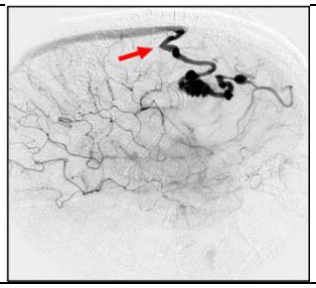	
(B)	**Venous stenosis** (e.g. of proximal straight sinus. Arrow indicates location of stenosis. Curved line indicates the normal patent straight sinus.)	**Venous congestion** (e.g. Congestion of cortical veins [red arrows] or venous hypertension, which are straining to drain the sylvian vein territory via multiple small collaterals into the superior sagittal sinus [white arrow])	**Venous ectasia** (Dilatation with a greater than 2-fold calibre change in any draining vein)	
(C)	5 (4.90)	87 (85.3)	83 (81.4)	
(A)	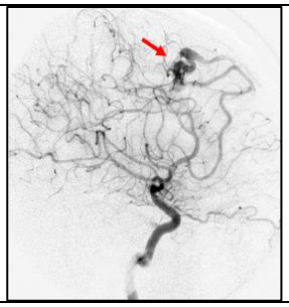			
(B)	Venous varix	Venous reflux	Venous sinus thrombosis	
(C)	35 (34.3)	34 (33.3)	0	

(A)	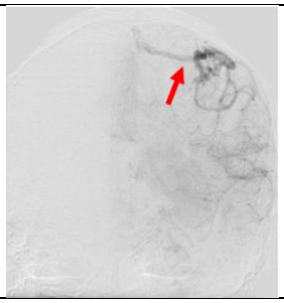	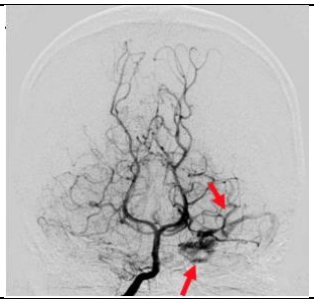	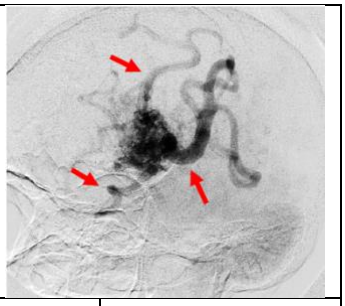	
(B) number of draining veins	1	2	3	Multiple
(C)	22 (21.6)	13 (12.7)	13 (12.7)	54 (52.9)
(A)	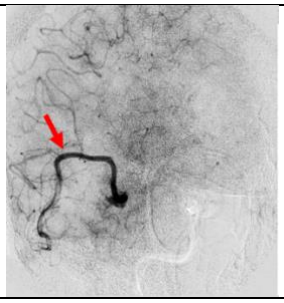	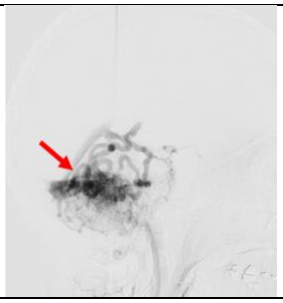	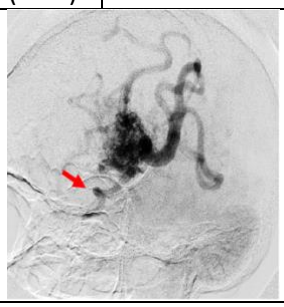	
(B) Pial vein course length	Long	Short	Deep	
(C)	44 (43.1)	33 (32.4)	25 (24.5)	
(B) Artery: vein ratio	<1:1	1:1	>1:1	
(C)	15 (14.7)	50 (49.0)	36 (35.3)	

Arterial, then venous features, are listed together with examples from DSAs of the relevant features. Artery: vein ratios are also listed. Red arrows indicate the abnormality.

Nidus features

Most cAVMs reviewed had a diameter of less than 3 cm and had a low SMG (mostly SMG 2) (37%) (Table 2.3.5). A majority of 77 (75.5%) had a compact border with 25 (24.5%) having a diffuse border (Figure 2.3.2). A high flow shunt was noted in 91 patients (89%).

Table 2.3.5: Spetzler Martin Grades listed with the associated number of cAVMs

Spetzler-Martin Grade	Number of cAVMs (%)
I	25 (24.5)
II	38 (37.3)
III	23 (22.5)
IV	12 (11.8)
V	3 (2.94)

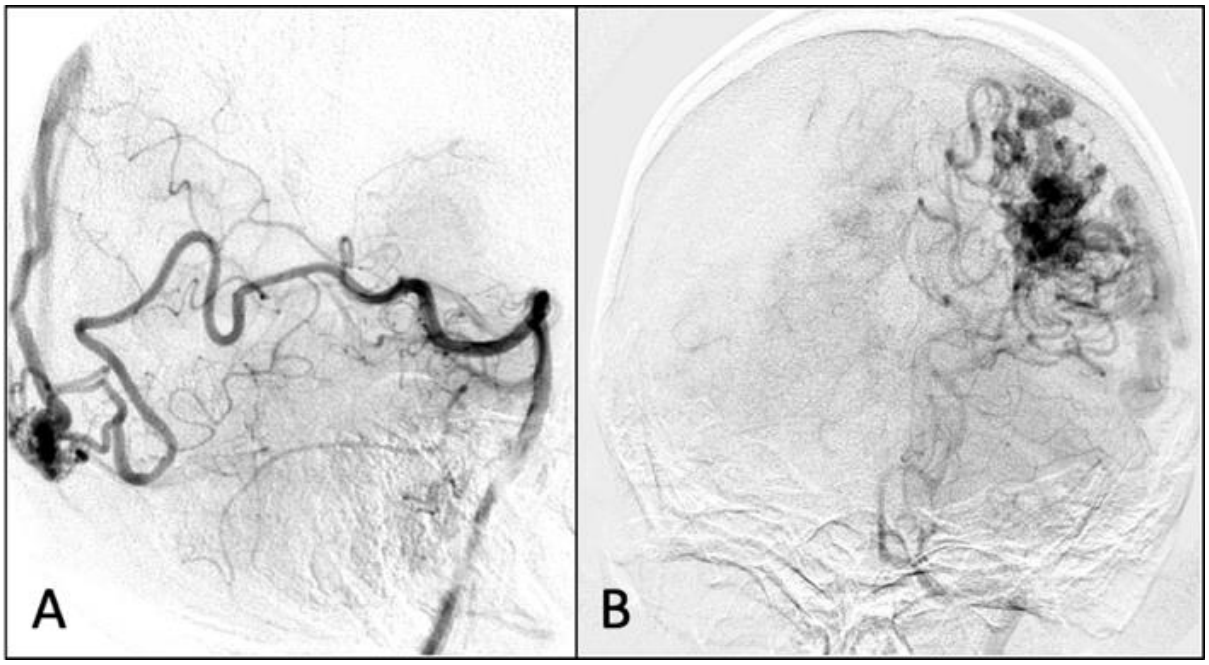

Figure 2.3.2 (A) Compact nidus border and (B) diffuse nidus border demonstrated on angiograms.

Angiogenesis

Angiogenesis was observed in 39 out of 102 cAVMs (38.2%) (Table 2.3.6, Figures 2.3.3 & 2.3.4). Two patients had two cAVMs each, but there was no angiogenesis in either. There was a complete border of angiogenesis in 12 cases (11.8%) (Figure 2.3.4). In most cases in which angiogenesis was observed, it was confined to specific parts of the cAVM nidus, rather than completely surrounding the nidus. As described previously, the median angiogenesis volume was 0.31 cm^3.

Table 2.3.6 Anatomical locations of angiogenesis relative to cerebral arteriovenous malformation (cAVM) nidus and the number of cAVMs in which each of these are present.

Anatomical position of angiogenesis	Number of cAVMs (102), (%)
superior	24 (23.5)
inferior	19 (18.6)
lateral	49 (48.0)
medial	15 (14.7)
anterior	17 (16.7)
posterior	15 (14.7)
border	12 (11.8)

Most cAVMs have angiogenesis at a combination of anatomical locations, e.g. superior and lateral.

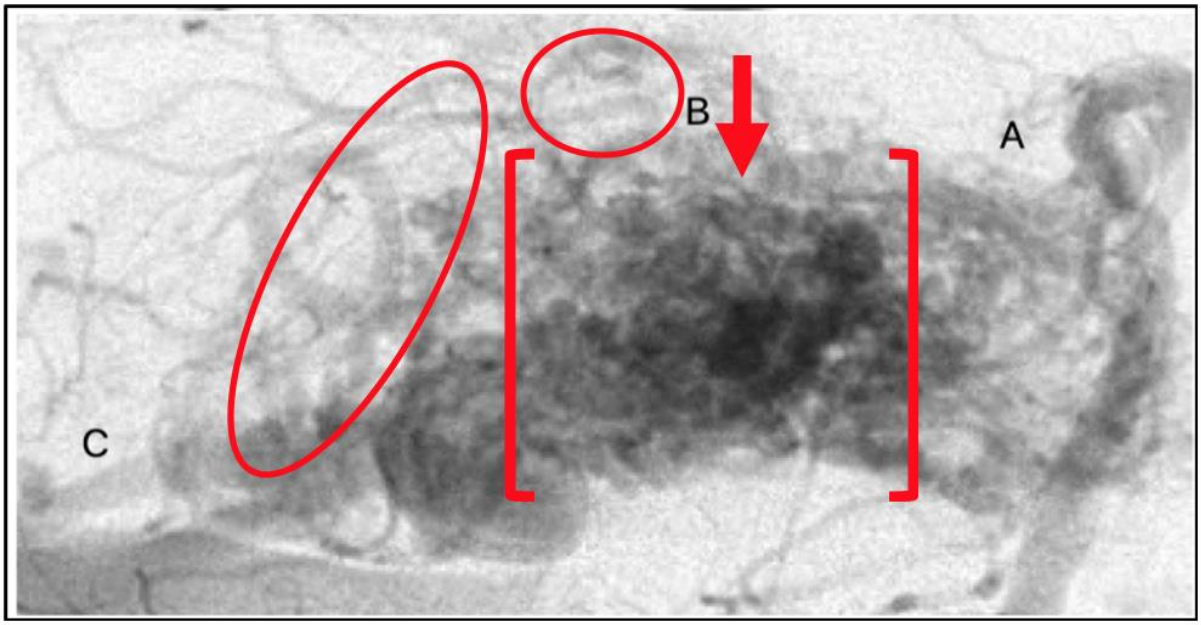

Figure 2.3.3: Perinidal angiogenesis on angiogram

An increased number of smaller calibre, perinidal vessels that do not supply the shunt, with the nidus at the centre. Oval and circle indicate the bordering angiogenesis. (A) feeding artery; (B) Thick arrow, with surrounding brackets, indicates nidus; (C) draining vein.

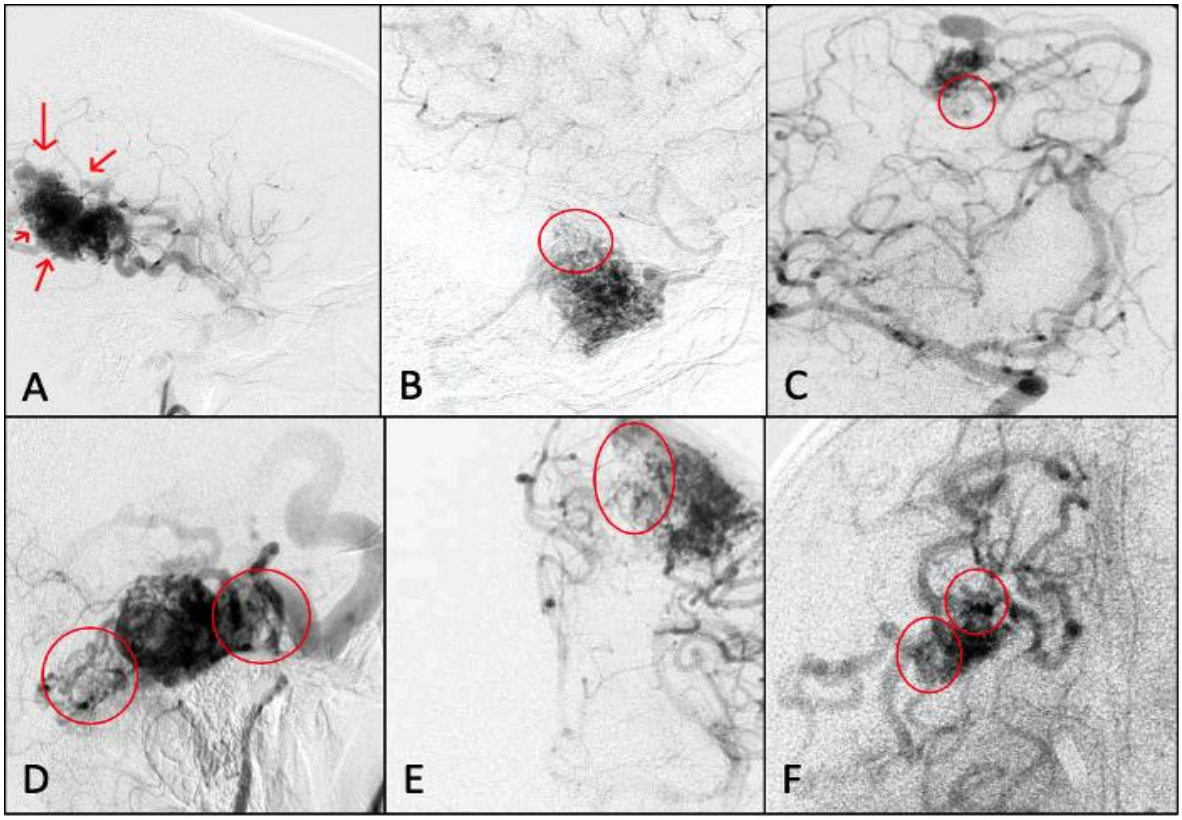

Figure 2.3.4: Different areas of perinidal angiogenesis on angiograms
Highlighted by red circles and, in one panel, red arrows: (A) narrow border of angiogenesis all around nidus indicated by red arrows; (A) narrow border; (B) superior; (C) inferior; (D) anterior and posterior; (E) medial (F) superior and lateral.

Association of angiogenesis with angioarchitectural features

Multicollinearity was tested using the variance inflation factor, which demonstrated that between the various investigated variables, there was no substantial correlation. The angioarchitectural features that are significantly associated with the presence of angiogenesis are listed (Table 2.3.7). Our results demonstrate that arterial ectasia and the artery: vein ratio were significantly associated with angiogenesis, the strongest being arterial ectasia, based on the odds ratio.

Univariate analysis was performed for all angioarchitectural features in relation to angiogenesis, including arterial and nidal features, as well as features related to venous occlusion. Significant associations with angiogenesis were found for arterial ectasia, artery: vein ratio, venous reflux, and venous congestion (Table 2.3.7). Multivariate analysis of the four strongest predictors from the univariate analysis (arterial ectasia, artery: vein ratio,

venous reflux, and venous congestion) revealed that the only factors showing an independent association were arterial ectasia (OR 16.6 [95% CI = 4.65 – 59.6]) and artery: vein ratio (4.28 [95% CI = .956 – 19.15]). In other words, the odds of angiogenesis were 16.6-fold higher if there was arterial ectasia, and 4.28-fold higher with a greater artery to vein ratio.

Table 2.3.7: Univariate analyses of angiographic features thought to be related to angiogenesis as well as multivariate analysis for selected features.

Factor	Angiogenesis present N (%) 39 (38.2)	Angiogenesis absent N (%) 63 (61.8)	Univariate analysis	Multivariate analysis
Number of artery feeders **1** **2** **≥3**	 2/39 (5.13) 3/39 (7.69) 34/39 (87.2)	 7/63 (11.1) 9/63 (14.3) 47/63 (74.6)	Chi-square 2.35, p = .309	Not included
Arterial ectasia	19/39 (48.7)	22/63 (34.9)	Chi-square 11.6, ***p = .001***	OR 16.6 (95% CI = 4.65 – 59.6) ***p = 5.5e-10***
Aneurysms	10/39 (25.6)	15/63 (23.1)	Chi-square .346, p = .557	Not included
Compact border	32/39 (82.1)	45/63 (71.4)	Chi-square 1.47, p = .225	Not included
High flow shunt	35/39 (89.7)	56/63 (88.9)	Chi-square .272, p = .602	Not included
Number of draining veins **1** **2** **≥3**	 10/39 (25.6) 6/39 (15.4) 22/39 (2.56)	 12/63 (19.0) 7/63 (11.1) 45/63 (71.4)	Chi-square 1.26, p = .532	Not included
Artery: vein ratio **<1:1** **1:1** **>1:1**	 4/39 (10.3) 15/39 (38.5) 20/39 (51.3)	 11/63 (17.5) 35/63 (55.6) 17/63 (27.0)	Chi-square 6.21, ***p = .045***	OR 4.28 (95% CI = .956 – 19.15) ***p = .048***
Venous reflux	31/39 (79.5)	61/63 (96.8)	Chi-square 8.19, ***p = .004***	OR .121 (95% CI = .013 – 1.159) p = .067
Venous stenosis	3/39 (7.7)	2/63 (3.17)	Chi-square 1.06, p = .368	Not included
Venous congestion	29/39 (74.4)	58/63 (92.1)	Chi-square 6.02, ***p = .014***	OR .971 (95% CI = .178 – 5.29) p = .972
Venous drainage **Superficial** **Deep** **Both**	 21/39 (53.8) 5/39 (12.8) 13/39 (33.3)	 30/63 (47.6) 18/63 (28.6) 15/63 (23.8)	Chi-square 2.37, p = .306	Not included
Pial vein length **< 3 cm** **>3 cm** **deep**	 14/39 (35.9) 19/39 (48.7) 6/39 (15.4)	 19/63 (30.2) 25/63 (39.7) 19/63 (30.2)	Chi-square 2.85, p = .241	Not included

Multivariate analysis revealed significance for arterial ectasia and artery: vein ratio.

Observer reliability

Observer agreement was compared for multiple angioarchitectural features considered important in the pathophysiology of a cAVM. This consisted of features broadly belonging to three groups: those related to the feeding arteries, nidus, and draining veins (Figures 2.3.5 and 2.3.6, Appendix 1). Features related to the arterial component were the number of feeding arteries, arterial ectasia, and aneurysms. Nidus characteristics were the three diameters (AP, CC and LL), nidus border, eloquence, and high flow shunt. Venous features included venous drainage, number of draining veins, venous varix, venous ectasia, venous stenosis, and venous reflux. An aspect combining multiple features was the SMG.

As Figures 2.3.5 and 2.3.6, and Appendix 1 show, intra-observer agreement was better for every aspect compared to inter-observer agreement.

Intra-observer agreement

Most intra-observer agreement was strong, with exceptions being venous varix, aneurysms and venous ectasia. It ranged from perfect for AP and CC diameters ($\kappa = 1$, [95% CI, 1 – 1]) to slight for aneurysms ($\kappa = .138$, [95% CI, 1.47 – 2.45]) and venous ectasia ($\kappa = .200$, [95% CI, -0.0568 – 0.457]) (Figure 2.3.5, Appendix 1). Venous stenosis was positively identified both times in all cases. This meant it was not possible to compare agreement for venous stenosis as all readings were the same the second time. For angiogenesis, there was substantial agreement ($\kappa = .762$, [95% CI, .450 – 1.07]).

Inter-observer agreement

Inter-observer agreement between three pairs of observers (observers 1, 2, and 3) was compared across the same angioarchitecture features as above (Figure 2.3.6, Appendix 1). Inter-observer agreement was greatest at a rating of perfect for pial course length (observers 2 and 3, $\kappa = 1$, [95% CI, 1 – 1]) and substantial for venous drainage (observers 1 and 2, $\kappa = .696$, [95% CI, .017 – 1.22]), and poorest at a rating of less than chance for AP and CC diameter (for both, this was for observers 1 and 2 with $\kappa = -.2$, [95% CI, -0.488 – 0.088]), venous stenosis

(observers 1 and 2, κ = -.143, [95% CI, -0.339 – 0.339]), and aneurysms (observers 1 and 3, κ = -0.316, [95% CI, -0.018 – -0.614]). For angiogenesis, there was fair (observers 1 and 3, κ = .2, [95% CI, -0.356 – 0.757]) to substantial inter-observer agreement (for observers 2 and 3, κ = .688, [95% CI, .312 - 1.064]). The latter comparison was statistically significant.

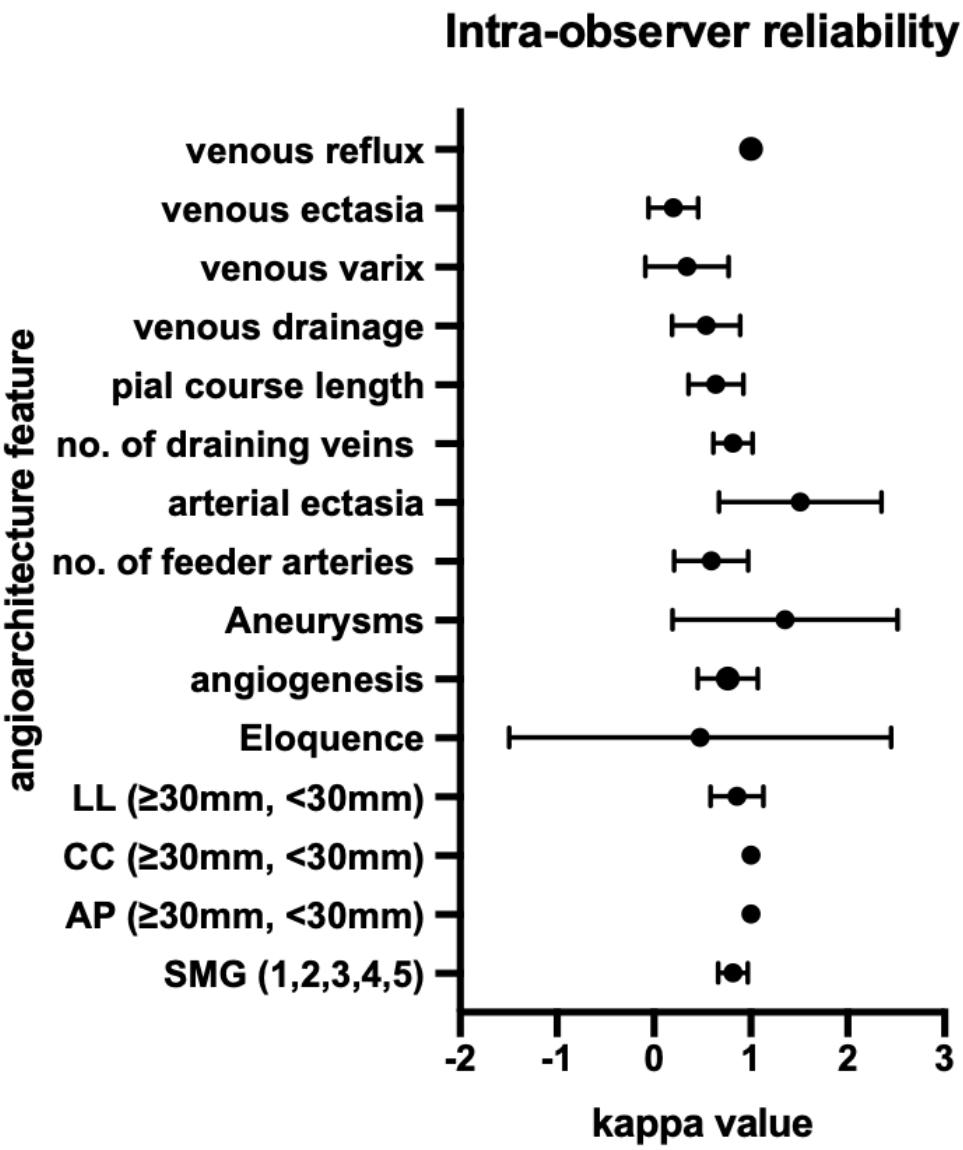

Figure 2.3.5: Forest plot summarising extent of intra-observer agreement
Measured by the unweighted or weighted kappa, shown as odds ratios with 95% confidence intervals. Qualitative ranges for the extent of agreement are as follows: 0.8 to 1 = almost perfect; 0.6 to 0.8 = substantial; 0.4 to 0.6 = moderate; 0.2 to 0.4 = fair; 0 to 0.2 = slight; < 0 = agree less than chance. Venous stenosis, border, and high flow shunt are not included as we were unable to perform an intra-observer comparison as all values were the same in the second reading.

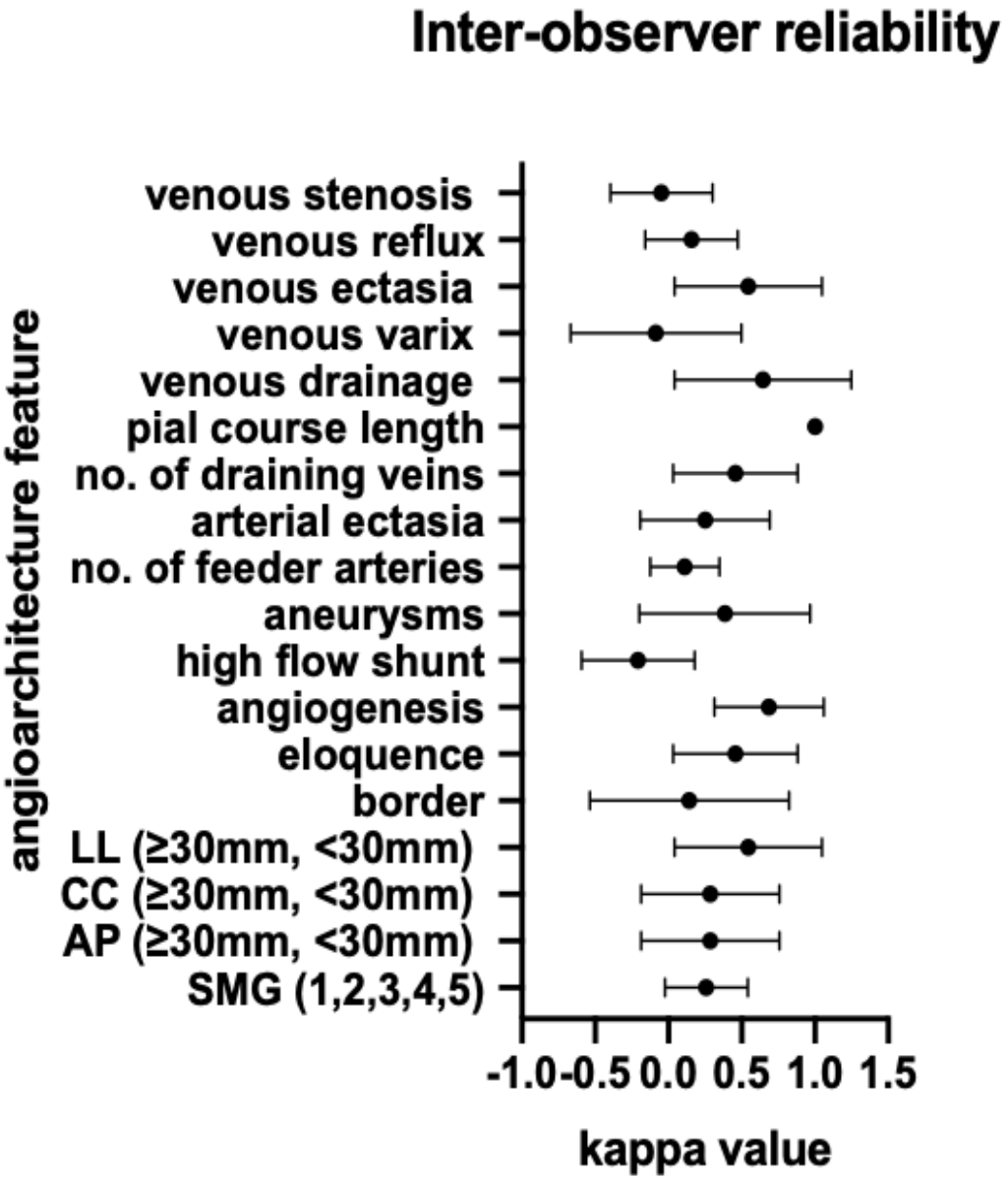

Figure 2.3.6: Forest plot summarising extent of inter-observer agreement
Measured by the unweighted or weighted kappa, shown as odds ratios with 95% confidence intervals. Qualitative ranges for the extent of agreement are as follows: 0.8 to 1 = almost perfect; 0.6 to 0.8 = substantial; 0.4 to 0.6 = moderate; 0.2 to 0.4 = fair; 0 to 0.2 = slight; < 0 = agree less than chance.

Angiogram quality

Subjective assessment of angiogram quality was mostly considered to be average (Table 2.3.8). Formally assessing angiogram quality revealed that 92.2% angiograms demonstrated the complete venous drainage system and 96.1% had a minimum of three views, but few had five or six vessels injected (31.4%) or recorded the frame rate (26.5%) (Table 2.3.9). Most angiograms were of average quality (65 cases). Observer agreement did not show any relationship with angiogram quality.

Table 2.3.8: Subjective quality of angiograms

Angiogram quality	**Number of images (total = 102, 100%)**
average	65, 63.7%
good	29, 28.4%
excellent	4, 3.92%

Table 2.3.9: Objective quality of angiograms reviewed using four features as listed.

Quality feature	**Number of images feature present in (total = 102, 100%)**
Complete venous drainage demonstrated	94, 92.2%
At least three views (anteroposterior, lateral and oblique)	98, 96.1%
Five or six vessel angiography	32, 31.4%
Frame rate recorded	27, 26.5%

The associated number of angiograms each feature is present in is shown.

2.4 Discussion

Using our definition of angiogenesis, a moderate frequency of angiogenesis was observed with 38.2% of cAVMs having angiogenesis. Angiogenesis could be reliably determined during both intra-observer assessment and inter-observer assessment. There were significant associations between angiogenesis and features of artery: vein ratio, and arterial ectasia. As far as we know, no other research group so far has tried to quantify angiogenesis or evaluate its relationship to other angioarchitectural features.

Overall, our sample population was similar to other reported series and provides some support for the wider applicability of our observations. Large natural-history studies report an average age of 32-39 years.[86–91] and a lower male to female ratio compared to our series which had slightly more males (58%) than females (42%). Most patients in our series presented with haemorrhage (53%): this is similar to other studies (42%, 52%).[92,11] Fewer (30%) presented with seizures, which is again comparable to others' findings (29%, 23%).[87,88] In contrast, 48% had other symptoms, which was similar to one study (48%), but far higher than another (8%).[9,92] No studies have provided frequencies for each treatment, despite describing the possible treatment modalities in their sample populations.[32,6,93] Most patients recovered well and were asymptomatic after treatment, with 58 cases having the best outcome of GOS 5 and mRS 0.

A mixture of the JWG standards and commonly known terms were used to compile the definitions used to study the angiographic characteristics.[30] When defining angiogenesis, we have expanded on the classical definition by Valavanis: we defined it as a border of small calibre vessels, not solely present between the nidus and feeding arteries (Figure 2.3.3).[2] This definition is recognised by other authors as well as by practising surgeons who encounter these vessels at the time of cAVM surgical excision.[76] This border may completely surround the nidus or, more often, may be incomplete.

For our study sample, angiogenesis was observed as a border in a minority of cases: in only 12 cases, angiogenesis was seen to completely encircle the nidus (30.8% of all cAVMs with

angiogenesis) (Figure 2.3.4). The remaining 27 cases had varying degrees of angiogenesis, but no complete border (69.2%) (Table 2.3.6).

Univariate analysis revealed significant associations between angiogenesis and certain features of venous occlusion (venous reflux and venous congestion). Venous stenosis, on the other hand, was not found to be significantly associated. With respect to other angioarchitectural features, only arterial ectasia and artery: vein ratio were significantly associated with angiogenesis. Multivariate analysis, however, only revealed an independent association for angiogenesis with arterial ectasia and artery: vein ratio. As described in Section 1.12, venous occlusion reduces cerebral perfusion by causing passive congestion.[94] This could result in tissue hypoxia, which triggers the release of angiogenic factors, mediated by hypoxia-inducible factor (HIF-1α). These include VEGF, ANG-1, and placenta growth factor (PlGF).[69] This is why it would be plausible to expect an association of venous occlusion with angiogenesis. We have not shown this possibly due to insufficient sample numbers, or varying angiogram quality.

Artery: vein ratio and arterial ectasia were the features showing an independent significant association with angiogenesis. Apart from the mechanism just described for angioarchitectural features associated with venous occlusion, a higher artery: vein ratio may also increase the likelihood of angiogenesis as a result of a higher pressure within the nidus. This may induce relative venous engorgement within the nidus and exert mass effect on the surrounding parenchyma resulting in tissue hypoxia. A high artery: vein ratio may result in a form of venous hypertension, which is localised and angiographically occult, compared to venous congestion that is more widespread and visible. Arterial ectasia may be an indicator of vascular remodelling and thus occur simultaneously with angiogenesis. It has been hypothesised that matrix metalloproteinases (MMP) are implicated in the development of arterial ectasia via angiogenic signalling.[95]

As there was fair to substantial inter-observer agreement, we would argue that angiogenesis can be reasonably determined. In particular, this is because the analyses and observations were done by a doctor with little experience in interpreting cerebral angiograms. We would

anticipate that the inter-observer agreement would be higher if angiograms were being analysed by expert neuroradiologists.

Our observer agreement was evaluated using a method adapted from Al Shahi et al.[77] To date, there are four studies alone that have investigated the reliability of different observers describing cAVM angioarchitecture.[77,96,97,98] Unlike these studies, our emphasis was on the identification and measurement of angiogenesis.

Al Shahi et al also reported on the inter-observer agreement for angiogenesis, observing only slight inter-observer agreement as compared to substantial agreement in our study.[77] The reason for this is unclear but may relate to the quality of imaging used for the Al Shahi et al's study. Angiogenesis was not studied in Iancu-Gontard and Du et al's study, whilst in Braileanu et al's study of 36 cases, the assessment of interobserver agreement was limited to cAVM border diffuseness.[96,97,98] Agreement for this varied from fair to substantial and although the diffuseness of a cAVM to assess surgical planes is not the same as our definition of angiogenesis, it may still be more representative of the angiogenesis that we are describing.

We accept that the overall agreement between readers was variable when other aspects of angioarchitecture were considered. The best agreement in our study was limited to elementary angioarchitectural characteristics (i.e. characteristics that are well-defined such as the presence of an aneurysm or a measurement), for example when measuring nidus diameter. However, when identifying more challenging and complicated features such as venous ectasia, agreement was weaker. This has implications for clinical management given that the SMG only had fair inter-observer agreement (κ = .292). The SMG is often used in classifying cAVM to guide treatment modality and also allows for morbidity predictions following surgical excision. Similarly, agreement regarding the occurrence of aneurysms varied from fair (κ = .385) to less than chance (κ = -0.143): this is important as haemorrhage is considered more likely to occur if they are present.[99]

Inter-observer agreement for venous drainage varied from substantial (κ = .696) to fair (κ = .273). However, in the cases where there was disagreement, this was due to either mixed drainage into superficial and deep systems (e.g. draining into the superior sagittal sinus, SSS,

and into the deep venous system via the basal vein of Rosenthal, or into the transverse sinus and via the right superficial middle cerebral vein into the cavernous sinus) or drainage into a combination of venous sinuses (e.g. drains to straight sinus and transverse sinus, or into the SSS and straight sinus).

It is clear that there are variable levels of reliability in interpreting cAVM morphology from the four published observer agreement studies, with no clear pattern accounting for this. Iancu-Gontard had higher rates of agreement compared to the other studies, which may be due to the availability of imaging modalities other than angiography.[96] There appeared to be better reliability for size, when measured alone (e.g. CC diameter), but not when as part of the SMG. The variation in observer agreement appears to apply to the full gamut of angioarchitecture from feeders to veins.

The reasons for the problem are not clear. A contributing factor may be the need for clearer definitions in angioarchitecture. Differing angiogram quality and techniques (e.g. high and low frame rate) would also need to be considered. There have been attempts at standardising the nomenclature (the JWG and Jayaraman et al),[30,100] and further efforts are required to enhance conformity of reporting, including setting standards for angiography technique.

There were a number of limitations with our study. There were mainly four problems with assessing observer agreement. For assessing intra- and inter-observer agreement, the sample size of twenty and ten was comparatively small. The overall study sample size of 100 was also small, although they were consecutive cases. There was significant variation in observer experience: observer 2 had the most (consultant), and observer 1 had the least (third-year registrar). Both were neurosurgeons. We were unable to recruit a neuroradiologist to the observer agreement study. Specialist radiologist reporting with more extensive radiological experience would likely improve agreement, but non-specialist neurosurgical reporting is more likely to apply surgical experience to reporting, e.g. when considering whether a lesion is eloquent. Observers were aware of patients' clinical presentation and demographics: they were therefore unblinded. Angiogram quality varied between cases, and was good in the more recent images, but average in the older ones. There was no consistency in terms of types of views or vessel injections. There was also a lack of uniformity with the measurement unit

as some machines had millimeter scales, while most had pixel scales. We assumed the diameters of the BA and the genu of the ICA's petrous segment to be 3.17 mm and 5 mm respectively, even though this is a generalisation, and there is a natural variation amongst patients. The addition of standardised calibration markers to the Centricity imaging program may be a solution. We were unable to view all images due to lack of accessibility: this was the case for a total of 43 patients. Of these, in 23 cases, both CTs and MRIs were unavailable, and in 20 cases, only MRIs were unavailable. The occurrence of hydrocephalus, mass effect, or perinidal gliosis could not be commented on. It was also more difficult to localise the cAVM. Lastly, the sample data may not be a true representation of the national population as it has been derived from the referrals made to a tertiary neuroscience centre.

Future work would use a larger sample size to investigate the associations with angiogenesis and to assess observer agreement. Performing the reliability study with neuroradiologists who have more experience with image interpretation may improve results (though this did not occur in the literature described). To enhance the identification of angiogenesis, the next study planned was to utilise parametric imaging. Colour-coded DSA (based on cerebral blood flow) is referred to as parametric imaging.[101] As just described, it is challenging to categorise cAVM angioarchitecture on DSA with poor overall reliability.[31] This may partly be due to the image resolution. Colour improves the effectiveness of image processing and facilitates tasks requiring visual search and recognition, particularly with increasing complexity.[102] Colour imaging could facilitate the detection of abnormal vessels associated with angiogenesis. Colour-coding facilitates diagnosis, planning of treatment, and determining treatment success.[103] It could enable measurement of the functionality of cerebral circulation e.g. calculating the blood flow, with no additional radiation dose.[104] Other applications include an enhanced detection of cAVM shunting or vessel stenosis intra-operatively, and assessing results of interventional treatment.[101,105]

In conclusion, we identified angiogenesis in 38.2% of cases in our sample. We reliably identified angiogenesis during both intra- and inter-observer agreement studies. A significant association was detected between angiogenesis and both artery: vein ratio and arterial ectasia. This was the first study to conduct a detailed investigation into angiogenesis. This is a significant contribution to enhancing our knowledge on cAVM development.

Chapter 3: Reporting of angioarchitecture on angiograms in patients with cerebral arteriovenous malformations – a systematic review

3.1 Introduction

As described in Chapter 1, the young suffer from a greater risk of death and disability from cAVMs.[89] The fact that cAVM treatment is associated with significant morbidity and mortality poses additional challenges. Treatment is currently aimed at shrinking or excising the lesion, usually after it has ruptured or caused symptoms. Management decisions require a case-by-case multidisciplinary discussion balancing risks and benefits: there is no definitive algorithm for management. This is because there is little understanding of the pathophysiology underpinning cAVMs.

Typically, digital subtraction angiography (DSA) is used to classify cAVMs. cAVM presentation is believed to rely on its angioarchitecture (the morphology of cAVM anatomy). The latter may also be used to guide treatment.

cAVMs have a complex morphology and they are comparatively rare, with each malformation being unique. This makes classifying cAVMs consistently challenging for clinicians managing them. As shown in chapter 2, although there was good intra-observer agreement on the characterisation of cAVM angioarchitecture, the inter-observer agreement was poor.[77]

A consensus document was published by the Joint Working Group (JWG) of the Technology Assessment Committee: this provides elementary and clear definitions of terms and recommends which clinical and radiological cAVM features should be described and noted.[30] Although we used the JWG definitions in Chapter 2, given our results and given the poor inter-rater reliability observed by other authors,[77,97] it was decided to systematically review the cAVM angioarchitecture literature to help in the understanding of poor reporting reliability.

Objectives

The aim of this study was to systematically review the cAVM angioarchitecture literature with a view of providing a narrative, describing:

1. the proportion of identified publications that use the JWG reporting terminology,
2. which of the JWG reporting standards were used,
3. if there were any differences between the definitions used in the identified publications and those used in the JWG document,
4. any novel angiographic features reported that are not mentioned by the JWG, and
5. which professionals were responsible for cAVM reporting and their level of experience.

3.2 Methods

The review protocol was sent for registration to PROSPERO but not accepted due to "a perceived lack of direct impact on patient outcomes". Reporting was conducted in accordance with the Preferred Reporting Items for Systematic Reviews and Meta-Analyses (PRISMA) statement. The PRISMA checklist was used to ensure clear reporting of the systematic review results.[106]

Eligibility criteria

Publications were searched from 1st January 2001 (as this was the year the JWG standards were published) and limited to human subjects. There was no restriction on age, sex or article type, except review articles. Language was restricted to English. All human studies on cAVM were included such as case-control studies, retrospective studies, cohort studies, case series and individual case reports. There have not been any randomised controlled trials published so far.

Population

The population consisted of all cAVM patients, regardless of age or gender.

Intervention

There was no intervention except that all patients must have had DSAs.

Comparison

There was nothing to compare against.

Outcomes

The primary outcomes for each research question were regarding the description of the angioarchitecture of a cAVM and are listed (Table 3.2.1). The study design was not restricted as described.

Studies were excluded if they discussed cavernous malformations, dural arteriovenous (AV) fistulae, angiomas, capillary telangiectasias, Vein of Galen Malformations or other angiographically occult vascular malformations. Unpublished data was not included.

Table 3.2.1: Review questions listed with an explanation for each question

1	**What proportion of identified publications use the Joint Writing Group (JWG) cAVM reporting standard?**
The number of publications using the JWG reporting standards was divided by the overall number of eligible review publications.	
2.	**Which of the JWG reporting standards is and is not used?**
The angiographic features studied in each publication was assessed.	
3.	**Is there any difference in the definitions used in the publications reviewed compared to the original JWG reporting standards?**
When comparing definitions in the JWG against the reviewed publication, any disparities were detailed and documented.	
4.	**Are there any other angiographic feature(s) that are reported that do not appear in the JWG document?**
The relevant additional angiographic features associated with their respective definitions were listed.	
5.	**Which professionals (and with what experience) were involved in reporting?**
The participating reporters' specialties were noted, including their years of experience.	

Information sources

A database search was performed using the electronic bibliographic databases, EMBASE and Medline. The search strategy for Medline is recorded below and this was conducted on 15/07/19. It was repeated again on 10/9/20 to update the search. One reviewing author (SD) performed the initial search. The updated search was performed by a second author (MW). There was independent assessment by an experienced librarian and another reviewing author (HP). In addition to the electronic searches, we conducted citation tracking, checked the reference lists of the included studies, and perused the list of similar articles provided by PubMed.

Search Strategy

To conduct searches of the Medline electronic bibliographic database, combinations of the following search terms were used to identify all relevant literature, and ensure no relevant literature is omitted.

Medical Subheadings: ((Arteriovenous Malformations OR Arteriovenous Malformations, Intracranial) AND (Brain OR Intracranial)) AND (angioarchitecture OR angiogram OR angiographic OR aneurysm OR venous OR ectasia OR nidus OR angiogenesis OR varix)

Text Words: ((Arteriovenous Malformations OR Arteriovenous Malformations, Intracranial) AND (Brain OR Intracranial)) AND (angioarchitecture OR angiogram OR angiographic OR aneurysm OR venous OR ectasia OR nidus)

Study selection

Studies were selected if they included any of the features mentioned in the search strategy. Titles and abstracts were reviewed to decide whether studies were eligible according to the pre-specified inclusion criteria. The figure demonstrates how articles were excluded (Figure 3.3.1). The final number of articles selected was 219.

Data collection process

Data extraction was performed by two independent reviewers. The full text version of these studies was retrieved and both inclusion and exclusion criteria reviewed again. Any disagreements regarding inclusions of papers were discussed between the two reviewers.

Pre-designed and piloted proforma were used for data extraction and to collect information according to study question.

Data items

All the individual data items collected from each paper are listed below (Table 3.2.2).

Table 3.2.2: Description of all data items collected.

Variables	Description
Author	First author of paper
Journal, year, centre, country	As described
Study type	As described
Number of cases & study duration	As described
Definitions given	Angioarchitectural definitions given
Definition difference	If the definition differed from the JWG, this was described here
Fields included & similarities to JWG	Aspects of angioarchitecture described in the study are listed, including placing them in bold if the definitions were the same as the JWG definitions
cAVM diagnostic criteria	How a cAVM is defined in the study
Method of DSA/ imaging	Imaging techniques used in the study
DSA method: injection/ views/ structures	During DSA, which vessels were injected (internal carotid or external carotid or vertebral arteries), which views (anteroposterior, lateral or oblique), which structures were visible on the angiogram
Calibration method	Which vessel diameter is used to convert units on radiology software to mm
Fields used in JWG that were not described	As described
Focus of study	Study objective
Specialists involved, level of experience, how many	Specialists collecting data, their level of experience, and the number of professional involved
Intra-rater/ inter-rater reliability reported	Whether reliability was assessed for the same observer (at different time-points) or between different observers
Statistical test used	As described

DSA = digital subtraction angiography

Risk of bias in individual studies

Risk of bias was determined by two independent reviewers. For the studies in question, bias/quality of publication was analysed by using a modified version of a score of case series analyses (Table 3.2.3).

Table 3.2.3: Quality assessment questions for every study

1.	Diagnosis: Are diagnostic criteria (as defined) for cAVM clearly identified and met in clinical studies?
2.	Is the method of cerebral angiography described, including the arterial injections, views taken, and what structures are included in a standard view?
3.	Is the method of calibration described?
4.	Are the cerebral angiograms reported on by two blinded neuroradiologist(s)?
5.	Was the data on the patients collected over a short period of time in sufficient numbers?
6.	Is intra-rater reliability reported for each publication?

Summary measures

The principal summary measures are the number of studies following the JWG terminology and the angioarchitectural fields described.

Synthesis of results

This review was done to provide a narrative to:

1. assess if cAVM angioarchitecture is described in a standard fashion,
2. determine which features are described less frequently,
3. decide if there are additional features that need to be added to the JWG reporting standard.

Risk of bias across studies

Publication bias was assessed, as well as selective reporting bias.

Role of the author in the project

My role consisted of performing the database search (including citation and reference tracking), data extraction, analysis and writing the report. My primary supervisor, Mr Patel, independently assessed the data. My research registrar colleague, Mueez Waqar, performed the updated search.

3.3 Results

Study search

The search strategy identified 4306 publications, among which 3206 were screened by title, and 306 were screened by abstract. A manual review of the citations of the included articles and similar articles yielded further citations (114), which were screened by title/abstract. In total, 219 articles were selected for full-text review. They reported the angiogram findings for 54, 148 individuals. Full data extraction for the qualitative synthesis in this study was performed on the studies identified from the initial search and from the manual review of citations. The process for identifying articles for this narrative review is summarised in Figure 3.3.1.

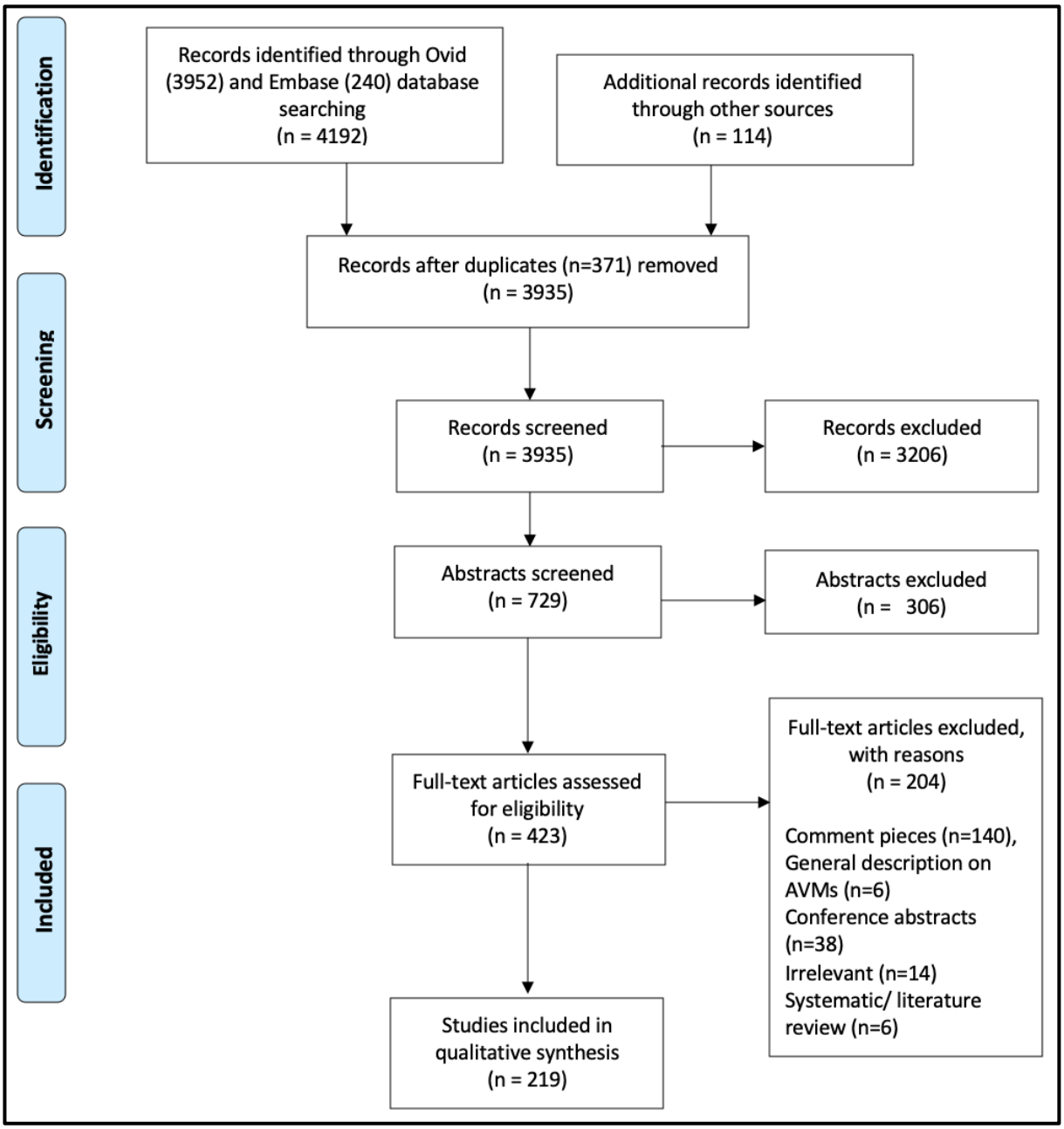

Figure 3.3.1: PRISMA flowchart demonstrating screening process for article selection

Study designs

The most common study type was retrospective (63%), followed by prospective (27.9%) (Figure 3.3.2). Far less common were case reports (2.7%), and studies that were both prospective and retrospective (2.7%).

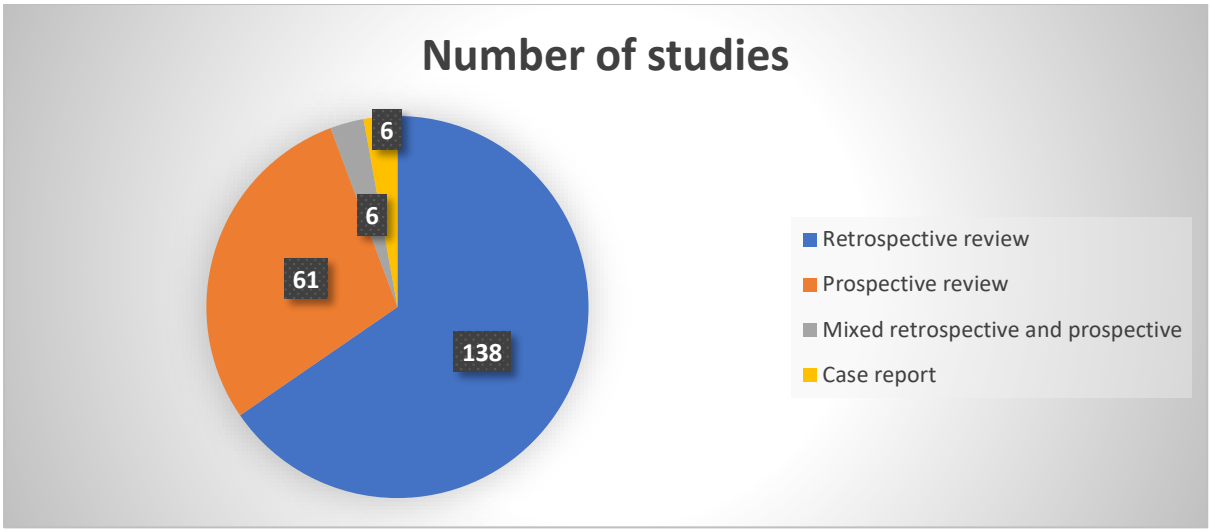

Figure 3.3.2: The different study types included in the systematic review and the numbers of each type encountered

Publication Trends

The studies spanned from 2001 to 2020 (the JWG report was published in 2001). The number of patients in each study ranged from 1 to 3923. The median was 120 (interquartile range: 30 to 278). The countries individually publishing the highest number of studies were China (16%) and the United States of America (17.4%).

Beijing Tiantan Hospital produced most of the data published, with data from this single centre contributing to 26 (74.3%) of the studies from China and 11.9% overall (Table 3.3.1). Out of these 26 studies conducted from Beijing Tiantan Hospital, the commonest author groups were Lv, Wu, Jiang, Yang, Li, Sun, Zhang, and Tong, Wu, Lin, Cao, Zhao, Wang, Zhang, Zhao (five studies for each author group). However, the same sample population was used three times for each of these two author groups (Table 3.3.2). In the USA, the majority of the studies were published from the University of California (San Francisco) which accounted for 18 (8.2%) of overall publications. The author group with the most publications here was Halim, Singh, Johnston, Higashida, Dowd, Lawton, and Young (three studies). In the same institution, Du, Dowd, Johnston, Young, and Lawton used the same study population for two studies (Table 3.3.2).

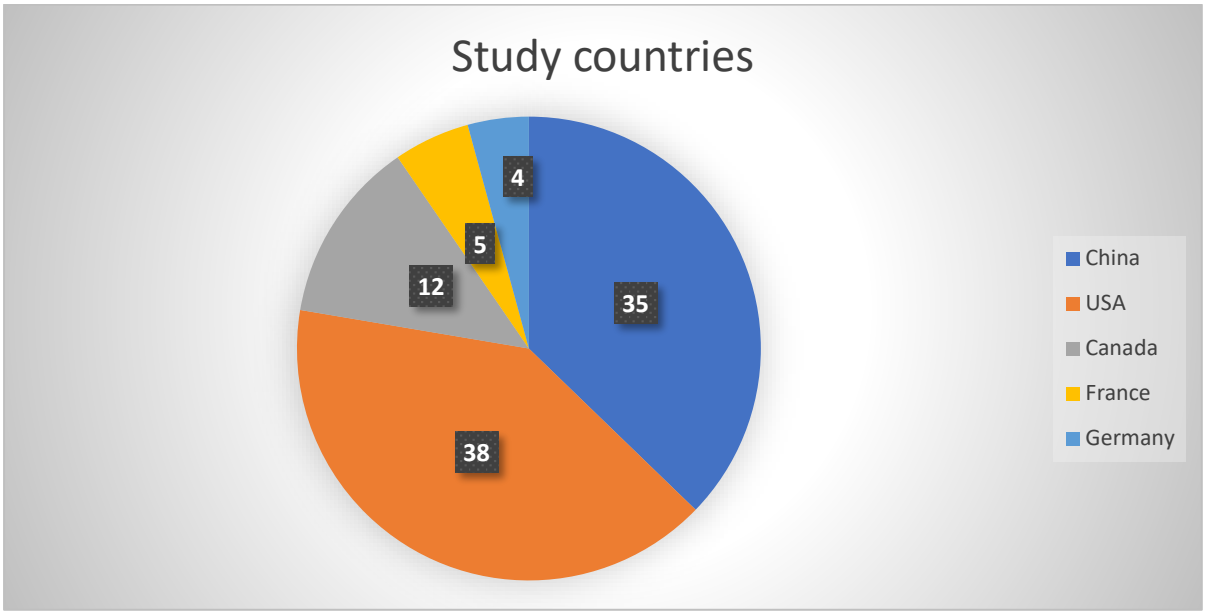

Figure 3.3.3: Commonest countries producing studies included in the systematic review and the numbers from each country encountered.
The following are percentages for each country: USA (17.4%), China (16.0%), Canada (5.5%), France (2.3%), Germany (1.8%).

Table 3.3.1: Commonest study cities and departments with numbers of studies for each

Study city & hospital	Number of studies (%)
Beijing: Beijing Tiantan Hospital	26 (11.9)
San Francisco: University of California	18 (8.2)
Charlottesville: University of Virginia	7 (3.2)
New York: Columbia University	6 (2.7)

Several studies used the same study populations, occasionally with a few more cases added due to an extension of the study duration by a few years (Table 3.3.2). Ding et al and Stapf et al used the same population for four (1.8%) publications each. Lv et al and Tong et al used their populations for three (1.4%) publications each. Out of the whole study population identified by the systematic search, it is estimated that 1422 patients (2.6%) were duplicated, 607 (1.1%) triplicated, and 1942 (3.6%) patients were quadruplicated. The data, therefore, applies to 45 881 (84.7%).

Table 3.3.2: Author groups with same or overlapping study populations, with the number of studies each, and the mean sample size for each group

Author group with overlapping study populations	Number of studies (%)	Mean sample size
Beijing Tiantan Hospital		
Lv, Wu, Jiang, Yang, Li, Sun, Zhang[99,107,108]	3 (1.4)	302
Ma, Kim, Chen, Wu, Ma, Su, Zhao[109,110]	2 (0.9)	108
Tong, Wu, Lin, Cao, Zhao, Wang, Zhang, Zhao[111–113]	3 (1.4)	225
The First Affiliated Hospital of Guangzhou Medical University		
Pan, Feng, Vinuela, He, Wu, Zhan[114,115]	2 (0.9)	152
University of California, San Francisco		
Du, Dowd, Johnston, Young, Lawton[98,116]	2 (0.9)	304
John Hopkins University, Baltimore		
Yang, Liu, Hung, Braileanu, Wang, Caplan, Colby, Coon, Huang[117,118]	2 (0.9)	123
University of Virginia, Charlottesville		
Ding, Starke, Quigg, Yen, Xu, Przybylowski, Dodson, Sheehan[119,120,121,122]	4 (1.8)	1400
University of Illinois, Urbana-Champaign		
Shakur, Valyi-Nagy, Amin-Hanjani, Ya'qoub, Aletich, Charbel, Alaraj[123,124,125]	3 (1.4)	80
Columbia University, New York		
Stapf, Mohr, Pile-Spellman, Sciacca, Hartmann, Schumacher, Mast[126–129]	4 (1.8)	542
Hopital Lariboisiere, Paris		
Choi, Mast, Hartmann, Marshall, Stapf[130,131]	2 (0.9) – same study population as Stapf et al	735

Authors by topics studied

The above research groups specialised in certain topics.

Yang et al investigated paediatric cAVMs (one study on haemorrhage and one on seizures) [117,118]. Ma et al had an interest in children with haemorrhagic presentations. [109,110,132] Abla et al studied cAVM haemorrhage. [133,134] Tong et al reported on cerebellar AVMs. [113,135,136] Lv et al presented cAVM and aneurysms in two studies. [107,137] Stein studied aneurysms associated with cAVMs. [138,139] Shakur et al analysed haemodynamics in cAVMs.[125,140–142] Pan et al described angioarchitecture in relation to haemorrhage and embolisation.[114,115] Stefani studied angiographic features of cAVMs associated with haemorrhage.[143,144] Ding et al summarised outcomes of SRS in treating cAVMs.[119,120,145]

Topics reported

Children were the focus population in 23 studies (10.5%). The natural history of untreated cAVMs in children is considered worse than in adults.[146] Children are also considered to have a higher annual risk of haemorrhage, and a higher incidence of basal ganglia and posterior fossa AVMs, most of which present with large haemorrhages. Conversely, only one study focused on the elderly.[147]

Given the clinical importance of being able to predict haemorrhage, angioarchitecture (including location) was most commonly analysed in relation to the occurrence of haemorrhage(65papers).[42,80,88,89,91,147–191,109–111,99,143,114,144,127,129,132–134,118,113,122] Forty-five papers reported the overall angioarchitectural risk factors predictive of haemorrhage or cAVM rupture.[109–111,149–152,99,80,153–161,143,114,42,89,91,162–168,144,127,129,132–134,118,113,170–173,147] Other studies specifically investigated the association of cAVM-related aneurysms with a presentation of haemorrhage (nine publications),[127,178,166,137,192,175,176,181] whilst three studied the association of venous angioarchitectural features.[152,153,161] Three papers studied whether aspects of cAVM haemodynamics affected the likelihood of cAVM rupture.[160,161,193] Two papers studied the association of race and angioarchitectural features with haemorrhage.[174,88]

Seizures, the second commonest cAVM presentation was the focus of investigation in 12 studies.[194–203,121,117] Three papers analysed predictive factors for seizures.[194,202,117] Finally, five

studies assessed the occurrence of neurological deficit, four of which also studied predictors of this presentation.[108,204–207]

Standard imaging was compared against novel imaging techniques in four studies.[208–211] Three studies assessed haemodynamics in relation to angioarchitecture.[212,189,141] Different forms of pre-operative imaging were investigated in two studies.[213,214]

Eleven papers studied various grading scores.[98,208,215–223] The SMG score was the most commonly analysed, but others included the Spetzler-Ponce, Lawton-Young, and Pollock-Flickinger. Out of these 11 studies, seven assessed and proposed different grading systems: one to predict seizures in cAVM patients,[222] and the rest to grade cAVMs based on angioarchitecture.[216–220,223] For the latter, the variables used for the scores were various combinations of haematoma volume, intraventricular haemorrhage, number of draining veins, deep venous drainage, cAVM size, eloquence, nidus diffuseness, nidus location, arterial feeders (type and numbers), lesion-to-eloquence distance, as well as the non-radiological features of Glasgow Coma Scale, age, emergency surgery, and preoperative neurological status.

Four papers assessed the observer reliability of different cAVM grading scales.[98,208,215,221] Frisoli et al demonstrated both excellent intra and interobserver agreement in using the compactness score.[221] For the SMG, Ognard et al had substantial inter-observer agreement between 4D DSA and 2D DSA.[208] Griessenauer et al tested the Spetzler-Ponce grade (interrater agreement varied from fair to strong) and the Pollock-Flickinger scale (agreement was excellent).[215] Du et al showed good agreement for SMG.[98] Observer reliability in describing cAVM angioarchitecture was assessed in four studies.[96,77,97,98] Agreement ranged from poor to good for both inter and intra-rater comparisons.

Angioarchitectural characteristics were also reported in association with treatments. The most studied treatment was embolisation,[205,115,216,181,184,2,100,224–248,96,218,188] followed by surgery,[205,249–254,255–261,229,230,232,126,233,136,213,236,204,147] and then stereotactic radiosurgery (SRS) [242,262–268,250,212,229,232,233,236,148,255,182,239,198] (35, 25 and 19 publications respectively).

Patient outcomes, efficacy and/or morbidity after embolisation were assessed (14 studies). The effects of angioarchitecture on the success and efficacy of embolisation was investigated in three studies.[235,269,115] Complications in relation to angioarchitecture post-embolisation was investigated in seven papers,[234,225,207,115,226,227,264] with another two specifically studying risk factors for neurological deficits and haemorrhage.[184,188]

Ten publications reported on outcomes, results and experiences of treating cAVMs with surgical excision and in relation to angioarchitecture,[205,236,260,258,261,229,136,257,252,204] and two studies assessed the risk factors for recurrence and long-term prognosis after surgical resection.[249,259] Six papers studied clinical outcomes after SRS,[263,242,265,212,268,267] with two publications reporting on how angioarchitectural features affected obliteration,[268,262] and two reported on how angioarchitecture changed post-SRS.[242,270] Five papers reported the results of multimodal treatment (varying combinations of embolisation, surgical resection and/or SRS) in relation to angioarchitecture.[147,173,271,233,232]

Quality of studies

The raw data from the 219 articles is presented in Appendix 2. The quality of studies included in the systematic review was assessed using certain criteria: several of these criteria were not fulfilled (Tables 3.3.3 and 3.3.4).

Forty-eight studies (out of a total of 219) used the definitions recommended by the JWG (Table 3.3.4). Thirty-three publications reported using the JWG standards. Out of these, the same population was used for four publications,[128,127,126,87] a separate population was used for two publications,[143,144] and a further population was used in another two studies.[109,110] cAVM diagnostic criteria were described in 39 studies (Table 3.3.3). The type of arterial injections used (e.g. vertebral artery) was specified in 15 papers (Table 3.3.3). Twenty-three studies described the specific views used in the DSA. The method of calibration was only detailed in three studies. The number of patients in each study was recorded in most cases (216 papers). Observer reliability was assessed in 21 publications (none of which used the same sample populations). The duration of data collection was reported in 183 studies. Statistics were conducted in 181 studies.

Table 3.3.3: Studies included in the systematic review were assessed for quality or bias by comparing them to the criteria listed in this table.

Quality assessment criteria	Number of studies N (%)
cAVM diagnostic criteria	39 (17.8)
DSA method: arterial injections	15 (6.8)
DSA method: views	23 (10.5)
Calibration method	3 (1.4)
Number of patients in series recorded	216 (98.6)
Duration of data collection recorded	183 (83.6)
Observer reliability reported (unspecified)	21 (9.6)
Inter-rater reliability assessed	15 (6.8)
Statistics performed	181 (82.6)
Statistical test to assess observer variability	14 (6.4)

This quality assessment was based on recommendations by a modified version of a score of case series analyses.

Risk of bias within studies

The commonest bias for all studies was small population size. Apart from the studies that assessed observer reliability (21), none of them ensured angiograms were reported separately by two reviewers (regardless of profession).

The more detailed table lists studies that did not assess cAVM treatment (Table 3.3.4). Most studies did not fulfil multiple criteria for quality assessment, and none satisfied all the criteria. Al Shahi, Imbesi, and Kandai et al were the highest quality papers.

Table 3.3.4: Publications listed by authors in alphabetic order, associated with criteria assessing study quality.

Study author	a	b	c	d	e	f	g
Abla 2014							
Abecassis							
Al-Shahi							
Al-Tamimi							
Alen							
Alexander							
Anderson							
Benson							
Bharatha							
Blanc							
Braileanu							
Brunozzi 2017							
Brunozzi 2019							
Burkhardt							
Chang							
Chen							
Choi 2006							
Choi 2009							
Chowdhury							
Cuong							
D'Aliberti							
De Blasi							
de Castro-Afonso							

Study author	a	b	c	d	e	f	g
Dinc 2019							
Dinc 2018							
Ding 2017							
Ding 2015							
Dos Santos							
Du 2005							
Du 2016							
Ellis							
Fierstra							
Fleetwood							
Fok							
Frisoli							
Fukuda 2016							
Fukuda 2017							
Fullerton							
Galletti							
Garcin							
Gauvrit							
Geibprasert							
Griessenauer							

Study Author	a	b	c	d	e	f	g
Guo							
Halim 2004							
Halim 2002							
Hernesniemi							
Hetts							
Hofmeister							
Huang							
Hung 2019							
Iancu-Gontard							
Illies							
Imbesi							
Iryo							
Jayaraman 2012							
Jiang							
Jiao							
Jin							
Kakizawa							
Kandai							
Kellner							
Khaw							
Kim 2004							
Kim 2007							
Kim 2014							
Kouznetsov							

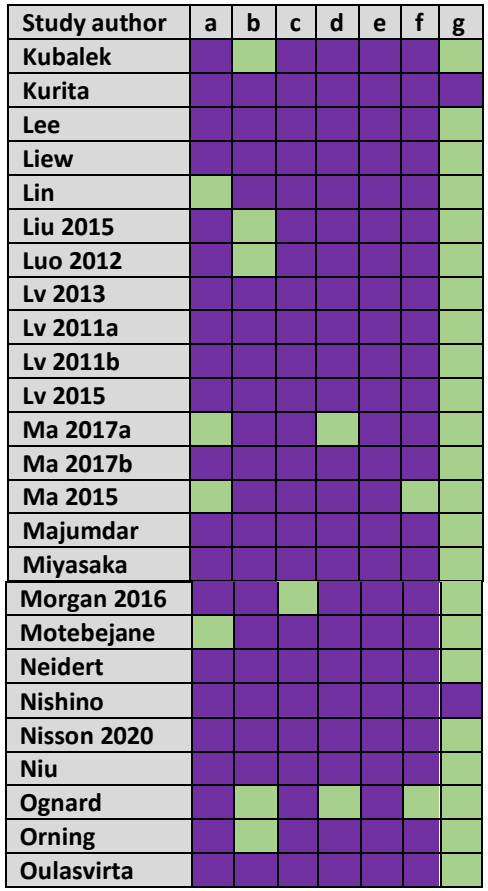

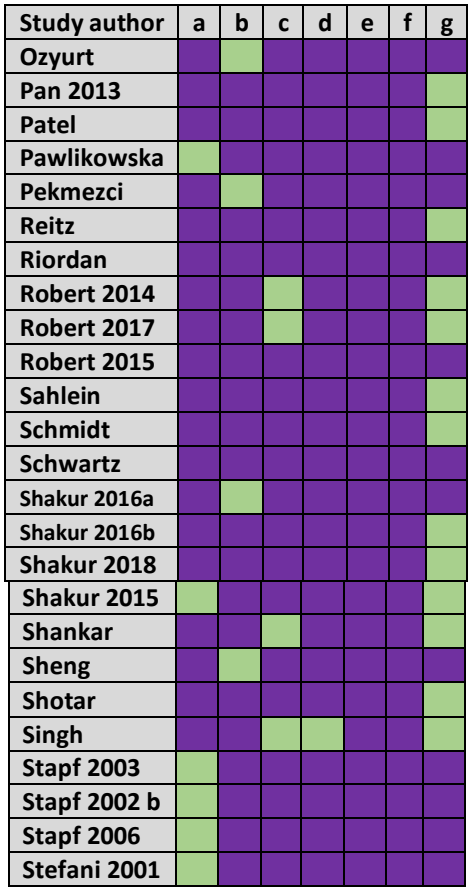

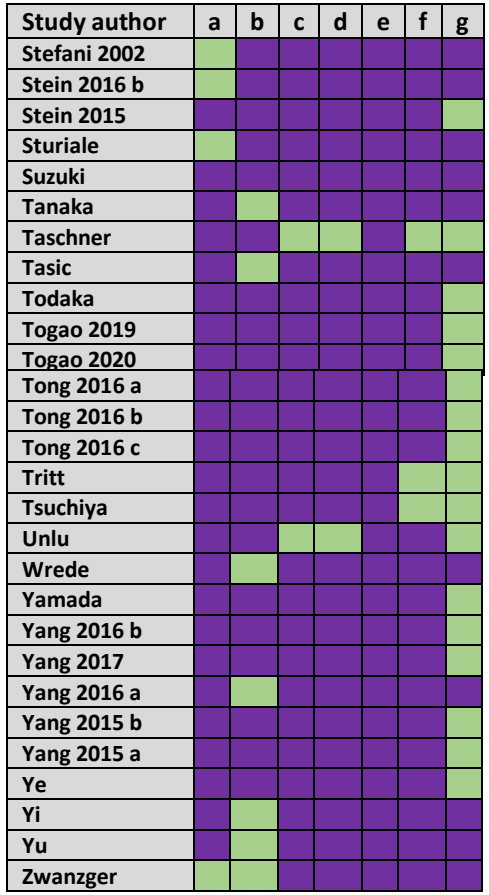

The list excludes studies related to treatment modalities. As demonstrated, no single study satisfies all criteria, and in most cases, several criteria are unfulfilled. Green boxes indicate criteria fulfilled; purple boxes indicate criteria absent. a = JWG standard used; b = cAVM diagnostic criteria; c = DSA method: arterial injections; d = DSA method: views; e = Calibration method; f = Inter-rater reliability assessed; g = Statistics performed

Number of studies reporting individual angioarchitectural features

Most studies described nidus size, location, venous drainage, feeding arteries, cAVM haemorrhage, and aneurysms (Figure 3.3.4). Venous reflux was reported the least, followed by cAVM border, and venous ectasia (or pouch/ varix).

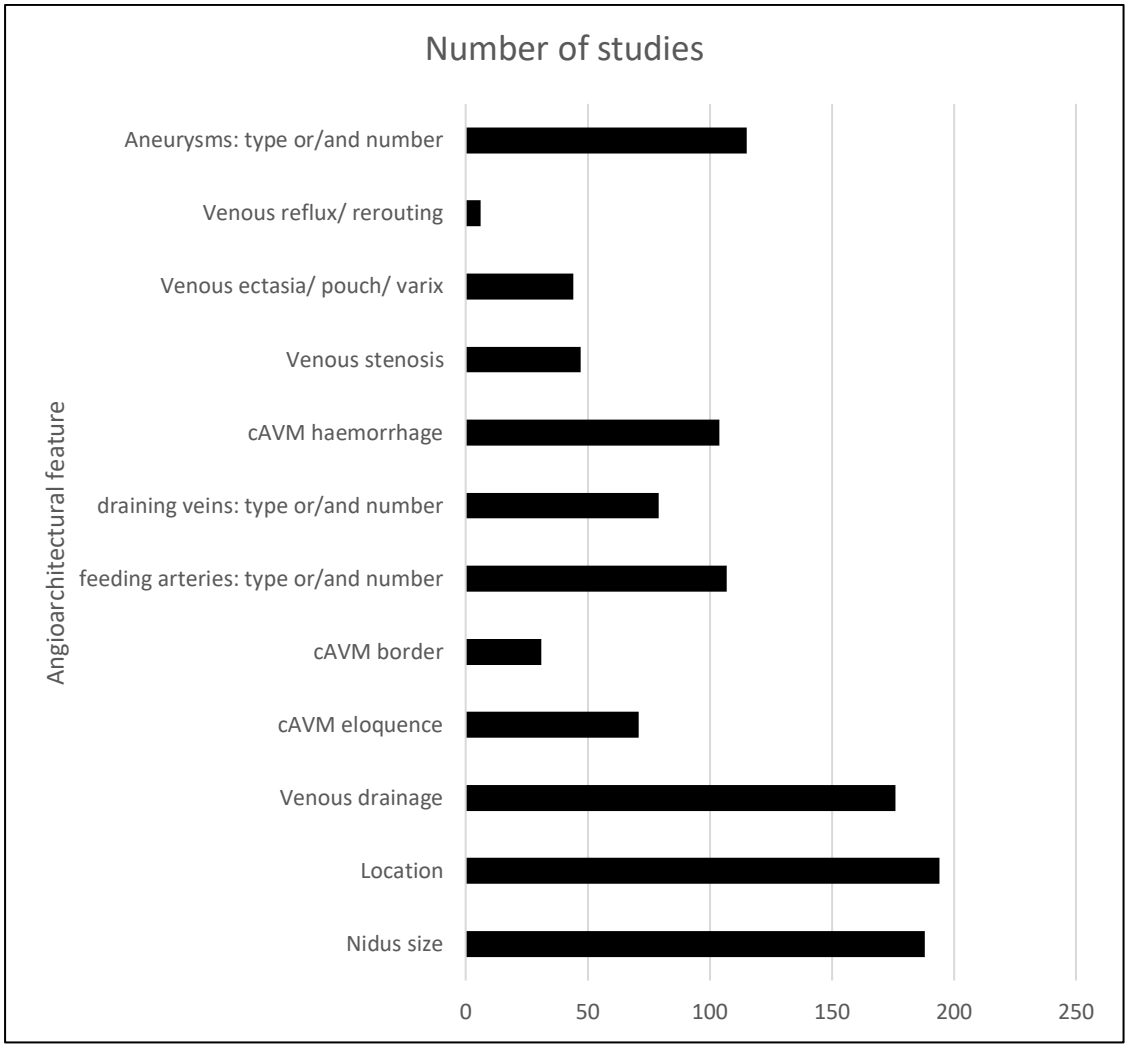

Figure 3.3.4: Key angiographic features listed in the Joint Writing Group's recommendations, and the frequency with which these were reported on and defined in the studies identified

The common angioarchitectural features are listed with the associated number of studies (Table 3.3.5). These are studies that followed the definitions stipulated by the JWG. Forty-eight studies (21.9%) used the same definitions as the JWG for at least one angioarchitectural feature.[134,152,272–282,193,130,131,91,155,158,185,178,179,159,80,263,162,163,166,188,184,99,109,186,266,42,149,13,126–129,138,111,113,117,169]

No studies described all the angiographic features recommended by the JWG. Ma, Stapf, and Stefani et al always used the JWG definitions in all their publications. Angioarchitecture was not described beyond size, location or border in five studies.[221,283,284,183,258]

Table 3.3.5: Angiographic features that were defined as per the JWG definition and the number of studies that used the definition for each feature

Angiographic feature	**Number of studies (%)**
AVM size	10 (4.4)
Aneurysm	6 (2.7)
Feeding artery	7 (3.1)
Venous stenosis	3 (1.3)
Venous ectasia	7 (3.1)
Venous drainage	16 (7.1)

A large number of studies used a variety of the recommended angiographic features, though not necessarily defining these features in the same way (Table 3.3.6). The most commonly described features were AVM size (175 papers), venous drainage (173 papers), and AVM location (153 papers). The least described feature was AVM border (29 papers). Four features were not reported at all: number of vessels to be embolised, Moyamoya-type changes, pial-to-pial collateralisation, and intravascular pressure measurements.

Table 3.3.6: Angiographic features recommended for reporting cAVMs by the JWG associated with the number of studies that record each feature.

Angiographic feature described by the JWG	**Number of studies (%)**
Clinical presentation	108 (48)
AVM size	175 (78)
AVM location	153 (68)
Eloquence	72 (32)
AVM border	29 (12.9)
AVM haemorrhage	109 (48.4)
Venous drainage	173 (76.9)
Number of draining veins	71 (31.6)
Venous stenosis	47 (20.9)
Venous ectasia	42 (18.7)
Feeding artery	88 (39.1)
Aneurysm	121 (53.8)
Number of vessels to be embolised	0
Moyamoya-type changes	0
Pial-to-pial collateralisation	0
Intravascular pressure measurements	0

They may have different definitions for these features compared to that stipulated by the JWG.

Angiographic features with different definitions

Several angiographic features were given definitions that differed from those provided by the JWG (Table 3.3.7). Almost all the features described in the JWG guideline were given different definitions and these included venous stenosis, occlusion and ectasia, deep venous drainage, nidus border and size, aneurysm (including flow-related aneurysm), cAVM location, eloquence, type of feeders, arterial feeders, and haemorrhagic presentation.

cAVM location was not described by the JWG. This feature had the largest range of definitions in other publications (Table 3.3.7). Some specified what constitutes deep, cortical, and/or infratentorial [89,99,108,159,165,285] or dichotomised location into supratentorial and infratentorial.[107,112,162,257] There were further categorisations into posterior fossa and periventricular by Ma et al. [281]

Venous ectasia was the feature with the second-most variations of definition. Whereas the JWG defines it as double the calibre change in any draining venous channel, some are more specific defining venous ectasia as at least 50% increase in original vessel diameter, [286] or dilatation twice as large as the vein diameter, [115] or 1.5 times larger than the contralateral vessel. [287] Two papers are broader in their definitions, describing venous ectasia as a markedly ectatic vein [222] or an abnormal dilatation.[143,144]

Aneurysms were defined as a saccular luminal dilatation of parent feeding vessels by the JWG. Most papers have essentially stated the aneurysm should be double the width of the artery (Table 3.3.7), with only one definition stating the diameter is at least the same as that of the parent vessel. [91]

Table 3.3.7: Angiographic features with definitions that are different from those provided by JWG. The different definitions are listed accompanied by the publications in which they were described.

Angiographic feature	JWG definition	Study definition
Venous stenosis	In two angiographic views, narrowing of any draining vein outflow pathway. Proximal venous outflow tract used as denominator.	reduction of ≥ 50% in vein diameter (Shankar, Yi, Lv 2011, Lv 2013, Luo, Lin, Stefani 2002 a and b, Jiang, Brunozzi 2017, Ellis, Wu) 50% focal reduction of venous diameter (Pan 2013, Pan 2014) >50% stenosis within a draining vein (Shakur b 2018) Focal luminal narrowing less than 50% of adjacent normal venous diameter in main drainage vein (Hu)
Venous occlusion	Filling defect in dural venous sinus excluding arachnoid granulations.	Occurs if a blind-ending vein is visualised exiting the lesion (Alexander).
Venous ectasia/ dilation	In any draining venous channel, double the calibre change	Markedly ectatic vein (Shankar) Abnormal dilatation (Stefani 2002 a and b) At least 50% increase in original vessel diameter observed in any portion of the vessel (Brunozzi 2017) Focal dilatations at least twice as large as the vein diameter (Pan 2014) Dilated drainage was at least 1.5 times larger than the contralateral (Panni)
Deep venous drainage	If any or all of the drainage is through deep veins, e.g. the internal cerebral veins, basal veins, or precentral cerebral veins	Any drainage through the internal cerebral veins, basal veins, or precentral cerebral veins (Lin). Defined as venous drainage through periventricular, galenic, or cerebellar pathways (Yamada).
Nidus border	Peninsula of normal brain parenchyma within the cAVM nidus protruding into what is surgically or radiosurgically treatable nidus, versus a well-demarcated border	Compact or diffuse (Taeshineetanakul, Sahlein) A compact border occurs if there is little neural tissue within the nidus leading to defined borders between the brain and AVM. With a diffuse border, there is a ragged margin and loose nidus, as if the compact tangle of vessels was unravelled (Du 2007). Compact (angiographically well demarcated) vs diffuse (noncompact lesion with an unclear margin) (Daou)
Nidus size	Measured on MRI in sagittal, coronal and axial views, and, on angiogram	On angiogram, in lateral and anteroposterior views, maximum linear diameter in any plane (Kandai)

	in lateral and anteroposterior injections. The cAVM's largest diameter in each axis is chosen: length, width, and height.	Imbesi: technique devised as part of study objective Maximum nidus diameter on initial CT or MR images (Lee 2002) The diameter of the AVM's greatest dimension in centimeters (Liew)
Aneurysm	Saccular luminal dilatation of parent feeding vessel	Saccular dilation of lumen more than double the width of artery that carried the dilation (Lv 2013, Khaw, Ma 2017, Ma 2015, Stapf 2006, Stapf 2003, Choi 2006) Saccular arterial dilatation with a diameter at least equal to parent artery (da Costa 2009) Lesion with a diameter at least twice that of the parent vessel (Lai). Dilation of lumen more than double the width of parent arterial vessel (Schmidt)
Flow-related aneurysm	Aneurysm lying on a pathway carrying non-nutritive blood feeding the AVM shunt	Aneurysm is located upstream of the ipsilateral internal carotid artery (Lin) Aneurysm located beyond the circle of Willis (Hu)
AVM location	No definition provided. Described as topographic locations.	Classified into these areas: eloquence, cortical, deep and infratentorial. Deep refers to involvement of the ventricular nuclei, thalami, ventricles, and diencephalon. Cortical refers to the cerebral surface. Infratentorial refers to the brainstem and cerebellum. (Lv 2011, Lv 2013, Luo) Deep as above. Superficial if on the surface of the cerebrum and cerebellum (Lv 2015). Categorised into frontal, temporal, parietal, occipital, corpus callosum, basal ganglia, insular, brainstem and cerebellum. Also divided into deep (basal ganglia, thalamus, cerebellum, and corpus callosum) and superficial (all the rest of locations) (Stefani 2002b, Ma 2017). Involvement of the AVM in a specific brain region (Yang 2017) Classified into superficial (frontal, temporal, parietal, occipital), deep (basal ganglia, thalamus, paracallosal, and intraventricular), and infratentorial (brain stem and cerebellum) (Huang). Classified as supratentorial (frontal, temporal, parietal, occipital, including combinations of these,

		basal ganglia, thalamus, corpus callosum, ventricles, and multiple lobes) and infratentorial (brainstem, cerebellum, cerebellopontine angle). (Tong 2016a) Classified as superficial (frontal, temporal, parietal, occipital) or deep (insular, basal ganglia, thalamus, corpus callosum, brainstem, or cerebellum) (Yamada). Divided into supratentorial (any lobar +/- deep cerebral) and infratentorial (brainstem, peduncles, vermis, cerebellar hemisphere, deep cerebellar nuclei, any combination) (Khaw). Classified as either supratentorial or infratentorial, and more specifically cerebellar or pontomesencephalic (Pohjola). Categorised as lobar (any cortical or subcortical frontal, temporal, parietal, occipital), deep (basal ganglia, thalamus, corpus callosum, internal capsule) and infratentorial (brainstem or cerebellum) (Garcin, Stapf 2003, Stapf 2006, Stapf 2002) Cortical AVM location is when the nidus centre is in the frontal, temporal, parietal, or occipital lobes. (Ding c 2015) Superficial if in the cortex and subcortical white matter. Deep if in the corpus callosum, thalamus, basal ganglia, brainstem, cerebellar peduncles, and deep cerebellar nuclei (Jin). Divided into deep (basal ganglia, thalamus, cerebellum, and corpus callosum) and superficial (all the rest of locations). Posterior fossa location defined as brainstem, cerebellum or both. Periventricular location if nidus contacted the ependymal lining of ventricle (Ma 2015).
Eloquence	Reported as per Spetzler-Martin score and no definition provided	Present if regions involved are the deep cerebellar nuclei, cerebellar peduncles or brainstem (da Costa 2008, Tong 2016c, Tong 2016d, Lai). Present if next to the sensorimotor cortex, language areas, visual cortex, hypothalamus, thalamus, internal capsule brainstem, cerebellar peduncles, or deep cerebellar nuclei (Soltanolkotabi, Hofmeister, Ding c 2015). Defined as any cerebellar AVM located in deep nuclei or cerebellar peduncles (Nisson 2020)
Type of feeders	Perforators are vessels which are normally end arteries. Branches	Types of feeders classified into two categories: cortical branches and perforators (Lv 2013, Luo)

	normally go on to divide further.	
Arterial feeders	An arterial structure that angiographically demonstrates a flow contribution to the AV shunt.	Branches deriving from the anterior, middle or posterior cerebral arteries or cerebellar arteries (Taschner) Any arterial contribution to the nidus (Yang 2015b)

AV = arteriovenous

Additional angioarchitectural features

Numerous studies described further angioarchitectural features which were not mentioned in the JWG report (Table 3.3.8). These features included perinidal angiogenesis, AVM nidus, different locations, and various venous, arterial and aneurysmal features. Both the most widely reported and less common ones are described here, along with a narrative.

Nidus

The nidus is the central component of the cAVM, important when considering its size and location. AVM nidus was defined by three authors.[128,129,162,288] Stapf and Khaw described this in terms of the vascular mass included when measuring cAVM size. Mohr, however, was more specific, defining it as the junction between the feeders and draining veins (in the absence of capillaries).

Perinidal angiogenesis was described by Shankar, Valavanis, Taeshineetanakul and Hu. [267,289–291] Valavanis' defines it as a vascular network between the nidus and ends of the feeding arteries, but Shankar described it as an indirect supply to the peripheral cAVM from secondary feeding arteries. In contrast, Taeshineetanakul and Hu believe it is a new network of vessels (a merge between arteries and capillaries) in the white matter surrounding a cAVM. Perinidal angiogenesis is believed to be induced by hypoxia, which triggers the process of new vessel formation. [29]

An angiopathic AVM was described as a large brain AVM demonstrating distinctive angiogenetic features to separate it from a "classical" brain AVM.[275] Deep AVM location was defined in three ways by different authors.[91,189,267] Other locations defined were borderzone, posterior fossa, and periventricular. [129,132]

Artery

Arterial dilatation, arterial ectasia, and feeding artery enlargement are different variations of an enlarged artery. Arterial ectasia was simply characterised as dilated feeding vessels.[162] Feeding artery enlargement and arterial enlargement were both described as an arterial feeder 150% wider than the contralateral corresponding vessel, [267,287] whereas arterial dilatation was defined as a 50% increase.[201]

For a dominant arterial afferent, dominance was defined as a composite of vessel diameter and contribution of nidal flow.[255] Du used the term deep perforator to refer to lateral and medial lenticulostriates, thalamoperforators and brainstem perforators. [116]

Vein

Venous varix, variceal enlargement, venous aneurysm, and venous pouch are all slightly different variations of a dilated vein. Venous varix had three different definitions by different authors. [108,114,268,285] The first two authors simply defined a venous varix as a markedly ectatic vein. Daou similarly described it as a focal aneurysmal dilation. Pan, however, more specifically described it as a focal dilation at least twice the vein diameter. Variceal enlargement and venous aneurysm was described by one author alone. [176] Venous pouch was defined by three authors. [176,267,292] Chen describes a venous pouch as the focal aneurysmal dilation of a proximal draining vein. D'Aliberti defines it as a bleb on nidus venules, unrelated to a draining vein. Hu, more specifically, categorised a venous pouch as such if the diameter of any draining vein was greater than double.

Venous recruitment, venous obstacle and venous kinking were all defined by Yi.[150] Venous recruitment was defined as anastomoses between long circumferential arteries, which supply adjacent regions. For venous obstacle, various structures were listed, including the tentorial edge, and foramen of Monro. Venous kinking refers to a severe change in a draining vein direction. Similarly, venous rerouting (venous reflux into veins separate from cAVM drainage), and pseudophlebitic pattern (corkscrew-like dilated veins draining normal brain parenchyma in the late venous phase) were explained by one author.[267] Venous congestion was characterised by Fierstra as cortical vein dilation, in response to restriction of venous outflow.[293] Long draining vein was defined as greater than 3cm by a couple of authors,[203,294]

whereas main draining vein was specified as a vein with the shortest time to drain to major sinuses.[189,267] Variceal enlargement was defined as venous wall blebs resulting from progressive wall wearing.[176]

Other features

Flow pattern was estimated by Panni by determining the number of DSA frames between the first depiction of the nidus and the first visualisation of a vein.[287] On the other hand, flow steal was any contrast opacification of the AVM after contrast injection in other arterial branches other than main arterial feeders.[295] A fistulous cAVM component referred to direct shunting between the feeding artery and draining vein, in the absence of an intervening nidus network, with a shorter transit time than other AVM parts.[201]

Aneurysms were classified in similar ways. They were divided into three categories with slight variations in nomenclature: intranidal (found in AVM nidus),[238,268] flow-related or prenidal or feeding arterial or perinidal (lying on supplying arteries),[165,108,137,238,268] and unrelated (remote).[108,137] Only D'Aliberti defined a venous aneurysm as one located in or very close to the nidus, originating at the start of the main AVM drainage.[176]

Table 3.3.8: The most commonly described additional angiographic features (with their associated definitions) that are not listed in the Joint Writing Group standards

Angiographic feature	Definition	Number of studies
AVM nidus	the vascular mass included in the AVM size measurement (Stapf 2003, Stapf 2006, Khaw) the junction between the feeding arteries and draining veins, without a capillary bed (Mohr)	4
Perinidal angiogenesis	Vascular network within brain parenchyma between the nidus and feeding artery terminal segment, without visible AV shunts (Valavanis) Indirect supply to the AVM periphery from arterial branches other than the main arterial feeders (Shankar) The formation of a new network of arteriocapillaries in the white matter around an AVM in reaction to hypoxia. This is caused by the steal effect from a high flow nidus in the perinidal brain. (Taeshineetanakul, Hu)	4
Deep location	Includes basal ganglia, internal capsule, thalamus, and corpus callosum (Lin) The larger portion of the nidus is localised in deep white matter tracts, basal ganglia and thalamus, peri-ventricular regions, or posterior fossa. (da Costa 2009) Includes the cerebellum, thalamus, basal ganglia, internal capsule, corpus callosum, and brainstem (Hu).	3
Venous varix	Markedly ectatic vein (Lv 2013, Luo) Focal dilatations at least twice as large as the vein diameter (Pan 2013) Focal aneurysmal dilation in the draining venous system (Daou)	4
Venous pouch	Proximal draining vein's focal aneurysmal dilation (Chen 2017) Bleb that originates on the nidus venules with no defined relationship with a draining vein (D'Aliberti) Change of greater than 200% in the focal venous diameter of any drainage vein (Hu)	3

AV = arteriovenous

Professions conducting studies

The most common profession conducting these studies were neuroradiologists/ neuro-interventionalists (101 studies) and neurosurgeons (60 studies) (Table 3.3.9). A neuropathologist was involved in one study.

Table 3.3.9: Professionals involved in study and frequency of the studies found

Professional	**Number of studies (%)**
Neurosurgeon	67 (30.6)
Neuroradiologist	59 (26.9)
Neuro-interventionalist/Interventional neuroradiologist	42 (19.2)
Neurologist	21 (9.3)
Neuropathologist	1 (0.4)
Not mentioned	35 (15.6)

3.4 Discussion

This review shows that few studies followed the standards of the JWG (only 33 papers) since they were published 20 years ago.[30] This review also shows that most authors consider cAVM angioarchitecture as size, location and venous drainage as suggested by the observation that most studies reported venous drainage (76.9%), cAVM size (78%), and cAVM location (68%).

Given that over 200 publications were reviewed as providing data on angioarchitecture, it appears that the morphological appearance of a cAVM on angiography is considered important. This is supported by the observations that most of the studies reviewed have tried to relate angioarchitecture to clinical presentation.

This systematic review is the first of its kind and so it is difficult to relate our observations to the literature, but this narrative review can provide some insight into what has been observed.

Most studies described nidus size, location, venous drainage, feeding arteries, cAVM haemorrhage, and aneurysms. cAVM nidus location was the most commonly reported feature, and venous reflux was reported the least.

The reason for this is not clear but is likely to be related to features that are easier to observe and describe. Given the wide range of angioarchitectural features described by the JWG, and particularly given the poor inter-rater reliability of these measures, this is understandable. In addition, full descriptive angioarchitectural classification is time-consuming and requires experience and knowledge (given the rare nature of the disease) that takes time to accumulate. This may not always be available for scientific purposes. Some of this may be due to the fact that the mainstay of treatment was previously surgical excision and the surgical grading scale (SMG) has historically been the most recognisable.

Diversity in reporting different components of the morphology of a cAVM may also be related to the initial purpose of the study and hence may differ between studies that considered

efficacy of treatment compared to those that considered associations between angioarchitectural features and clinical presentation.

Difficulties and differences also probably arise from the variation in interpretation, lack of appreciation of the availability of the JWG definitions and also lack of standard definitions used for certain angioarchitectural features. It was observed that the widest variation of definitions was applied to venous ectasia and this may explain why venous features were least reported. There should be better dissemination of the JWG definitions to compensate for their reduced availability.

Some time has passed since the publication of the JWG definitions and, not unsurprisingly, several papers have reported on additional aspects of angioarchitecture which the JWG did not mention. A justification of why these features should also be recommended in the criteria proposed by the JWG is included for the more significant ones. These additional features are also crucial in understanding cAVMs to varying extents. These features are perinidal angiogenesis, deep location, venous and arterial dilatation. Angiogenesis is vital to the formation and development of a cAVM.[2] It is useful to report as it may also indicate a recently formed cAVM. Locations are crucial to define to facilitate discussions based on a shared understanding of where each term describing a particular location refers to. A deep cAVM may be more problematic to treat and is associated with haemorrhage.[89,296,114] Venous dilatation is helpful to describe as it indicates if there is high or low-pressure flow in the cAVM, with a larger vein reducing the pressure in a cAVM.[108,114,268,285,176, 165,197] This could possibly have major consequences, including making it less likely for the cAVM to rupture. Arterial dilatation[162,267,287,201] is salient information to include in a report: a dilated artery implies high-pressure flow in a cAVM, particularly if combined with a single vein of regular dimensions. This is related to our finding in Chapter 2 that arterial ectasia is significantly associated with angiogenesis, which may be due to this high cAVM pressure exerting mass effect on the surrounding parenchyma and inducing hypoxia.

The argument of including the full angioarchitectural representation is of greater relevance particularly when considering association studies. The ability to explore inter-relationships

has been greatly advanced with the advent of machine learning so that the appropriate variable can be considered appropriately for an association or predictive study.

It is also clear from the literature that the technical quality of publications on the whole is low. Most studies were retrospective and from small single centre series, reducing the statistical power of the study. Data reported from larger series lacked the full consideration of angioarchitecture and often the same dataset was used for association studies which compromises the validity of their observations.

In addition to features that may need to be added to the JWG criteria, four JWG features were not mentioned by any study: the number of vessels to be embolised, Moyamoya-type changes, pial-to-pial collateralisation, and intravascular pressure measurements and consideration should be given to removing these from the JWG guidelines. The fact that these features were not mentioned at all indicates the lack of practical benefit of knowing about these features.

Only 21 studies looked at reliability of reporting, and although there was good intra-rater reliability (in the five studies that assessed both intra and inter-rater reliability), inter-rater reliability was generally poor. This lack of consistency of reporting has not been tested by recent studies using a contemporary dataset acquired on current state-of-the-art angiographic machines, with images viewable on high quality digital screens using software permitting an enhanced three-dimensional appreciation. There are now studies which have interrogated the benefits of parametric imaging and these technologies may help overcome some of the limitations of the past.

There are other challenges that need to be overcome such as the reporting bias towards retrospective studies, which formed the majority of the review results. There is an inability to check on certain data (if there is need for clarification or any missing data). Retrospective studies are less representative of the natural history of the studied disease. A very small proportion of studies (2.7%) were case reports. These are the lowest quality of evidence mainly due to the high likelihood of bias when reporting these single cases.

Another common limitation was a tertiary centre referral bias. AVM cases referred to tertiary neurosurgery units may be more severe with higher haemorrhage and recurrent haemorrhage rates. Follow-up data collection is more difficult as much of this occurs outside the tertiary unit and needs to be obtained by correspondence. Additionally, obliteration confirmation by DSA is more challenging as patients may not be able to return to the institution, they may refuse to have another angiogram, there may be a reduced interventional capacity, or they may have the angiogram elsewhere.

A large proportion of studies was published by research groups in Beijing and San Francisco. This meant the results may not be generalisable to populations in other countries or, even, in other departments or cities. The same sample populations were used in multiple publications. This was due to different aspects of data analysis being published separately. However, this piecemeal publication may result in some redundant information in a subsequent paper. Including multiple papers using the same study participants in a systematic review or meta-analysis can reduced the validity of the results and undermine the derived conclusions. It is also misleading as, at first glance, the separate publications could be taken to represent independent samples of data collected.

Although an extensive number of search results were identified, this could have been expanded by not limiting the language to English, and by including the grey literature.

There remains a challenge in creating uniformity in reporting cAVMs and a common language. Understanding angioarchitecture in detail may pave the way to explaining patients' clinical presentation, anticipating future disease manifestations and prognosis,[297] and deciding on the most effective and least risky treatment plan.

Having a unified method of describing cAVMs would facilitate discussions about patient management. Describing cAVMs using a common language would simplify multidisciplinary team discussions. This would help in deciding on the most appropriate management for the patient concerned. Another factor to consider is pre-procedure planning, across all modalities i.e. surgical excision, embolisation, and SRS. With standardised reporting and terminology,

planning may be more streamlined and treatment protocols more consistent. Clear definitions would also advance our knowledge of cAVM natural history.

This review would support the need to establish another working group to incorporate the additional angiographic features aforementioned and to include more specific definitions for some of the features that were left open to interpretation. These recommendations should then be widely publicised and incorporated into national and local guidelines: including professionals from every country would facilitate the distribution of these guidelines. A further incentive would be to audit the use of the recommended terminology in cAVM reporting on an annual basis and offer a reward to the most compliant institutions.

There is a need to improve current management of cAVMs. Establishing a shared language for describing cAVMs would build a strong foundation on which to continue prospective research.

Chapter 4: Developing a zebrafish model of a human cerebral arteriovenous malformation

4.1 Introduction

Up to the present moment, a readily accessible, clinically applicable and valid in vivo disease model, which imitates every feature of a human cAVM does not exist. The lack of availability of suitable pre-clinical animal models on which to test various treatments has restricted the evolution of therapies.

Early versus later life

Cerebral angiogenesis initiates at the embryonic stage based on experimental data: the brain develops quickly during this time.[298,299] Although broadly-speaking, cAVMs are accepted to be congenital, there is proof in favour of growth in later life (e.g. following an ischaemic stroke).[72] Ordinarily, cAVMs are localised abnormalities, limited to specific organs.[300] If growth occurred during the process of angiogenesis or vasculogenesis, they would tend to be global lesions instead.

Two-hit hypothesis and limitations of current animal models

Angiogenic signalling is required to trigger cAVM formation. Investigations have indicated that development of an arteriovenous (AV) shunt (the hallmark of a cAVM) requires the neurovasculature to have an inherent genetic susceptibility and a secondary angiogenic clinically relevant stimulus (two-hit hypothesis).[45,46] The first hit is often a mutation or variant in a cAVM risk gene e.g. as seen in HHT (see section 1.11).[301] The second-hit is a successive environmental stimulus, for instance, vascular injury, radiation, trauma, hypoxia, or inflammation. This stimulus induces an angiogenic response, which under genetic risk conditions leads to uncontrolled angiogenesis and formation of a cAVM. Nielsen et al have described how the hypothesis was generated from localised cAVM development and incomplete penetration in *Alk1*+/- and *Eng*+/- mice.[302] A second-hit (a secondary process or additional genetic defect) needs to be applied to the genetically engineered model to produce

a cAVM. The fact that cAVMs first present in adolescence or early adulthood, hints towards the two-hit hypothesis.[303]

Current animal model systems have limitations in terms of clinical translation, but this might be because they do not really mimic the two-hit hypothesis. Primarily, three categories of cAVM animal models currently exist, which include a fistula model, the carotid rete mirabile, and genetically engineered models, with each having their benefits and disadvantages. A fistula (an abnormal connection between an artery and a vein), without the presence of a nidus, does not truly represent a cAVM.[304] However, a fistula is relatively simple to surgically engineer in the absence of a genetic susceptibility: it imitates the ambience of venous hypertension which occurs in the surrounding cerebral parenchyma after cAVM excision and this hypertension induces angiogenesis. The carotid rete mirabile similarly lacks a nidus and is also extracranial.[47] Its advantage lies in the fact that it is a naturally occurring structure, which produces changes similar to the pathological properties of a human cAVM. Although cAVMs are mostly sporadic which may make genetically engineered models less representative, they present a susceptible environment in which to study the disease. It must be noted that to test the two-hit hypothesis, genetic models are crucial to permit us to test various angiogenic stimuli. These animals have a homogenous genetic composition, allowing for greater result reproducibility.[305]

Hereditary Haemorrhagic Telangiectasia and genetic risk factors

Hereditary Haemorrhagic Telangiectasia (HHT) is a rare autosomal dominant disorder, characterised by the presence of multiple systemic vascular abnormalities, including in the brain.[306] AVMs are amongst these abnormalities. There are two types: HHT1 (more commonly associated with congenital AVMs, particularly pulmonary and cerebral) and HHT2 (more frequently associated with hepatic AVMs).[307,308] They can present with stroke, epistaxis, and mucocutaneous telangiectases. HHT1 is caused by loss of function mutations in *ENG* (which codes for endoglin). Endoglin is a transforming growth factor-β1 (TGF-β1) receptor-associated glycoprotein, found on endothelial cell surfaces.[45] TGF-β1 is involved in vascular endothelial cell proliferation, increasing or inhibiting it depending on the subtype.[16] Loss of function mutations in *ALK1* (coding for activin receptor-like kinase 1, also a TGF-β1 receptor on

endothelial cell surfaces) causes HHT2.[45] Both proteins are crucial to the integrity and the normal structure of adult vasculature.

To produce models of cAVM, experimental mouse models have been employed that were genetically manipulated to study the consequences of deletions on the *Alk1* (HHT2) and *Eng* (HHT1) genes (Table 4.1.1). *Eng* and *Alk1* heterozygous mutant mice models are viable: peripheral AVMs emerge in adulthood, and, sporadically, they develop aberrations in their cerebral vasculature (niduses of dilated vessels and AV shunts).[52,53] However, global homozygous *Alk1* and *Eng* deletions result in lethal embryonic vascular defects, including fused and dilated artery-vein pairs related to haemorrhagic complications, inducing death in utero.[50,51] Two investigations demonstrated marked activation of cerebral microvascular dysplasia with induction using vascular endothelial growth factor (VEGF) in *Alk1*+/- or *Eng*+/- mice, and this can be heightened further by accumulations in local tissue perfusion rates for the *Alk1* +/- mice.[45,46] The anomalous vessels were limited to the VEGF injection site and were spiralled, twisted, clustered, and large.[45] Interestingly, intracranial AVMs do not develop, but extracranial AVMs do, implying the adult mouse brain does not support new vessel formation and angiogenesis.[55,56] An endothelial Cre transgenic line was used to produce multiple inducible knockout systems.[309] When *Alk1* knockout mice had their skin wounded, vascular dysplasia and direct arteriovenous connections were noted: this hints at an aberrant response to physical harm. It also generally supports the two-hit hypothesis, albeit in the skin rather than the brain.

There are a few disadvantages with using genetic mouse models, which are important to consider for our experiment. The specialist expertise and tools needed to assemble the models restrict their accessibility. They also lack a cardinal cAVM pathognomonic property: a nidus. Human cerebral AVMs typically grow in a stereotyped, categorisable, anatomical and topological pattern: genetic models have not been able to reproduce this. Stereotyped development helps as the arterial and venous constituents are dictated by the cAVM position in the brain, which indicates likely interruption of anatomy.

Table 4.1.1: Animal models that have been genetically manipulated to study AVMs.

Animal models	Authors, year	Animal	Age	Application
VEGF stimulation in *Alk1*+/- and *Eng*+/- models	Hao 2010[46]	mice	adult	To determine if VEGF application ("response-to-injury") triggers abnormal vascular dysplasia in *Alk1*+/- mice brains
VEGF stimulation in *Eng*+/- model	Xu 2004[45]	mice	8-10 weeks	To determine if using VEGF to cause focal hyperstimulation of angiogenesis causes cerebral blood vessel malformations
Wounding (as an angiogenic stimulus) *Alk1* +/- model	Park 2009[309]	mice	adult	To determine if environmental or physiological factors and genetic ablation are required for AVMs to evolve
Thalidomide stimulation in heterozygous *Eng* +/- models	Lebrin 2010[310]	mice	7 days	To determine if thalidomide treatment promotes maturation of vessels

VEGF = vascular endothelial growth factors; alk1 = activin-like kinase 1; eng = endoglin; AVMs = arteriovenous malformations.

Environmental risk factors and angiogenesis

We hypothesised, based on mouse models developed by others and from clinical observations, that if a clinically relevant angiogenic stimulus is given in the embryonic stages, this may induce the formation of cAVMs in later life in genetically susceptible individuals.[45] No experiment has so far tested a clinically relevant stimulus (e.g. intracerebral haemorrhage, ICH) to study the two-hit hypothesis. Injury to the head or brain can trigger the cascade of events that lead to angiogenesis.[45,46,311] An angiogenic response is activated by haemorrhage-induced brain injury, which leads to cAVM formation.[311] Apart from ICH and brain injury, angiogenesis is also triggered by infection and venous occlusion.[312,313] The expression of VEGF is related to cerebral venous occlusion. Experimental venous hypertension triggers VEGF, resulting in the formation of new vessels in the dura, whereas VEGF antagonists can dampen the extent of hypoxia and oedema related to venous occlusion.[312,313]

Sprague-Dawley rats had spontaneous ICH induced by the stereotactic injection of collagenase type VII into the globus pallidus in two studies.[314,315] In Tang et al's study,

angiogenesis was detected using haematoxylin-eosin staining and double immunolabelling.[314] VEGF expression was observed using immunohistochemistry and polymerase chain reaction. Luo et al identified angiogenesis only using double immunolabelling and detected HIF-1 expression with the same techniques as for VEGF.[315] ICH has therefore been shown to cause VEGF-induced angiogenesis, so from an experimental point of view, this might be a useful clinically relevant stimulus to test the two-hit hypothesis in a genetically susceptible model. Multiple cellular responses are triggered by ICH, apart from responses restoring haemostasis: this is all involved in secondary brain injury. Ischaemia, vasogenic and cytotoxic oedema (due to blood-brain barrier breakdown), raised intracranial pressure, and oxidative damage are common consequences of ICH, all resulting in brain cell death.[316] Coagulation pathway activation and haem toxicity also occur secondary to ICH.

The zebrafish model

Zebrafish are well-suited for human disease modelling thanks to their high fecundity, small size, phenotype recognition, ease of drug administration and a remarkable degree of genetic conservation to mammals.[59] The availability of numerous transgenic reporter lines that express different fluorescent proteins in various tissues, coupled with larval transparency, make zebrafish a powerful model system for visualising cellular processes (e.g. neuroendothelial development) in live intact animals.[59] External fertilisation and embryogenesis are other benefits (as opposed to mice): this simplifies the application of stimuli and any manipulation during early life. There is conservation of numerous disease mechanisms amongst vertebrates, which make the findings of zebrafish studies applicable to human disease. Genetic manipulation can be used to reproduce a phenotype in zebrafish cranial circulation that resembles the early stages of human cAVM development.[60,61] cAVMs and other cerebrovascular diseases have been modelled in zebrafish using various genetic techniques.[59,62] This involves accurate manipulation of the gene of significance to scrutinise the phenotype.[59] Procedures to manipulate the gene comprise of clustered, regularly interspaced, short palindromic repeats (CRISPR), CRISPR-associated systems, morpholino oligonucleotide knockdowns, zinc-finger nucleases, and transcription activator-like effector nucleases (TALEN).

To explore HHT disease mechanisms, *alk1* mutant zebrafish have been developed by Roman et al.[61,300] An ENU mutagenesis screen was initially used to identify this *alk1* germline mutant model.[61] A TGFβ type 1 receptor is encoded by *alk1*: this receptor is expressed in endothelial cell walls. *Alk1* homozygous mutant zebrafish, much like mice, die prematurely subsequent to a severe vascular developmental defect, whereas, in heterozygotes, development is normal.[61] There are a multitude of molecular, morphological, and functional defects in *alk1* knockouts, which are comparable to defects in cAVM patients. The majority of blood cells flow in a few dilated cranial vessels and do not perfuse the tail or trunk at 2 days post-fertilisation (dpf). Shortly after, at 3 to 4 dpf, cerebral and pericardial oedema develop, all signs of high-output cardiac failure. By 7 to 10 dpf, they perish and therefore are not useful for studying cAVM development in later life. Although dilated vessels and shunting were reproduced by these models, there was no abnormal neurovascular architecture or pattern.[60,61] Although it is unclear why heterozygotes have a normal physical appearance and do not develop a phenotype, they may be helpful to test the cAVM two-hit hypothesis as they portray a genetically susceptible animal.

Additionally, to improve visualisation of the vasculature, the *alk1* mutation was crossed onto a kinase insert domain receptor-like green fluorescent protein (*kdrl*: GFP) transgenic background, to visualise endothelial cells.[317]

An environmental stimulus, such as ICH, could be applied to zebrafish as a clinically relevant stimulus to study angiogenesis. Unlike with rats, ICH can be induced in zebrafish larvae following exposure to atorvastatin.[318] The 'bubblehead' mutant line is another ICH model, which displays hydrocephalus in association with spontaneous ICH.[318] Crilly et al provided evidence that spontaneous ICH in zebrafish larvae is similar to human ICH in the inflammatory and pathological phenotypes it produces.

Methods used in zebrafish for clearing, staining, and imaging

In this study, we aim to develop a zebrafish model of cAVM by testing the two-hit hypothesis using a clinically relevant angiogenic stimulus during early life (ICH) in genetically susceptible individuals (*alk1* heterozygous mutants). As we hypothesise cAVMs will develop later in life,

we will require a methodology that will allow us to visualise intact neurovasculature in whole animals. Protocols for imaging tissue in optically cleared adult zebrafish exist.[65] However, such techniques have not been utilised before either in the context of cAVMs in zebrafish, or specifically using the *alk1*$^{+/-}$*; kdrl:* GFP line.[65,319]

To permit the viewing of cranial vasculature in an intact specimen, the dissolution of opaque matter is essential. Histological sectioning is one method of visualisation, but this can cause a loss of delicate structures, tearing and distortion. Clearing allows for the visualisation of intact internal anatomy. There are two major subdivisions of existing tissue-clearing protocols: aqueous-based and organic solvent-based clearing methods.[320] Clearing methods include three-dimensional imaging of solvent-cleared organs (3DISCO).[321] Based on this, other methods have emerged: fluorescence (FDISCO) and ultimate (uDISCO).[320,322] They all cause maximum tissue transparency and shrinkage. However, a problem faced is the quenching of endogenous fluorescence, which is resolved with FDISCO. The reagents of FDISCO are tetrahydrofuran (THF), a dehydrating agent, and dibenzylether (DBE), a refractive index matching agent, but the key differences from the other techniques are the ambient adjustments in pH and temperature. A pH of 9.0 and temperature of 4°C permit the dual advantages of preservation of exogenous and endogenous fluorescence, as well as a reduced processing time. These temperature and pH levels have been found to stabilise GFP.[323,324]

Immunohistochemistry is useful to overcome the challenges of fluorescence quenching or tissue penetration while clearing occurs.[65] It provides an exogenous antibody stain: antibodies conjugated to enzymes activate reactions, which result in identifiable compounds forming.[325] These compounds permit the localisation of certain antigens in an organic specimen. Useful choices for labelling whole brains are small antibodies and membrane-bound reporter lines.[65,326]

Aims and hypothesis

Our long-term hypothesis is that genetic and environmental risk factors during early life may induce cAVM development detectable in later life. The overarching aim of this study is to combine a zebrafish genetic risk factor model (heterozygous mutant *alk1)* with an

environmental stimulus (ICH) model to generate an animal model which can be used to test the two-hit hypothesis of cAVM in the future. Specifically, to do this we will:

1. induce ICH in heterozygous *alk1* zebrafish larvae and raise them to adulthood;
2. optimise a protocol for visualisation of the neurovasculature in intact, fixed adult zebrafish.

4.2 Methods

List of reagents

Table 4.2.1: list of reagents which are abbreviated in this section

Abbreviation	Full name
PTU	Phenylthiourea
MS222	Tricaine Methanesulfonate
DMSO	Dimethylsulfoxide
NaOH	Sodium hydroxide
PFA	Paraformaldehyde
PBS	Phosphate-buffered saline
PBS-T	PBS containing 0.1% Triton-X solution
SSC	Saline Sodium Citrate
BSA	Bovine Serum Albumin
THF	Tetrahydrofuran
DBE	Dibenzyl Ether

List of primers

Table 4.2.2: primers used for Polymerase Chain Reaction

Primer direction	Sequence
alk1 forward primer (Eurofin)	5'-CACGGTCCAACTAAGGCATGAAAACACCTT-3'
alk1 reverse primer (Eurofin)	5'-GTGTGCTATGGCTGGTTTG-3'

Zebrafish

Zebrafish Husbandry

Zebrafish were maintained at the University of Manchester Biological Services Facility according to the recommended environmental and care conditions: this included a temperature of 28.5°C and a pH of 7. The University of Manchester Ethical Review Board approved all zebrafish experiments described in this chapter. Experiments performed on zebrafish aged less than 5 dpf did not require a licence as per Home Office regulations. The animals have unprotected status up to and including 5 dpf. All procedures performed on older animals required a project licence: this included breeding, genotyping and protocols required

for imaging older fish. Breeding, genotyping and experiments using adult zebrafish were performed under Home Office project licence P132EB6D7. The author obtained her Home Office personal licence I71868873 in August 2019. This was thereafter used for breeding, genotyping, administering substances by immersion, performing live imaging, to terminally anaesthetise zebrafish perfused with a fixative via immersion, and for clearing.

Zebrafish strains

As mentioned in the 'Introduction', the transgenic *alk1*$^{+/-}$; *kdrl*: GFP line was used. Wild-types (WT; *kdrl*: GFP) were crossed with heterozygous mutants (*alk1*$^{+/-}$; *kdrl*: GFP) to produce a ~50:50 ratio of WT; *kdrl*: GFP and *alk1*$^{+/-}$; *kdrl*: GFP embryos to which stimuli were applied. Mutant and wild-types were housed separately. As previously described, homozygous mutants do not survive past 10 dpf and cannot be studied in adulthood.[61]

Embryo collection

E3 embryo water was poured into clean petri dishes. This is a medium for harvesting embryos, composed of 'instant ocean' sea salts (60 µg/ml) and methylene blue (0.5ppm) (Sigma-Aldrich). After natural spawning at 28°C in breeding boxes, embryos were collected and transferred into these dishes. Within 24 hours post-fertilisation (hpf), unfertilised and/or dead embryos were discarded.

Embryo dechorionating

Embryos (both WT; *kdrl*: GFP and *alk1*$^{+/-}$; *kdrl*: GFP genotypes) at ~27 hpf were manually dechorionated using a pair of sharp dissecting forceps (Dumont) and subsequently transferred to clean petri dishes containing fresh embryo water.

Phenylthiourea treatment

Phenylthiourea (PTU) was added to E3 water to prevent zebrafish larvae forming melanin.[327] This consisted of solubilising 0.03g PTU in embryo water. The dechorionated embryos (at ~27 hpf) were bathed in PTU. They were incubated in PTU until the experiment's end (at 72 hpf),

refreshing the solution daily. The remaining embryos were sacrificed by a lethal overdose of tricaine methanesulfonate (MS222) and freezing at -20°C.

ICH model – Atorvastatin treatment

Atorvastatin calcium salt trihydrate (ATV) (Sigma-Aldrich Merck PZ0001) was solubilised in 1% dimethyl sulfoxide (DMSO) (Sigma-Aldrich) to produce a 0.5µM stock concentration. This was stored in aliquots at -20°C. At 28hpf, embryos were bathed in a mixture of PTU and ATV (at 1.5µM). An age-matched sibling group was left untreated in PTU as a control. Eighteen embryos were placed in each well (of a six-well plate), except the untreated group, which had nine. They were kept in an incubator at 28°C for 24 hours. At ~52 hpf, embryos with visible brain haemorrhages (ICH+) were identified and separated from those without haemorrhages (ICH-). The ATV was discarded, and the larvae were kept in fresh PTU alone. They were inspected again at ~72 hpf. Subsequently, their DNA was extracted for genotyping. Prior to extraction, they were imaged with an apochromatic fluorescent stereo microscope (Leica DFC7000 T M165 FC), using the software Leica Application Suite X, to view fluorescent blood vessels.

DNA extraction

DNA extraction of each embryo involved siphoning off the existing solution from each eppendorf. Subsequently, 30µL of 50µM sodium hydroxide (NaOH) was added. The samples were heated to 95°C for 20 minutes (and mixed by vortexing half-way through), then cooled on ice for 2 minutes. Finally, 3 µL of 1M TRIS-HCl at pH 8 was added. The eppendorfs were vortexed, then centrifuged at maximum speed for 1 minute. The supernatant was subsequently used as a DNA template for Polymerase Chain Reaction (PCR).

Genotyping

PCR was conducted in a thermocycler (BIOER GenePro) to amplify the DNA. The reagents were Master Mix (Thermo Scientific DreamTaq), nuclease-free water (Thermo Scientific), a forward 5'-CACGGTCCAACTAAGGCATGAAAACACCTT-3' and reverse 5'-GTGTGCTATGGCTGGTTTG-3' primer (Eurofin). The forward primer ends just 5' to the mutation: it contains a single mismatch (underlined), which creates a BsaJI restriction site in the wild-type sequence.[61] A

Touchdown program setting of 65-55°C and annealing for 60°C for 35 cycles was used (Tables 4.2.3 & 4.2.4). Gel electrophoresis confirmed PCR amplicons. PCR products were separated by running them on a 3% agarose gel. The 3% gel was imaged using an ultraviolet transilluminator (G:box) and GeneSys software. DNA digestion was performed by adding PCR product to BSaJI enzyme and cutsmart buffer (both from New England Biolabs), and nuclease-free water (Table 4.2.5). The mixture was heated at 60°C for 2 hours, followed by 80°C for 20 minutes. This digested product was separated by gel electrophoresis (Figure 4.2.1). For both PCR and digested products, 5 µL was transferred into each well.

Table 4.2.3: Polymerase Chain Reaction components for one sample

Ingredients	**Volume for 1 sample (µL)**
DNA	3
Master Mix (2X conc)	15
nuclease-free water	8
forward primer (10µM)	2
reverse primer (10µM)	2

Table 4.2.4: Touchdown steps for Polymerase Chain Reaction

	Step	**Temperature (°C)**	**Time (s)**
1	denature	98	40
2	touchdown anneal	65-55	40
Repeat 10 cycles			
3	denature	98	40
4	anneal	60	30
5	elongate	72	120
Repeat 35 cycles			
6	elongate	72	600
7	hold	10	-

Table 4.2.5: Digestion components for one sample

Ingredients	**Volume for 1 sample (µL)**
PCR product	7
nuclease-free water	10
BSaJI	1
Cutsmart buffer (10X conc)	2

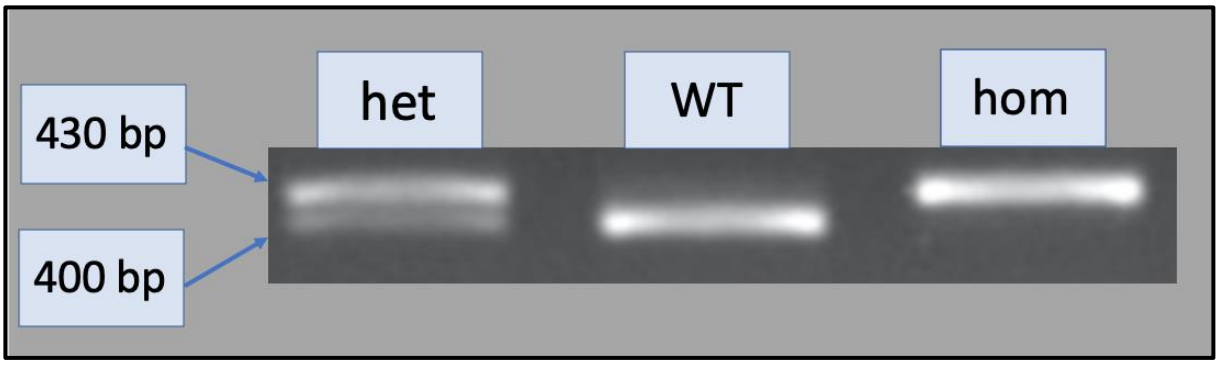

Figure 4.2.1: Appearances of digested DNA product on agarose gel under an ultraviolet transilluminator.
het = heterozygous, WT = wild type, hom = homozygous. Two bands indicate a heterozygous digestion product (430 and 400 base pairs length), a single 400 base pair (bp) further down, and a 430 base pair further up. A single 430bp indicates homozygous product. A single 400bp indicates a wild type product.

The above protocol was performed as 3 biological replicates to ensure reliability of results.

Raising haemorrhaged larvae to adulthood

A clutch of 104 larvae, which were treated with atorvastatin, and were ICH+ and positive for *kdrl*:GFP signal, were raised to adulthood with the aim of investigating whether their cerebral vasculature developed cAVMs.

Immunohistochemistry and clearing

Tissue preparation

An *alk1*$^{+/-}$*;kdrl:*GFP adult zebrafish was sacrificed by a lethal overdose of MS222 via immersion (Table 4.2.6). It was fixed overnight in 4% paraformaldehyde (PFA) at 4°C in the dark (Table 4.2.6, Figure 4.3.3). It was subsequently washed in phosphate-buffered saline (PBS). The zebrafish scales were removed under a light microscope (Leica) with a scalpel (Swann-Morton). The specimen was immersed and agitated in a bleaching solution over 5 minutes at room temperature. The eyes were then removed using sharp dissecting forceps (Dumont) (Figure 4.3.3).

Immunohistochemistry

All steps were performed at 4°C in the dark (by wrapping in aluminium foil) with agitation, using a 4°C roller (PORKKA). The specimen was initially rinsed in a PBS containing 0.1% Triton-X (PBS-T) solution for 1 hour (Table 4.2.6, Figure 4.2.2). This was followed by rinsing in a blocking buffer overnight. The specimen was incubated in fresh blocking buffer and primary antibody for 7 days. The zebrafish was rinsed in PBS-T solution for four hours, with the solution being replaced hourly. It was then incubated in PBS-T solution containing secondary antibody for another 7 days in the same environment. The specimen was, once again, rinsed in PBS-T solution for four hours, with the solution replaced hourly.

Table 4.2.6: Solutions and compositions.

Solution	**Components**	**Receptacle**
MS222	2g tricaine, 500ml distilled water, 10.5ml Tris (pH 8.0) – total pH 7.0	500ml bottle
PBS	5 tablets of PBS, 1000ml distilled water	1000ml bottle
4% PFA	10 ml of 16% PFA, 30ml PBS	50ml falcon
Bleach solution	3.9ml distilled water, 5ml H_2O_2, 0.25ml 20X SSC, 0.5ml formamide	15ml falcon
PBS-T solution	PBS, 150 µls of 0.3% Triton-X	50ml falcon
Blocking buffer	PBS, 150 µl of 0.3% Triton-X, 1ml of 2% normal goat serum, 0.5g of 1% BSA	50ml falcon
Blocking/ primary antibody mixture	primary antibody, rabbit-anti-GFP (ThermoFisher, A11122) diluted 1:500 with blocking solution	50ml falcon
Blocking/ secondary antibody mixture	secondary antibody, goat-anti-rabbit Alexa 555 (ThermoFisher, A21429) diluted 1:750 with 1XPBS-Tx 0.3%	50ml falcon

PFA - paraformaldehyde, PBS - phosphate-buffered saline, BSA - bovine serum albumin

FDISCO clearing protocol

All the steps were performed with THF under the fume hood. All incubations were done in a glass vial with gentle agitation on ice. All solutions were prepared first and then cooled to 4°C before addition to the sample. The specimen was immersed in increasing concentrations of THF solutions (Table 4.2.7, Figure 4.2.2), followed by DBE.

Table 4.2.7: Steps for FDISCO protocol.

Steps for FDISCO protocol
THF
a. Add 50 % THF mixed with distilled water for 24 hours b. Add 70 % THF mixed with distilled water for 24 hours c. Add 80 % THF mixed with distilled water for 24 hours d. Add 100 % THF two or three times for 24 hours
DBE
Incubate for 24 hours and store in DBE in airtight glass chambers at 4°C in the dark

THF - tetrahydrofuran, DBE – dibenzyl ether.

Two-photon and confocal microscopy

Two-photon microscopy (Leica SP8 Upright Multiphoton) was used to image the zebrafish brains and whole zebrafish. The specimens were mounted on glass dishes filled with DBE. Either a 16x oil immersion lens or multi-immersion lens was used. Images were viewed using IMARIS.

Confocal microscopy (Leica SP8 inverted) was attempted but did not provide adequate resolution.

Role of the author in the project

I produced the larval ICH models using atorvastatin treatment and genotyped them. I also performed the adult zebrafish tissue processing, immunohistochemistry, and clearing. The zebrafish brains were dissected out of the whole specimen by my second supervisor, Dr Paul Kasher, and post-doctoral research associate, Dr Siobhan Crilly. Two-photon imaging was performed by senior neuroscience lecturer, Dr Ingo Schiessl.

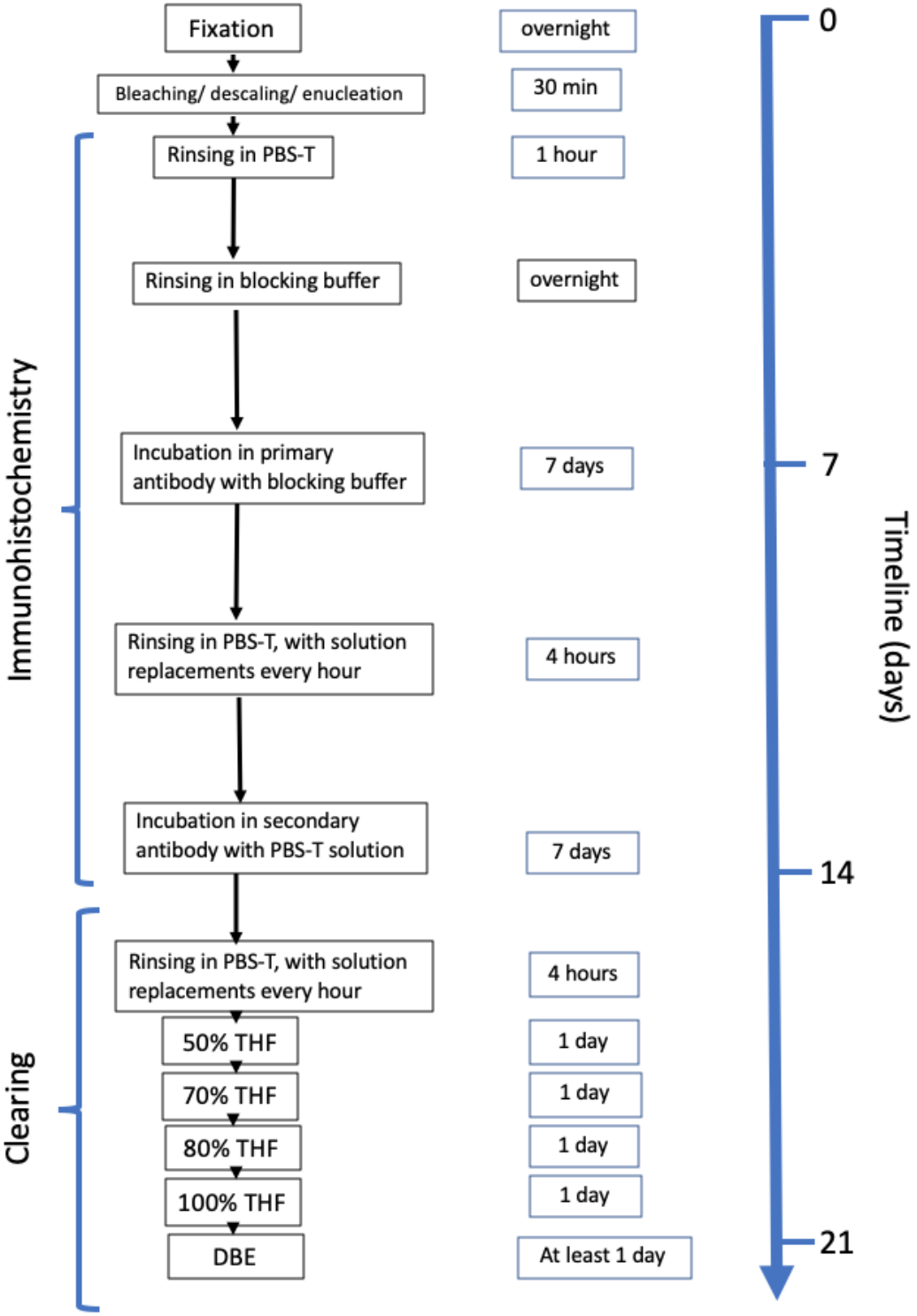

Figure 4.2.2: Protocol timeline demonstrating steps of whole adult *alk1*$^{+/-}$*;kdrl*:GFP+ zebrafish immunohistochemistry, followed by clearing.
Final timeline was reduced by 15 days as the whole zebrafish appeared to retain endogenous fluorescent signal when subjected to clearing, without antibody staining (see section 'Final protocol timeline' of 'Results'). Abbreviations: THF – tetrahydrofuran; DBE – dibenzyl ether.

4.3 Results

Inducing ICH in alk1 zebrafish larvae

In order to produce a clinically relevant angiogenic stimulus, ICH was induced.[301] ATV is known to cause neuroendothelial weakness and spontaneous vessel rupture at the larval stage.[328] Light and fluorescent microscopy was used to observe ICH in the transparent larvae. Following exposure to 1.5µM ATV, an average of 82% of zebrafish larvae were ICH+, and 17% were ICH- (comparable to Crilly et al.)[318] The untreated group were ICH- as expected. Both groups of larvae were imaged at 3 dpf under a brightfield or fluorescent microscope (Fig 4.3.1).

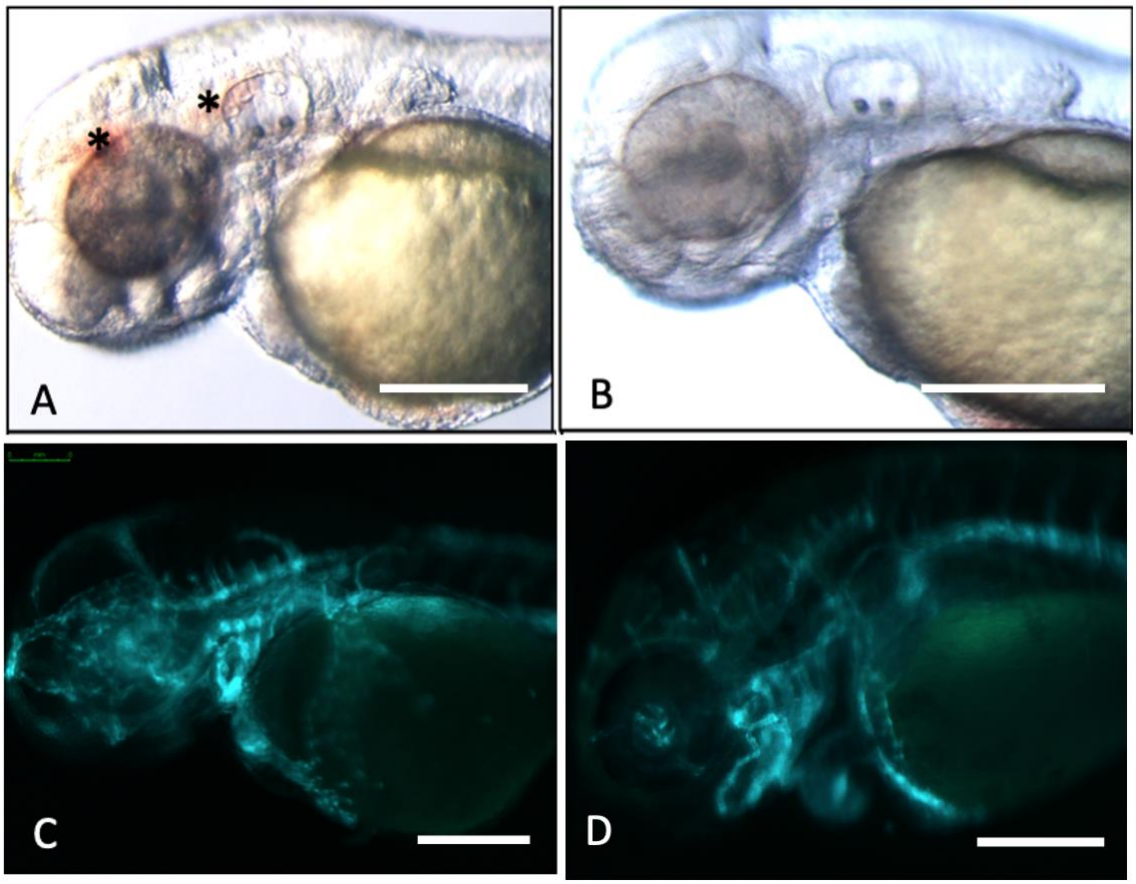

Figure 4.3.1: ATV-induced ICH in *alk1*$^{+/-}$*; kdrl*: GFP+ zebrafish larvae.
Lateral head images of treated zebrafish larvae at 3 days post fertilisation, treated with atorvastatin and phenylthiourea at 28 hours post fertilisation. Scale bars represent 250 µm. (A) with intracranial haemorrhage (ICH) (*), under a brightfield microscope, magnification x 10.0; (B) without ICH, under a brightfield microscope, magnification x 10.0; (C) with ICH, under a fluorescent microscope, magnification x 8.0; (D) without ICH, under a fluorescent microscope, magnification x 8.0.

Genotyping was performed to determine whether heterozygotes were more likely to sustain ICH than WTs. Three biological replicates were performed, however genotyping for the third

replicate failed so this replicate was discarded from the analysis. No statistically significant difference was found between the frequencies of WT and heterozygous mutants in the ICH+ group (Figure 4.3.2, Table 4.3.1). As a WT and heterozygote incross was performed, we expected Mendelian ratios of roughly 50:50 of both genotypes: our findings agreed with this.

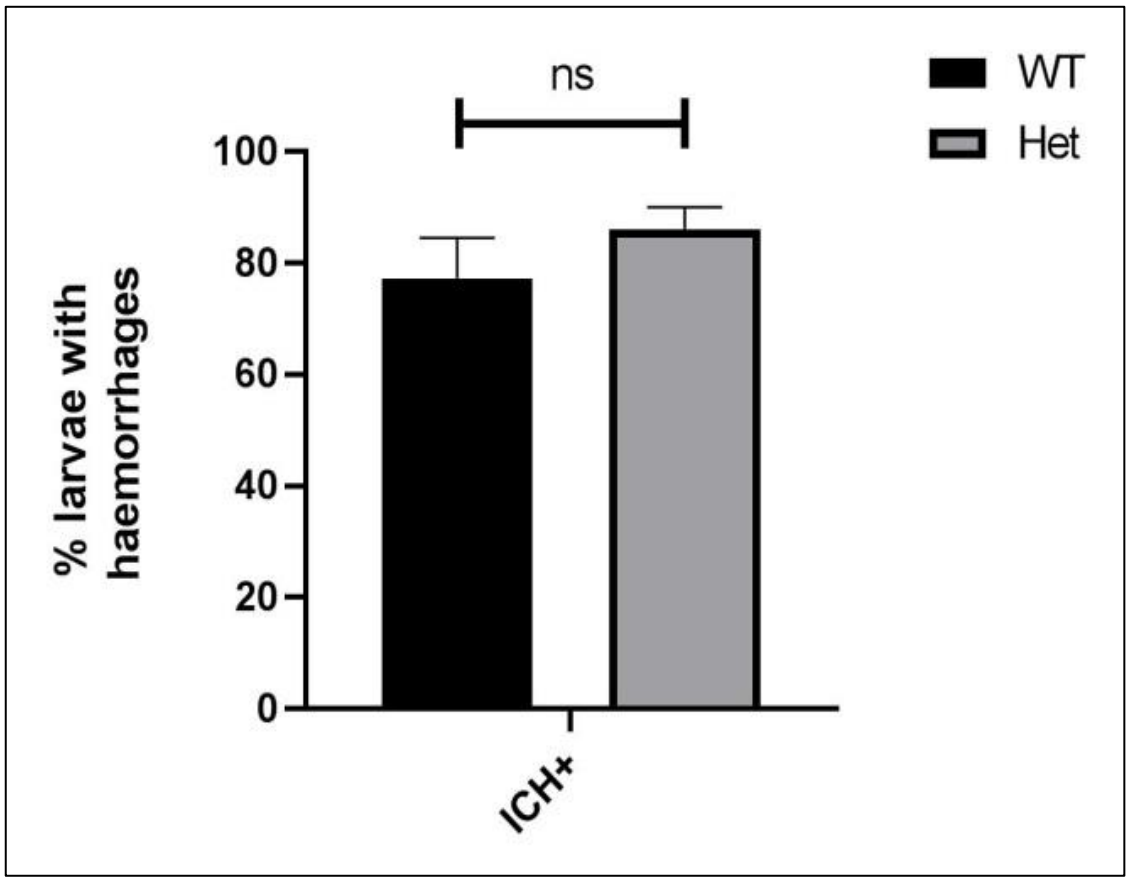

Figure 4.3.2: Alk1 heterozygous larvae are not more susceptible to ICH
Atorvastatin-treated (1.5 µM concentration, dissolved in DMSO) zebrafish larvae that have haemorrhaged (ICH+), showing relative proportions of wild-types (WT) and heterozygotes (het). This includes the data of two biological replicates. Error bars show SEM. There are roughly equal numbers of WT (n = 14, 13) and het (n = 15, 16) with no statistical significance between the two when an unpaired t-test was performed.

Table 4.3.1: Numbers and percentages of wild types (WT) and heterozygotes (het) within haemorrhaged (ICH+) and non-haemorrhaged (ICH-) groups, following ATV treatment

	WT (N (%))		**Het (N (%))**	
ICH+	14 (82.4)	13 (72.2)	15 (83.3)	16 (88.9)
ICH-	3 (17.6)	5 (27.8)	3 (16.7)	2 (11.1)

Adult zebrafish immunohistochemistry and clearing

As described in Sections 1.1, 1.9, and 4.1, cAVMs are understood to form due to a congenital insult, but they are usually diagnosed in young adults. After we applied an angiogenic stimulus at the larval stage, we were therefore expecting to observe a cAVM developing at the adult stage. To effectively image adult brains, immunohistochemistry followed by clearing has been used by other studies.[65,320,322] The ATV induction was repeated and 104 mixed genotype larvae (all having developed ICH) were raised to adulthood to attempt to detect cAVMs in later life. Following genotyping, WT and heterozygote specimens (one pair at 8 and another at 11 months of age) were taken for antibody staining and clearing. The primary antibody used was rabbit-anti-GFP and the secondary antibody was goat-anti-rabbit Alexa 555. The final cleared specimens allowed visualisation of internal organs (Figure 4.3.3).

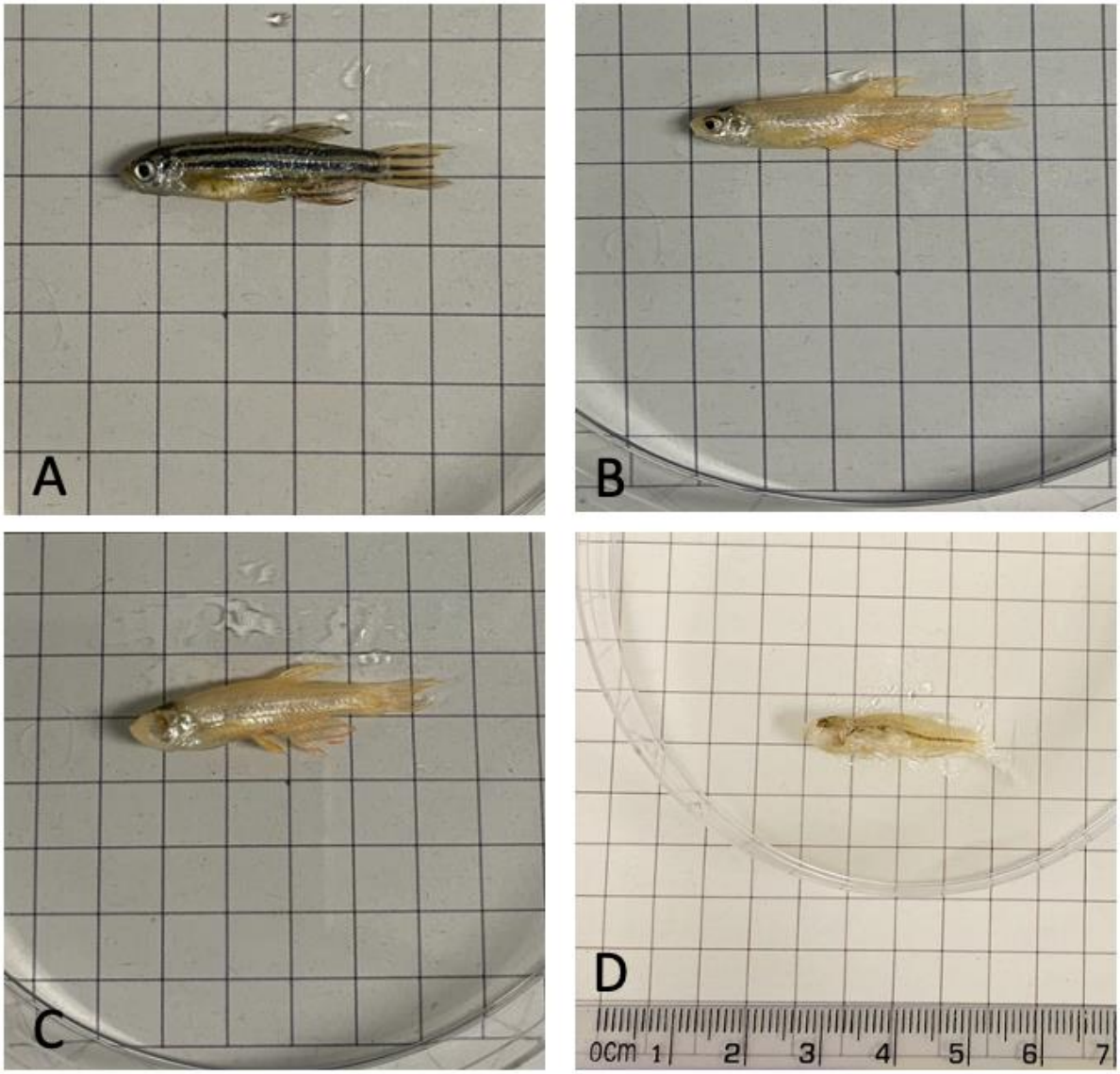

Figure 4.3.3: Stages of adult zebrafish preparation prior to imaging.
Specimen is an 11-month-old *alk1+/-; kdrl*: GFP+ zebrafish. (A) After overnight fixation. (B) After bleaching. (C) After enucleation. (D) After clearing. Each square represents 6mm.

As part of the optimisation process, we initially imaged the brain in isolation as we were concerned with identifying cAVMs. We dissected out the brain of an untreated *alk1*$^{+/-}$ *;kdrl:GFP+* zebrafish and, subsequently, repeated the process and dissected out the right hemisphere to ensure there was full antibody penetration through to the centre of the brain under a stereo fluorescent microscope (Figure 4.3.4). This microscope was used to generally assess whether fluorescence was visible, but not visualise the vessels in detail.

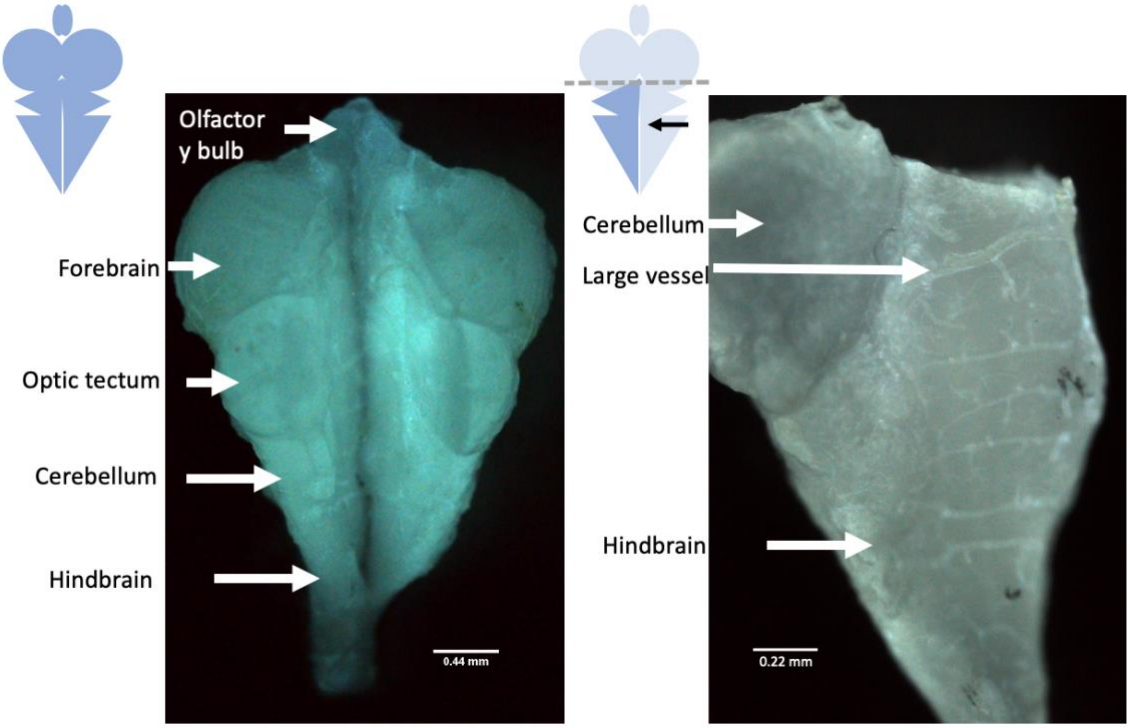

Figure 4.3.4: Six-month-old *alk1*$^{+/-}$*;kdrl*:GFP+ zebrafish brain under stereo fluorescent microscope.
Prior to dissecting the brain, immunohistochemistry was performed on the whole zebrafish specimen. Schematics above each panel indicate the location/orientation of the specimen. Left panel demonstrates ventral surface of whole adult zebrafish brain. Scale bar represents 0.44 mm. Right panel demonstrates the right cerebellum and hindbrain, with fluorescent vessels visible on the medial surface, confirming good penetration of antibody stain through to the centre of the brain. Scale bar represents 0.22mm.

Adult zebrafish two-photon microscopy

It is well-established that two-photon microscopy allows for three-dimensional imaging, particularly within intact tissues of relatively thick specimens. Although confocal microscopy allows sectioning into thicker tissues, its limitations lie in the bleaching of out of focus planes and tissue scattering of excitation and emission photons: this reduces the penetration depth.

Two-photon microscopy provided a clear demonstration of most cerebral vessels in the whole zebrafish brain (Figures 4.3.5 and 'zebrafish brain 2 photon' on https://www.dropbox.com/sh/45w3vuh5271q4h4/AAAdN86jspaFXKlfg9k15etta?dl=0).
Initially a whole brain was imaged without immunohistochemistry (Figure 4.3.5 A to C) to determine whether clearing allowed full visualisation of vessels. Cerebral vasculature in all external surfaces of the brain were well-delineated, but for internal surfaces, endogenous fluorescence appeared to have been quenched. Consequently, immunohistochemistry using

an anti-GFP antibody was performed to improve signal. After confirming internal visibility of fluorescence (Figure 4.3.4), the right hemisphere was imaged (Figure 4.3.5 D to F). The second attempt demonstrated full visibility of all fluorescent vessels, regardless of depth.

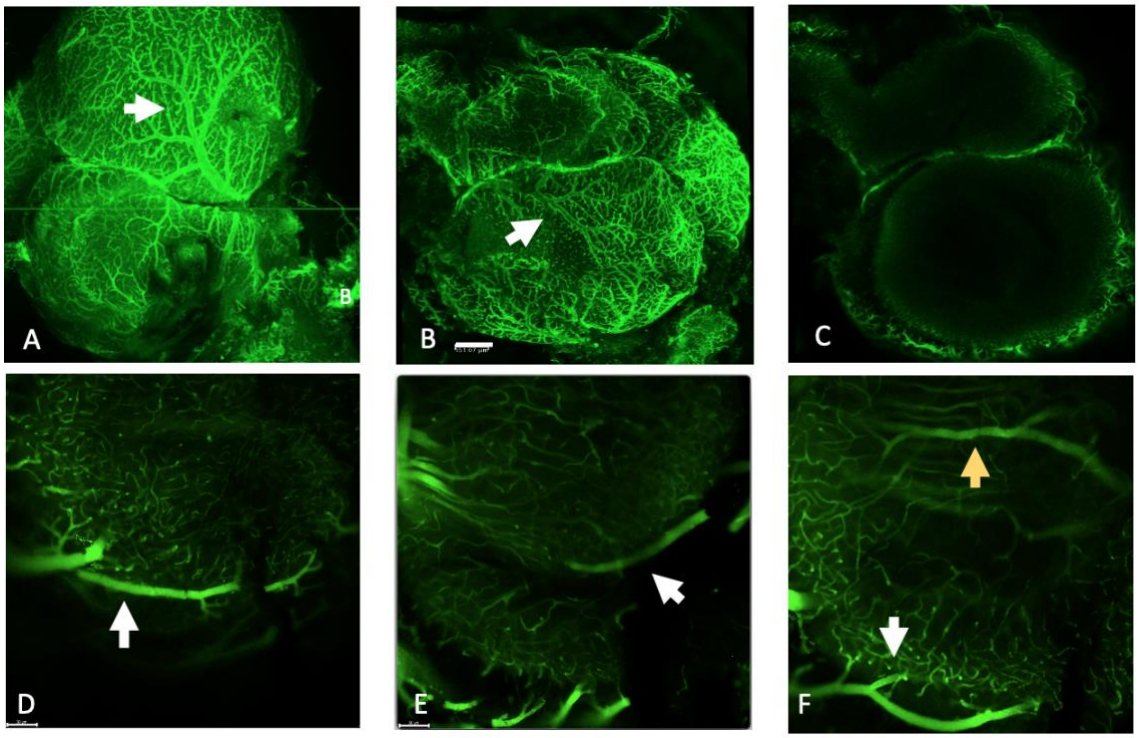

Figure 4.3.5: Optimisation of two-photon microscopy using alk1 zebrafish whole brains.
All images produced using IMARIS. For A to C, 18-month-old *alk1*$^{+/-}$;*kdrl*:GFP zebrafish whole brain was imaged for endogenous GFP signal. White arrows indicate large cortical arteries. (A), dorsal view, optic tectum visible. (B) Same brain, lateral surface, scale bar represents 151.07 µm. (C) When imaging internally, vessels not visible. For D to F, six-month-old *alk1*$^{+/-}$;*kdrl*:GFP zebrafish brain right hemisphere was imaged. Immunohistochemistry was performed using an anti-GFP antibody. Going from D to F, z stacks are moving from the lateral surface to the medial surface. Scale bar represents 50 µm. Yellow arrow indicates large vein. (D) Lateral surface (E) Middle stack (F) Medial surface.

Others have found that clearing shrinks tissues by ~40% so that the small zebrafish brain is even more difficult to handle and mount for imaging.[322] To overcome this, we repeated the process with whole adult zebrafish. We performed whole zebrafish antibody staining, followed by clearing, on ATV-treated specimens (see 'Methods').

Imaging using the confocal microscope proved unsuccessful (Figure 'IMG_2442.MOV' on https://www.dropbox.com/sh/45w3vuh5271q4h4/AAAdN86jspaFXKlfg9k15etta?dl=0).

Two-photon imaging provided an excellent demonstration of all the vessels in the body. An overview of the anterior body of the zebrafish specimen is demonstrated (Figure 4.3.6). This is the first time two-photon imaging has been performed in this transgenic species in a completely cleared specimen.

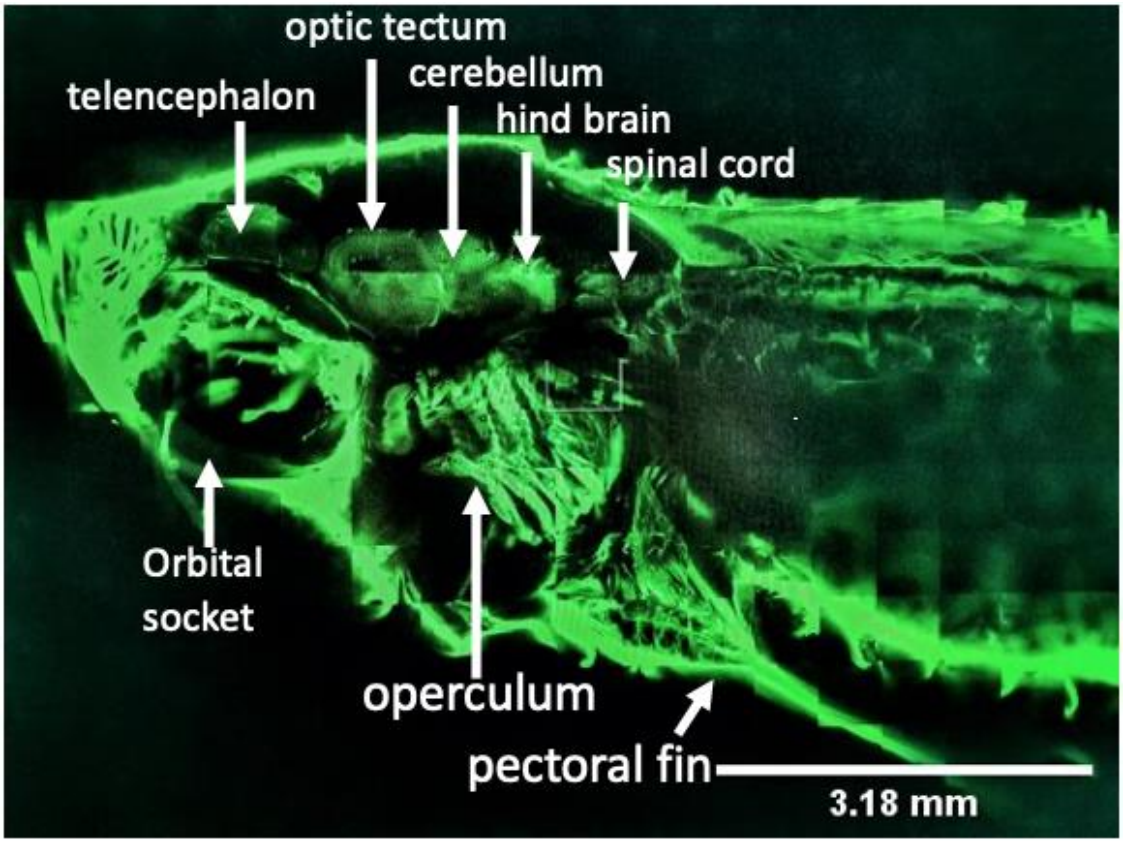

Figure 4.3.6: Annotated overview of zebrafish head using two-photon microscope. Images produced with IMARIS. Eight-month-old *alk1*$^{+/-}$; *kdrl*: GFP+ zebrafish, which was ATV-treated at 24 hpf and developed ICH, which cleared by 4 dpf. Zebrafish brain visible (due to fluorescent vessels) against background of autofluorescence.

The cerebral vasculature in the telencephalon and tectum opticum has been recorded, and a 3D rendering created (Figures 4.3.8, 'Series006_Median001_chan01' and 'Cleared Fish Brain 3D Surface Movie-1' on https://www.dropbox.com/sh/45w3vuh5271q4h4/AAAdN86jspaFXKlfg9k15etta?dl=0).

Even through the intact skull and subcutaneous tissue, immunohistochemistry followed by clearing, permitted exquisitely detailed views of the vessels (Figures 4.3.7 A - C). For the final step, to evaluate whether it was possible to reduce the protocol's duration, immunohistochemistry was omitted. The imaging quality retained its clarity (Figures 4.3.7 D -

F) with the invaluable benefits of reducing the labour, resources and time required. In these two specimens, no abnormal vascular malformations were detected.

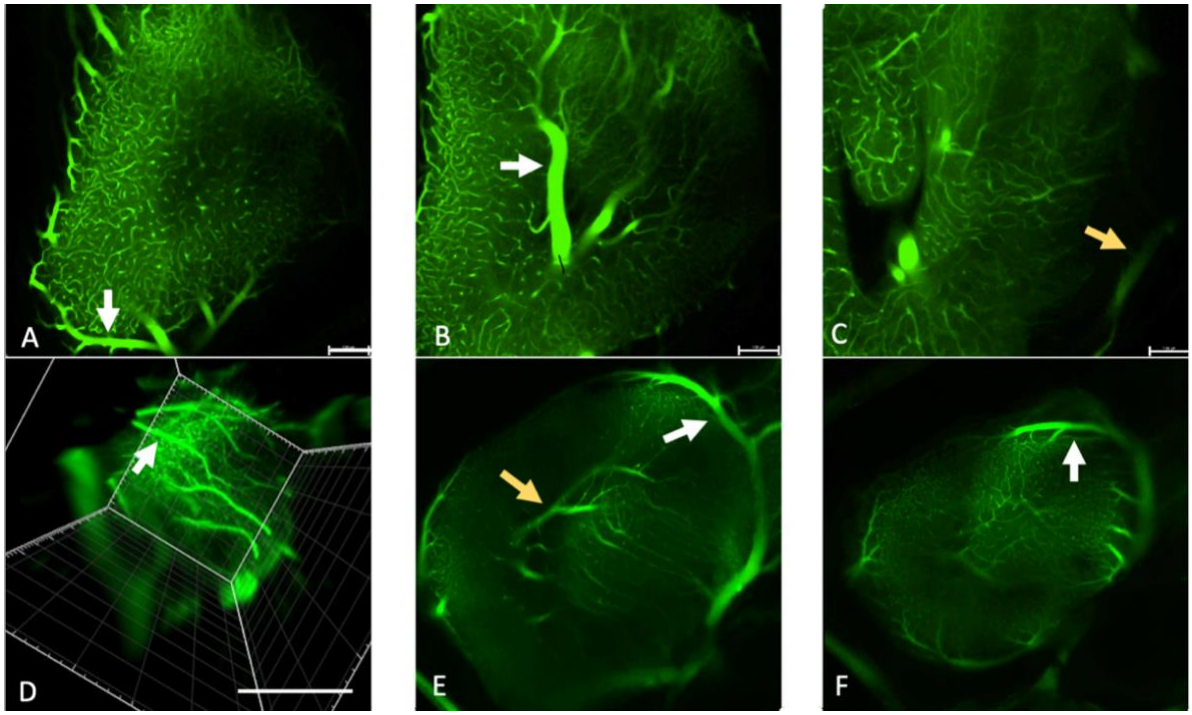

Figure 4.3.7: Optimisation of two-photon microscopy using whole body cleared adult *alk1*$^{+/-}$*;kdrl*:GFP zebrafish.

Images produced with IMARIS. Demonstration of *alk1*$^{+/-}$;*kdrl*:GFP heterozygous zebrafish brains, who were ATV-treated at 24 hpf and developed intracerebral haemorrhages during larval stages. White arrows indicate large arteries and yellow arrows large veins. For A to C, eight-month-old adults were imaged. An oil immersion lens was used, providing improved resolution. These were antibody-stained prior to clearing. Scale bar represents 100µm (A) lateral surface, (B) mid-section, (C) section around the habenula. For D to F, 11-month-old adults were imaged. These were not antibody-stained, but the fluorescence was nevertheless preserved. Resolution was restricted by the multi-immersion lens that had to be used. Scale bar represents 300µm. (D) 3D view of mid-section. (E) mid-section of telencephalon. (F) lateral surface of telencephalon

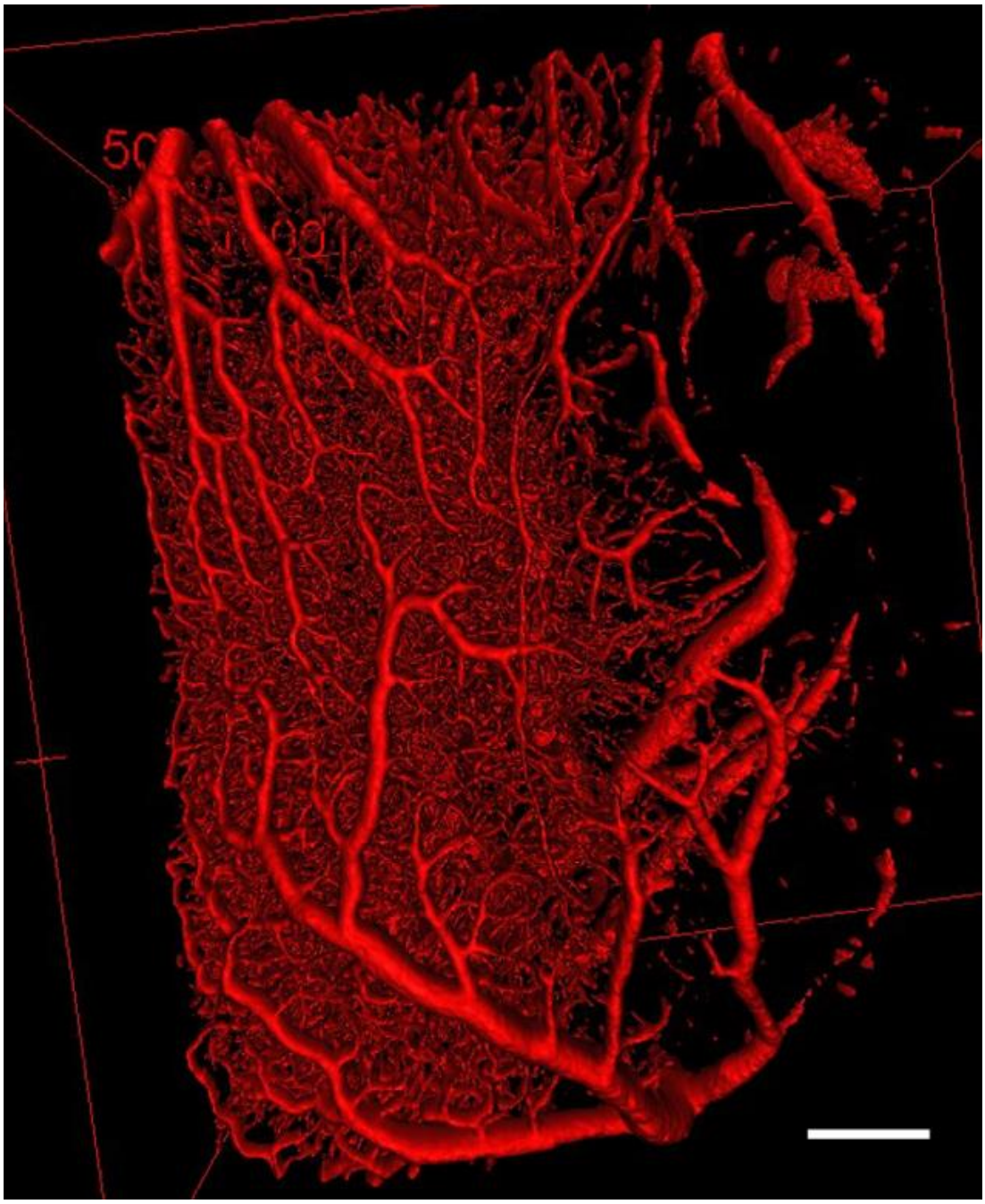

Figure 4.3.8: 3D rendering of a section of the adult zebrafish brain vasculature.
Images acquired of eight-month-old (antibody-stained) *alk1*$^{+/-}$;*kdrl*:GFP zebrafish were processed using IMARIS and the surpass tool to render 3D images. Section from telencephalon. Scale bar represents 50 µm.

Final protocol timeline

As Figure 4.3.7 D-F demonstrates excellent preservation of fluorescence using the FDISCO clearing protocol, despite no prior immunohistochemistry, the final optimised protocol was considerably reduced in duration and cost (Fig 4.3.9).

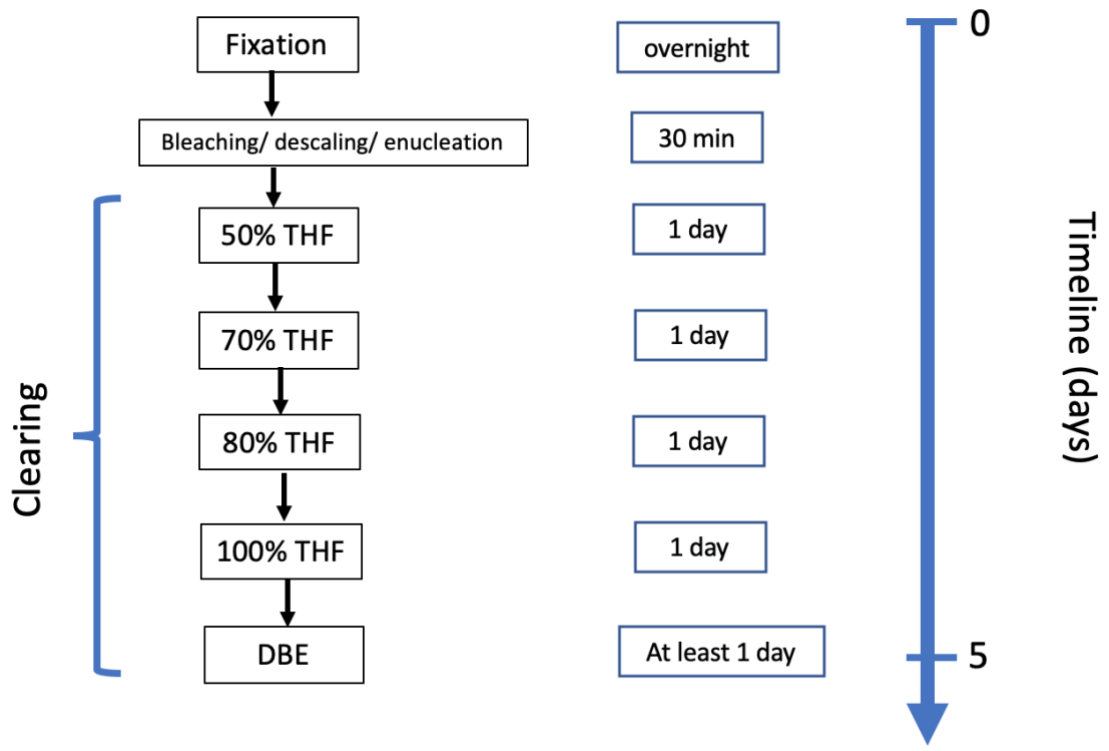

Figure 4.3.9: Final protocol timeline.
Demonstrating steps of whole *alk1*$^{+/-}$*;kdrl*:GFP+ zebrafish preparation prior to imaging. Final timeline was reduced by 15 days as the whole zebrafish appeared to retain their fluorescence when subjected to clearing despite the lack of antibody staining. Abbreviations: THF – tetrahydrofuran; DBE – dibenzyl ether. Steps involved in fixation and bleaching are described in 'Methods'.

4.4 Discussion

We demonstrate here that it is possible to raise *alk1* heterozygous zebrafish larvae, which had ICH induced at the larval stage, to adulthood. Additionally, we successfully optimised an original protocol to visualise neurovasculature in fixed and cleared intact adult *alk1*$^{+/-}$*;kdrl*: GFP zebrafish. This has the potential to be an effective experimental in vivo system for studying the two-hit hypothesis in the development of cAVMs.

Although cAVMs are a disease affecting a young population, they represent a source of high mortality when they rupture. Our knowledge of their development is poor, making an animal cAVM model critical to further our understanding. Studies have shown that, as part of a two-hit hypothesis, the formation of a cAVM requires an environmental trigger (an angiogenic stimulus) as the second hit adding to a genetic predisposition in the neurovasculature while the organism is immature.[301] Potential second hits are inflammation, injury to vessels, mechanical trauma, ultraviolet light radiation, and other angiogenic stimuli.[301] The timing of the second hit is not well-established, but possibly occurs sometime between childhood and adulthood, since cAVMs commonly manifest in young adults. cAVMs in humans, unlike in genetic animal models, generally grow in a classifiable, stereotyped, topological and anatomical pattern. In terms of translational relevance, a particular discrepancy with the VEGF-stimulated mouse models is that direct application of VEGF is artificial and potentially less reliable for studying the effect of a brain injury during the neonatal stage, for example.

The strategy we employed in engineering a dependable cAVM animal model consisted of a two-hit model: a clinically relevant angiogenic stimulus was provided to a genetically altered and susceptible immature zebrafish. This was innovative, having not been applied to zebrafish before. There are inherently several requirements: there must be genetic vulnerability and immaturity, to which a clinically relevant angiogenic stimulus should be applied for the growth of a cAVM later in life (during adulthood). Numerous pieces of evidence support this hypothesis. A helpful tactic was proposed by Kim et al, where the aim is to focus on genes associated with the human AVM phenotype.[300] We used the *ALK1* gene for our study, which is associated with HHT2. A germline mutant *alk1* zebrafish model was employed in our experiment.[61] Earlier studies that exposed *Alk1* mutant mice to VEGF (triggering abnormal

cerebral capillary dysplasia) were used as foundations for our study.[45,46] Although an interceding nidus was absent, in both these studies, fistulae were generated. Numerous activating agents were discovered for the occurrence of childhood CVST.[74] A known angiogenesis stimulus is venous occlusion, which leads to cerebral hypoxia.[329] If we accept that CVST induces venous occlusion, it is possible to predict that factors activating CVST would also induce cAVM growth. Finally, experimental evidence is required that permits identification of the age at which the angiogenic stimulus is applied for the evolution of cerebral angiogenesis. This is at the neonatal stage according to rodent studies.[55,56] In adulthood, according to Carlson et al, angiogenesis does not develop in the brain, but in the liver and skin. A mixture of studies was thus required to enable us to construct this two-hit hypothesis for a cAVM animal model.

According to the hypothesis, for cAVMs to develop in brains, the cerebral environment must support angiogenesis by possessing an inherent weakness, in terms of an immature brain (which has remaining angiogenic potential), or a genetic defect like HHT. In reaction to an angiogenic stimulus, cAVMs develop.[55,56,309,330] We can subject an experimental model to an angiogenic stimulus, though the type of clinically relevant stimulus is unknown. It is also possible to inject VEGF directly. As discussed in Section 1.9, 'Pathogenesis', other angiogenic factors include TGF, bFGF, and ANG-1. VEGF upregulation is the mechanism by which hypoxia triggers angiogenesis.[67,69] This requires several pro-angiogenic pathways to be upregulated to encourage vessel growth.[69] Accumulation of HIFα in cells (a dominant angiogenesis regulator) occurs in the presence of hypoxia. In the local environment with reduced oxygen, multiple pro-angiogenic genes are regulated by the HIF pathway, including VEGF, to induce angiogenesis. Vascular permeability is stimulated by these pro-angiogenic factors: they also nurture endothelial cell proliferation and trigger consequent sprouting, followed by migration, adhesion, and ultimately, tube formation. Studies have demonstrated that mouse embryos die with HIFα ablation, which highlights its essential role.[331,332]

In our experiment, ICH was induced in *alk1* WT and heterozygous siblings. *Alk1* heterozygous zebrafish larvae were not more likely to haemorrhage than their wild type siblings. This may be a consequence of the high ATV dose used, which caused haemorrhage even in the absence of genetic vulnerability. Only two replicates were performed which did not provide sufficient

power for the experiment. There was a slight trend towards an increase in the *alk1* heterozygotes, so if more (e.g. six) replicates were used, ICH may have been found to occur more often in heterozygotes. Different doses of ATV were attempted to achieve an appropriate portion of more haemorrhaged vs non-haemorrhaged larvae to allow for sufficient numbers to raise to adulthood. Since the drug with the specific dose used is known to cause ICH,[318] the likelihood of detecting neurovascular instability in heterozygous larvae (in the absence of any external stimulus) was poor. In future, an ATV dose response experiment could be performed, i.e., repeat the ATV experiment with different doses (0.5 µM, 1 µM, and 1.25 µM in DMSO) to see if we can achieve equal numbers of ICH+ and ICH- and compare the genotypes better. In future, also larger numbers of untreated heterozygous larvae could be observed to assess for any neurovascular instability.

Few studies so far have developed a clearing protocol in zebrafish, and none in the *alk1*$^{+/-}$*; kdrl:*GFP line.[65,319] Clearing enables three-dimensional imaging of an intact whole specimen without delicate tissue damage. This is advantageous compared to sectioning, which importantly results in tissue loss, but is also comparatively laborious and slow.[333] Sample destruction is a common result of automated sectioning.[320] Aqueous-based clearing has been used for smaller specimens such as insects.[334] Clearing based on organic solvents (e.g. FDISCO, 3DISCO) results in the greatest tissue shrinkage and transparency which markedly facilitates imaging, though it can be disadvantageous if the pre-treated specimen is small.[322] Dehydration also hardens the specimen but allows some flexibility to be retained to aid in handling. FDISCO has the added benefit of preserving endogenous fluorescence.[320] Organic solvent tissue clearing has been used to render transparency in large, fixed biological samples, in, for instance, mice, young rats, zebrafish, and tumour specimens.[334,65] Tissue sections can vary in thickness from several centimeters to ~100 µm. It has commonly been used in mice to study neurons, vessels, and amyloid plaques.[334,322] We used this technique as we required an intact specimen, three-dimensional imaging and a high resolution to detect the presence of a cAVM in a small zebrafish brain (average length ~4mm).[335]

While optimising our protocol for visualising the cerebral neurovasculature, we ran a pilot study. This involved subjecting genetically susceptible zebrafish (*alk1*$^{+/-}$*;kdrl:GFP*) to an angiogenic stimulus at the larval stage in the form of atorvastatin (which induced

intracerebral haemorrhage, i.e., a brain injury). These specimens' brains were then studied in adulthood using the developing protocol. If a cAVM was present, a tangle of abnormal vessels would be visible, either on the surface or in deeper structures: this was notably absent. Although no cAVM was identified in the four specimens studied, our protocol was successfully optimised. We did not look at sufficient numbers of specimens. Our study's main focus was to optimise the protocol for future larger studies. Based on existing literature, power calculations should be performed to determine appropriate sample sizes for identifying significant frequencies of the presence of cAVMs in ICH+ larvae in comparison to ICH-. Comparable mouse models noticed 89% of heterozygous specimens developed abnormal microvasculature (representative of cAVMs): this percentage may be anticipated in zebrafish specimens.[45]

Since our work to visualise the neurovasculature is very preliminary, there was limited detail of the precise vessels and anatomical sections of the brain. To improve the protocol, neuroanatomical sectioning of the brain should be performed prior to imaging with labels to assist with orientation. Colocalisation of arteries and veins could further assist identification of vessels, in particular in detecting a shunt between an artery and a vein.[336] This technique will have a transformative impact on the future imaging of cAVMs and other vascular abnormalities.

Future work could use this protocol for a larger scale study with zebrafish being imaged at a younger age, e.g. three months. This would be the start of adulthood, allowing us to study if an insult to the immature infant brain produces a cAVM in maturity.[337] Since it is unknown at what stage a cAVM would develop, if at all, the brains should be studied at monthly intervals: these different ages combined with the larger sample size would increase the chances of cAVM detection.

We used the angiogenic stimulus of spontaneous ICH (induced by ATV exposure). As described in section 1.7, other stimuli which could be attempted include exposure to agents to mimic a viral infection (using e.g. Polyinosinic: polycytidylic acid, poly (I:C)), fever, and dehydration. Poly(I:C) is an immunostimulant commonly used to induce anti-viral responses in vivo.[338] Fever could be imitated by placing larvae in an incubator with raised temperature e.g. at 34°C.

Reducing the volume of embryo water for harvesting larvae could be used to reproduce dehydration. Besides clinically relevant stimuli, a direct angiogenic stimulus such as VEGF could be injected through e.g. an adeno-associated viral vector.[339] The other aforementioned angiogenic factors, such as TGF, could also be directly introduced.

A further consideration for future optimisation of these protocols is through the use of other genetically modified zebrafish strains. A transgenic *eng* zebrafish model has been engineered as a model of HHT1 using TALENs. Since cAVMs are more common in this subtype of the disease, the use of this particular zebrafish strain in future work may be beneficial.[308,340] Unlike homozygous *alk1* models, the homozygous *eng* mutant zebrafish survive to adulthood. Endothelial cells cannot limit their surface areas in vessels deficient of *eng*. This leads to vessel dilatation, worsening pre-existing arteriovenous shunting, reminiscent of cAVMs. The *Notch 3* and *Notch 4* genes have been associated with AVMs.[341,57] Defective Notch signalling is present in zebrafish *mindbomb* (*mib*) mutants, which could also be used as models.[58] *Mib* encodes a ubiquitin ligase necessary for *Notch* signalling to be efficiently activated by Delta. The loss-of-function mutations in the mutants cause defects in vasculature. *Notch* signalling has also been inhibited by treatment using 10 µmol/L of LY411575, a gamma-secretase inhibitor from 23 to 48 hpf.[342] A transgenic *Notch3* specimen has been created by inserting a commercially available *notch3* allele, which was produced using insertional mutagenesis.[343]

To characterise cAVM pathology, different transgenic reporter backgrounds (other than the endothelial cell-specific lineage *kdrl:*GFP) could be used. These include the erythroid-specific *gata1*:dsRed,[344] neutrophil-specific BAC*mpo*:GFP,[345] endothelial cell and leucocyte-specific *fli1*:EGFP,[346] endothelial cell-specific double-transgenic *flt1*:YFP, *kdr-l*:RFP,[347] and macrophage-specific *mpeg1*:GAL4-Vp16/UAS:nfsB-mCherry and *mpeg1*:Gal4-VP16/UAS:Kaede/*mpx*:EGFP.[326] Trialling different reporter backgrounds might demonstrate improved vessel differentiation using certain backgrounds.

If these experiments result in cAVMs developing, novel therapeutic strategies could be attempted. One method would be pharmacological intervention to cause the lesion to regress or prevent it from becoming symptomatic. Anti-angiogenic agents are likely candidates, such as bevacizumab, which binds to VEGF, inhibiting its binding to cell-surface receptors and its

involvement in signalling pathways.[348] It is a recombinant humanised monoclonal antibody to VEGF. Another agent which blocks VEGF is aflibercept, a recombinant fusion VEGF protein, which binds to placental growth factor (PlGF), VEGF-A and VEGF-B.[348] These agents are currently used in chemotherapy. Tetracyclines (such as doxycycline) are matrix metalloproteinase inhibitors, which improve vascular stability and reduce the likelihood of rupture.[349] Thalidomide is an immunomodulator, which acts on the platelet-derived growth factor (PDGF)β receptor to enhance vascular pericyte coverage, stabilising the blood brain barrier, and could consequently, stabilise the cAVM, lessening haemorrhage risk.[349]

Another treatment strategy could involve gene therapy, targeting genes associated with cAVM development. VEGF could be blocked using soluble FMS-like tyrosine kinase 1 delivered using injected adeno-associated viral vector serotype-9. This has a high binding affinity for VEGF, thus inhibiting cAVM formation or reducing its severity.[350] Repression of *NOTCH-4* expression reverses vascular defects and AVMs: doxycycline could be orally administered to achieve this.[55] Overexpression of *ALK1* function could prevent AVM development.[351] This could be performed using drugs increasing *ALK1* expression or, less feasibly, viral delivery of wild-type *ALK1*.

Our innovative optimised protocol permits 3D visualisation of whole zebrafish brains. This could be used to investigate other cerebral vascular abnormalities, such as dural arteriovenous fistulae or cavernomas. It could likewise be used to image axons or monitor stem cell proliferation. Imaging axons would enable us to improve our understanding of neuroanatomy, how neural circuits function, and help to detect various diseases, including myelin pathologies, brain or spinal cord injury, and neurodegenerative disorders (e.g. multiple sclerosis). Stem cell proliferation is useful to observe to understand normal development and provide insight into the health of tissues. Better knowledge of neural stem cell proliferation and differentiation mechanisms furthers our understanding of cancer therapy and regenerative medicine.

Likely due to non-genetic reasons, the *alk1* zebrafish generation used did not breed optimally, so there was significant variation in egg quality and the likelihood of acquiring eggs from one week to another. As such, it was challenging to get adequate numbers of eggs for the

experiments. Transferring larvae from the petri dish to the nursery tank posed a comparable problem with survival.

Adult zebrafish, treated with atorvastatin at the larval stage, were imaged at advanced ages of 8 and 11 months, which was older than we planned (due to the pandemic). To enable a good penetration of the clearing solutions and immunohistochemistry, zebrafish eyes had to be enucleated. There was a risk of damage to cerebral parenchyma in the process. We were limited by the lens type used for two-photon microscopy as demonstrated by the poorer resolution of images in 11-month-old zebrafish specimens, compared to those eight months of age.

In conclusion, we implemented the two-hit hypothesis and an imaging protocol. We used ATV to induce ICH at the larval stage and raised to adulthood *alk1* heterozygous zebrafish larvae. We accomplished our objective in optimising an innovational protocol to image the entire adult *alk1* zebrafish neurovasculature. This protocol will, moving forward, be of undoubted practical benefit for multiple research groups, particularly in investigating cAVM development.

Chapter 5: General discussion

5.1 Major findings

The research work presented in this thesis has addressed the essential aims to (1) form a moderate agreement on the presence of angiogenesis on angiograms, (2) demonstrate that no consensus exists in the current literature when reporting the angioarchitecture of cAVMs, (3) optimise a protocol for visualisation of the neurovasculature in intact, fixed *alk1* adult zebrafish.

5.2 Detecting angiogenesis in angiograms

Apart from demonstrating a reliable identification of angiogenesis during both intra and inter-observer agreement, we also identified a moderate frequency of angiogenesis. Improving our understanding of angiogenesis is worthwhile as it can hinder obliteration. Incomplete embolisation after an AVM has been shown to induce angiogenesis, which often results in inadequate obliteration when followed by SRS.[352,291] Angiogenesis has been physically recognised intraoperatively in the form of perinidal friable vessels, that have poor quality walls.[353]

We found a significant association between angiogenesis and artery: vein ratio, as well as arterial ectasia. To the best of the author's knowledge, this has not been previously identified in the literature. This suggests that treating arterial ectasia may reverse the process of angiogenesis, which may, in turn, cause the cAVM to be less active. The hypothesis discussed in Chapter 1 where venous occlusion was thought to trigger angiogenesis led to the proposal of a questionnaire of mothers of cAVM patients to identify if any risk factors of childhood venous sinus thrombosis (a form of venous occlusion) occurred in utero or in early childhood.

The quality of angiograms was very variable which could have contributed to discrepancies in agreement. Image resolution for the older angiograms (prior to 2010) was poorer. Standardising the technique of angiography (e.g. having a minimum number of vessels injected) would aid future studies on observer agreement. As per the definition described in Section 2.1, the visualisation of angiogenesis is subjective, accounting for the variability in

detection. Parametric imaging, which is colour coded DSA, facilitates and allows the identification of angiogenesis to be more objective. It would consequently also enable easier measurements of the quantity of angiogenesis. The efficiency of image processing and visual recognition is improved with colour.[102] All the temporal data in a series of angiograms can be summarised using colour-intensity projection images into one composite image.[105] This could have a benefit for planning stereotactic treatment compared to using a single early phase DSA image. Other benefits of parametric imaging include measuring cerebral circulation's functionality[104] and improving the intra-operative recognition of cAVM vessel stenosis or shunting.[101]

When interpreting the angiograms, we noted the variability in reporting: consequently, we performed a systematic review to assess what the literature has published on AVM angioarchitecture. We also recognised that angiogenesis was rarely, if ever, reported. In our review of the literature, we therefore also noted whether angiogenesis was mentioned, described and quantified.

The observation of cAVM vessels using angiography, and particularly the use of parametric imaging, led to the proposal of using colocalisation to separately identify zebrafish arteries, veins, and subsequently, potentially detect angiogenesis. In our experiment, we were able to clearly visualise fluorescent vessels. However, there was no striking difference in the appearances of arteries compared to veins.

5.3 Systematic review on reporting of cAVM angioarchitecture

The review findings confirmed our suspicions that there is a lack of uniformity in the way cAVMs are reported, with the majority not following JWG recommendations. Only 48 studies (out of a total of 219) used the latter report's definitions, with 33 specifically reporting that they used the JWG standards. Numerous studies described novel angioarchitectural features additional to those mentioned in the JWG report.

Haemorrhage appeared to be the presentation which triggered the most publications describing cAVM angioarchitecture. Certain features were identified which were associated with a higher frequency of haemorrhage (Table 5.3.1): deep location,[89,110,114] periventricular location,[109] infratentorial location,[99,113] single draining vein,[99] long draining vein,[109] deep venous drainage,[110,111,99,113,114] single arterial feeder,[99,113] perforating feeder,[114] reduced venous ectasia,[110] presence of venous varices,[99] aneurysm occurrence,[99] fast arteriovenous shunting,[110] cAVM size <3cm[99] or ≥ 3cm.[111] Treating cAVMs with these features with greater urgency may help reduce cAVM morbidity and mortality. As discussed in Sections 1.3 and 1.7, studies correlated certain clinical features with specific angioarchitectural features, though the findings were not consistent enough to be able to devise a grading system (Table 5.3.1).

Table 5.3.1: Clinical features associated with cAVM angioarchitectural features

Clinical feature	Angioarchitectural feature
Haemorrhage	Deep location, periventricular location, infratentorial location, single draining vein, long draining vein, deep venous drainage, single arterial feeder, perforating feeder, reduced venous ectasia, venous varices, aneurysms, fast arteriovenous shunting, small <3cm or large cAVM size ≥ 3cm
Seizure	cortical location, temporal or frontal locations, absence of aneurysms, middle cerebral artery and cortical feeders, varices, long pial draining vein, venous congestion
Focal neurological deficit	vascular steal, venous ectasia, deep location

These features would need to be confirmed over several studies for it to be possible to use in a grading system. Certain studies have findings that contradict other study findings.

Similar to our angiogram review described in Chapter 2, only four studies assessed observer reliability in reporting cAVM angioarchitecture.[77,96,97,98] These studies are useful to demonstrate the variability in agreement in identifying cAVM features as a lack of standardisation in nomenclature contributes to the variability in management decisions.

Our systematic review used two databases for identifying eligible studies, which future work could improve on by expanding the number of databases. Additionally, we limited our search strategy to English and the published literature: in future, we could remove any language limitation and include the grey literature. We did not exclude studies that were of poor quality to ensure a comprehensive inclusion of the existing literature to assess the global use of the JWG standards. However, this meant that the majority of studies did not describe the full angioarchitecture.

Similar to the difficulties encountered in AVM nomenclature, intracranial cerebral aneurysms lack standardised terminology.[354] This would be useful to enable a shared language for research purposes, facilitating interpretation and a trustworthy comparison between different studies. Aneurysms occur in approximately 2% of the population, making them more prevalent than AVMs, further highlighting the importance of creating a uniform language with which to describe and report them.[355]

To date and to our knowledge, there have not been any publications exposing the significantly reduced adherence to the JWG report. National and international societies responsible for setting standards and guidelines for AVMs and their management can play a crucial role in advertising the JWG recommendations: the level of authority they possess means they are best placed for endorsing and disseminating such guidance. Another method of increasing usage of the recommended terminology would be for journals to request that any AVM-related submissions adhere to them.

5.4 Developing a zebrafish model of human cAVMs

Our experiment demonstrated that we can induce ICH in *alk1* heterozygous zebrafish larvae, and subsequently, raise them to adulthood. In the process, we developed a novel protocol to observe the cerebral vasculature in these intact adult specimens.

As far as we know, to date, there have not been any publications describing the production of ICH in *alk1+/-* zebrafish larvae using atorvastatin and raising them to adulthood. This has been performed in other transgenic embryos.[318,328] An ICH model using a chemical approach is advantageous as there is relative homogeneity in the ICH produced, and it is non-invasive (and hence, beneficial for animal welfare).

The two-photon microscope provided crystal clear images with high resolution but was time-consuming. It may also be challenging to obtain detailed structural information on the vasculature.[356] Light-sheet microscopy allows a larger area to be imaged with high acquisition speed. It may be possible to perform this without compromising on the resolution and would be an option for future work.[356] The optimised protocol could be used to further our understanding of tissue response to trauma by studying stem cell proliferation. The latter could also enhance our knowledge of ageing (in which stem cells become depleted) or of embryogenesis (where stem cells differentiate and give rise to new organs). Additionally, the protocol could enable studies on the immune system.

Unlike in our human angiogram study, we identified major zebrafish vessel types based on their anatomical location, but for smaller vessels, distinguishing between arteries and veins was far less straightforward. Colocalisation could enable us to make this distinction, facilitating the identification of a cAVM. One method involves double transgenic labelling with all endothelial cells (ECs) expressing GFP, and arterial ECs expressing red fluorescent protein: this enables veins (green) and arteries (yellow) to be differentiated.[336]

It may be possible to detect the development of a cAVM by labelling angiogenic factors in the adult zebrafish, at which stage normal vascular development is expected have been completed. Using a marker for VEGF or HIF-1a could help identify the occurrence of

angiogenesis. Fluorescent ligands which are analogues of anti-angiogenic $VEGF_{165}b$ have been used to label VEGF-A, which is then visualised using bioluminescence resonance energy transfer (BRET).[357] GFP has been used as a reporter to observe the transcriptional activity of HIF-1a with in vivo imaging using fluorescence resonance energy transfer (FRET).[358]

If cAVMs are identified, it may be that their incidence in *alk1* zebrafish would be 4.3% (similar to that of the general population) or higher (as noted in experimental mouse models discussed in Chapter 4).[7] Zebrafish *alk1* mutants can not only be used to study cAVMs, but also HHT and AVMs in other organs. Systemic AVMs are characteristic of HHT: specifically, in HHT2 (associated with the *ALK1* mutation) AVMs typically occur in the liver.[308,307] Telangiectasias are also common in the gastrointestinal tract. Identification of AVMs could be followed by trials to obliterate them using anti-angiogenic agents as discussed in Section 4.4.

5.5 Conclusion

Throughout this study, we have enhanced our understanding of the development of cAVMs. We propose an angiographic definition of cAVMs to consist of an abnormal tangle of blood vessels, with an artery feeding into a nidus, which drains into a vein, with the pathognomonic features being a shunt, a nidus and early venous drainage. We demonstrated it is possible to reliably identify angiogenesis on cAVM angiograms, and that angiogenesis is associated with arterial ectasia and artery: vein ratio. Our systematic review demonstrated a lack of standardisation when describing the angioarchitecture of cAVMs. We have successfully produced a protocol to observe the neurovasculature of an intact adult zebrafish model.

References

1. Kim H, Su H, Weinsheimer S, Pawlikowska L. Brain arteriovenous malformation pathogenesis: A response-to-injury paradigm. *Intracerebral Hemorrhage Res From Bench to Bedside*. 2011;(111):83-92. doi:http://dx.doi.org/10.1007/978-3-7091-0693-8_14
2. Valavanis A, Pangalu A, Tanaka M. Endovascular treatment of cerebral arteriovenous malformations with emphasis on the curative role of eembolisation. *Swiss Arch Neurol Psychiatry*. 2004;155(7):341-347.
3. Geibprasert S, Pongpech S, Jiarakongmun P, Shroff M, Armstrong D, Krings T. Radiologic assessment of brain arteriovenous malformations: What clinicians need to know. *Radiographics*. 2010;30(2):483-501. doi:http://dx.doi.org/10.1148/rg.302095728
4. Kim EJ, Vermeulen S, Li FJ, Newell DW. A review of cerebral arteriovenous malformations and treatment with stereotactic radiosurgery. *Transl Cancer Res*. 2014;3(4):399-410. doi:10.3978/j.issn.2218-676X.2014.07.07
5. Cockroft KM. Unruptured brain arteriovenous malformations should be treated conservatively: no. *Stroke*. 2007;38(12):3310-3311. doi:10.1161/STROKEAHA.107.504613
6. Choi JH, Mohr JP. Brain arteriovenous malformations in adults. *Lancet Neurol*. 2005;4(5):299-308. doi:10.1016/S1474-4422(05)70073-9
7. McCormick W, Rosenfield D. Massive brain hemorrhage: a review of 144 cases and an examination of their causes. *Stroke*. 1973;4(6):946-954.
8. Perret G, Nishioka H. An Analysis of 545 Cases of Cranio-Cerebral Arteriovenous Malformations and Fistulae Reported to the Cooperative Study. *Journak Neurosurg*. 1966;25:467-490.
9. Brown RJ, Wiebers D, Torner J, O'Fallon W. Incidence and prevalence of intracranial vascular malformations in Olmsted County, Minnesota, 1965 to 1992. *Neurology*. 1996;46(4):949-952.
10. Al-Shahi R, Fang J, Lewis S, Warlow C. Prevalence of adults with brain arteriovenous malformations: A community based study in Scotland using capture-recapture analysis. *J Neurol Neurosurg Psychiatry*. 2002;73(5):547-551. doi:10.1136/jnnp.73.5.547 LK - http://sfx.library.uu.nl/utrecht?sid=EMBASE&issn=00223050&id=doi:10.1136%2Fjnnp.73.5.547&atitle=Prevalence+of+adults+with+brain+arteriovenous+malformations%3A+A+community+based+study+in+Scotland+using+capture-recapture+analysis&stitle=J.+Neurol.+Neurosurg.+Psychiatry&title=Journal+of+Neurology+Neurosurgery+and+Psychiatry&volume=73&issue=5&spage=547&epage=551&aulast=Al-Shahi&aufirst=R.&auinit=R.&aufull=Al-Shahi+R.&coden=JNNPA&isbn=&pages=547-551&date=2002&auinit1=R&aui
11. Can A, Gross BA, Du R. The natural history of cerebral arteriovenous malformations. *Handb Clin Neurol Arter Cavernous Malformations*. 2017;143(Chapter 2):15-24. doi:10.3171/2012.10.JNS121280
12. Laakso A, Dashti R, Seppänen J, et al. Long-term excess mortality in 623 patients with brain arteriovenous malformations. *Neurosurgery*. 2008;63(2):244-253. doi:10.1227/01.NEU.0000320439.27895.24
13. Stapf C, Labovitz DL, Sciacca RR, Mast H, Mohr JP, Sacco RL. Incidence of adult brain arteriovenous malformation hemorrhage in a prospective population-based stroke

survey. *Cerebrovasc Dis*. 2002;13(1):43-46. doi:10.1159/000047745
14. Yasargil M. A Legacy of Microneurosurgery: Memoirs, Lessons, and Axioms. *Neurosurgery*. 1999;45(5).
15. Thomas J, Surendran S, Abraham D, Sasankan S, Bhaadri S, Rajavelu B. Gene expression analysis of nidus of cerebral arteriovenous malformations reveals vascular structures with deficient differentiation and maturation. *PLoS One*. 2018;13(6):e0198617. doi:http://dx.doi.org/10.1371/journal.pone.0198617
16. Moftakhar P, Hauptman J, Malkasian D, Martin N. Cerebral arteriovenous malformations. Part 1: cellular and molecular biology. *Neurosurg Focus*. 2009;26(5):1-15.
17. Vasudevan A, Bhide P. Monitoring endothelial cell development and migration in the embryonic CNS. *PROTOCOL*. 2008:1-4.
18. Kim H, Marchuk DA, Pawlikowska L, et al. Genetic considerations relevant to intracranial hemorrhage and brain arteriovenous malformations. *Acta Neurochir Suppl*. 2008;(105):199-206. doi:10.1007/978-3-211-09469-3_38
19. Hashimoto N, Nozaki K. Do cerebral arteriovenous malformations recur after angiographically confirmed total extirpation? *Crit Rev Neurosurg*. 1999;25(9(3)):141-146.
20. Deshpande DH, Vidyasagar C. Histology of the Persistent Embryonic Veins in Arteriovenous Malformations of the Brain. *Acta Neurochir (Wien)*. 1980;53:227-236.
21. Bederson J, Wiestler O, Brüstle O, Roth P, Frick R, Yaşargil M. Intracranial venous hypertension and the effects of venous outflow obstruction in a rat model of arteriovenous fistula. *Neurosurgery*. 1991;29(3):341-350.
22. Derdeyn CP, Zipfel GJ, Albuquerque FC, et al. Management of Brain Arteriovenous Malformations: A Scientific Statement for Healthcare Professionals from the American Heart Association/American Stroke Association. *Stroke*. 2017;48(8):e200-e224. doi:10.1161/STR.0000000000000134
23. Tanabe S, Uede T, Nonaka T, Ohtaki M, Hashi K. Diagnosis of cerebral arteriovenous malformations with three-dimensional CT angiography. *J Clin Neurosci*. 1998;5:33–38.
24. Josephson C, White P, Krishan A, Al-Shahi Salman R. Computed tomography angiography or magnetic resonance angiography for detection of intracranial vascular malformations in patients with intracerebral haemorrhage. *Cochrane Database Syst Rev*. 2014;9:CD009372. doi:10.1002/14651858.CD009372.pub2.
25. Spetzler R, Martin N. A proposed grading system for arteriovenous malformations. *J Neurosurg*. 1986;65(4):476-483.
26. Lawton M, Kim H, McCulloch C, Mikhak B, Young W. A Supplementary Grading Scale for Selecting Patients with Brain Arteriovenous Malformations for Surgery. *Neurosurgery*. 2010;66(4):702-713. doi:10.1227/01.NEU.0000367555.16733.E1.A
27. Pollock B, Flickinger J. A proposed radiosurgery-based grading system for arteriovenous malformations. *J Neurosurg*. 2002;96(1):79-85.
28. Starke RM, Komotar RJ, Otten ML, et al. Adjuvant embolization with n-butyl cyanoacrylate in the treatment of cerebral arteriovenous malformations: Outcomes, complications, and predictors of neurologic deficits. *Stroke*. 2009;40(8):2783-2790. doi:10.1161/STROKEAHA.108.539775
29. Valavanis A, Yasargil M. The endovascular treatment of brain arteriovenous malformations. *Adv Tech Stand Neurosurg*. 1998;24:131-214.
30. Committee JWG of the TA, Neuroradiology AS of I and T, Neurosurgery JS on C,

Surgeons a S of the AA of N. Reporting Terminology for Brain Arteriovenous Malformation Clinical and Radiographic Features for Use in Clinical Trials. *Stroke*. 2001;32(6):1430-1442. doi:10.1161/01.STR.32.6.1430

31. Al-Shahi R, Pal N, Lewis SC, Bhattacharya JJ, Sellar RJ, Warlow CP. Observer agreement in the angiographic assessment of arteriovenous malformations of the brain. *Stroke*. 2002;33(6):1501-1508. doi:10.1161/01.STR.0000018318.83802.18
32. The Arteriovenous Malformations Study Group. Arteriovenous Malformations of the Brain in Adults. *N Engl J Med*. 1999;340(23):1812-1818.
33. Panagiotopoulos V, Gizewski E, Asgari S, Regel J, Forsting M, Wanke I. Embolization of Intracranial Arteriovenous Malformations with Ethylene-Vinyl Alcohol Copolymer (Onyx). *Am J Neuroradiol*. 2009;30(1):99-106. doi:10.3174/ajnr.a1314
34. Gobin Y, Laurent A, Merienne L, et al. Treatment of brain arteriovenous malformations by embolization and radiosurgery. *J Neurosurg*. 1996;85(1):19-28.
35. Vollherbst DF, Chapot R, Bendszus M, Möhlenbruch MA. Glue, Onyx, Squid or PHIL? Liquid Embolic Agents for the Embolization of Cerebral Arteriovenous Malformations and Dural Arteriovenous Fistulas. *Clin Neuroradiol*. 2021. doi:10.1007/s00062-021-01066-6
36. Elsenousi A, Aletich VA, Alaraj A. Neurological outcomes and cure rates of embolization of brain arteriovenous malformations with n-butyl cyanoacrylate or Onyx: a meta-analysis. *J Neurointerv Surg*. 2016;8(3):265-272. doi:https://dx.doi.org/10.1136/neurintsurg-2014-011427
37. Lunsford L, Kondziolka D, Flickinger J, et al. Stereotactic radiosurgery for arteriovenous malformations of the brain. *J Neurosurg*. 1991;75(4):12-24.
38. Flickinger JC, Pollock BE, Kondziolka D, Lunsford LD. A dose-response analysis of arteriovenous malformation obliteration after radiosurgery. *Int J Radiat Oncol Biol Phys*. 1996;36(4):873-879. doi:10.1016/S0360-3016(96)00316-1
39. Lang M, Moore N, Rasmussen PA, Bain M. Treatment Outcomes of A Randomized Trial of Unruptured Brain Arteriovenous Malformation-Eligible Unruptured Brain Arteriovenous Malformation Patients. *Neurosurgery*. 2018;83(3):548-555.
40. Kano H, Flickinger JC, Yang H, et al. Stereotactic radiosurgery for Spetzler-Martin Grade III arteriovenous malformations. *J Neurosurg*. 2014;120(4):973-981. doi:10.3171/2013.12.jns131600
41. Mohr J, Parides M, Stapf C, et al. Medical management with or without interventional therapy for unruptured brain arteriovenous malformations (ARUBA): a multicentre, non-blinded, randomised trial. *Lancet*. 2014;383(9917):614-621.
42. Pawlikowska L, Tran M, Achrol A, et al. Polymorphisms in genes involved in inflammatory and angiogenic pathways and the risk of hemorrhagic presentation of brain arteriovenous malformations. *Stroke*. 2004;35(10):2294-2299. doi:http://dx.doi.org/10.1161/01.STR.0000141932.44613.b1
43. Kim H, Hysi PG, Pawlikowska L, et al. Common variants in interleukin-1-beta gene are associated with intracranial hemorrhage and susceptibility to brain arteriovenous malformation. *Cerebrovasc Dis*. 2009;27(2):176-182. doi:10.1159/000185609
44. Hashimoto T, Lawton M, Wen G, et al. Gene Microarray Analysis of Human Brain Arteriovenous Malformations. *Neurosurgery*. 2004;54(2):410-425. doi:http://dx.doi.org/10.1227/01.NEU.0000103421.35266.71
45. Xu B, Wu YQ, Huey M, et al. Vascular Endothelial Growth Factor Induces Abnormal Microvasculature in the Endoglin Heterozygous Mouse Brain. *J Cereb Blood Flow*

Metab. 2004;24(2):237-244. doi:10.1097/01.WCB.0000107730.66603.51
46. Hao Q, Zhu Y, Su H, et al. VEGF Induces More Severe Cerebrovascular Dysplasia in Eng+/- than in Alk1+/- Mice. *Transl Stroke Res*. 2010;1(3):197-201. doi:10.1007/s12975-010-0020-x
47. Chaloupka JC, Vinuela F, Robert J, Duckwiler GR. An in vivo arteriovenous malformation model in swine: Preliminary feasibility and natural history study. *Am J Neuroradiol*. 1994;15(5):945-950.
48. Pietilä T, Zabramski J, X A, et al. Animal Model for Cerebral Arteriovenous Malformation. *Acta Neurochir (Wien)*. 2000;142(11):1231–1240.
49. Wang S-S, Li C-H, Zhang X-J, Wang R-M. Investigation of the mechanism of dural arteriovenous fistula formation induced by high intracranial venous pressure in a rabbit model. *BMC Neurosci*. 2014;15(1):101. doi:10.1186/1471-2202-15-101
50. Choi E-J, Walker E, Shen F, et al. Minimal Homozygous Endothelial Deletion of Eng with VEGF Stimulation is Sufficient to Cause Cerebrovascular Dysplasia in the Adult Mouse. *Cerebrovasc Dis*. 2012;33(6):540-547. doi:10.1159/000337762.Minimal
51. Alsina-Sanchis E, Garcia-Ibanez Y, Figueiredo AM, et al. ALK1 loss results in vascular hyperplasia in mice and humans through PI3K activation. *Arterioscler Thromb Vasc Biol*. 2018;38(5):1216-1229. doi:10.1161/ATVBAHA.118.310760
52. Satomi J, Mount RJ, Toporsian M, et al. Cerebral vascular abnormalities in a murine model of hereditary hemorrhagic telangiectasia. *Stroke*. 2003;34(3):783-789. doi:10.1161/01.STR.0000056170.47815.37
53. Srinivasan S, Hanes MA, Dickens T, et al. A mouse model for hereditary hemorrhagic telangiectasia (HHT) type 2. *Hum Mol Genet*. 2003;12(5):473-482. doi:10.1093/hmg/ddg050
54. Hao Q, Zhu Y, Su H, et al. VEGF Induces More Severe Cerebrovascular Dysplasia in Eng+/- than in Alk1+/- Mice. *Transl Stroke Res*. 2010;1(3):197-201. doi:10.1007/s12975-010-0020-x
55. Carlson TR, Yan Y, Wu X, et al. Endothelial expression of constitutively active Notch4 elicits reversible arteriovenous malformations in adult mice. *Proc Natl Acad Sci U S A*. 2005;102(28):9884-9889. doi:10.1073/pnas.0504391102
56. Murphy PA, Lam MTY, Wu X, et al. Endothelial Notch4 signaling induces hallmarks of brain arteriovenous malformations in mice. *Proc Natl Acad Sci U S A*. 2008;105(31):10901-10906. doi:10.1073/pnas.0802743105
57. Hill-Felberg S, Wu HH, Toms SA, Dehdashti AR. Notch receptor expression in human brain arteriovenous malformations. *J Cell Mol Med*. 2015;19(8):1986-1993. doi:10.1111/jcmm.12580
58. Itoh M, Kim CH, Palardy G, et al. Mind bomb is a ubiquitin ligase that is essential for efficient activation of notch signaling by delta. *Dev Cell*. 2003;4(1):67-82. doi:10.1016/S1534-5807(02)00409-4
59. Walcott BP, Peterson RT. Zebrafish models of cerebrovascular disease. *J Cereb Blood Flow Metab*. 2014;34(4):571-577. doi:10.1038/jcbfm.2014.27
60. Corti P, Young S, Chen C-Y, et al. Interaction between alk1 and blood flow in the development of arteriovenous malformations. *Development*. 2011;138(8):1573-1582. doi:10.1242/dev.060467
61. Roman BL, Pham VN, Lawson ND, et al. Disruption of acvrl1 increases endothelial cell number in zebrafish cranial vessels. *Development*. 2002;129(12):3009-3019. http://www.ncbi.nlm.nih.gov/pubmed/12050147.

62. Walcott BP. BMP signaling modulation attenuates cerebral arteriovenous malformation formation in a vertebrate model. *J Cereb Blood Flow Metab*. 2014;34(10):1688-1694. doi:10.1038/jcbfm.2014.134
63. Kawasaki J, Aegerter S, Fevurly RD, et al. RASA1 functions in EPHB4 signaling pathway to suppress endothelial mTORC1 activity. *J Clin Invest*. 2014;124(6):2774-2784. doi:10.1172/JCI67084
64. Hartung T. Thoughts on limitations of animal models. *Park Relat Disord*. 2008;14(SUPPL.2):83-85. doi:10.1016/j.parkreldis.2008.04.003
65. Lindsey BW, Douek AM, Loosli F, Kaslin J. A whole brain staining, embedding, and clearing pipeline for adult zebrafish to visualize cell proliferation and morphology in 3-dimensions. *Front Neurosci*. 2018;11(JAN). doi:10.3389/fnins.2017.00750
66. Hao Q, Su H, Marchuk DA, et al. Increased tissue perfusion promotes capillary dysplasia in the ALK1-deficient mouse brain following VEGF stimulation. *Am J Physiol - Hear Circ Physiol*. 2008;295(6):2250-2256. doi:10.1152/ajpheart.00083.2008
67. Plate K. Mechanisms of Angiogenesis in the Brain. *J Neuropathol Exp Neurol*. 1999;58(4):313-320.
68. Adair T, Montani J. *Angiogenesis*.; 2010.
69. Krock BL, Skuli N, Simon MC. Hypoxia-Induced Angiogenesis: Good and Evil. *Genes and Cancer*. 2011;2(12):1117-1133. doi:10.1177/1947601911423654
70. Shweiki D, Itin A, Soffer D, Keshet E. Vascular endothelial growth factor induced by hypoxia may mediate hypoxia-initiated angiogenesis. *Nature*. 1992;359(6398):843-845. doi:10.1038/359843a0
71. Bergeron M, Yu AY, Solway KE, Semenza GL, Sharp FR. Induction of hypoxia-inducible factor-1 (HIF-1) and its target genes following focal ischaemia in rat brain. *Eur J Neurosci*. 1999;11(12):4159-4170. doi:10.1046/j.1460-9568.1999.00845.x
72. Pabaney AH, Reinard KA, Kole MK, et al. Management of arteriovenous malformations in the elderly: A single-center case series and analysis of outcomes. *J Neurosurg*. 2016;125(1):145-151. doi:http://dx.doi.org/10.3171/2015.6.JNS15293
73. Shidoh S, Kobayashi M, Akaji K, Kano T, Tanizaki Y, Mihara B. De Novo Arteriovenous Malformation after Aneurysm Clipping. *NMC case Rep J*. 2017;4(3):89-92. doi:10.2176/nmccrj.cr.2016-0272
74. Dlamini N, Billinghurst L, Kirkham FJ. Cerebral Venous Sinus (Sinovenous) Thrombosis in Children. *Neurosurg Clin N Am*. 2010;21(3):511-527. doi:10.1016/j.nec.2010.03.006
75. Geibprasert S, Pongpech S, Jiarakongmun P, Shroff M, Armstrong D, Krings T. Radiologic Assessment of Brain Arteriovenous Malformations: What Clinicians Need to Know. *RadioGraphics*. 2010;30(2):483-501.
76. Kozyrev D, Thiarawat P, Jahromi B, et al. "Dirty coagulation" technique as an alternative to microclips for control of bleeding from deep feeders during brain arteriovenous malformation surgery. *Acta Neurochir (Wien)*. 2017;159(5):855-859. doi:http://dx.doi.org/10.1007/s00701-017-3138-8
77. Al-Shahi R, Pal N, Lewis SC, Bhattacharya JJ, Sellar RJ. Observer agreement in the angiographic assessment of arteriovenous malformations of the brain. *Stroke*. 2002;33(6):1501-1508. doi:http://dx.doi.org/10.1161/01.STR.0000018318.83802.18
78. Kothari RU, Brott T, Broderick J, et al. The ABCs of Measuring Intracerebral Hemorrhage Volumes. *Stroke*. 1996;27(8):1304-1305. doi:10.1161/01.STR.27.8.1304
79. Won S-Y, Zagorcic A, Dubinski D, et al. Excellent accuracy of ABC/2 volume formula compared to computer-assisted volumetric analysis of subdural hematomas. *PLoS One*.

2018;13(6):e0199809-e0199809. doi:10.1371/journal.pone.0199809
80. Kandai S, Abdullah MS, Naing NN. Angioarchitecture of brain arteriovenous malformations and the risk of bleeding: An analysis of patients in Northeastern Malaysia. *Malaysian J Med Sci*. 2010;17(1):44-48.
81. Del Brutto OH, Mera RM, Costa AF, Del Brutto VJ. Basilar Artery Diameter Is Inversely Associated with Fetal Type Circle of Willis. *Eur Neurol*. 2017;78(3-4):217-220. doi:10.1159/000480430
82. Pico F, Labreuche J, Gourfinkel-An I, Amarenco P. Basilar artery diameter and 5-year mortality in patients with stroke. *Stroke*. 2006;37(9):2342-2347. doi:10.1161/01.STR.0000236058.57880.03
83. Tanaka M, Sakaguchi M, Miwa K, et al. Basilar artery diameter is an independent predictor of incident cardiovascular events. *Arterioscler Thromb Vasc Biol*. 2013;33(9):2240-2244. doi:10.1161/ATVBAHA.113.301467
84. Peduzzi P, Concato J, Kemper E, Holford T, Feinstein A. A Simulation Study of the Number of Events per Variable in Logistic Regression Analysis. *J Clin Epidemiol*. 1996;49(12):1373-1379. doi:10.1016/j.amepre.2003.12.002
85. Landis JR, Koch GG. The Measurement of Observer Agreement for Categorical Data Published by : International Biometric Society Stable URL : http://www.jstor.org/stable/2529310. *Biometrics*. 1977;33(1):159-174. doi:10.2307/2529310
86. Pollock BE, Flickinger JC, Lunsford LD, Bissonette DJ, Kondziolka D. Factors That Predict the Bleeding Risk of Cerebral Arteriovenous Malformations. *Stroke*. 1996;27(1):1-6.
87. Stapf C, Mast H, Sciacca RR, et al. Predictors of hemorrhage in patients with untreated brain arteriovenous malformation. *Neurology*. 2006;66(9):1350-1355. doi:http://dx.doi.org/10.1212/01.wnl.0000210524.68507.87
88. Kim H, Sidney S, McCulloch CE, et al. Racial/ethnic differences in longitudinal risk of intracranial hemorrhage in brain arteriovenous malformation patients. *Stroke*. 2007;38(9):2430-2437. doi:http://dx.doi.org/10.1161/STROKEAHA.107.485573
89. Yamada S, Takagi Y, Nozaki K, Kikuta K-I, Hashimoto N. Risk factors for subsequent hemorrhage in patients with cerebral arteriovenous malformations. *J Neurosurg*. 2007;107(5):965-972. doi:http://dx.doi.org/10.3171/JNS-07/11/0965
90. Hernesniemi J, Dashti R, Juvela S, Vaart K, Niemela M. Natural history of brain arteriovenous malformations: A long-term follow-up study of risk of hemorrhage in 238 patients. *Neurosurgery*. 2008;63(5):823-829. doi:http://dx.doi.org/10.1227/01.NEU.0000330401.82582.5E
91. Da Costa L, Wallace M, Ter Brugge K, O'Kelly C, Willinsky R, Tymianski M. The natural history and predictive features of hemorrhage from brain arteriovenous malformations. *Stroke*. 2009;40(1):100-105. doi:http://dx.doi.org/10.1161/STROKEAHA.108.524678
92. Al-Shahi R, Fang J, Lewis S. Prevalence of adults with brain arteriovenous malformations: A community based study in Scotland using capture-recapture analysis. *J Neurol Neurosurg Psychiatry*. 2002;73(5):547-551. doi:http://dx.doi.org/10.1136/jnnp.73.5.547
93. Al-Shahi R, Stapf C. The Prognosis and Treatment of Arteriovenous Malformations of the Brain. *Pract Neurol*. 2005;5(4):194-205. doi:10.1111/j.1474-7766.2005.00326.x
94. Lawton MT, Jacobowitz R, Spetzler RF. Redefined role of angiogenesis in the pathogenesis of dural arteriovenous malformations. *J Neurosurg*. 1997;87(2):267-274.

doi:10.3171/jns.1997.87.2.0267
95. Pico F, Jacob MP, Labreuche J, et al. Matrix metalloproteinase-3 and intracranial arterial dolichoectasia. *Ann Neurol*. 2010;67(4):508-515. doi:10.1002/ana.21922
96. Iancu-Gontard D, Weill A, Guilbert F, Nguyen T, Raymond J. Inter- and intraobserver variability in the assessment of brain arteriovenous malformation angioarchitecture and endovascular treatment results. *Am J Neuroradiol*. 2007;28(3):524-527. http://ovidsp.ovid.com/ovidweb.cgi?T=JS&PAGE=reference&D=emed10&NEWS=N&AN=46481898.
97. Braileanu M, Yang W, Caplan J, et al. Interobserver Agreement on Arteriovenous Malformation Diffuseness Using Digital Subtraction Angiography. 2016;95:535-541.
98. Du R, Dowd C, Johnston S, Young WL. Interobserver variability in grading of brain arteriovenous malformations using the Spetzler-Martin system. *Neurosurgery*. 2005;57(4). doi:http://dx.doi.org/10.1093/neurosurgery/57.4.668
99. Lv X, Wu Z, Jiang C, Yang X, Li Y, Sun Y. Angioarchitectural characteristics of brain arteriovenous malformations with and without hemorrhage. *World Neurosurg*. 2011;76(1-2):95-99. doi:http://dx.doi.org/10.1016/j.wneu.2011.01.044
100. Jayaraman M, Meyers P, Derdeyn CP, et al. Reporting standards for angiographic evaluation and endovascular treatment of cerebral arteriovenous malformations. *J Neurointerv Surg*. 2012;4(5):325-330. doi:http://dx.doi.org/10.1136/neurintsurg-2011-010173
101. Ionita C, Garcia V, Bednarek D, et al. Effect of injection technique on temporal parametric imaging derived from digital subtraction angiography in patient specific phantoms. *Proc SPIE Int Soc Opt Eng*. 2014:2-17. doi:10.1117/12.2041347.Effect
102. Cole BL, Maddocks JD, Sharpe K. Visual search and the conspicuity of coloured targets for Colour vision normal and Colour vision deficient Observers. *Clin Exp Optom*. 2004;87(4-5):294-304. doi:10.1111/j.1444-0938.2004.tb05058.x
103. Strother CM, Bender F, Deuerling-Zheng Y, et al. Parametric color coding of digital subtraction angiography. *Am J Neuroradiol*. 2010;31(5):919-924. doi:10.3174/ajnr.A2020
104. Benndorf G. Color-coded digital subtraction angiography: The end of a monochromatic era? *Am J Neuroradiol*. 2010;31(5):925-927. doi:10.3174/ajnr.A2077
105. Cover KS, Lagerwaard FJ, Van Den Berg R, Buis DR, Slotman BJ. Color intensity projection of digitally subtracted angiography for the visualization of brain arteriovenous malformations. *Neurosurgery*. 2007;60(3):511-514. doi:10.1227/01.NEU.0000255331.49791.B4
106. Moher D, Liberati A, Tetzlaff J, Altman DG. Preferred reporting items for systematic reviews and meta-analyses: The PRISMA statement. *BMJ*. 2009;339(7716):332-336. doi:10.1136/bmj.b2535
107. Lv X, Li Y, X. Y, C. J. Characteristics of arteriovenous malformations associated with cerebral aneurysms. *World Neurosurg*. 2011;76(3-4):288-291. doi:http://dx.doi.org/10.1016/j.wneu.2011.03.022
108. Lv X, Li Y, Yang X, Jiang C. Characteristics of brain arteriovenous malformations in patients presenting with nonhemorrhagic neurologic deficits. *World Neurosurg*. 2013;79(3-4):484-488. doi:http://dx.doi.org/10.1016/j.wneu.2012.04.006
109. Ma L, Kim H, Chen X-L, Wu C-X, Ma J, Su H. Morbidity after Hemorrhage in Children with Untreated Brain Arteriovenous Malformation. *Cerebrovasc Dis*. 2017;43(5-6):231-241. doi:http://dx.doi.org/10.1159/000458731

110. Ma L, Chen XL, Chen Y, Wu CX, Ma J, Zhao YL. Subsequent haemorrhage in children with untreated brain arteriovenous malformation: Higher risk with unbalanced inflow and outflow angioarchitecture. *Eur Radiol*. 2017;27(7):2868-2876. doi:10.1007/s00330-016-4645-3
111. Tong X, Wu J, Lin F, et al. Risk Factors for Subsequent Hemorrhage in Patients with Cerebellar Arteriovenous Malformations. *World Neurosurg*. 2016;92:47-57. doi:http://dx.doi.org/10.1016/j.wneu.2016.04.082
112. Tong X, Wu J, Lin F, et al. The Effect of Age, Sex, and Lesion Location on Initial Presentation in Patients with Brain Arteriovenous Malformations. *World Neurosurg*. 2016;87:598-606.
113. Tong X, Wu J, Lin F, et al. Cerebellar Arteriovenous Malformations: Clinical Feature, Risk of Hemorrhage and Predictors of Posthemorrhage Outcome. *World Neurosurg*. 2016;92:206-217. doi:http://dx.doi.org/10.1016/j.wneu.2016.05.006
114. Pan J, Feng L, Vinuela F, He H, Wu Z. Angioarchitectural characteristics associated with initial hemorrhagic presentation in supratentorial brain arteriovenous malformations. *Eur J Radiol*. 2013;82(11):1959-1963. doi:http://dx.doi.org/10.1016/j.ejrad.2013.05.015
115. Pan J, He H, Feng L, Vinuela F, Wu Z. Angioarchitectural characteristics associated with complications of embolization in supratentorial brain arteriovenous malformation. *Am J Neuroradiol*. 2014;35(2):354-359. doi:http://dx.doi.org/10.3174/ajnr.A3643
116. Du R, Keyoung H, Dowd C, Young W. The effects of diffuseness and deep perforating artery supply on outcomes after microsurgical resection of brain arteriovenous malformations. *Neurosurgery*. 2007;60(4):638-648. doi:http://dx.doi.org/10.1227/01.NEU.0000255401.46151.8A
117. Yang W, Westbroek E, Anderson-Keightly H, et al. Male gender associated with post-treatment seizure risk of pediatric arteriovenous malformation patients. *Neurosurgery*. 2017;80(6):899-906. doi:http://dx.doi.org/10.1093/neuros/nyx018
118. Yang W, Anderson-Keightly H, Westbroek E, et al. Long-term hemorrhagic risk in pediatric patients with arteriovenous malformations. *J neurosurg Pediatr*. 2016;18:329–338.
119. Ding D, Yen C-P, Xu Z, Starke R, Sheehan JP. Radiosurgery for low-grade intracranial arteriovenous malformations. *J Neurosurg*. 2014;121:457–467.
120. Ding D, Yen C-P, Starke RM, Xu Z, Sheehan JP. Radiosurgery for ruptured intracranial arteriovenous malformations. *J Neurosurg*. 2014;121:470–481.
121. Ding D, Starke R, Quigg M, et al. Cerebral Arteriovenous Malformations and Epilepsy, Part 1: Predictors of Seizure Presentation. *World Neurosurg*. 2015;84(3):645-652. doi:http://dx.doi.org/10.1016/j.wneu.2015.02.039
122. Ding D, Chen C, Starke R, et al. Risk of Brain Arteriovenous Malformation Hemorrhage Before and After Stereotactic Radiosurgery. *Stroke*. 2019;50(6):1384-1391. doi:http://dx.doi.org/10.1161/STROKEAHA.118.024230
123. Shakur SF, Amin-Hanjani S, Mostafa H, Charbel FT, Alaraj A. Hemodynamic Characteristics of Cerebral Arteriovenous Malformation Feeder Vessels with and Without Aneurysms. *Stroke*. 2015;46(7):1997-1999. doi:10.1161/STROKEAHA.115.009545
124. Shakur S, Valyi-Nagy T, Amin-Hanjani S, et al. Effects of nidus microarchitecture on cerebral arteriovenous malformation hemodynamics. *J Clin Neurosci*. 2016;26:70-74. doi:10.1016/j.jocn.2015.10.011

125. Shakur S, Amin-Hanjani S, H. M, V.A. A, F.T. C. Relationship of pulsatility and resistance indices to cerebral arteriovenous malformation angioarchitectural features and hemorrhage. *J Clin Neurosci*. 2016;33:119-123. doi:http://dx.doi.org/10.1016/j.jocn.2016.02.034
126. Stapf C, Connolly E, Schumacher H, Sciacca RR, H. M, J. P-S. Dysplastic vessels after surgery for brain arteriovenous malformations. *Stroke*. 2002;33(4):1053-1056. doi:http://dx.doi.org/10.1161/hs0402.105319
127. Stapf C, Mohr J, Pile-Spellman J, et al. Concurrent arterial aneurysms in brain arteriovenous malformations with haemorrhagic presentation. *J Neurol Neurosurg Psychiatry*. 2002;73(3):294-298. doi:http://dx.doi.org/10.1136/jnnp.73.3.294
128. Stapf C, Khaw A, Sciacca R, et al. Effect of Age on Clinical and Morphological Characteristics in Patients With Brain Arteriovenous Malformation. *Stroke*. 2003;34(11):2664-2669. doi:http://dx.doi.org/10.1161/01.STR.0000094824.03372.9B
129. Stapf C, Mast H, Sciacca R, et al. Predictors of hemorrhage in patients with untreated brain arteriovenous malformation. *Neurology*. 2006;66(9):1350-1355.
130. Choi JH, Mast H, Sciacca RR, et al. Clinical outcome after first and recurrent hemorrhage in patients with untreated brain arteriovenous malformation. *Stroke*. 2006;37(5):1243-1247. doi:10.1161/01.STR.0000217970.18319.7d
131. Choi J, Mast H, Hartmann A, Marshall R, Pile-Spellman J, J.P. M. Clinical and morphological determinants of focal neurological deficits in patients with unruptured brain arteriovenous malformation. *J Neurol Sci*. 2009;287(1-2):126-130. doi:http://dx.doi.org/10.1016/j.jns.2009.08.011
132. Ma L, Huang Z, Chen X-L, et al. Periventricular Location as a Risk Factor for Hemorrhage and Severe Clinical Presentation in Pediatric Patients with Untreated Brain Arteriovenous Malformations. *Am J Neuroradiol*. 2015;36(8):1550-1557. doi:http://dx.doi.org/10.3174/ajnr.A4300
133. Abla A, Nelson J, Rutledge W, Young W, Kim H, Lawton M. The natural history of AVM hemorrhage in the posterior fossa: comparison of hematoma volumes and neurological outcomes in patients with ruptured infra- and supratentorial AVMs. *Neurosurg Focus*. 2014;37(3):1-13.
134. Abla A, Nelson J, Kim H, Hess C, Tihan T, Lawton M. Silent Arteriovenous Malformation Hemorrhage and the Recognition of "Unruptured" Arteriovenous Malformation Patients Who Benefit From Surgical Intervention. *Neurosurgery*. 2015;76(5):592–600.
135. Tong X, Wu J, Lin F, et al. Risk Factors for Subsequent Hemorrhage in Patients with Cerebellar Arteriovenous Malformations. *World Neurosurg*. 2016;92(3):47-57. doi:10.1016/j.wneu.2016.04.082
136. Tong X, Wu J, Cao Y, et al. Microsurgical Outcome of Unruptured Brain Arteriovenous Malformations: A Single-Center Experience. *World Neurosurg*. 2017;99:644-655. doi:http://dx.doi.org/10.1016/j.wneu.2016.12.088
137. Lv X, Wu Z, Li Y, Jiang C, X. Y. Cerebral arteriovenous malformations associated with flow-related and circle of willis aneurysms. *World Neurosurg*. 2011;76(5):455-458. doi:http://dx.doi.org/10.1016/j.wneu.2011.04.015
138. Stein K-P, Wanke I, Forsting M, et al. Associated aneurysms in supratentorial arteriovenous malformations: Impact of aneurysm size on haemorrhage. *Cerebrovasc Dis*. 2015;39(2):122-129. doi:http://dx.doi.org/10.1159/000369958
139. Stein K-P, Wanke I, Forsting M, Oezkan N, Huetter B, Sandalcioglu I. Associated aneurysms in infratentorial arteriovenous malformations: Role of aneurysm size and

comparison with supratentorial lesions. *Cerebrovasc Dis*. 2016;41(5-6):219-225. doi:http://dx.doi.org/10.1159/000443540
140. Shakur S, Valyi-Nagy T, S. A-H, et al. Effects of nidus microarchitecture on cerebral arteriovenous malformation hemodynamics. *J Clin Neurosci*. 2016;26:70-74. doi:http://dx.doi.org/10.1016/j.jocn.2015.10.011
141. Shakur S, Amin-Hanjani S, M. A, et al. Changes in pulsatility and resistance indices of cerebral arteriovenous malformation feeder arteries after embolization and surgery. *Stroke*. 2016;124(1):7-12. doi:http://dx.doi.org/10.1080/01616412.2016.1258970
142. Shakur S, Amin-Hanjani S, H. M, F.T. C. Hemodynamic characteristics of cerebral arteriovenous malformation feeder vessels with and without aneurysms. *J Cereb Blood Flow Metab*. 2016;36(Supplement 1):167-168. doi:http://dx.doi.org/10.1177/0271678X16639009
143. Stefani M, Porter P, terBrugge KG, Montanera W, Willinsky R. Angioarchitectural factors present in brain arteriovenous malformations associated with hemorrhagic presentation. *Stroke*. 2002;33(4):920-924. doi:http://dx.doi.org/10.1161/01.STR.0000014582.03429.F7
144. Stefani M, Porter P, Terbrugge KG, Montanera W, Willinsky R. Large and deep brain arteriovenous malformations are associated with risk of future hemorrhage. *Stroke*. 2002;33(5):1220-1224. doi:http://dx.doi.org/10.1161/01.STR.0000013738.53113.33
145. Ding D, Starke R, Kano H, et al. Stereotactic radiosurgery for Spetzler-Martin Grade III arteriovenous malformations: An international multicenter study. *J Neurosurg*. 2017;126(3):859-871. doi:http://dx.doi.org/10.3171/2016.1.JNS152564
146. Di Rocco C, Tamburrini G, Rollo M. Cerebral arteriovenous malformations in children. *Acta Neurochir (Wien)*. 2000;142(2):145-158. doi:10.1007/s007010050017
147. Tong X, Wu J, Lin F, et al. Brain arteriovenous malformations in elderly patients: clinical features and treatment outcome. *Acta Neurochir (Wien)*. 2015;157(10):1645-1654. doi:http://dx.doi.org/10.1007/s00701-015-2521-6
148. Yen C-P, Schlesinger D. Natural history of cerebral arteriovenous malformations and the risk of hemorrhage after radiosurgery. A. N, H. K, L.D L, eds. *Gamma Knife Radiosurgery Brain Vasc Malformations*. 2013;27:5-21. doi:http://dx.doi.org/10.1159/000341616
149. Sahlein D, Mora P, Becske T, Huang P, Jafar J, Connolly E. Features predictive of brain arteriovenous malformation hemorrhage: Extrapolation to a physiologic model. *Stroke*. 2014;45(7):1964-1970. doi:http://dx.doi.org/10.1161/STROKEAHA.114.005170
150. Yi HJ, Hwang HS, Kim K, Shin I, Choi I. Angioarchitectural characteristics associated with the risk of hemorrhage in intracranial arteriovenous malformations. *Neurosurg Q*. 2016;26(4):329-335. doi:http://dx.doi.org/10.1097/WNQ.0000000000000193
151. Kubalek R, Moghtaderi A, Klisch J, Berlis A, Quiske A, Schumacher M. Cerebral arteriovenous malformations: Influence of angioarchitecture on bleeding risk. *Acta Neurochir (Wien)*. 2003;145(12):1045-1052. doi:10.1007/s00701-003-0143-x
152. Alexander M, Cooke D, Nelson J, et al. Association between Venous Angioarchitectural Features of Sporadic Brain Arteriovenous Malformations and Intracranial Hemorrhage. *AJNR Am J Neuroradiol*. 2015;36(5):949-952. doi:http://dx.doi.org/10.3174/ajnr.A4224
153. Kellner C, McDowell M, Phan M, et al. Number and location of draining veins in pediatric arteriovenous malformations: Association with hemorrhage. *J Neurosurg Pediatr*. 2014;14(5):538-545. doi:http://dx.doi.org/10.3171/2014.7.PEDS13563
154. Du X, Li X, Wang S, et al. Risk factors for hemorrhage in patients with cerebral

arteriovenous malformations. *Int J Clin Exp Med*. 2016;9(3):6649-6655. http://www.ijcem.com/files/ijcem0019824.pdf.
155. Ellis M, Armstrong D, Vachhrajani S, et al. Angioarchitectural features associated with hemorrhagic presentation in pediatric cerebral arteriovenous malformations. *J Neurointerv Surg*. 2013;5(3):191-195. doi:http://dx.doi.org/10.1136/neurintsurg-2011-010198
156. Reitz M, von Spreckelsen N, Vettorazzi E, et al. Angioarchitectural Risk Factors for Hemorrhage and Clinical Long-Term Outcome in Pediatric Patients with Cerebral Arteriovenous Malformations. *World Neurosurg*. 2016;89:540-551. doi:https://dx.doi.org/10.1016/j.wneu.2016.02.050
157. Niu H, Cao Y, Wang X, Xue X, Yu L, Yang M. Relationships between hemorrhage, angioarchitectural factors and collagen of arteriovenous malformations. *Neurosci Bull*. 2012;28(5):595-605. doi:http://dx.doi.org/10.1007/s12264-012-1271-1
158. Fok EWS, Poon WL, Tse KS, et al. Angiographic factors associated with haemorrhagic presentation of brain arteriovenous malformation in a Chinese paediatric population. *Hong Kong Med J = Xianggang yi xue za zhi*. 2015;21(5):401-406. doi:http://dx.doi.org/10.12809/hkmj144339
159. Jin H, Lenck S, Krings T, et al. Interval angioarchitectural evolution of brain arteriovenous malformations following rupture. *J Neurosurg*. 2019;131(1):96-103. doi:http://dx.doi.org/10.3171/2018.2.JNS18128
160. Illies T, Forkert N, Saering D, et al. Persistent hemodynamic changes in ruptured brain arteriovenous malformations. *Stroke*. 2012;43(11):2910-2915. doi:http://dx.doi.org/10.1161/STROKEAHA.112.669945
161. Todaka T, Hamada J, Kai Y, Morioka M, Ushio Y. Analysis of Mean Transit Time of Contrast Medium in Ruptured and Unruptured Arteriovenous Malformations: A Digital Subtraction Angiographic Study. 2003;34:2410-2414. doi:10.1161/01.STR.0000089924.43363.E3
162. Khaw A, Mohr J, Sciacca RR, et al. Association of Infratentorial Brain Arteriovenous Malformations with Hemorrhage at Initial Presentation. *Stroke*. 2004;35(3):660-663. doi:http://dx.doi.org/10.1161/01.STR.0000117093.59726.F9
163. Kim H, Al-Shahi Salman R, McCulloch C, Stapf C. Untreated brain arteriovenous malformation: Patient-level meta-analysis of hemorrhage predictors. *Neurology*. 2014;83(7):590-597. doi:http://dx.doi.org/10.1212/WNL.0000000000000688
164. Yu J, Nicholson A, Nelson J, et al. Predictors of intracranial hemorrhage volume and distribution in brain arteriovenous malformation. *Interv Neuroradiol*. 2018;24(2):183-188. doi:http://dx.doi.org/10.1177/1591019917749819
165. Huang Z, Peng K, Chen C, et al. A Reanalysis of Predictors for the Risk of Hemorrhage in Brain Arteriovenous Malformation. *J Stroke Cerebrovasc Dis*. 2018;27(8):2082-2087. doi:http://dx.doi.org/10.1016/j.jstrokecerebrovasdis.2018.03.003
166. Kim E, Halim A, Dowd C, et al. The relationship of coexisting extranidal aneurysms to intracranial hemorrhage in patients harboring brain arteriovenous malformations. *Neurosurgery*. 2004;54(6):1349-1358. doi:http://dx.doi.org/10.1227/01.NEU.0000124483.73001.12
167. Ai X, Ye Z, Xu J, You C. The factors associated with hemorrhagic presentation in children with untreated brain arteriovenous malformation: A meta-analysis. *J Neurosurg Pediatr*. 2019;23(3):343-354. doi:http://dx.doi.org/10.3171/2018.9.PEDS18262
168. Ding D, Starke RM, Kano H, et al. International multicenter cohort study of pediatric

brain arteriovenous malformations. Part 1: Predictors of hemorrhagic presentation. *J Neurosurg Pediatr*. 2017;19(2):127-135. doi:https://dx.doi.org/10.3171/2016.9.PEDS16283
169. Yang W, Liu A, Hung AL, et al. Lower Risk of Intracranial Arteriovenous Malformation Hemorrhage in Patients With Hereditary Hemorrhagic Telangiectasia. *Neurosurgery*. 2016;78(5):684-693. doi:https://dx.doi.org/10.1227/NEU.0000000000001103
170. Halim A, Johnston S, Singh V, et al. Longitudinal risk of intracranial hemorrhage in patients with arteriovenous malformation of the brain within a defined population. *Stroke*. 2004;35(7):1697-1702. doi:http://dx.doi.org/10.1161/01.STR.0000130988.44824.29
171. Miyasaka Y, Kurata A, Irikura K, Tanaka R, Fujii K. The influence of vascular pressure and angiographic characteristics on haemorrhage from arteriovenous malformations. *Acta Neurochir (Wien)*. 2000;142(1):39-43. doi:10.1007/s007010050005
172. Shakur S, Liesse K, Amin-Hanjani S, Carlson AP, Aletich VA, Charbel FT. Relationship of cerebral arteriovenous malformation hemodynamics to clinical presentation, angioarchitectural features, and hemorrhage. *Neurosurgery*. 2016;63(Supplement1):136-140. http://journals.lww.com/neurosurgery.
173. Dinc N, Won SY, Quick-Weller J, Berkefeld J, Seifert V, Marquardt G. Prognostic variables and outcome in relation to different bleeding patterns in arteriovenous malformations. *Neurosurg Rev*. 2019;42(3):731-736. doi:10.1007/s10143-019-01091-7
174. Yang W, Caplan J, Ye X, et al. Racial Associations with Hemorrhagic Presentation in Cerebral Arteriovenous Malformations. *World Neurosurg*. 2015;84(2):461-469. doi:http://dx.doi.org/10.1016/j.wneu.2015.03.050
175. Orning J, Amin-Hanjani S, Hamade Y, et al. Increased prevalence and rupture status of feeder vessel aneurysms in posterior fossa arteriovenous malformations. *J Neurointerv Surg*. 2016;8(10):1021-1024. doi:http://dx.doi.org/10.1136/neurintsurg-2015-012005
176. D'Aliberti G, Talamonti G, Cenzato M, et al. Arterial and venous aneurysms associated with arteriovenous malformations. *World Neurosurg*. 2015;83(2):188-196. doi:http://dx.doi.org/10.1016/j.wneu.2014.05.037
177. Guo Y, Saunders T, Su H, et al. Silent intralesional microhemorrhage as a risk factor for brain arteriovenous malformation rupture. *Stroke*. 2012;43(5):1240-1246. doi:10.1161/STROKEAHA.111.647263
178. Halim A, Singh V, Johnston S, et al. Characteristics of brain arteriovenous malformations with coexisting aneurysms: A comparison of two referral centers. *Stroke*. 2002;33(3):675-679. doi:http://dx.doi.org/10.1161/hs0302.104104
179. Hung AL, Yang W, Jiang B, et al. The Effect of Flow-Related Aneurysms on Hemorrhagic Risk of Intracranial Arteriovenous Malformations. *Clin Neurosurg*. 2019;85(4):466-475. doi:10.1093/neuros/nyy360
180. Huo X, Jiang Y, Lv X, Yang H, Zhao Y. Gamma Knife surgical treatment for partially embolized cerebral arteriovenous malformations. *J Neurosurg*. 2016;124(3):767-776. doi:http://dx.doi.org/10.3171/2015.1.JNS142711
181. Lockwood J, Scullen T, Mathkour M, et al. Endovascular Management of a Ruptured Basilar Perforator Artery Aneurysm Associated with a Pontine Arteriovenous Malformation: Case Report and Review of the Literature. *World Neurosurg*. 2018;116:159-162. doi:http://dx.doi.org/10.1016/j.wneu.2018.05.051
182. Zipfel G, Bradshaw P, Bova F. Do the morphological characteristics of arteriovenous malformations affect the results of radiosurgery? *J Neurosurg*. 2004;101(3):393-401.

doi:http://dx.doi.org/10.3171/jns.2004.101.3.0393
183. Riordan CP, Orbach DB, Smith ER, Scott RM. Acute fatal hemorrhage from previously undiagnosed cerebral arteriovenous malformations in children: A single-center experience. *J Neurosurg Pediatr*. 2018;22(3):244-250. doi:10.3171/2018.3.PEDS1825
184. Lv X, Wu Z, Jiang C, et al. Endovascular treatment accounts for a change in brain arteriovenous malformation natural history risk. *Interv Neuroradiol*. 2010;16(2):127-132. doi:http://dx.doi.org/10.1177/159101991001600203
185. Fullerton HJ, Achrol AS, Johnston SC, et al. Long-term hemorrhage risk in children versus adults with brain arteriovenous malformations. *Stroke*. 2005;36(10):2099-2104. doi:10.1161/01.STR.0000181746.77149.2b
186. Majumdar M, Tan LA, Chen M. Critical assessment of the morbidity associated with ruptured cerebral arteriovenous malformations. *J Neurointerv Surg*. 2016;8(2):163-167. doi:10.1136/neurintsurg-2014-011517
187. Sturiale CL, Puca A, Calandrelli R, et al. Relevance of bleeding pattern on clinical appearance and outcome in patients with hemorrhagic brain arteriovenous malformations. *J Neurol Sci*. 2013;324(1-2):118-123. doi:10.1016/j.jns.2012.10.016
188. Lai L-F, Chen J-X, Zheng K, et al. Posterior fossa brain arteriovenous malformations: Clinical features and outcomes of endovascular embolization, adjuvant microsurgery and radiosurgery. *Clin Neuroradiol*. 2018;28(1):17-24. doi:http://dx.doi.org/10.1007/s00062-016-0514-3
189. Lin T, Yang H, C.C. L, et al. Stasis index from hemodynamic analysis using quantitative DSA correlates with hemorrhage of supratentorial arteriovenous malformation: a cross-sectional study. *J Neurosurg*. 2020:1-9. doi:http://dx.doi.org/10.3171/2019.1.JNS183386
190. Schmidt N, Reitz M, Raimund F, Treszl A, Grzyska U, Westphal M. Clinical relevance of associated aneurysms with arteriovenous malformations of the posterior fossa. *Trends Neurovascular Surg*. 2011;(112):131-135. doi:http://dx.doi.org/10.1007/978-3-7091-0661-7_23
191. Tasic G, Jovanovic V, Djurovic B, et al. Natural course of the arteriovenous malformations of the brain initially presented by hemorrhage: analysis of a clinical series of 39 patients. *Turk Neurosurg*. 2011;21(3):280-289. http://ovidsp.ovid.com/ovidweb.cgi?T=JS&PAGE=reference&D=emed12&NEWS=N&AN=560003809.
192. Kouznetsov E, Weill A, Ghostine JS, Gentric JC, Raymond J, Roy D. Association between posterior fossa arteriovenous malformations and prenidal aneurysm rupture: Potential impact on management. *Neurosurg Focus*. 2014;37(3):37-40. doi:10.3171/2014.6.FOCUS14219
193. Burkhardt J, Chen X, Winkler EA, Cooke DL, Kim H. Delayed Venous Drainage in Ruptured Arteriovenous Malformations Based on Quantitative Color-Coded Digital Subtraction Angiography. *World Neurosurg*. 2017;104:619-627. doi:http://dx.doi.org/10.1016/j.wneu.2017.04.120
194. Shankar J, Menezes R, Pohlmann-Eden B, Wallace C, TerBrugge K, Krings T. Angioarchitecture of Brain AVM Determines the Presentation with Seizures: Proposed Scoring System. *Am J Neuroradiol*. 2013;34(5):1028 LP - 1034. doi:10.3174/ajnr.A3361
195. Jiang P, Lv X, Wu Z, Li Y, Jiang C, Yang X. Characteristics of brain arteriovenous malformations presenting with seizures without acute or remote hemorrhage. *Neuroradiol J*. 2011;24(6):886-888.

doi:http://dx.doi.org/10.1177/197140091102400610
196. Motebejane M, Royston D, Kabera G, Harrichandparsad R, Kaminsky I. Demographic and angioarchitectural features associated with seizures presentation in patients with brain arteriovenous malformations in Durban, KwaZulu-Natal, South Africa. *Interdiscip Neurosurg Adv Tech Case Manag*. 2018;11:14-18. doi:http://dx.doi.org/10.1016/j.inat.2017.09.010
197. Liu S, Chen HX, Mao Q, You C, Xu JG. Factors associated with seizure occurrence and long-term seizure control in pediatric brain arteriovenous malformation: A retrospective analysis of 89 patients. *BMC Neurol*. 2015;15(1):1-8. doi:10.1186/s12883-015-0402-5
198. Cordero-Tous N, Jorques-Infante AM, Santos-Martin L, et al. Angiographic characteristics of epileptogenic arteriovenous malformations and effectiveness in the seizure control after treatment with radiosurgery. *J radiosurgery SBRT*. 2014;3(2):103-110. http://www.ncbi.nlm.nih.gov/pubmed/29296391%0Ahttp://www.pubmedcentral.nih.gov/articlerender.fcgi?artid=PMC5675482.
199. Hoh B, Chapman P, Loeffler J, Carter B, Ogilvy CS. Results of multimodality treatment for 141 patients with brain arteriovenous malformations and seizures: factors associated with seizure incidence and seizure outcomes. *Neurosurgery*. 2002;51(2):303-311.
200. Galletti F, Costa C, Cupini LM, et al. Brain arteriovenous malformations and seizures: An Italian study. *J Neurol Neurosurg Psychiatry*. 2014;85(3):284-288. doi:http://dx.doi.org/10.1136/jnnp-2013-305123
201. Wu C-C, Guo W-Y, Chung W-Y, et al. Angioarchitecture and Posttreatment Magnetic Resonance Imaging Characteristics of Brain Arteriovenous Malformations and Long-Term Seizure Control After Radiosurgery. *World Neurosurg*. 2016;87:277-282. doi:http://dx.doi.org/10.1016/j.wneu.2015.10.070
202. Fierstra J, Conklin J, Krings T, et al. Impaired peri-nidal cerebrovascular reserve in seizure patients with brain arteriovenous malformations. *Brain*. 2011;134(1):100-109. doi:http://dx.doi.org/10.1093/brain/awq286
203. Benson JC, Chiu S, Flemming K, Nasr DM, Lanzino G, Brinjikji W. MR characteristics of unruptured intracranial arteriovenous malformations associated with seizure as initial clinical presentation. *J Neurointerv Surg*. 2020;12(2):186-191. doi:10.1136/neurintsurg-2019-015021
204. Ravindra V, Bollo R, Eli I, et al. A study of pediatric cerebral arteriovenous malformations: Clinical presentation, radiological features, and long-term functional and educational outcomes with predictors of sustained neurological deficits. *J Neurosurg Pediatr*. 2019;24(1):1-8. doi:http://dx.doi.org/10.3171/2019.2.PEDS18731
205. Hartmann A, Mast H, Mohr J, et al. Determinants of staged endovascular and surgical treatment outcome of brain arteriovenous malformations. *Stroke*. 2005;36(11):2431-2435. doi:http://dx.doi.org/10.1161/01.STR.0000185723.98111.75
206. Hartmann A, Pile-Spellman J, Stapf C, et al. Risk of endovascular treatment of brain arteriovenous malformations. *Stroke*. 2002;33(7):1816-1820. doi:http://dx.doi.org/10.1161/01.STR.0000020123.80940.B2
207. Jordan J, Llibre J. Predictors of neurological deficit after endovascular treatment of cerebral arteriovenous malformations and functional repercussions in prospective follow-up. *Neuroradiol J*. 2014;27(6):718-724. doi:http://dx.doi.org/10.15274/NRJ-

2014-10095
208. Ognard J, Magro E, Caroff J, Ben Salem D, Andouard S, Nonent M. A new time-resolved 3D angiographic technique (4D DSA): Description, and assessment of its reliability in Spetzler-Martin grading of cerebral arteriovenous malformations. *J Neuroradiol*. 2018;45(3):177-185. doi:http://dx.doi.org/10.1016/j.neurad.2017.11.004
209. Gauvrit J, Leclerc X, Oppenheim C, et al. Three-dimensional dynamic MR digital subtraction angiography using sensitivity encoding for the evaluation of intracranial arteriovenous malformations: A preliminary study. *Am J Neuroradiol*. 2005;26(6):1525-1531. http://ovidsp.ovid.com/ovidweb.cgi?T=JS&PAGE=reference&D=emed9&NEWS=N&AN=43733456.
210. Cuong N, Luu V, Tuan T, et al. Conventional digital subtractional vs non-invasive MR angiography in the assessment of brain arteriovenous malformation. *Clin Neurol Neurosurg*. 2018;169:29-33. doi:http://dx.doi.org/10.1016/j.clineuro.2018.03.022
211. Singh R, Gupta V, Ahuja C, Kumar A, Mukherjee K. Role of time-resolved-CTA in intracranial arteriovenous malformation evaluation at 128-slice CT in comparison with digital subtraction angiography. *Neuroradiol J*. 2018;31(3):235-243. doi:http://dx.doi.org/10.1177/1971400917744403
212. Paul L, Casasco A, Kusak M, Martinez N, G. R. Results for a series of 697 Arteriovenous malformations treated by gamma knife: Influence of angiographic features on the obliteration rate. *Neurosurgery*. 2014;75(5):568-582. doi:http://dx.doi.org/10.1227/NEU.0000000000000506
213. Tsuchiya K, Katase S, Yoshino A, J. H. MR-angiogram-added surface anatomy scanning of superficial cerebral arteriovenous malformations. *Eur Radiol*. 2002;12(9):2330-2334. http://ovidsp.ovid.com/ovidweb.cgi?T=JS&PAGE=reference&D=emed7&NEWS=N&AN=36940333.
214. Suzuki H, Maki H. Evaluation of cerebral arteriovenous malformations using image fusion combining three-dimensional digital subtraction angiography with magnetic resonance imaging. *Turk Neurosurg*. 2012;22(3):341-345. doi:http://dx.doi.org/10.5137/1019-5149.JTN.5527-11.0
215. Griessenauer CJ, Miller JH, Agee BS, et al. Observer reliability of arteriovenous malformations grading scales using current imaging modalities: Clinical article. *J Neurosurg*. 2014;120(5):1179-1187. doi:10.3171/2014.2.JNS131262
216. Willinsky RA, Goyal M, TerBrugge K, Montanera W, Wallace MC, Tymianski M. Embolisation of small (< 3 cm) brain arteriovenous malformations: Correlation of angiographic results to a proposed angioarchitecture grading system. *Interv Neuroradiol*. 2001;7(1):19-27. doi:10.1177/159101990100700102
217. Jiao, Lin F, Wu J, et al. A supplementary grading scale combining lesion-to-eloquence distance for predicting surgical outcomes of patients with brain arteriovenous malformations. *J Neurosurg*. 2018;128(2):530-540. doi:http://dx.doi.org/10.3171/2016.10.JNS161415
218. Robert T, Blanc R, Sylvestre P, et al. A proposed grading system to evaluate the endovascular curability of deep-seated arteriovenous malformations. *J Neurol Sci*. 2017;377:212-218. doi:10.1016/j.jns.2017.04.020
219. Neidert M, Lawton M, Mader M, et al. The AVICH Score: A Novel Grading System to Predict Clinical Outcome in Arteriovenous Malformation-Related Intracerebral Hemorrhage. *World Neurosurg*. 2016;92:292-297.

doi:http://dx.doi.org/10.1016/j.wneu.2016.04.080
220. Nisson PL, Fard SA, Walter CM, et al. A novel proposed grading system for cerebellar arteriovenous malformations. *J Neurosurg*. 2020;132(4):1105-1115. doi:10.3171/2018.12.JNS181677
221. Frisoli F, Lang S, Vossough A, et al. Intrarater and interrater reliability of the pediatric arteriovenous malformation compactness score in children: Clinical article. *J Neurosurg Pediatr*. 2013;11(5):547-551. doi:http://dx.doi.org/10.3171/2013.2.PEDS12465
222. Shankar JJS, Menezes RJ, Pohlmann-Eden B, Wallace C, TerBrugge K, Krings T. Angioarchitecture of brain AVM determines the presentation with seizures: Proposed scoring system. *Am J Neuroradiol*. 2013;34(5):1028-1034. doi:10.3174/ajnr.A3361
223. Shotar E, Debarre M, Sourour NA, et al. Retrospective study of long-term outcome after brain arteriovenous malformation rupture: The RAP score. *J Neurosurg*. 2018;128(1):78-85. doi:10.3171/2016.9.JNS161431
224. Ahmed A. Endovascular venous approach in the treatment of ruptured intra-cerebral arterio-venous malformation. *Egypt J Radiol Nucl Med*. 2014;45(2):439-441. doi:http://dx.doi.org/10.1016/j.ejrnm.2013.12.010
225. Downer J, Cellerini M, Corkill R, Lalloo S, Kuker W. Decision-making in the scheduling of endovascular treatment after brain arteriovenous malformation haemorrhage: A retrospective single centre study. *Neuroradiol J*. 2011;24(6):879-885. doi:http://dx.doi.org/10.1177/197140091102400609
226. Kocur D, Przybylko N, Hofman M, Jamroz T, Ignatowicz A, Baron J. Endovascular treatment of small cerebral arteriovenous malformations as a primary therapy. *Polish J Radiol*. 2018;83:e143-e150. doi:http://dx.doi.org/10.5114/pjr.2018.75621
227. Ledezma C, Hoh B, Carter B, Pryor J, Putman C. Complications of cerebral arteriovenous malformation embolization: Multivariate analysis of predictive factors. *Neurosurgery*. 2006;58(4):602-610. doi:http://dx.doi.org/10.1227/01.NEU.0000204103.91793.77
228. Liu J, Lv M, Lv X, He H, Liu A, Qian Z. Curative Glubran 2 embolization of cerebral arteriovenous malformations patient selection and initial results. *Interv Neuroradiol*. 2014;20(6):722-728. doi:http://dx.doi.org/10.15274/INR-2014-10063
229. Robert T, Blanc R, Ciccio G, et al. Endovascular treatment of posterior fossa arteriovenous malformations. *J Clin Neurosci*. 2016;25:65-68. doi:http://dx.doi.org/10.1016/j.jocn.2015.05.051
230. Sandalcioglu I, Asgari S, Wende D, et al. Proliferation activity is significantly elevated in partially embolized cerebral arteriovenous malformations. *Cerebrovasc Dis*. 2010;30(4):396-401. doi:http://dx.doi.org/10.1159/000319568
231. Soltanolkotabi M, Schoeneman S, Alden T, et al. Onyx embolization of intracranial arteriovenous malformations in pediatric patients: Clinical article. *J Neurosurg Pediatr*. 2011;3(4):A5-A6. doi:http://dx.doi.org/10.3171/2013.1.PEDS12286
232. Sorenson T, Lanzino G, Flemming K, Nasr D, S.Y. C, B.E. P. Clinical outcome of brainstem arteriovenous malformations after incomplete nidus obliteration. *J Clin Neurosci*. 2019;65:66-70. doi:http://dx.doi.org/10.1016/j.jocn.2019.03.009
233. Stein K-P, Wanke I, Oezkan N, et al. Multiple cerebral arterio-venous malformations: impact of multiplicity and hemodynamics on treatment strategies. *Acta Neurochir (Wien)*. 2016;158(12):2399-2407. doi:http://dx.doi.org/10.1007/s00701-016-2989-8
234. Haw C, Terbrugge K, Willinsky R. Complications of embolization of arteriovenous malformations of the brain. *J Neurosurg*. 2006;104(2):226-232. doi:http://dx.doi.org/10.3171/jns.2006.104.2.226

235. Viana D, De Castro-Afonso L, Nakiri G, Monsignore L, Trivelato F, B.O. C. Extending the indications for transvenous approach embolization for superficial brain arteriovenous malformations. *J Neurointerv Surg*. 2017;9(11):1053-1059. doi:http://dx.doi.org/10.1136/neurintsurg-2017-013113
236. Weber W, Kis B, Siekmann R, Kuehne D. Endovascular treatment of intracranial arteriovenous malformations with onyx: Technical aspect. *Am J Neuroradiol*. 2007;28(2):371-377. http://ovidsp.ovid.com/ovidweb.cgi?T=JS&PAGE=reference&D=emed10&NEWS=N&AN=46281065.
237. Zheng T, Wang Q, Liu Y-Q, et al. Clinical features and endovascular treatment of intracranial arteriovenous malformations in pediatric patients. *Child's Nerv Syst*. 2014;30(4):647-653. doi:http://dx.doi.org/10.1007/s00381-013-2277-3
238. Zhu G, Li G, He X, et al. Endovascular treatment of cerebellar arteriovenous malformations: management of associated aneurysms first or later. *Neurol Sci*. 2016;37(1):67-72. doi:http://dx.doi.org/10.1007/s10072-015-2359-y
239. Hung Y, Mohammed N, Jose T, et al. The impact of preradiosurgery embolization on intracranial arteriovenous malformations: a matched cohort analysis based on de novo lesion volume. *J Neurosurg*. 2020;133(October):1156-1167. doi:10.3171/2019.5.JNS19722.J
240. Iosif C, De Lucena A, Abreu-Mattos L, et al. Curative endovascular treatment for low-grade Spetzler-Martin brain arteriovenous malformations: A single-center prospective study. *J Neurointerv Surg*. 2019;11(7):699-705. doi:http://dx.doi.org/10.1136/neurintsurg-2018-014390
241. Jayaraman M, Marcellus ML, Hamilton S, et al. Neurologic complications of arteriovenous malformation embolization using liquid embolic agents. *Am J Neuroradiol*. 2008;29(2):242-246. doi:http://dx.doi.org/10.3174/ajnr.A0793
242. Luo C, Guo W, Teng M, et al. Fistula components of brain arteriovenous malformations: Angioarchitecture analysis and embolization prior to gamma-knife surgery. *J Chinese Med Assoc*. 2014;156(1):85-92. doi:http://dx.doi.org/10.1016/j.jcma.2013.01.011
243. Mangiafico S, Cellerini M, Villa G, Nistri M, Ammannati F. Disappearance of a cerebral arteriovenous malformation after partial endovascular embolisation. *Interv Neuroradiol*. 2001;7(1):41-46. http://ovidsp.ovid.com/ovidweb.cgi?T=JS&PAGE=reference&D=emed7&NEWS=N&AN=32509698.
244. Stiefel M, Al-Okaili R, Weigele J, Hurst R. De novo aneurysm formation and regression after brain arteriovenous malformation embolization: case report. *Surg Neurol*. 2007;67(1):99-101. doi:http://dx.doi.org/10.1016/j.surneu.2006.02.046
245. Van Rooij W, Jacobs S, Sluzewski M, Van Der Pol B, Beute G. Curative embolization of brain arteriovenous malformations with onyx: Patient selection, embolization technique, and results. *Am J Neuroradiol*. 2012;33(7):1299-1304. doi:http://dx.doi.org/10.3174/ajnr.A2947
246. Iosif C, Mendes GAC, Saleme S, et al. Endovascular transvenous cure for ruptured brain arteriovenous malformations in complex cases with high Spetzler-Martin grades. *J Neurosurg*. 2015;122(5):1229-1238. doi:http://dx.doi.org/10.3171/2014.9.JNS141714
247. Robert T, Blanc R, Ciccio G, et al. Angiographic factors influencing the success of endovascular treatment of arteriovenous malformations involving the corpus callosum. *J Neurointerv Surg*. 2015;7(10):715-720.

doi:https://dx.doi.org/10.1136/neurintsurg-2014-011271
248. Blanc R, Seiler A, Robert T, et al. Multimodal angiographic assessment of cerebral arteriovenous malformations: a pilot study. *J Neurointerv Surg*. 2015;7(11):841-847. doi:https://dx.doi.org/10.1136/neurintsurg-2014-011402
249. Morgan M, Patel N, Simons M, Ritson E. Influence of the combination of patient age and deep venous drainage on brain arteriovenous malformation recurrence after surgery. *J Neurosurg*. 2012;117(5):934-941. doi:http://dx.doi.org/10.3171/2012.8.JNS12351
250. Morgan M, Hermann Wiedmann M, Stoodley MA. Microsurgery for Spetzler-Ponce Class A and B arteriovenous malformations utilizing an outcome score adopted from Gamma Knife radiosurgery: A prospective cohort study. *J Neurosurg*. 2017;127(5):1105-1116. doi:http://dx.doi.org/10.3171/2016.8.JNS161275
251. Nisson P, Fard SA, Meybodi AT, et al. The Unique Features and Outcomes of Microsurgically Resected Cerebellar Arteriovenous Malformations. *World Neurosurg*. 2018;120:e940-e949. doi:http://dx.doi.org/10.1016/j.wneu.2018.08.194
252. Pai B, Nagaraj N. Is Temporary Proximal Artery Clipping in Arteriovenous Malformation Surgery Safe? *Turk Neurosurg*. 2019;29(2):164-170. doi:http://dx.doi.org/10.5137/1019-5149.JTN.22071-17.2
253. Potts M, Young WL. Deep arteriovenous malformations in the basal ganglia, thalamus, and insula: Microsurgical management, techniques, and results. *Neurosurgery*. 2013;73(3):417-429. doi:http://dx.doi.org/10.1227/NEU.0000000000000004
254. Tanaka K, Matsumoto S, Yamada T, et al. Elevated end-diastolic ratio of the common carotid artery due to cerebral arteriovenous malformation: Two case reports. *Radiol Case Reports*. 2018;13(4):917-920. doi:http://dx.doi.org/10.1016/j.radcr.2018.06.007
255. Donzelli G, Nelson J, McCoy D, et al. The effect of preoperative embolization and flow dynamics on resection of brain arteriovenous malformations. *J Neurosurg*. 2019:1-9. doi:http://dx.doi.org/10.3171/2019.2.JNS182743
256. Zhao J, Wang S, Li J, Qi W, Sui D, Zhao Y. Clinical characteristics and surgical results of patients with cerebral arteriovenous malformations. *Surg Neurol*. 2005;63(2):156-161. doi:10.1016/j.surneu.2004.04.021
257. Pohjola A, Lehto H, Hafez A, Oulasvirta E, Koroknay-Pal P. Arteriovenous Malformations of the Posterior Fossa: Focus on Surgically Treated Patients Presenting with Hemorrhage. *World Neurosurg*. 2018;116:e934-e943. doi:http://dx.doi.org/10.1016/j.wneu.2018.05.138
258. Han SJ, Englot DJ, Kim H, Lawton MT. Brainstem arteriovenous malformations: anatomical subtypes, assessment of “occlusion in situ” technique, and microsurgical results. *J Neurosurg*. 2015;122(1):107-117. doi:https://dx.doi.org/10.3171/2014.8.JNS1483
259. Liu L, Li H, Zheng J, Wang S, Zhao J. Sylvian fissure arteriovenous malformations: Long-term prognosis and risk factors. *Neurosurg Rev*. 2013;36(4):541-549. doi:http://dx.doi.org/10.1007/s10143-013-0470-1
260. Maher CO, Scott RM. Linear vein-based arteriovenous malformations in children: Clinical article. *J Neurosurg Pediatr*. 2009;4(1):12-16. doi:10.3171/2009.1.PEDS08329
261. Lang S-S, Beslow L, Bailey R, Vossough A, Ekstrom J, G.G. H. Follow-up imaging to detect recurrence of surgically treated pediatric arteriovenous malformations: Clinical article. *J Neurosurg Pediatr*. 2012;9(5):497-504. doi:http://dx.doi.org/10.3171/2012.1.PEDS11453

262. Taeshineetanakul P, Krings T, Geibprasert S, et al. Angioarchitecture determines obliteration rate after radiosurgery in brain arteriovenous malformations. *Neurosurgery*. 2012;71(6):1071-1078. doi:10.1227/NEU.0b013e31826f79ec
263. Kasliwal M, Kale S, Gupta A, Kiran N, Sharma M. Outcome after hemorrhage following Gamma Knife surgery for cerebral arteriovenous malformations: Clinical article. *J Neurosurg*. 2009;110(5):1003-1009. doi:http://dx.doi.org/10.3171/2008.10.17675
264. Machnowska M, Taeshineetanakul P, Geibprasert S, et al. Factors determining the clinical complications of radiosurgery for AVM. *Can J Neurol Sci*. 2013;40(6):807-813. doi:http://dx.doi.org/10.1017/S0317167100015936
265. Nagaraja S, Lee K, Coley S, et al. Stereotactic radiosurgery for brain arteriovenous malformations: Quantitative MR assessment of nidal response at 1 year and angiographic factors predicting early obliteration. *Neuroradiology*. 2006;48(11):821-829. doi:http://dx.doi.org/10.1007/s00234-006-0131-y
266. Parkhutik V, Lago A, Tembl J, Vazquez J, Aparici F, Mainar E. Postradiosurgery hemorrhage rates of arteriovenous malformations of the brain: Influencing factors and evolution with time. *Stroke*. 2012;43(5):1247-1252. doi:http://dx.doi.org/10.1161/STROKEAHA.111.635789
267. Hu YS, Lee CC, Wu HM, et al. Stagnant venous outflow predicts brain arteriovenous malformation obliteration after gamma knife radiosurgery without prior intervention. *Neurosurgery*. 2020;87(2):338-347. doi:10.1093/neuros/nyz507
268. Daou BJ, Palmateer G, Thompson BG, et al. Stereotactic Radiosurgery for Brain Arteriovenous Malformations: Evaluation of Obliteration and Review of Associated Predictors. *J Stroke Cerebrovasc Dis*. 2020;29(8):1-9. doi:10.1016/j.jstrokecerebrovasdis.2020.104863
269. Robert T, Blanc R, Ciccio G, et al. Angiographic factors influencing the success of endovascular treatment of arteriovenous malformations involving the corpus callosum. *J Neurointerv Surg*. 2015;7(10):715-720. doi:http://dx.doi.org/10.1136/neurintsurg-2014-011343.121
270. van den Berg R, Buis D, Lagerwaard F, Lycklama A Nijeholt G. Extensive white matter changes after stereotactic radiosurgery for brain arteriovenous malformations: A prognostic sign for obliteration? *Neurosurgery*. 2008;63(6):1064-1069. doi:http://dx.doi.org/10.1227/01.NEU.0000330413.73983.02
271. Nishino K, Hasegawa H, Morita K, Fukuda M, Ito Y, Y. F. Clinical characteristics of arteriovenous malformations in the cerebellopontine angle cistern. *J Neurosurg*. 2017;126(1):60-68. doi:http://dx.doi.org/10.3171/2015.12.JNS152190
272. Anderson R, McDowell, Kellner C, et al. Arteriovenous malformation-associated aneurysms in the pediatric population: Clinical article. *J Neurosurg Pediatr*. 2012;9(1):11-16. doi:http://dx.doi.org/10.3171/2011.10.PEDS11181
273. Brunozzi D, Amin-Hanjani S, Charbel FT, Mohammaden M, A. A. Ratio of arteriovenous malformation draining vein to adjacent venous sinus diameter is associated with increased risks of vein stenosis. *Stroke*. 2019;50(Supplement 1). doi:http://dx.doi.org/10.1161/str.50.suppl_1.TP579
274. Yi HJ, Hwang HS, Kim KS, Shin IY, Choi I, Jang IB. Angioarchitectural characteristics associated with the risk of hemorrhage in intracranial arteriovenous malformations. *Neurosurg Q*. 2016;26(4):329-335. doi:10.1097/WNQ.0000000000000193
275. Chowdhury AH, Khan SU, Rahman KM, et al. Clinical and morphological pattern of brain arteriovenous malformations (BAVMs) in a Tertiary Care Hospital in Bangladesh

Neurology. *BMC Res Notes*. 2015;8(1):1-7. doi:10.1186/s13104-015-1717-4
276. Da Costa LD, Thines L, Dehdashti AR, et al. Management and clinical outcome of Posterior fossa arteriovenous malformations: Report on a singlecentre 15-year experience. *J Neurol Neurosurg Psychiatry*. 2009;80(4):376-379. doi:10.1136/jnnp.2008.152710
277. Dos Santos M, Demartini Jr. Z, Matos L, Spotti A, Tognola W, A.A. DS. Angioarchitecture and clinical presentation of brain arteriovenous malformations. *Arq Neuropsiquiatr*. 2009;67(2 A):316-321. doi:http://dx.doi.org/10.1590/S0004-282X2009000200031
278. Fukuda K, Majumdar M, Masoud H, et al. Multicenter assessment of morbidity associated with cerebral arteriovenous malformation hemorrhages. *J Neurointerv Surg*. 2017;9(7):664-668. doi:https://dx.doi.org/10.1136/neurintsurg-2016-012485
279. Garcin B, Houdart E, Porcher R, Manchon E, Saint-Maurice J, D. B. Epileptic seizures at initial presentation in patients with brain arteriovenous malformation. *Neurology*. 2012;78(9):626-631. doi:http://dx.doi.org/10.1212/WNL.0b013e3182494d40
280. Hofmeister C, Stapf C, Hartmann A, et al. Demographic, Morphological, and Clinical Characteristics of 1289 Patients With Brain Arteriovenous Malformation. *Stroke*. 2000;31:1307-1310.
281. Ma L, Huang Z, Chen X-L, et al. Periventricular Location as a Risk Factor for Hemorrhage and Severe Clinical Presentation in Pediatric Patients with Untreated Brain Arteriovenous Malformations. *AJNR Am J Neuroradiol*. 2015;36(8):1550-1557. doi:https://dx.doi.org/10.3174/ajnr.A4300
282. Yang W, Caplan JM, Ye X, et al. Racial Associations with Hemorrhagic Presentation in Cerebral Arteriovenous Malformations. *World Neurosurg*. 2015;84(2):461-469. doi:https://dx.doi.org/10.1016/j.wneu.2015.03.050
283. Imbesi SG, Knox K, Kerber CW. Reproducibility Analysis of a New Objective Method for Measuring Arteriovenous Malformation Nidus Size at Angiography. *AJNR Am J Neuroradiol*. 2002;23(March):412-415.
284. Ozyurt O, Dincer A, Erdem Yildiz M, et al. Integration of arterial spin labeling into stereotactic radiosurgery planning of cerebral arteriovenous malformations. *J Magn Reson Imaging*. 2017;46(6):1718-1727. doi:http://dx.doi.org/10.1002/jmri.25690
285. Luo J, Lv X, Jiang C, Wu Z. Brain AVM characteristics and age. *Eur J Radiol*. 2012;81(4):780-783. doi:10.1016/j.ejrad.2011.01.086
286. Brunozzi D, A.E. H, S.F. S, A. L, C.-Y. H, F.T. C. Contrast time-density time on digital subtraction angiography correlates with cerebral arteriovenous malformation flow measured by quantitative magnetic resonance angiography, angioarchitecture, and hemorrhage. *Clin Neurosurg*. 2018;83(2):210-216. doi:http://dx.doi.org/10.1093/neuros/nyx351
287. Panni P, Gallotti AL, Gigliotti CR, et al. Impact of flow and angioarchitecture on brain arteriovenous malformation outcome after gamma knife radiosurgery: the role of hemodynamics and morphology in obliteration. *Acta Neurochir (Wien)*. 2020;162(7):1749-1757. doi:10.1007/s00701-020-04351-4
288. Mohr J, Kejda-Scharler J. Diagnosis and treatment of arteriovenous malformations topical collection on stroke. *Curr Neurol Neurosci Rep*. 2013;13(2):324. doi:http://dx.doi.org/10.1007/s11910-012-0324-1
289. Shankar J, Menezes R, B. P-E, C. W, K. T. Angioarchitecture of brain AVM determines the presentation with seizures: Proposed scoring system. *Am J Neuroradiol*. 2013;34(5):1028-1034. doi:http://dx.doi.org/10.3174/ajnr.A3361

290. Valavanis A, Pangalu A. Endovascular treatment of cerebral arteriovenous malformations with emphasis on the curative role of embolisation. *Interv Neuroradiol*. 2005;11(7):341-347. http://ovidsp.ovid.com/ovidweb.cgi?T=JS&PAGE=reference&D=emed9&NEWS=N&AN=41645453.
291. Taeshineetanakul P, Schwartz ML, S. G, et al. Angioarchitecture determines obliteration rate after radiosurgery in brain arteriovenous malformations. *Neurosurgery*. 2011;71(SUPPL. 1):61-62. doi:http://dx.doi.org/10.1227/NEU.0b013e31826f79ec
292. Chen X, Cooke DL, D. S, et al. Higher flow is present in unruptured arteriovenous malformations with Silent intralesional microhemorrhages. *Stroke*. 2017;48(10):2881-2884. doi:http://dx.doi.org/10.1161/STROKEAHA.117.017785
293. Fierstra J, Spieth S, L. T, et al. Severely impaired cerebrovascular reserve in patients with cerebral proliferative angiopathy. *J Neurosurg Pediatr*. 2011;17(SUPPL. 1):310-315. doi:http://dx.doi.org/10.3171/2011.6.PEDS1170
294. Wu C-C, Guo W-Y, Chung W-Y, Wu H-M. Angioarchitecture and Posttreatment Magnetic Resonance Imaging Characteristics of Brain Arteriovenous Malformations and Long-Term Seizure Control After Radiosurgery. 2016;87:277-282.
295. de Castro-Afonso L, Nakiri G, Oliveira R, Santos M, A.C.D. S, H.R. M. Curative embolization of pediatric intracranial arteriovenous malformations using Onyx: the role of new embolization techniques on patient outcomes. *Neuroradiology*. 2016;58(6):585-594. doi:http://dx.doi.org/10.1007/s00234-016-1666-1
296. L. M, Y. C, Ma L, et al. Subsequent haemorrhage in children with untreated brain arteriovenous malformation: Higher risk with unbalanced inflow and outflow angioarchitecture. *Eur Radiol*. 2017;27(7):2868-2876. doi:http://dx.doi.org/10.1007/s00330-016-4645-3
297. Ogilvy CS, Stieg PE, Awad I, et al. Recommendations for the management of intracranial arteriovenous malformations: A statement for healthcare professionals from a special writing group of the Stroke Council, American Stroke Association. *Circulation*. 2001;103(21):2644-2657. doi:10.1161/01.CIR.103.21.2644
298. Robb L, Elefanty AG. The hemangioblast - An elusive cell captured in culture. *BioEssays*. 1998;20(8):611-614. doi:10.1002/(SICI)1521-1878(199808)20:8<611::AID-BIES3>3.0.CO;2-L
299. Mancuso M, Kuhnert F, Kuo C. Developmental Angiogenesis of the central Nervous System. *Lymphat Res Biol*. 2008;6(3-4):173-180. doi:10.1038/jid.2014.371
300. Kim H, Su H, Weinsheimer S, Pawlikowska L, Young W. Brain Arteriovenous Malformation Pathogenesis: A Response- to-Injury Paradigm. *Acta Neurochir Suppl*. 2011;111:83-92. doi:10.1007/978-3-7091-0693-8
301. Bernabeu C, Bayrak-Toydemir P, McDonald J, Letarte M. Potential Second-Hits in Hereditary Hemorrhagic Telangiectasia. *J Clin Med*. 2020;9(11):3571. doi:10.3390/jcm9113571
302. Nielsen CM, Huang L, Murphy PA, Lawton MT, Wang RA. Mouse models of cerebral arteriovenous malformation. *Stroke*. 2016;47(1):293-300. doi:10.1161/STROKEAHA.115.002869
303. Alvarez H, Perry V, Solle M, Castillo M. De novo cerebral arteriovenous malformation in a child with previous cavernous malformation and developmental venous anomaly: Case report. *J Neurosurg Pediatr*. 2012;9(3):327-330. doi:10.3171/2011.12.PEDS11312

304. Yassari R, Jahromi B. Dural arteriovenous fistula after craniotomy for pilocytic astrocytoma in a patient with protein S deficiency. *Surg Neurol*. 2002;58(1):59-64. doi:http://dx.doi.org/10.1016/S0090-3019%2802%2900730-9
305. Barré-Sinoussi F, Montagutelli X. Animal models are essential to biological research: Issues and perspectives. *Futur Sci OA*. 2015;1(4):4-6. doi:10.4155/fso.15.63
306. Putman CM, Chaloupka JC, Fulbright RK, Awad IA, White RI, Fayad PB. Exceptional multiplicity of cerebral arteriovenous malformations associated with hereditary hemorrhagic telangiectasia (Osler-Weber-Rendu syndrome). *Am J Neuroradiol*. 1996;17(9):1733-1742.
307. Sabbà C, Pasculli G, Lenato GM, et al. Hereditary hemorrhagic telangiectasia: Clinical features in ENG and ALK1 mutation carriers. *J Thromb Haemost*. 2007;5(6):1149-1157. doi:10.1111/j.1538-7836.2007.02531.x
308. Letteboer TGW, Mager JJ, Snijder RJ, et al. Genotype-phenotype relationship in hereditary haemorrhagic telangiectasia. *J Med Genet*. 2006;43(4):371-377. doi:10.1136/jmg.2005.035451
309. Park SO, Wankhede M, Lee YJ, et al. Real-time imaging of de novo arteriovenous malformation in a mouse model of hereditary hemorrhagic telangiectasia. *J Clin Invest*. 2009;119(11). doi:10.1172/JCI39482DS1
310. Lebrin F, Srun S, Raymond K, et al. Thalidomide stimulates vessel maturation and reduces epistaxis in individuals with hereditary hemorrhagic telangiectasia. *Nat Med*. 2010;16(4):420-428. doi:10.1038/nm.2131
311. Lo EH, Lok J, Ning MM, Whalen MJ. *Vascular Mechanisms in CNS Trauma*.; 2014. doi:10.1007/978-1-4614-8690-9
312. Li Q, Zhang Q, Huang QH, et al. A pivotal role of the vascular endothelial growth factor signaling pathway in the formation of venous hypertension-induced dural arteriovenous fistulas. *Mol Med Rep*. 2014;9(5):1551-1558. doi:10.3892/mmr.2014.2037
313. Zhu Y, Lawton MT, Du R, et al. Expression of hypoxia-inducible factor-1 and vascular endothelial growth factor in response to venous hypertension. *Neurosurgery*. 2006;59(3):687-695. doi:10.1227/01.NEU.0000228962.68204.CF
314. Tang T, Liu XJ, Zhang ZQ, et al. Cerebral angiogenesis after collagenase-induced intracerebral hemorrhage in rats. *Brain Res*. 2007;1175(1):134-142. doi:10.1016/j.brainres.2007.08.028
315. Luo JK, Zhou HJ, Wu J, Tang T, Liang QH. Electroacupuncture at Zusanli (ST36) accelerates intracerebral hemorrhage-induced angiogenesis in rats. *Chin J Integr Med*. 2013;19(5):367-373. doi:10.1007/s11655-013-1458-y
316. Lok J, Leung W, Murphy S, Butler W, Noviski N, Lo E. Intracranial haemorrhage - Mechanisms of Secondary Brain Injury. *Acta Neurochir (Wien)*. 2011;111:63-69. doi:10.1007/978-3-7091-0693-8
317. Choi J, Dong L, Ahn J, Dao D, Hammerschmidt M, Chen JN. FoxH1 negatively modulates flk1 gene expression and vascular formation in zebrafish. *Dev Biol*. 2007;304(2):735-744. doi:10.1016/j.ydbio.2007.01.023
318. Crilly S, Njegic A, Laurie SE, et al. Using zebrafish larval models to study brain injury, locomotor and neuroinflammatory outcomes following intracerebral haemorrhage. *F1000Research*. 2018;7:1617. doi:10.12688/f1000research.16473.1
319. Pende M, Vadiwala K, Schmidbaur H, et al. A versatile depigmentation, clearing, and labeling method for exploring nervous system diversity. *Sci Adv*. 2020;6(22).

doi:10.1126/sciadv.aba0365
320. Qi Y, Yu T, Xu J, et al. FDISCO: Advanced solvent-based clearing method for imaging whole organs. *Arch di Stud Urbani e Reg*. 2019;48(122):1-14. doi:10.1126/sciadv.aau8355
321. Belle M, Godefroy D, Dominici C, et al. A Simple Method for 3D Analysis of Immunolabeled Axonal Tracts in a Transparent Nervous System. *Cell Rep*. 2014;9(4):1191-1201. doi:10.1016/j.celrep.2014.10.037
322. Pan C, Cai R, Quacquarelli FP, et al. Shrinkage-mediated imaging of entire organs and organisms using uDISCO. *Nat Methods*. 2016;13:859. https://doi.org/10.1038/nmeth.3964.
323. Tsien RY. The green fluorescent protein. *Annu Rev Biochem*. 1998;67:509-544. doi:10.1146/annurev.biochem.67.1.509
324. Alkaabi KM, Yafea A, Ashraf SS. Effect of pH on thermal- and chemical-induced denaturation of GFP. *Appl Biochem Biotechnol*. 2005;126(2):149-156. doi:10.1385/ABAB:126:2:149
325. Duraiyan J, Govindarajan R, Kaliyappan K, Palanisamy M. Applications of immunohistochemistry. *J Pharm Bioallied Sci*. 2012;4(2):S307–S309.
326. Ellett F, Pase L, Hayman JW, Andrianopoulos A, Lieschke GJ. Mpeg1 Promoter Transgenes Direct Macrophage-Lineage Expression in Zebrafish. *Blood*. 2011;117(4):e49-e56. doi:10.1182/blood-2010-10-314120
327. Kirschbaum F. Investigations on the colour pattern of the zebra fish Brachydanio rerio (Cyprinidae, teleostei). *Wilhelm Roux's Arch Dev Biol*. 1975;177(2):129-152. doi:10.1007/BF00848526
328. Eisa-Beygi S, Hatch G, Noble S, Ekker M, Moon TW. The 3-hydroxy-3-methylglutaryl-CoA reductase (HMGCR) pathway regulates developmental cerebral-vascular stability via prenylation-dependent signalling pathway. *Dev Biol*. 2013;373(2):258-266. doi:10.1016/j.ydbio.2012.11.024
329. Zhang R, Zhu W. Vascular integrity in the pathogenesis of brain arteriovenous malformation. *Acta Neurochir Suppl*. 2016;121:29-35. doi:http://dx.doi.org/10.1007/978-3-319-18497-5_6
330. Sorensen LK, Brooke BS, Li DY, Urness LD. Loss of distinct arterial and venous boundaries in mice lacking endoglin, a vascular-specific TGFβ coreceptor. *Dev Biol*. 2003;261(1):235-250. doi:10.1016/S0012-1606(03)00158-1
331. Maltepe E, Schmidt J V., Baunoch D, Bradfield CA, Simon MC. Abnormal angiogenesis and responses to glucose and oxygen deprivation in mice lacking the protein ARNT. *Nature*. 1997;386(6623):403-407. doi:10.1038/386403a0
332. Ryan HE, Lo J, Johnson RS. HIF-1α is required for solid tumor formation and embryonic vascularization. *EMBO J*. 1998;17(11):3005-3015.
333. Li Y, Xu J, Wan P, Yu T, Zhu D. Optimization of GFP Fluorescence Preservation by a Modified uDISCO Clearing Protocol. *Front Neuroanat*. 2018;12(August):1-10. doi:10.3389/fnana.2018.00067
334. Ariel P. A beginner's guide to tissue clearing. *Int J Biochem Cell Biol*. 2017;84:35–39. doi:10.1016/j.biocel.2016.12.009.A
335. Maeyama K, Nakayasu H. Postembryonic neurogenesis in zebrafish (Danio rerio) brain: Presence of two different systems. *Zoolog Sci*. 2000;17(7):959-966. doi:10.2108/zsj.17.959
336. Geudens I, Coxam B, Silvanus A, et al. Artery-vein specification in the zebrafish trunk is

pre-patterned by heterogeneous Notch activity and balanced by flow-mediated fine-tuning. *Development*. 2019;146(16).
337. Singleman C, Holtzman NG. Growth and maturation in the zebrafish, Danio Rerio: A staging tool for teaching and research. *Zebrafish*. 2014;11(4):396-406. doi:10.1089/zeb.2014.0976
338. Zhou ZX, Zhang BC, Sun L. Poly(I:C) induces antiviral immune responses in Japanese flounder (Paralichthys olivaceus) that require TLR3 and MDA5 and is negatively regulated by Myd88. *PLoS One*. 2014;9(11):1-14. doi:10.1371/journal.pone.0112918
339. Chen W, Young W, Su H. Induction of Brain Arteriovenous Malformation in the Adult Mouse. *Methods Mol Biol*. 2014;1135(2):309-316. doi:10.1007/978-1-4939-0320-7
340. Sugden WW, Meissner R, Aegerter-Wilmsen T, et al. Endoglin controls blood vessel diameter through endothelial cell shape changes in response to haemodynamic cues. *Nat Cell Biol*. 2017;19(6):653-665. doi:10.1038/ncb3528
341. Delev D, Pavlova A, Grote A, et al. NOTCH4 gene polymorphisms as potential risk factors for brain arteriovenous malformation development and hemorrhagic presentation. *J Neurosurg*. 2017;126(5):1552-1559. doi:10.3171/2016.3.JNS151731
342. Rochon ER, Wright DS, Schubert MM, Roman BL. Context-specific interactions between Notch and ALK1 cannot explain ALK1-associated arteriovenous malformations. *Cardiovasc Res*. 2015;107(1):143-152. doi:10.1093/cvr/cvv148
343. Zaucker A, Mercurio S, Sternheim N, Talbot W, Marlow F. notch3 is essential for oligodendrocyte development and vascular integrity in zebrafish. *Dis Model Mech*. 2013;6(5):1246–1259.
344. Traver D, Paw BH, Poss KD, Penberthy WT, Lin S, Zon LI. Transplantation and in vivo imaging of multilineage engraftment in zebrafish bloodless mutants. *Nat Immunol*. 2003;4(12):1238-1246. doi:10.1038/ni1007
345. Renshaw SA, Loynes CA, Trushell DMI, Elworthy S, Ingham PW, Whyte MKB. A transgenic zebrafish model of neutrophilic inflammation. *Blood*. 2006;108(13):3976-3978. doi:10.1182/blood-2006-05-024075
346. Redd MJ, Kelly G, Dunn G, Way M, Martin P. Imaging macrophage chemotaxis in vivo: Studies of microtubule function in zebrafish wound inflammation. *Cell Motil Cytoskeleton*. 2006;63(7):415-422. doi:10.1002/cm.20133
347. Hogan BM, Bos FL, Bussmann J, et al. Ccbe1 is required for embryonic lymphangiogenesis and venous sprouting. *Nat Genet*. 2009;41(4):396-398. doi:10.1038/ng.321
348. Zirlik K, Duyster J. Anti-Angiogenics: Current Situation and Future Perspectives. *Oncol Res Treat*. 2018;41(4):166-171. doi:10.1159/000488087
349. Raper DMS, Winkler EA, Caleb Rutledge W, Cooke DL, Abla AA. An update on medications for brain arteriovenous malformations. *Neurosurgery*. 2020;87(5):871-878. doi:10.1093/neuros/nyaa192
350. Zhu W, Shen F, Mao L, et al. Soluble FLT1 Gene Therapy Alleviates Brain Arteriovenous Malformation Severity. *Stroke*. 2017;48(5):1420-1423. doi:10.1161/STROKEAHA.116.015713
351. Kim YH, Vu PN, Choe SW, et al. Overexpression of activin receptor-like kinase 1 in endothelial cells suppresses development of arteriovenous malformations in mouse models of hereditary hemorrhagic telangiectasia. *Circ Res*. 2020:1122-1137. doi:10.1161/CIRCRESAHA.119.316267
352. Buell TJ, Ding D, Starke RM, Webster Crowley R, Liu KC. Embolization-induced

angiogenesis in cerebral arteriovenous malformations. *J Clin Neurosci*. 2014;21(11):1866-1871. doi:10.1016/j.jocn.2014.04.010

353. Takemae T, Kobayashi S, Sugita K. Perinidal Hypervascular Network on Immediate Postoperative Angiogram after Removal of Large Arteriovenous Malformations Located Distant from the Arterial Circle of Willis Clinical Study I. *Neurosurgery*. 1993;33(3):400-406. doi:10.1080/00033799300200371
354. Meyers PM, Schumacher HC, Higashida RT, et al. Reporting Standards for Endovascular Repair of Saccular Intracranial Cerebral Aneurysms. *J Vasc Interv Radiol*. 2009;20(7 SUPPL.):S435-S450. doi:10.1016/j.jvir.2009.03.004
355. Rinkel GJE, Djibuti M, Algra A, Van Gijn J. Prevalence and risk of rupture of intracranial aneurysms: A systematic review. *Stroke*. 1998;29(1):251-256. doi:10.1161/01.STR.29.1.251
356. Kirst C, Skriabine S, Vieites-Prado A, et al. Mapping the Fine-Scale Organization and Plasticity of the Brain Vasculature. *Cell*. 2020;180(4):780-795.e25. doi:10.1016/j.cell.2020.01.028
357. Peach CJ, Kilpatrick LE, Friedman-Ohana R, et al. Real-Time Ligand Binding of Fluorescent VEGF-A Isoforms that Discriminate between VEGFR2 and NRP1 in Living Cells. *Cell Chem Biol*. 2018;25(10):1208-1218.e5. doi:10.1016/j.chembiol.2018.06.012
358. Berchner-Pfannschmidt U, Frede S, Wotzlaw C, Fandrey J. Imaging of the hypoxia-inducible factor pathway: Insights into oxygen sensing. *Eur Respir J*. 2008;32(1):210-217. doi:10.1183/09031936.00013408

Appendices

Appendix 1 - Kappa observer agreement

Table 1: The degree of intra-observer agreement for Observer 1 is shown with the angiographic features compared listed, with their corresponding Kappa statistic, and the matching degree of agreement.

Intra-observer comparison	Kappa statistic	Degree of agreement
Spetzler-Martin Grade (1, 2, 3, 4, 5)	**weighted**	
Observer 1	κ = .817 (95% CI, .663 – 0.970), ***p = 5.5e-10***	Near perfect
Nidus		
AP diameter (≥30mm, <30mm)	**unweighted**	
Observer 1	κ = 1 (95% CI, 1 - 1), ***p = 5.5e-10***	perfect
CC diameter (≥30mm, <30mm)	**unweighted**	
Observer 1	κ = 1 (95% CI, 1 - 1), ***p = 5.5e-10***	perfect
LL diameter (≥30mm, <30mm)	**unweighted**	
Observer 1	κ = .857 (95% CI, .587 – 1.13), ***p = 5.5e-10***	near perfect
Border (compact or diffuse)	**unweighted**	
Unable to perform intra-observer comparison as all values same in the second reading.		
Eloquence (yes or no)	**unweighted**	
Observer 1	0.733 (95% CI, -1.61 – 2.31), ***p = 0.001***	substantial
Additional features		
Angiogenesis (yes or no)	**unweighted**	
Observer 1	κ = .762 (95% CI, .450 – 1.07), ***p = .001***	substantial
High flow shunt (yes or no)	**unweighted**	
Unable to perform intra-observer comparison as all values same in the second reading.		
Aneurysms (yes or no)	**unweighted**	
Observer 1	κ = .138 (95% CI, 1.47 – 2.45), *p* = .531	slight
Arterial feeders		
Number of feeder arteries (1 vs 2 vs >=3)	**weighted**	
Observer 1	κ = .592 (95% CI, .210 – .973), ***p = 5.5e-10***	moderate
Arterial ectasia (yes or no)	**unweighted**	
Observer 1	κ = .612 (95% CI, 1.65 – 2.27), ***p = .003***	substantial
Draining veins		
Number of draining veins (1 vs 2 vs >=3)	**weighted**	
Observer 1	κ = .817 (95% CI, .615 – 1.019), ***p = 5.5e-10***	near perfect
Pial course length (short vs long vs deep)	**weighted**	
Observer 1	κ = .639 (95% CI, .356 – .922), ***p = .001***	substantial
Venous drainage (superficial vs deep vs both)	**weighted**	

Observer 1	κ = .540 (95% CI, .189 – .891), ***p = .002***	moderate
Venous varix (yes or no)	**unweighted**	
Observer 1	κ = .341 (95% CI, -.0882 - .770), p=.128	fair
Venous ectasia (yes or no)	**unweighted**	
Observer 1	κ = .200 (95% CI, -0.0568 – 0.457), p=.136	slight
Venous reflux (yes or no)	**unweighted**	
Observer 1	κ = 1 (95% CI, 1 - 1), ***p = 5.5e-10***	perfect
Venous stenosis (yes or no)	**unweighted**	
Unable to perform intra-observer comparison as all values same in the second reading.		

The second reading was performed 6 months later. If all the second readings were the same, no comparison could be made. Anteroposterior (AP), craniocaudal (CC) and laterolateral (LL) diameters are compared. Also, venous stenosis could not be compared.

Table 2: The degree of inter-observer agreement for angiographic features mentioned in above table is shown with the observers compared listed, with their corresponding Kappa statistic, and the matching degree of agreement.

Spetzler-Martin Grade (1, 2, 3, 4, 5)		
Observers compared	**Kappa statistic (weighted)**	**Degree of agreement**
3 and 1	κ = .259 (95% CI, -0.024 – 0.542), p=.161	fair
No data for 2		
Nidus		
AP diameter (≥30mm, <30mm)		
Observers compared	**Kappa statistic (unweighted)**	**Degree of agreement**
2 and 3	κ = 0 (95% CI, -0.600 – 0.600), p=1	slight
2 and 1	κ = -0.2 (95% CI, -0.488 – 0.088), p= .537	Less than chance
3 and 1	κ = .286 (95% CI, -0.186 – 0.758), p= .197	fair
CC diameter (≥30mm, <30mm)		
Observers compared	**Kappa statistic (unweighted)**	**Degree of agreement**
2 and 3	κ = 0.5 (95% CI, -0.019 – 1.02), p=.102	moderate
2 and 1	κ = -0.2 (95% CI, -0.488 – 0.088), p=.537	Less than chance
3 and 1	κ = .286 (95% CI, -0.186 – 0.758), p=.197	fair
LL diameter (≥30mm, <30mm)		
Observers compared	**Kappa statistic (unweighted)**	**Degree of agreement**
2 and 3	κ = 0.5 (95% CI, -0.019 – 1.02), p=.102	moderate
2 and 1	κ = 0.333 (95% CI, -0.406 – 1.07), p=.346	fair
3 and 1	κ = 0.545 (95% CI, 0.043 – 1.05), p=.053	moderate

Border		
Observers compared	**Kappa statistic (unweighted)**	**Degree of agreement**
2 and 3	Unable to perform intra-observer comparison as all values same in the second reading.	
2 and 1	κ = 0.143 (95% CI, -0.537 – 0.823), p=.673	slight
3 and 1	Unable to perform intra-observer comparison as all values same in the second reading.	
Additional features		
Angiogenesis	**unweighted**	
Observers compared	**Kappa statistic (unweighted)**	**Degree of agreement**
2 and 3	κ = .688 (95% CI, .312 - 1.064), ***p* = .001**	substantial
2 and 1	κ = .50 (95% CI, .016 – .984), **p = .027**	moderate
3 and 1	κ = .20 (95% CI, -0.356 – 0.757), *p* = .49	fair
High flow shunt (yes or no)	**unweighted**	
Observers compared	**Kappa statistic (unweighted)**	**Degree of agreement**
2 and 3	Unable to perform intra-observer comparison as all values same in the first reading.	
2 and 1	Unable to perform intra-observer comparison as all values same in the first reading.	
3 and 1	κ = -0.207 (95% CI, -0.593 – .179), *p* = .197	Less than chance
Aneurysms (yes or no)	**unweighted**	
Observers compared	**Kappa statistic (unweighted)**	**Degree of agreement**
2 and 3	κ = -0.143 (95% CI, -0.339 – 0.053), *p* = .686	Less than chance
2 and 1	κ = .385 (95% CI, -0.197 – 0.967), *p* = .168	fair
3 and 1	κ = -0.316 (95% CI, -0.018 – -0.614), *p* = .301	Less than chance
Arterial feeders		
Number of feeder arteries (1 vs 2 vs >=3)		
Observers compared	**Kappa statistic (weighted)**	**Degree of agreement**
2 and 1	κ = .111 (95% CI, -0.125 – .347), *p* = .408	slight
No data for 3		
Arterial ectasia		
Observers compared	**Kappa statistic (unweighted)**	**Degree of agreement**
2 and 3	Unable to perform intra-observer comparison as all values same in the first reading.	
2 and 1	κ = .250 (95% CI, -0.193 – 0.693), *p* = .285	fair
3 and 1	Unable to perform intra-observer comparison as all values same in the first reading.	
Draining veins		
Number of draining veins (1 vs 2 vs >=3)		
Observers compared	**Kappa statistic (weighted)**	**Degree of agreement**
2 and 3	κ = .172, (95% CI, - .327 – .672), p = .446	slight

2 and 1	κ = .500 (95% CI, .013 – 0.860), ***p* = .028**	moderate
3 and 1	κ = .333 (95% CI, -0.422 – 1.09), *p* = .414	fair
Pial course length		
Observers compared	**Kappa statistic (weighted)**	**Degree of agreement**
2 and 3	κ = 1 (95% CI, 1 – 1), ***p* = .005**	perfect
2 and 1	κ = .048 (95% CI, -0.453 – 0.549), *p* = .850	slight
3 and 1	κ = .167 (95% CI, -0.328 – 0.661), *p* = .490	slight
Venous drainage (superficial vs deep vs both)		
Observers compared	**Kappa statistic (weighted)**	**Degree of agreement**
2 and 3	κ = .273 (95% CI, -.201 – 0.747), p=.221	fair
2 and 1	κ = .696 (95% CI, .017 – 1.22), *p* = .053	substantial
3 and 1	κ = .40 (95% CI, -0.186 – 0.986), *p* = .134	moderate
Venous varix (yes or no)		
Observers compared	**Kappa statistic (unweighted)**	**Degree of agreement**
2 and 3	κ = .091 (95% CI, -0.112 – 0.294), p=.537	slight
2 and 1	κ = .263 (95% CI, -0.757 - .239), p=.168	fair
3 and 1	κ = .143 (95% CI, -0.537 - .823), p=.673	slight
Venous ectasia (yes or no)		
Observers compared	**Kappa statistic (unweighted)**	**Degree of agreement**
2 and 3	κ = .091 (95% CI, -0.112 – 0.294), p=.537	slight
2 and 1	κ = .250 (95% CI, -0.193 – 0.693), p=.285	fair
3 and 1	κ = .545 (95% CI, .043 – 1.05), p=.053	moderate
Venous reflux		
Observers compared	**Kappa statistic (unweighted)**	**Degree of agreement**
2 and 3	Unable to perform intra-observer comparison as all values same in the second reading.	
2 and 1	κ = .158 (95% CI, -0.158 – 0.474), p=.408	slight
3 and 1	Unable to perform intra-observer comparison as all values same in the first reading.	
Venous stenosis (yes or no)		
Observers compared	**Kappa statistic (unweighted)**	**Degree of agreement**
2 and 1	κ = -.143 (95% CI, -0.339 – 0.339), p=.686	Less than chance
Unable to compare with 3 as all values the same, i.e., no venous stenosis noted for any patient.		

AP = anteroposterior, CC = craniocaudal, LL = laterolateral diameters

Appendix 2 – Systematic Review article data collection

Author	Journal, year, centre, country	No. of cases, study duration	Definitions given	Fields included, & similarities to JWG (bold if same)	Method of angiography/ imaging, quality, calibration	Fields used in JWG that were not described	Focus of study	Specialists involved, level of experience, how many	Intra-rater/ inter-rater reliability reported	Statistical test used
Abecassis	Neurosurg Focus, 2014, Department of Neurological Surgery, University of Washington, Seattle, USA	n/a	none	Venous drainage, venous stenosis, concurrent aneurysm, clinical presentation, nidus size, location	angiography	date of presentation, imaging source and date, lesion side, handedness, BAVM eloquence, BAVM border with adjacent brain, BAVM haemorrhage, haemorrhage location, size, periventricular drainage, number of draining veins leaving nidus, number of veins reaching sinus, venous ectasia, venous reflux, sinus thrombosis feeding arteries, number of aneurysms, location,	To systematically review the literature to clarify the natural history of (BAVMs).	none	none	nil

						haemorrhage history, haemorrhage date, no of vessels to be embolised, Moyamoya-type changes, pial-to-pial collateralisation, intravascular pressure measurement				
Abla 2014	Neurosurg Focus, 2014, Department of Neurological Surgery, University of California, San Francisco,	154, 2001-2013	none	Posterior fossa location, associated aneurysm, AVM size, deep location, eloquence, deep venous drainage	DSA	clinical presentations, date of presentation, imaging source and date, lesion side, handedness, BAVM border with adjacent brain, BAVM haemorrhage, haemorrhage location, size, periventricular drainage, number of draining veins leaving nidus, number of veins reaching sinus, venous stenosis/ occlusion, venous ectasia, venous reflux,	To determine whether debilitating effects of first-time bleeding from an AVM in a previously intact patient with an unruptured AVM are more pronounced when AVMs are located in the posterior fossa.	nil	nil	t-tests, chi-square tests Univariate and multivariate logistic regression analyses Area under the receiver operating characteristic (AUROC) curve ordinal logistic regression

						sinus thrombosis feeding arteries, arterial aneurysms, number of aneurysms, location, haemorrhage history, haemorrhage date, no of vessels to be embolised, Moyamoya-type changes, pial-to-pial collateralisation, intravascular pressure measurement				
Abla 2015	Neurosurgery. 2015, Department of Neurological Surgery, University of California, San Francisco	242, 1997 - ???	Haemorrhage presentation	Seizure presentation, AVM size, deep venous drainage, eloquence, SMG, diffuse AVM, posterior fossa location, haemorrhage	CT, MRI, DSA	date of presentation, imaging source and date, lesion side, handedness, haemorrhage location, size, periventricular drainage, number of draining veins leaving nidus, number of veins reaching sinus, venous stenosis/ occlusion,	To better define features associated with unrecognized subgroup of unruptured AVM patients with silent haemorrhage.	Neurologist neuroradiologist neuropathologists	none	Fisher exact test (or χ^2 test) logistic regression model nonparametric correlation (Spearman's ρ)

						venous ectasia, venous reflux, sinus thrombosis feeding arteries, arterial aneurysms, number of aneurysms, location, haemorrhage history, haemorrhage date, no of vessels to be embolised, Moyamoya-type changes, pial-to-pial collateralisation, intravascular pressure measurement				
Ahmed	The Egyptian Journal of Radiology & Nuclear Medicine, 2014, Radiology Department, Cairo University, Egypt	One, ???	none	Clinical presentation, location, size, number of veins, venous drainage, venous stenosis, feeder arteries	CT, angiography	date of presentation, imaging source and date, lesion side, handedness, BAVM eloquence, BAVM border with adjacent brain, BAVM haemorrhage, haemorrhage location, size, periventricular drainage,	To describe transvenous endovascular treatment for a patient with an AVM in a case report	Neurosurgery, neuro-interventional team	none	n/a

						number of veins reaching sinus, venous ectasia, venous reflux, sinus thrombosis arterial aneurysms, number of aneurysms, location, haemorrhage history, haemorrhage date, no of vessels to be embolised, Moyamoya-type changes, pial-to-pial collateralisation, intravascular pressure measurement				
Ai	J Neurosurg Pediatr, 2019, West China Hospital of Sichuan University, Chengdu	n/a	none	AVM size, venous drainage, number of draining veins, feeder arteries, AVM location, diffuse morphology, venous ectasia, SMG	CT, DSA, MRI	clinical presentations, date of presentation, imaging source and date, lesion side, handedness, BAVM eloquence, BAVM haemorrhage, haemorrhage location, size, periventricular drainage,	To evaluate the predictors of haemorrhagic presentation in paediatrics patients with AVMs.	None	none	multivariate regression univariate regression fixed-effects model funnel plots and Begg's test

						number of veins reaching sinus, venous stenosis/ occlusion, venous reflux, sinus thrombosis arterial aneurysms, number of aneurysms, location, haemorrhage history, haemorrhage date, no of vessels to be embolised, Moyamoya-type changes, pial-to-pial collateralisation, intravascular pressure measurement				
Al-Shahi	Stroke, 2002, Western General Hospital, Scotland	40, Jan-May 2001	None	**Depth**, **Nidus diameter**, **No. of feeding arteries**, Feeding artery angiopathy, Angiogenesis, **collateral supply**, **nidus**	CT, MRI, MRA, 4-vessel DSA Nil else	Clinical presentation, date of presentation, imaging source and date, lesion side, handedness, BAVM haemorrhage including	to determine intraobserver and interobserver agreement in the characterisation of BAVM angioarchitecture on IADSA	5 experienced interventional neuroradiologists, 7-21 years consultant experience	yes	Kappa statistic, Bland & Altman analysis

				border, fistula in nidus, **no. of draining veins**/ nidus compartments, **SMG**, varices, **venous ectasia**, **stenosis**, **aneurysm and type**		location and size, no. of veins reaching sinus, venous reflux, sinus thrombosis, no. of vessels to be embolised, Moyamoya-type changes, intravascular pressure measurements				
Al-Tamimi	Childs Nerv Syst, 2011, Departments of Neurosurgery / Neuroradiology, Leeds General Infirmary, UK	3 patients, ???	Histological definition of cAVM	Clinical presentation, BAVM location, feeding arteries, venous drainage, number of draining veins leaving nidus, accessory fistulae, shunt, venous hypertension, cerebral atrophy, arterialised vein, venous varix	CT, MRI, DSA	date of presentation, imaging source and date, lesion side, handedness, BAVM size, BAVM eloquence, BAVM border with adjacent brain, BAVM haemorrhage, haemorrhage location, size, periventricular drainage, number of veins reaching sinus, venous stenosis/ occlusion, venous ectasia,	To present three cases of paediatric AVMs that demonstrated unusual features of high flow and significant shunting of blood without a clearly demonstrable nidus.	none	none	n/a

						venous reflux, sinus thrombosis arterial aneurysms, number of aneurysms, location, haemorrhage history, haemorrhage date, no of vessels to be embolised, Moyamoya-type changes, pial-to-pial collateralisation, intravascular pressure measurement				
Alen	J Neurosurg 2013, Department of Neurosurgery, Universidad Complutense de Madrid	28, 2000-2010	haemorrhage volume	AVM size, clinical presentation, haemorrhage volume, feeding arteries and size, associated arterial aneurysms, venous drainage, venous ectasia, venous stenosis,	MRI, MRA, DSA	date of presentation, imaging source and date, lesion side, handedness, BAVM location, BAVM eloquence, BAVM border with adjacent brain, haemorrhage location, periventricular drainage, number of draining veins leaving nidus,	To assess the clinical presentation, radiological features, therapeutic management, and outcome of a case series of micro-cAVMs	Neuroradiologist, neurosurgeon	none	nil

				calibre of venous outflow		number of veins reaching sinus, venous reflux, sinus thrombosis number of aneurysms, location, haemorrhage history, haemorrhage date, no of vessels to be embolised, Moyamoya-type changes, pial-to-pial collateralisation, intravascular pressure measurement				
Alexander et al	AJNR, 2015, University of California, San Francisco	519, 2001-2014	Venous stenosis, occlusion	**Lesion side**, **venous drainage**, degree of **venous stenosis**, **number of draining veins**, **venous ectasia**, **venous reflux**.	2D DSA, CT, MRI	Clinical presentation, date of presentation, imaging source and date, handedness, BAVM size, BAVM location, BAVM eloquence, BAVM border with adjacent brain,	To examine association between venous angioarchitectural features of brain AVMs and intracranial haemorrhage	5 neuroradiologists Nil else	none	Univariable and multivariable logistic regression analyses

						BAVM haemorrhage, haemorrhage location, size, periventricular drainage, number of veins reaching sinus, sinus thrombosis, feeding arteries, arterial aneurysms, number of aneurysms, location, haemorrhage history, haemorrhage date, no of vessels to be embolised, Moyamoya-type changes, pial-to-pial collateralisation, intravascular pressure measurement				
Anderson	J Neurosurg Paediatrics, 2012, Columbia	77, 1991-2010	none	Aneurysms, SMG, AVM side, AVM location,	angiography	clinical presentations, date of presentation,	To investigate the relationship of associated aneurysms in a large group of	attending neurosurgeon, endovascular neurosurgeon,	none	Univariate analyses

	University, Department of Neurological Surgery, New York			venous drainage, eloquence, AVM size, haemorrhage		imaging source and date, handedness, BAVM border with adjacent brain, haemorrhage location, size, periventricular drainage, number of draining veins leaving nidus, number of veins reaching sinus, venous stenosis/ occlusion, venous ectasia, venous reflux, sinus thrombosis feeding arteries, number of aneurysms, location, haemorrhage history, haemorrhage date, no of vessels to be embolised, Moyamoya-type changes, pial-to-pial collateralisation, intravascular pressure measurement	children with AVMs.	interventional neuroradiologist		Fisher exact test, chi-squared test, t-test, Wilcoxon signed-rank test, Mann-Whitney U-test logistic regression model

Arnaout	Neurosurg Focus 26, 2009, Department of Neurological Surgery, The Feinberg School of Medicine and McGaw Medical Centre, Northwestern University, Chicago, USA	n/a	none	Clinical presentation, annual bleeding rate	n/a	date of presentation, imaging source and date, lesion side, handedness, BAVM size, BAVM location, BAVM eloquence, BAVM border with adjacent brain, BAVM haemorrhage, haemorrhage location, size, venous drainage, periventricular drainage, number of draining veins leaving nidus, number of veins reaching sinus, venous stenosis/ occlusion, venous ectasia, venous reflux, sinus thrombosis feeding arteries, arterial aneurysms, number of aneurysms, location,	To review the literature on posterior fossa AVMs, in particular their annual rupture rates.	none	none	None Reported stats of other studies (multivariate analysis)

						haemorrhage history, haemorrhage date, no of vessels to be embolised, Moyamoya-type changes, pial-to-pial collateralisation, intravascular pressure measurement				
Benson	Department of neuroradiology, Mayo clinic, Rochester, Minnesota, Usa	165, 2000-2016	BAVM location, gliosis, SMG, AVMES,	BAVM location, AVM side, characteristics of AVMs and surrounding parenchyma, Spetzler-Martin (SM) grade (ie, size based on SM categorization as being <3 cm, 3–6 cm, or ≥6 cm, involvement of eloquent cortex, presence or absence of deep venous drainage, and SM grade), AVM Embocure Score (AVMES) (ie, number of arterial pedicles,	MRI, MRA, CTA, Angiography	clinical presentations, date of presentation, imaging source and date, lesion side, handedness, BAVM border with adjacent brain, BAVM haemorrhage, haemorrhage location, size, periventricular drainage, number of veins reaching sinus, venous stenosis/ occlusion, venous ectasia, venous reflux, sinus thrombosis	To identify Mri characteristics of unruptured intracranial aVMs associated with seizures at presentation.	Two neuroradiologists	nil	Student's t-test for continuous variables and χ^2 test for categorical variable

				number of draining veins, AVM nidus size, and vascular eloquence), and (3) location.		arterial aneurysms, number of aneurysms, location, haemorrhage history, haemorrhage date, no of vessels to be embolised, Moyamoya-type changes, pial-to-pial collateralisation, intravascular pressure measurement				
Bharatha	Stroke, 2012, Division of Neuroradiology, Dept. of Medical Imaging, St Michael's Hospital, University of Toronto, Toronto, Canada	1989 patients included in analysis (723 from UCSF and 1266 from UHN) Toronto database includes all patients, with confirmed bAVM diagnosis, referred to the UHN Toronto Brain Vascular	Multiplicity, HHT diagnosis	Clinical presentation, haemorrhage presentation, HHT diagnosis, BAVM location, number of BAVMs, eloquence, venous drainage, BAVM size, SMG, feeding artery	CT/CTA, MR/MRA or Angiography [DSA] 3 or 4 vessel catheter angiography and a subset underwent superselective angiography	clinical presentations, date of presentation, imaging source and date, lesion side, handedness, BAVM size, BAVM location, BAVM eloquence, BAVM border with adjacent brain, BAVM haemorrhage, haemorrhage location, size, venous drainage,	To quantitatively estimate the relationship between multiplicity of BAVMs and the diagnosis of hereditary haemorrhagic telangiectasia (HHT)	none	none	t tests/ chi-square tests Univariate logistic regression analysis Multivariable logistic regression analysis

		Malformation Study Group from 1984–2009. UCSF database: 2000–2010				periventricular drainage, number of draining veins leaving nidus, number of veins reaching sinus, venous stenosis/ occlusion, venous ectasia, venous reflux, sinus thrombosis feeding arteries, arterial aneurysms, number of aneurysms, location, haemorrhage history, haemorrhage date, no of vessels to be embolised, Moyamoya-type changes, pial-to-pial collateralisation, intravascular pressure measurement				
Blanc	J NeuroInterve nt Surg, 2015, Fondation	11, ?years	none	**Location**, SMG, **haemorrhage**, **arterial feeder**,	3D MRI, DSA, 3D rotational angiography (RA), superselective	clinical presentations date of presentation	To use multiple modalities in assessing the angiographic	interventional neuroradiologis t nil	none	none

	Rothschild Hospital, Paris			**aneurysms (proximal or distal)**	catheterisation,	imaging source and date lesion side handedness BAVM size BAVM eloquence BAVM border with adjacent brain venous drainage periventricular drainage number of draining veins leaving nidus number of veins reaching sinus venous stenosis/ occlusion venous ectasia venous reflux sinus thrombosis haemorrhage history haemorrhage date no of vessels to be embolised	features of BAVMs and for endovascular treatment (3D roadmap intracranial navigation, image fusion)			

						Moyamoya-type changes pial-to-pial collateralisation intravascular pressure measurement				
Boone	Journal of Clinical Neuroscience, 2016, Johns Hopkins School of Medicine, Baltimore	38, 1949–1989 or 1990–2011	none	Number of AVM, AVM laterality, AVM size, Venous drainage	Not mentioned	clinical presentations, date of presentation, imaging source and date, handedness, BAVM location, BAVM eloquence, BAVM border with adjacent brain, BAVM haemorrhage, haemorrhage location, size, periventricular drainage, number of draining veins leaving nidus, number of veins reaching sinus, venous stenosis/ occlusion, venous ectasia, venous reflux, sinus thrombosis	To examine clinical characteristics, treatment strategies, and annual haemorrhage incidence rate for patients with multiple AVM	none	none	Fisher's exact test Welch two-sample t-test

						feeding arteries, arterial aneurysms, number of aneurysms, location, haemorrhage history, haemorrhage date, no of vessels to be embolised, Moyamoya-type changes, pial-to-pial collateralisation, intravascular pressure measurement				
Braileanu	World Neurosurgery, 2016, Emory University School of Medicine, Atlanta	36, ? duration	BAVM border with adjacent brain	**BAVM location**, **BAVM border with adjacent brain**, **BAVM size**, **BAVM eloquence**, **venous drainage**, SMG	DSA	clinical presentations, date of presentation, imaging source and date, lesion side, handedness, BAVM haemorrhage, haemorrhage location, size, periventricular drainage, number of draining veins leaving nidus,	To assess interobserver agreement of AVM diffuseness among physicians of different specialties and training backgrounds using DSA	2 attending neurosurgeons, 1 attending interventional neuroradiologist, 1 senior neurosurgical resident (postgrad year 6) All >10 years experience	Yes for inter-observer	Kappa statistic, intraclass correlation coefficient

						number of veins reaching sinus, venous stenosis/ occlusion, venous ectasia, venous reflux, sinus thrombosis feeding arteries, arterial aneurysms, number of aneurysms, location, haemorrhage history, haemorrhage date, no of vessels to be embolised, Moyamoya-type changes, pial-to-pial collateralisation, intravascular pressure measurement				
Brinjikji	Department of Radiology	n/a 1990-2016	HHT	SMG	n/a	clinical presentations, date of presentation,	To identify studies on AVM prevalence	reference librarian (with over 30 years experience in		Chi-square analysis

		39 studies included in meta-analysis				imaging source and date, lesion side, handedness, BAVM size, BAVM location, BAVM eloquence, BAVM border with adjacent brain, BAVM haemorrhage, haemorrhage location, size, venous drainage, periventricular drainage, number of draining veins leaving nidus, number of veins reaching sinus, venous stenosis/ occlusion, venous ectasia, venous reflux, sinus thrombosis feeding arteries, arterial aneurysms, number of aneurysms, location, haemorrhage history,	and characteristics in the HHT population 4 databases (MEDLINE, EMBASE, Scopus and Web of Science)	systematic reviews and meta-analysis)		Heterogeneity of treatment effect across studies was evaluated using the I-squared (I^2) statistic

						haemorrhage date, no of vessels to be embolised, Moyamoya-type changes, pial-to-pial collateralisation, intravascular pressure measurement				
Brunozzi 2017	Neurosurgery, 2017, University of Illinois, Chicago	28, 2007-2014	venous ectasia, venous stenosis	**BAVM volume**, arterial ectasia, intranidal fistula, **intranidal aneurysm**, **venous ectasia**, **venous stenosis**, varix, single draining vein, **deep venous drainage**, **haemorrhagic presentation**, steal, **seizure**	DSA, QMRA	date of presentation imaging source and date lesion side handedness BAVM location BAVM eloquence BAVM border with adjacent brain BAVM haemorrhage haemorrhage location, size periventricular drainage number of draining veins leaving nidus number of veins reaching sinus	To assess contrast time-density time on DSA relative to AVM flow measured using quantitative MRA (QMRA)	none	none	Pearson's correlation, Wilcoxon rank sum test

						venous reflux sinus thrombosis feeding arteries arterial aneurysms number of aneurysms location haemorrhage history haemorrhage date no of vessels to be embolised Moyamoya-type changes pial-to-pial collateralisation intravascular pressure measurement				
Brunozzi 2019	World Neurosurgery, 2019, University of Illinois at Chicago, Chicago	243, 1997-2018	Venous stenosis	Haemorrhagic presentation, draining venous stenosis, degree of venous stenosis, adjacent venous draining sinus,	DSA	clinical presentations, date of presentation, imaging source and date, lesion side, handedness, BAVM size, BAVM location, BAVM eloquence,	To determine if the ratio of draining vein to adjacent sinus diameter might predict the development of venous stenosis	nil	nil	Pearson correlation test

				distance from draining vein stenosis to junction of adjacent draining sinus, number of draining veins		BAVM border with adjacent brain, haemorrhage location, size, venous drainage, periventricular drainage, number of veins reaching sinus, venous ectasia, venous reflux, sinus thrombosis feeding arteries, arterial aneurysms, number of aneurysms, location, haemorrhage date, no of vessels to be embolised, Moyamoya-type changes, pial-to-pial collateralisation, intravascular pressure measurement				
Buis	J Neurol, 2004, Department of Neuroradiology,	One, ???	none	Case report: Clinical presentation, location, size, venous drainage	MRI, DSA	date of presentation, imaging source and date, handedness, BAVM eloquence,	To describe a case report of a complete spontaneous obliteration of an BAVM and present results	none	none	none

	Amsterdam & Leiden University Medical Center Leiden, The Netherlands			Systematic review: Clinical presentation, location, lateralisation, size, venous drainage, number of draining veins, arterial feeders		BAVM border with adjacent brain, BAVM haemorrhage, haemorrhage location, size, periventricular drainage, number of veins reaching sinus, venous stenosis/ occlusion, venous ectasia, venous reflux, sinus thrombosis arterial aneurysms, number of aneurysms, location, haemorrhage history, haemorrhage date, no of vessels to be embolised, Moyamoya-type changes, pial-to-pial collateralisation, intravascular pressure measurement	of a systematic review			
Burkhardt	World Neurosurg, 2017, Department	71, 2010-2016	Deep venous drainage	SMG, number of feeding arteries, number of	DSA	clinical presentations, date of presentation,	To use catheter angiography to identify	neurosurgeon	nil	Mann-Whitney U test

	of Neurological Surgery, University of California San Francisco			draining veins, diffuse AVM nidus, AVM location, AVM size, deep venous drainage, haemorrhage		imaging source and date, lesion side, handedness, BAVM eloquence, haemorrhage location, size, periventricular drainage, number of veins reaching sinus, venous stenosis/ occlusion, venous ectasia, venous reflux, sinus thrombosis arterial aneurysms, number of aneurysms, location, haemorrhage date, no of vessels to be embolised, Moyamoya-type changes, pial-to-pial collateralisation, intravascular pressure measurement	hemodynamic parameters in ruptured and unruptured AVMs.			chi^2 test or Fisher exact test
Chang	Am J Neuroradiol, 2015, Department	21 for MRI, 14 for DSA	none	Feeder arteries, venous drainage,	MRI HYPRFlow & 3D TOF, DSA	clinical presentations, date of presentation,	To determine if the images obtained with HYPRFlow are	experienced neuroradiologists	none	Wilcoxon rank sum test 2-sample t test

	of Radiology, University of California, Los Angeles, USA			nidus size, SMG, flow analysis		imaging source and date, lesion side, handedness, BAVM location, BAVM eloquence, BAVM border with adjacent brain, BAVM haemorrhage, haemorrhage location, size, periventricular drainage, number of draining veins leaving nidus, number of veins reaching sinus, venous stenosis/ occlusion, venous ectasia, venous reflux, sinus thrombosis arterial aneurysms, number of aneurysms, location, haemorrhage history, haemorrhage date, no of vessels to be embolised, Moyamoya-type changes,	of adequate diagnostic image quality to delineate the major components of AVMs.			

						pial-to-pial collateralisation, intravascular pressure measurement				
Chen	Stroke, 2017, Centre for Cerebrovascular Research, Beijing	125, 1992 - 2016	venous pouch, feeding artery enlargement, mean transit time (MTT), diameter of a region of interest (ROI)	Demographics, clinical presentation, AVM location, SMG, flow-related aneurysms, venous drainage, **venous pouch** (varix), venous ectasia, **feeding artery**, haemodynamic parameters, mean transit time (MTT), diameter of a region of interest (ROI)	DSA	date of presentation, imaging source and date, lesion side, handedness, BAVM size, BAVM eloquence, BAVM border with adjacent brain, BAVM haemorrhage, haemorrhage location, size, periventricular drainage, number of draining veins leaving nidus, number of veins reaching sinus, venous stenosis/ occlusion, venous reflux, sinus thrombosis arterial aneurysms, number of aneurysms, location,	To hypothesise that flow would be faster in unruptured AVMs with haemosiderin compared to without haemosiderin	neurosurgeon, interventional neuroradiologist		Two-sided two-sample t-test for continuous variables, Fisher's exact test for categorical variables.

						haemorrhage history, haemorrhage date, no of vessels to be embolised, Moyamoya-type changes, pial-to-pial collateralisation, intravascular pressure measurement				
Choi 2006	Stroke, 2006, Stroke Center, The Neurological Institute, Columbia University Medical Center, New York,	241, 1989-2004	Haemorrhagic AVM presentation, recurrent haemorrhage, AVM location, venous drainage, arterial aneurysms	AVM size, AVM location, venous drainage, aneurysms, haemorrhage location	CT, MRI, DSA	clinical presentations, date of presentation, imaging source and date, lesion side, handedness, BAVM eloquence, BAVM border with adjacent brain, BAVM haemorrhage, size, periventricular drainage, number of draining veins leaving nidus, number of veins reaching sinus, venous stenosis/ occlusion, venous ectasia,	To determine the short- and the long-term neurological outcome in patients with untreated AVM after first and recurrent haemorrhage and to compare their outcome with a control sample of non-AVM–related intracerebral haemorrhage cases.	Neurologist, rest not mentioned	nil	Univariate statistical models including Wilcoxon Rank Sum test, Two Sample test, χ^2 test/Fisher exact test, multivar-iate logistic regression model

						venous reflux, sinus thrombosis feeding arteries, number of aneurysms, location, haemorrhage history, haemorrhage date, no of vessels to be embolised, Moyamoya-type changes, pial-to-pial collateralisation, intravascular pressure measurement				
Choi 2009	J Neurol Sci, 2009, Stroke Centre, The Neurological Institute/ Academic Interventional Neuroradiology, New York-Presbyterian Hospital/Columbia University Medical Center, New York, USA	735 or 53, 1989	Venous ectasia, haemorrhage presentation, initial BAVM presentation, pattern of feeding artery, venous drainage	AVM size, AVM location, feeding artery, venous drainage, venous ectasia, clinical presentation, haemorrhage presentation	CT, MRI, cerebral angiography	clinical presentations, date of presentation, imaging source and date, lesion side, handedness, BAVM eloquence, BAVM border with adjacent brain, BAVM haemorrhage, haemorrhage location, size, periventricular drainage,	To determine demographic and morphological AVM characteristics associated with FNDs.	none	none	Wilcoxon rank sum-test, χ2-test/Fisher's Exact test multivariate logistic regression models

						number of draining veins leaving nidus, number of veins reaching sinus, venous stenosis/ occlusion, venous reflux, sinus thrombosis arterial aneurysms, number of aneurysms, location, haemorrhage history, haemorrhage date, no of vessels to be embolised, Moyamoya-type changes, pial-to-pial collateralisation, intravascular pressure measurement				
Chowdhury	BMC Res Notes, 2015, Department of Neurology, Dhaka Medical College Hospital	60, 2010-2013	AVM, venous ectasia, intranidal aneurysm, venous stenosis, transit time and flow, feeding artery,	clinical presentation, AVM location, AVM size, pattern of flow through the AVMs, feeding arteries, BAVM eloquence, arterial aneurysms,	MRA, DSA	clinical presentations, date of presentation, imaging source and date, lesion side, handedness, BAVM size, BAVM location,	To examine the clinical and morphological pattern of brain AVMs along with their treatment and short-term outcome in a	neurosurgeons interventional neurologists	none	none

			angiopathic AVM	angiopathic AVM, venous drainage,		BAVM eloquence, BAVM border with adjacent brain, BAVM haemorrhage, haemorrhage location, size, venous drainage, periventricular drainage, number of draining veins leaving nidus, number of veins reaching sinus, venous stenosis/ occlusion, venous ectasia, venous reflux, sinus thrombosis feeding arteries, arterial aneurysms, number of aneurysms, location, haemorrhage history, haemorrhage date, no of vessels to be embolised, Moyamoya-type changes,	tertiary care hospital in Bangladesh.			

						pial-to-pial collateralisation, intravascular pressure measurement				
Cordero-Tous	Jour of Radiosurgery and SBRT, 2014, Hospital Universitario Virgen de la Nieves, Granada	237, 1996 - 2006	none	**BAVM border** with adjacent brain, **arterial aneurysms**, **number of aneurysms**, **feeding arteries**, **venous ectasia**, **venous stenosis**/ occlusion, angiogenesis, **BAVM size**, **clinical presentation**, treatment, **number of draining veins** leaving nidus, SMG,	CT, angiography	date of presentation, imaging source and date, lesion side, handedness, BAVM location, BAVM eloquence, BAVM haemorrhage, haemorrhage location, size, venous drainage, periventricular drainage, number of veins reaching sinus, venous reflux, sinus thrombosis location, haemorrhage history, haemorrhage date, no of vessels to be embolised, Moyamoya-type changes, pial-to-pial collateralisation,	To identify the angiographic characteristics of epileptogenic cAVMs and assess symptom control of the seizure after treatment with radiosurgery	Interventional neuroradiologists	none	Measures of central tendency & dispersion, absolute & relative frequencies for the qualitative variables calculated, Chi-square test with Yates correction, Fisher's exact test

						intravascular pressure measurement				
Cuong	Clinical Neurology and Neurosurgery, 2018, Radiology Department, Hanoi Medical University Hospital, Vietnam	14, 2016-2017	none	SMG, nidus size, venous drainage , AVM location, associated aneurysms, fistula	cDSA and MRI DSA	clinical presentations, date of presentation, imaging source and date, lesion side, handedness, BAVM eloquence, BAVM border with adjacent brain, BAVM haemorrhage, haemorrhage location, size, periventricular drainage, number of draining veins leaving nidus, number of veins reaching sinus, venous stenosis/ occlusion, venous ectasia, venous reflux, sinus thrombosis feeding arteries, number of aneurysms, location, haemorrhage history,	to compare this technique with a non-invasive MR angiography (MRI DSA) for (bAVM).	experienced radiologist	none	none

						haemorrhage date, no of vessels to be embolised, Moyamoya-type changes, pial-to-pial collateralisation, intravascular pressure measurement				
D'Aliberti	World Neurosurg, 2015, Departments of Neurosurgery / Neuroradiology, Niguarda Cà Granda Hospital, Milan	400, ???	Venous pouch, venous aneurysm, variceal enlargement	SMG, AVM size, venous drainage, recruitment, aneurysm type, aneurysm size, number of aneurysms, haemorrhage, venous pouch, venous aneurysm, variceal enlargement	DSA, CT, MRI	clinical presentations, date of presentation, imaging source and date, lesion side, handedness, BAVM location, BAVM eloquence, BAVM border with adjacent brain, haemorrhage location, size, periventricular drainage, number of draining veins leaving nidus, number of veins reaching sinus, venous stenosis/ occlusion, venous reflux, sinus thrombosis	To identify prioritisation based on haemorrhagic risk and indications for treatment of arterial and venous aneurysms associated with AVM	none	none	Fisher exact test general linear model with logistic link (using the standard as well as the exact algorithm) univariate and multivariate modeling

						feeding arteries, location, haemorrhage history, haemorrhage date, no of vessels to be embolised, Moyamoya-type changes, pial-to-pial collateralisation, intravascular pressure measurement				
Da Costa 2008	Stroke, 2008, Toronto Western Hospital	678, 1986-2004	AVM size, deep location, aneurysms, deep venous drainage	clinical presentation, deep venous drainage, deep AVM location, AVM size, aneurysms and location	CT, MRI, DSA	date of presentation, imaging source and date, lesion side, handedness, BAVM eloquence, BAVM border with adjacent brain, BAVM haemorrhage, haemorrhage location, size, periventricular drainage, number of draining veins leaving nidus, number of veins reaching sinus,	To examine the impact of demographic and angiographic features on the likelihood of future haemorrhage	nil	nil	Kaplan-Meier, Univariate survival analysis using the log rank test, Cox proportional hazards model for multivariate analysis, multivariate logistic regression

						venous stenosis/ occlusion, venous ectasia, venous reflux, sinus thrombosis feeding arteries, number of aneurysms, haemorrhage history, haemorrhage date, no of vessels to be embolised, Moyamoya-type changes, pial-to-pial collateralisation, intravascular pressure measurement				
Da Costa 2009	J Neurol Neurosurg Psychiatry, 2009, Division of Neuroradiology, Department of Medical Imaging, Toronto Western Hospital	106, 1989-2004	eloquence, deep venous drainage, associated aneurysms	AVM location, clinical presentation, deep venous drainage, AVM size, associated aneurysms, eloquence, venous stenosis, venous ectasia	MRI, DSA	date of presentation, imaging source and date, lesion side, handedness, BAVM border with adjacent brain, BAVM haemorrhage, haemorrhage location, size, periventricular drainage,	To describe a 15- year experience in the management of posterior fossa brain AVMs with a focus on clinical outcome.	nil	nil	Univariate analysis, multiple logistic regres- sion

						number of draining veins leaving nidus, number of veins reaching sinus, venous reflux, sinus thrombosis feeding arteries, number of aneurysms, location, haemorrhage history, haemorrhage date, no of vessels to be embolised, Moyamoya-type changes, pial-to-pial collateralisation, intravascular pressure measurement				

Daou	Journal of Stroke and Cerebrovascular Diseases, 2020, Departments of Neurosurgery, University of Michigan, Ann Arbor, Michigan	128, 1990-2018	venous varix, associated intranidal or perinidal aneurysm	AVM maximum diameter, venous drainage, eloquence, previous embolization, the Spetzler-Martin grading scale, radiosurgery-based AVM score (RBAS), the angio-architecture of the AVM, including presence of multiple arterial feeders or multiple draining veins, presence of a venous varix, large draining cortical vein, presence of an associated intranidal or perinidal aneurysm, compact vs diffuse nidus, AVM volume,	MRA, CTA, DSA	clinical presentations, date of presentation, imaging source and date, lesion side, handedness, BAVM haemorrhage, haemorrhage location, size, periventricular drainage, number of veins reaching sinus, venous stenosis/ occlusion, venous ectasia, venous reflux, sinus thrombosis, arterial aneurysms, number of aneurysms, location, haemorrhage history, haemorrhage date, no of vessels to be embolised, Moyamoya-type changes, pial-to-pial collateralisation,intravascular pressure measurement	to analyze our experience with linear accelerator (LINAC)-based SRS for brain AVMs, evaluate outcomes, assess factors associated with AVM obliteration and review the various reported predictors of AVM oblitera-tion.	nil	nil	Unpaired t-test, Chi-square, and Fisher's exact tests Univariate analysis stratification and relevant expansion covariates backwards multivariate logistic regression analysis

De Blasi	The Neuroradiology Journal, 2009, Department of Neuroradiology, Bari University Hospital, Italy	n/a	none	**Clinical presentation**, **number of draining veins**, **Venous stenosis, venous ectasia,** venous **associated aneurysm**, pressure in the feeding artery, **venous drainage, nidus size, location,** arterial stenosis, arterial ectasia, dural arterial supply, venous recruitment, angiogenesis, **arterial feeders, nidus borders,** intranidal shunt type, eloquence	angiography	date of presentation, imaging source and date, lesion side, handedness, BAVM eloquence, BAVM haemorrhage, haemorrhage location, size, periventricular drainage, number of veins reaching sinus, venous reflux, sinus thrombosis feeding arteries, number of aneurysms, location, haemorrhage history, haemorrhage date, no of vessels to be embolised, Moyamoya-type changes, pial-to-pial collateralisation, intravascular pressure measurement	To describe the Clinical Features and Classification of Brain AVMs and Cranial DAVFs	none	none	none

de Castro-Afonso	Neuroradiology, 2020, Division of Interventional Neuroradiology, Medical School of Ribeirão Preto, University of São Paulo, Brazil	203, 2010 - 2019	Ruptured AVM, AVM location, glomerular vs diffuse nidus, Flow steal	Previous haemorrhage, nidus location, nidus side, eloquence, nidus diameter, glomerular vs diffuse nidus, Flow steal effect of AVM, AVM-associated lesion (aneurysm, venous & arterial stenosis), venous drainage, single draining vein, single deep draining vein, draining vein diameter	DSA	clinical presentations, date of presentation, imaging source and date, lesion side, handedness, BAVM haemorrhage, haemorrhage location, size, periventricular drainage, number of draining veins leaving nidus, number of veins reaching sinus, venous ectasia, venous reflux, sinus thrombosis feeding arteries, number of aneurysms, location, haemorrhage history, haemorrhage date, no of vessels to be embolised, Moyamoya-type changes, pial-to-pial collateralisation,	To investigate the variables related with intracranial AVM rupture and to examine the association of draining vein diameters and AVM haemorrhage.	five interventional neuroradiologists	nil	chi-square or Fisher's exact tests Mann-Whitney test or Student t test Univariate and multivariate logistic regression analyses variable inflation factor

						intravascular pressure measurement				
Dinc 2019	Neurosurgical Review, 2019, Department of Neurosurgery, Goethe University Hospital Frankfurt	158, 2002-2017	none	Clinical presentation, SMG, aneurysm, deep drainage, AVM location, haemorrhage volume, eloquence	CT, MRI, DSA	date of presentation, imaging source and date, lesion side, handedness, BAVM size, BAVM border with adjacent brain, haemorrhage location, periventricular drainage, number of draining veins leaving nidus, number of veins reaching sinus, venous stenosis/ occlusion, venous ectasia, venous reflux, sinus thrombosis feeding arteries, number of aneurysms, location, haemorrhage history, haemorrhage date, no of vessels to be embolised,	To evaluate different bleeding patterns in haemorrhages due to an AVM and their impact on outcome in terms of risk and treatment stratification.	neuroradiologist	none	Fisher exact test unpaired t test forward stepwise multiple logistic regression analysis.

						Moyamoya-type changes, pial-to-pial collateralisation, intravascular pressure measurement				
Dinc 2018	Journal of Clinical Neuroscience, 2018, Department of Neurosurgery, Goethe University Hospital, Frankfurt	316, 2005-2015	AVM size	AVM location, AVM size, SMG, venous drainage, associated aneurysms	3D 4 vessel DSA, MRI	clinical presentations, date of presentation, imaging source and date, lesion side, handedness, BAVM eloquence, BAVM border with adjacent brain, BAVM haemorrhage, haemorrhage location, size, periventricular drainage, number of draining veins leaving nidus, number of veins reaching sinus, venous stenosis/ occlusion, venous ectasia, venous reflux, sinus thrombosis feeding arteries,	To compare features of supratentorial and infratentorial AVMs.	neurosurgeons, neuroradiologists, radiosurgeons	none	Fisher´s exact, chi square-test, Mann-Whitney U test multivariate analysis stepwise forward WALD model

						number of aneurysms, location, haemorrhage history, haemorrhage date, no of vessels to be embolised, Moyamoya-type changes, pial-to-pial collateralisation, intravascular pressure measurement				
Ding 2013	Neurosurgery, 2013, Department of Neurological Surgery, Uni-versity of Virginia	134, 1989 - 2009	none	Clinical presentation, AVM location, venous drainage, number of draining veins, AVM diameter, AVM volume, SMG	DSA, MRI	date of presentation, imaging source and date, lesion side, handedness, BAVM eloquence, BAVM border with adjacent brain, BAVM haemorrhage, haemorrhage location, size, periventricular drainage, leaving nidus, number of veins reaching sinus,	To evaluate the outcomes of radiosurgery on primary motor or somatosensory cortex AVMs and compare them with radiosurgery outcomes in a matched cohort of non-eloquent lobar AVMs.	nil	nil	univariate Cox regression analyses, Multivariate analysis, Kaplan-Meier survival analysis

						venous stenosis/ occlusion, venous ectasia, venous reflux, sinus thrombosis feeding arteries, arterial aneurysms, number of aneurysms, location, haemorrhage history, haemorrhage date, no of vessels to be embolised, Moyamoya-type changes, pial-to-pial collateralisation, intravascular pressure measurement				
Ding 2017	J neurosurg Pediatr, 2017, University of Virginia, Charlottesville, Virginia	357,	Eloquence, location	Prior haemorrhage status, AVM diameter, volume, eloquence,	CT, DSA, MRI	clinical presentations, date of presentation, imaging source and date, lesion side,	To evaluate the incidence and determine the predictors of haemorrhagic presentation	nil	none	unpaired, 2 indepen-dent–samples Student t-test or Wilcoxon

				deep venous drainage, associated aneurysms, SMG		handedness, BAVM location, BAVM border with adjacent brain, BAVM haemorrhage, haemorrhage location, size, periventricular drainage, number of draining veins leaving nidus, number of veins reaching sinus, venous stenosis/ occlusion, venous ectasia, venous reflux, sinus thrombosis feeding arteries, number of aneurysms, location, haemorrhage history, haemorrhage date, no of vessels to be embolised, Moyamoya-type changes, pial-to-pial collateralisatio n,	in paediatric AVM patients.			rank-sum test Pearson's chi-square or Fisher's exact test logistic regression analysis multivariate models

						intravascular pressure measurement				
Ding 2015	World Neurosurg, 2015, Department of Neurological Surgery, University of Virginia, Charlottesville, USA	1007, 1989-2013	AVM location, eloquence,	Seizure presentation, AVM location, eloquence, AVM size, venous drainage, number of draining veins, associated aneurysms and type, SMG, prior haemorrhage	MRI, DSA	date of presentation, imaging source and date, lesion side, handedness, BAVM border with adjacent brain, BAVM haemorrhage, haemorrhage location, size, periventricular drainage, number of veins reaching sinus, venous stenosis/ occlusion, venous ectasia, venous reflux, sinus thrombosis feeding arteries, number of aneurysms, location, no of vessels to be embolised, Moyamoya-type changes, pial-to-pial collateralisation,	To determine the factors associated with seizure presentation in AVM patients.	none	none	chi-square test independent (two sample), unpaired Student's t-tests Univariate & multivariate logistic regression analysis stratification and relevant expansion covariates

						intravascular pressure measurement				
Ding 2019	Stroke, 2019, Department of Neurosurgery, University of Louisville, USA	2320, 1987-2014	none	prior AVM haemorrhage, prior AVM intervention, location, eloquence, venous drainage, AVM size, associated arterial aneurysms, SMG	angiography	clinical presentations, date of presentation, imaging source and date, lesion side, handedness, BAVM border with adjacent brain, BAVM haemorrhage, haemorrhage location, size, periventricular drainage, number of draining veins leaving nidus, number of veins reaching sinus, venous stenosis/ occlusion, venous ectasia, venous reflux, sinus thrombosis feeding arteries, number of aneurysms, location, haemorrhage date, no of vessels to be embolised,	To evaluate and compare the rates of pre- and post-SRS AVM haemorrhage and identify risk factors.	neurosurgeon	none	Student t or Mann-Whitney U tests Pearson $\chi 2$ or Fisher exact tests multivariate logistic regression models Kaplan-Meier analyses, log-rank test

						Moyamoya-type changes, pial-to-pial collateralisation, intravascular pressure measurement				
Donzelli	**J Neurosurg**, 2020, UCSF School of Medicine and Departments of Anesthesia and Perioperative Care, San Francisco, California	319, 2006-2017	Cmax/ROI, dominant arterial afferent	BAVM size, BAVM eloquence, venous drainage, BAVM border with adjacent brain, BAVM haemorrhage,	DSA	clinical presentations, date of presentation, imaging source and date, lesion side, handedness, BAVM location, haemorrhage location, size, periventricular drainage, number of draining veins leaving nidus, number of veins reaching sinus, venous stenosis/ occlusion, venous ectasia, venous reflux, sinus thrombosis feeding arteries, arterial aneurysms, number of aneurysms, location,	to characterize the role of pre-microsurgical embolization on traditional surgical performance variables.	neurointerventional radiologist	nil	Fisher's exact tests for categorical variables t-tests for continuous variables regression analyses: simple and multivariable linear and logistic regression models

						haemorrhage history, haemorrhage date, no of vessels to be embolised, Moyamoya-type changes, pial-to-pial collateralisation, intravascular pressure measurement				
Dos Santos	Arq Neuropsiquiatr, 2009, Hospital de Base, Sao Paulo	170, 2001-2007	location, BAVM haemorrhage	**Clinical presentation**, **BAVM size**, **BAVM eloquence**, **location**, **side**, **number of feeding arteries**, **aneurysms**, **venous drainage pattern**, number and presence of **venous stenosis or ectasia**, SMG, **BAVM haemorrhage**	CT, MRI	date of presentation imaging source and date handedness BAVM border with adjacent brain BAVM haemorrhage haemorrhage location, size periventricular drainage number of draining veins leaving nidus number of veins reaching sinus venous reflux	To correlate the angioarchitecture of BAVMs with their clinical presentation	none	none	Univariate and multivariate statistical models

						sinus thrombosis number of aneurysms haemorrhage history haemorrhage date no of vessels to be embolised Moyamoya-type changes pial-to-pial collateralisation intravascular pressure measurement				
Downer	The Neuroradiology Journal, 2011, Department of Neuroradiology, John Radcliffe Hospital; Oxford, UK	50, 2007-2010	none	SMG, location, AVM size, haemorrhage, aneurysm, venous varix, venous stenosis, number of draining veins, venous drainage, fistula,	CT, DSA	clinical presentations, date of presentation, imaging source and date, lesion side, handedness, BAVM eloquence, BAVM border with adjacent brain, haemorrhage location, size, periventricular drainage, number of veins reaching sinus,	To determine factors that lead to early endovascular intervention and to investigate whether early intervention has the same complication rate as late intervention in a single centre.	neurointerventional consultant and fellow	none	two-tailed Fisher exact test, or Chi square test two-tailed Mann Whitney U-test

						venous reflux, sinus thrombosis feeding arteries, number of aneurysms, location, haemorrhage history, haemorrhage date, no of vessels to be embolised, Moyamoya-type changes, pial-to-pial collateralisation, intravascular pressure measurement				
Du 2005 et al	Neurosurgery, 2005, University of California, San Francisco	224, 1997 - 2003	none	**BAVM size**, **venous drainage**, **eloquence**, SMG	angiography	clinical presentations date of presentation imaging source and date lesion side handedness BAVM location BAVM border with adjacent brain BAVM haemorrhage	To assess interobserver variability in grading BAVMs using SMG	Neurosurgeon, neuroradiologist Nil else	Inter-rater reliability	Cohen K analysis, Wilcoxon signed-rank test, univariate logistic regression analysis, multivariate analysis.

						haemorrhage location & size, periventricular drainage number of draining veins leaving nidus number of veins reaching sinus venous stenosis/ occlusion venous ectasia venous reflux sinus thrombosis feeding arteries arterial aneurysms number of aneurysms location haemorrhage history haemorrhage date no of vessels to be embolised Moyamoya-type changes				

						pial-to-pial collateralisation intravascular pressure measurement				
Du 2007	Neurosurgery, 2007, Department of Neurological Surgery, University of California, San Francisco	304, 1997-2005	AVM border, deep perforators	AVM size, eloquence, venous drainage, SMG, previous haemorrhage, AVM border, deep perforators	DSA	clinical presentations, date of presentation, imaging source and date, lesion side, handedness, BAVM location, BAVM haemorrhage, haemorrhage location, size, periventricular drainage, number of draining veins leaving nidus, number of veins reaching sinus, venous stenosis/ occlusion, venous ectasia, venous reflux, sinus thrombosis arterial aneurysms, number of aneurysms, location, haemorrhage date,	To determine whether diffuseness of an AVM increases its surgical risk beyond what is predicted by the Spetzler-Martin grading scale and that this risk is compounded by the presence of deep perforators.	Neurosurgeon, neuroradiologist neurologist/nurse clinician (for mRS scores)	none	χ^2 and Mann-Whitney tests of association Univariate & multivariate logistic regression analysis

						no of vessels to be embolised, Moyamoya-type changes, pial-to-pial collateralisation, intravascular pressure measurement				
Du 2016 et al	Int J Clin Exp Med, 2016, Weifang's People's Hospital, Weifang	139, 2005-2014	none	**BAVM site**, **BAVM size**, **feeding artery types**, number of feeding arteries, **type of draining veins**, **number of draining veins**,	CT, MRI, CTA, MRA, cerebral DSA	clinical presentation date of presentation imaging source and date lesion side handedness BAVM eloquence BAVM border with adjacent brain BAVM haemorrhage haemorrhage location, size periventricular drainage number of veins reaching sinus venous stenosis/ occlusion venous ectasia	To explore the associations between risk factors and cAVM haemorrhage	None	None	t-test, chi-square, Fisher's exact test, Kaplan-Meier, univariate or multivariate Cox proportional hazards regression model

						venous reflux sinus thrombosis arterial aneurysms number of aneurysms location haemorrhage history haemorrhage date no of vessels to be embolised Moyamoya-type changes pial-to-pial collateralisation intravascular pressure measurement				
Ellis	J NeuroInterv ent Surg, 2013, Hospital for Sick Children, Toronto	135, 2000 - 2011	venous pouches, venous ectasia, venous stenosis, BAVM location, BAVM border	Age, gender, past medical history, **clinical presentation**, **BAVM location**, **BAVM size**, **venous drainage**, SMG, **border**, **number of draining veins**	**angiography**	date of presentation imaging date lesion side handedness BAVM eloquence BAVM haemorrhage haemorrhage location, size periventricular drainage	To study angioarchitectural features associated with ruptured paediatric BAVMs	none	none	t-test, Pearson's chi square test, Fisher's exact test, Univariate and multivariate logistic regression analysis

				(single or multiple), venous pouches, **venous ectasia**, **venous stenosis**, **sinus thrombosis**, **associated aneurysms**		number of veins reaching sinus venous reflux feeding arteries number of aneurysms location haemorrhage history haemorrhage date no of vessels to be embolised Moyamoya-type changes pial-to-pial collateralisation intravascular pressure measurement				
Fierstra et al	Brain, 2011, Division of Neuroradiology, Toronto Western Hospital	20, ???	Venous congestion	Clinical presentation, type of feeding artery, AVM size, SMG, AVM location, venous congestion, type of AVM nidus	DSA, MRI-based quantitative cerebrovascular reactivity mapping	date of presentation, imaging source and date, lesion side, handedness, BAVM eloquence, BAVM border with adjacent brain,	To determine whether seizure-prone patients with BAVMs exhibit impaired cerebrovascular reserve or morphological angiographic features	Neuroradiologist	nil	independent sample t-tests, Fisher's Exact test, multivariate exact logistic regression

						BAVM haemorrhage, haemorrhage location, size, venous drainage, periventricular drainage, number of draining veins leaving nidus, number of veins reaching sinus, venous stenosis/ occlusion, venous ectasia, venous reflux, sinus thrombosis arterial aneurysms, number of aneurysms, location, haemorrhage history, haemorrhage date, no of vessels to be embolised, Moyamoya-type changes,	predictive of seizures			

						pial-to-pial collateralisation, intravascular pressure measurement				
Fleetwood	J Neurosurg, 2003, Department of Neurosurgery, Division of Neuroradiology, Stanford University, USA	96, 1986-2001	none	AVM location, feeder arteries, venous drainage, AVM size, SMG, haemorrhage, clinical presentation	none	date of presentation, imaging source and date, lesion side, handedness, BAVM eloquence, BAVM border with adjacent brain, haemorrhage location, size, periventricular drainage, number of draining veins leaving nidus, number of veins reaching sinus, venous stenosis/ occlusion, venous ectasia, venous reflux, sinus thrombosis arterial aneurysms, number of aneurysms, location, haemorrhage history,	To retrospectively assess the natural history of AVMs involving the basal ganglia and thalamus, from the time of clinical diagnosis to the time of initial treatment.	none	none	none

						haemorrhage date, no of vessels to be embolised, Moyamoya-type changes, pial-to-pial collateralisation, intravascular pressure measurement				
Fok et al	Hong Kong Med J, 2015, Queen Elizabeth Hospital, Jordan, Hong Kong	67, 2005-2013	location, BAVM haemorrhage, border	**location**, **size**, **morphology/ border**, **venous drainage**, **draining vein (multiple or single)**, **intranidal aneurysm**, varix, **venous stenosis**, **feeding artery (multiple or single)**, **origin of feeder, BAVM haemorrhage**	DSA	clinical presentations date of presentation imaging source and date lesion side handedness BAVM eloquence BAVM haemorrhage haemorrhage location, size periventricular drainage number of veins reaching sinus venous ectasia venous reflux sinus thrombosis	To assess angiographic factors associated with haemorrhagic presentation in paediatric BAVMs	2 interventional neuroradiologists (7 and 15 years experience)	Any discrepancy in reviews was resolved by mutual consensus	Chi squared test, Fisher's exact test, student's t test, logistic regression, univariate & multivariate analysis

						arterial aneurysms number of aneurysms location haemorrhage history haemorrhage date no of vessels to be embolised Moyamoya-type changes pial-to-pial collateralisation intravascular pressure measurement				
Frisoli	J Neurosurg Pediatr, 2013, Department of Neurosurgery, University of Pennsylvania Medical Center	24, ???	none	AVM border	Angiography, CTA, MRI, MRA	clinical presentations, date of presentation, imaging source and date, lesion side, handedness, BAVM size, BAVM location, BAVM eloquence, BAVM haemorrhage, haemorrhage location, size, venous drainage,	To evaluate the intra and interrater reliability of our AVM compactness score.	paediatric neuroradiologist paediatric neurosurgeon paediatric neuroradiology fellow paediatric interventional radiologist	Both inter and intra (9 months apart for first radiologist)	kappa (κ)

						periventricular drainage, number of draining veins leaving nidus, number of veins reaching sinus, venous stenosis/ occlusion, venous ectasia, venous reflux, sinus thrombosis feeding arteries, arterial aneurysms, number of aneurysms, location, haemorrhage history, haemorrhage date, no of vessels to be embolised, Moyamoya-type changes, pial-to-pial collateralisation, intravascular pressure measurement				
Fukuda 2016	World Neurosurgery, 2016, Fukuoka University	11, Aug 2012 – Mar 2014	none	**clinical presentations**, relationship between nidus/	DSA	date of presentation, imaging source and date,	To determine the morbidity associated with initial cerebral AVM	2 neuro-interventionalists	Yes for inter-observer agreement	Cohen's kappa coefficient

	Hospital, Fukuoka			fistulous point, **feeding arteries**, **number of draining veins leaving nidus**.		lesion side, handedness, BAVM size, BAVM location, BAVM eloquence, BAVM border with adjacent brain, BAVM haemorrhage, haemorrhage location, size, venous drainage, periventricular drainage, number of veins reaching sinus, venous stenosis/ occlusion, venous ectasia, venous reflux, sinus thrombosis arterial aneurysms, number of aneurysms, location,	rupture in patients presenting to tertiary medical centers.			

						haemorrhage history, haemorrhage date, no of vessels to be embolised, Moyamoya-type changes, pial-to-pial collateralisation, intravascular pressure measurement				
Fukuda 2017	J NeuroInterve nt Surg, 2017, Rush Medical College, Chicago, Illinois, USA	101, 2008-2014	Cerebral AVM, deep venous drainage, associated aneurysms	Clinical presentation, Haemorrhage presentation, Haemorrhage size, Haemorrhage location, AVM size, AVM location, venous drainage, associated aneurysm, midline shift	DSA, MRI, CTA, CT	clinical presentations, date of presentation, imaging source and date, lesion side, handedness, BAVM size, BAVM location, BAVM eloquence, BAVM border with adjacent brain, BAVM haemorrhage, haemorrhage location, size, venous drainage,	To determine the morbidity associated with initial cerebral AVM rupture in patients presenting to tertiary medical centres.	Neurosurgeon/neurologist to determine outcome (mRS) Not specified for angio review	none	analysis of variance F-test Student's t-test χ^2 test

						periventricular drainage, number of draining veins leaving nidus, number of veins reaching sinus, venous stenosis/ occlusion, venous ectasia, venous reflux, sinus thrombosis feeding arteries, arterial aneurysms, number of aneurysms, location, haemorrhage history, haemorrhage date, no of vessels to be embolised, Moyamoya-type changes, pial-to-pial collateralisation, intravascular pressure measurement				
Fullerton	Stroke, 2005, University of California, San Francisco	400, 2000-2004	ICH	Venous drainage, small AVM, clinical presentation	CT, MRI, DSA	date of presentation, imaging source and date, lesion side, handedness,	To compare the risk of ICH in children	nil	nil	Kaplan–Meier survival analyses

						BAVM location, BAVM eloquence, BAVM border with adjacent brain, BAVM haemorrhage, haemorrhage location, size, periventricular drainage, number of draining veins leaving nidus, number of veins reaching sinus, venous stenosis/ occlusion, venous ectasia, venous reflux, sinus thrombosis feeding arteries, arterial aneurysms, number of aneurysms, location, haemorrhage history, haemorrhage date, no of vessels to be embolised, Moyamoya-type changes,	versus adults with BAVM			Cox proportional hazards regression analyses Chi square tests Log-rank tests and univariate and multivariate

						pial-to-pial collateralisation, intravascular pressure measurement				
Galletti	J Neurol Neurosurg Psychiatry, 2014, Universita degle Studi di Perugia, Perugi	101, 2002-2012	none	Sex, age, seizure type, AVM size, AVM location, AVM side, AVM topography, AVM nidus, arterial feeder, venous drainage, number of draining veins, pseudoaneurysms	angiography	clinical presentations, date of presentation, imaging source and date, handedness, BAVM eloquence, BAVM haemorrhage, haemorrhage location, size, periventricular drainage, number of veins reaching sinus, venous stenosis/ occlusion, venous ectasia, venous reflux, sinus thrombosis arterial aneurysms, number of aneurysms, location, haemorrhage history, haemorrhage date, no of vessels to be embolised,	To evaluate seizures as first clinical manifestation of AVMs in relation to angioarchitectural features of these vascular anomalies	Neurosurgeons, neurologists for patient assessment. Interventional neuroradiologists for DSA review	none	Chi squared test, multivariate logistic regression

						Moyamoya-type changes, pial-to-pial collateralisation, intravascular pressure measurement				
Garcin	Neurology, 2012, Department of Neurology, Paris	155, 2003-2006	**Initial AVM presentation (haemorrhagic and non-haemorrhagic), AVM size AVM location**, **feeding arteries, venous drainage venous ectasia**	**Clinical presentation** (seizure, focal neurological deficit, headache, other, haemorrhage-associated with above symptoms), **AVM size**, **AVM location**, **feeding artery**, **venous drainage, venous ectasia**	CT, MRI, DSA	date of presentation, imaging source and date, lesion side, handedness, BAVM eloquence, BAVM border with adjacent brain, BAVM haemorrhage, haemorrhage location, size, periventricular drainage, number of draining veins leaving nidus, number of veins reaching sinus, venous stenosis/ occlusion, venous reflux, sinus thrombosis arterial aneurysms, number of aneurysms,	To identify the morphologic predictors of symptomatic epilepsy in patients with AVMs	Neurosurgeons, neuroradiologists, neurologists	none	Univariate & multivariate logistic regression models

						location, haemorrhage history, haemorrhage date, no of vessels to be embolised, Moyamoya-type changes, pial-to-pial collateralisation, intravascular pressure measurement				
Gauvrit	Am J Neuroradiol, 2005, Department of Neuroradiology (J.-Y.G., X.L., H.R., J.-P.P.), EA 2691, Roger Salengro Hospital, University Hospital of Lille, Lille, France	11, 2003 - 2004	Venous drainage	venous drainage, clinical presentations, BAVM location, BAVM size,	DSA, 3D MRA, MRI	date of presentation, imaging source and date, lesion side, handedness, BAVM eloquence, BAVM border with adjacent brain, BAVM haemorrhage, haemorrhage location, size, periventricular drainage, number of draining veins leaving nidus, number of veins reaching sinus, venous stenosis/ occlusion,	**to develop 3D dynamic MR digital subtraction angiography with high temporal resolution**	four neuroradiologists	Yes, interobserver & intertechnique agreement	Kappa statistic

						venous ectasia, venous reflux, sinus thrombosis feeding arteries, arterial aneurysms, number of aneurysms, location, haemorrhage history, haemorrhage date, no of vessels to be embolised, Moyamoya-type changes, pial-to-pial collateralisation, intravascular pressure measurement				
Geibprasert	J Neurosurg, 2009, Department of Radiology, Ramathibodi Hospital, Bangkok, Thailand	8, 2000-2007	none	AVM location, AVM size, venous drainage, draining veins	angiography	clinical presentations, date of presentation, imaging source and date, lesion side, handedness, BAVM eloquence, BAVM border with adjacent brain, BAVM haemorrhage,	To present possible pathological mechanisms, clinical and imaging findings, and to describe the management and outcome in patients with hydrocephalus due to unruptured	none	none	none

						haemorrhage location, size, periventricular drainage, number of veins reaching sinus, venous stenosis/ occlusion, venous ectasia, venous reflux, sinus thrombosis feeding arteries, arterial aneurysms, number of aneurysms, location, haemorrhage history, haemorrhage date, no of vessels to be embolised, Moyamoya-type changes, pial-to-pial collateralisation, intravascular pressure measurement	pial brain AVMs			
Griessenauer	J Neurosurg, 2014, University of Alabama at Birmingham	15, ?duration	none	SMG, **BAVM size, BAVM eloquence**, **venous drainage**, Pollock-	MR, CTA, DSA	clinical presentations, date of presentation,	To examine observer reliability of frequently used AVM grading	1 vascular neurosurgeon, 2 neuroradiologists, 2 senior	Yes	Kappa analysis, Kendall's coefficient of concordance, interclass

				Flickinger grade, **BAVM location**, BAVM volume		imaging source and date, lesion side, handedness, BAVM border with adjacent brain, BAVM haemorrhage, haemorrhage location, size, periventricular drainage, number of draining veins leaving nidus, number of veins reaching sinus, venous stenosis/ occlusion, venous ectasia, venous reflux, sinus thrombosis feeding arteries, arterial aneurysms, number of aneurysms, location,	scales, including the 5-tier S-M scale, 3-tier Spetzler-Ponce scale and the Pollock-Flickinger scale, using current imaging modalities	neurosurgical residents		correlation coefficient

						haemorrhage history, haemorrhage date, no of vessels to be embolised, Moyamoya-type changes, pial-to-pial collateralisation, intravascular pressure measurement				
Gross	J Neurosurg, 2013, Department of Neurological Surgery, Brigham and Women's Hospital and Harvard Medical School, Boston, USA	Nine natural history studies with 3923 patients and 18,423 patient-years of follow-up	none	clinical presentations, BAVM location, venous drainage, arterial aneurysms, BAVM size, prior haemorrhage	none	date of presentation, imaging source and date, lesion side, handedness, BAVM eloquence, BAVM border with adjacent brain, BAVM haemorrhage, haemorrhage location, size, periventricular drainage, number of draining veins leaving nidus, number of veins reaching sinus,	To provide overall arteriovenous malformation (AVM) hemorrhage rates and to elucidate significant risk factors for hemorrhage.	none	none	meta-analyses of hazard ratios using a random-effects approach. Publication bias was assessed using the Egger regression test and rank correlation with the Kendall tau for each categorical

						venous stenosis/ occlusion, venous ectasia, venous reflux, sinus thrombosis feeding arteries, number of aneurysms, location, haemorrhage date, no of vessels to be embolised, Moyamoya-type changes, pial-to-pial collateralisation, intravascular pressure measurement				factor considered in the Cox proportional hazards regression model.
Guo	Stroke, 2012, Centre for Cerebrovascular Research, Department of Anaesthesia and Perioperative Care, University of California, San Francisco, USA	975, 1992 and 2011	none	Clinical presentation, haemorrhage presentation, previous haemorrhage, venous drainage, eloquence, AVM deep location, aneurysm (associated/ not), AVM size	CT, MR, DSA	date of presentation, imaging source and date, lesion side, handedness, BAVM border with adjacent brain, haemorrhage location, size, periventricular drainage, number of draining veins leaving nidus,	To investigate whether bAVM silent intralesional microhemorrhage (asymptomatic bleeding in the nidal compartment) might serve as a marker for increased risk of symptomatic intracranial haemorrhage	attending neuro-interventional radiologist	none	t tests chi-squared tests univariate and multivariable logistic regression Cox proportional hazards analysis

						number of veins reaching sinus, venous stenosis/ occlusion, venous ectasia, venous reflux, sinus thrombosis feeding arteries, number of aneurysms, location, haemorrhage date, no of vessels to be embolised, Moyamoya-type changes, pial-to-pial collateralisation, intravascular pressure measurement				Kaplan-Meier survival curves, log-rank tests
Halim 2002	Stroke, 2002, University of California, San Francisco	82, 2000-2001	AVM size, venous drainage, feeding artery, arterial aneurysms, ***clinical presentation*** (not defined in general but defined individually):	Clinical presentation, AVM haemorrhage, AVM size, venous drainage, associated arterial aneurysms and types (including nidal)	CT, MRI, angiography	date of presentation, imaging source and date, lesion side, handedness, BAVM location, BAVM eloquence, BAVM border with adjacent brain, haemorrhage location, size,	To study the association between coexisting aneurysms and initial presentation with intracranial haemorrhage in patients with BAVM evaluated at	attending interventional neuroradiologist	none	Wilcoxon rank-sum test Fisher exact test Pearson chi 2 test logistic regression

			BAVM haemorrhage, seizure, focal deficit, headache, other, incidental.			periventricular drainage, number of draining veins leaving nidus, number of veins reaching sinus, venous stenosis/ occlusion, venous ectasia, venous reflux, sinus thrombosis feeding arteries, number of aneurysms, haemorrhage history, haemorrhage date, no of vessels to be embolised, Moyamoya-type changes, pial-to-pial collateralisation, intravascular pressure measurement	two tertiary-care centres.			complete multivariate model
Halim 2004	Stroke, 2004, Departments of Anesthesia and Perioperative Care, Center for Cerebrovascul	790, 1961 - 2001	nil	BAVM size, BAVM haemorrhage, venous drainage,	Not mentioned	clinical presentations, date of presentation, imaging source and date, lesion side, handedness, BAVM location,	To demonstrate that initial clinical presentation with ICH is associated with a higher	Not mentioned	nil	univariate and multivariate Cox proportional hazards models Stratified analyses

	ar Research, University of California, San Francisco					BAVM eloquence, BAVM border with adjacent brain, haemorrhage location, size, periventricular drainage, number of draining veins leaving nidus, number of veins reaching sinus, venous stenosis/ occlusion, venous ectasia, venous reflux, sinus thrombosis feeding arteries, arterial aneurysms, number of aneurysms, location, haemorrhage history, haemorrhage date, no of vessels to be embolised, Moyamoya-type changes, pial-to-pial collateralisatio n,	rate of subsequent ICH in the natural course before any treatment is undertaken.			backward stepwise ap-proach Kaplan–Meier curves paired (McNemar) χ^2 tests.

						intravascular pressure measurement				
Hartmann 2002	Stroke, 2002, Stroke Center, Neurological Institute, New York Presbyterian Hospital, USA	233, 1991-1998	none	clinical presentations, BAVM size, BAVM location, feeding arteries, SMG, arterial aneurysms, venous drainage, eloquence,	DSA	date of presentation, imaging source and date, lesion side, handedness, BAVM eloquence, BAVM border with adjacent brain, BAVM haemorrhage, haemorrhage location, size, periventricular drainage, number of draining veins leaving nidus, number of veins reaching sinus, venous stenosis/ occlusion, venous ectasia, venous reflux, sinus thrombosis number of aneurysms, location, haemorrhage history, haemorrhage date, no of vessels to be embolised,	to prospectively and independently assess treatment outcome after embolization therapy of brain AVMs with modern embolization techniques and to analyze determinants of treatment-related neurological deficits.	Neurologist mentioned	none	Univariate statistics (chi square or, when appropriate, Fisher's exact test, *t* test) and forward stepwise multiple logistic regression

						Moyamoya-type changes, pial-to-pial collateralisation, intravascular pressure measurement				
Hartmann 2005	Stroke, 2005, Doris and Stanley Tananbaum Stroke Center, Neurological Institute, Columbia University College of Physicians and Surgeons, New York, USA	119, 1991-1999	SMG	Clinical presentation, haemorrhage presentation, AVM diameter, AVM deep arterial feeders, borderzone AVM location, AVM location, concurrent arterial aneurysms, SMG, AVM size, venous drainage, eloquence	angiography	date of presentation, imaging source and date, lesion side, handedness, BAVM haemorrhage, haemorrhage location, size, periventricular drainage, number of draining veins leaving nidus, number of veins reaching sinus, venous stenosis/ occlusion, venous ectasia, venous reflux, sinus thrombosis number of aneurysms, location, haemorrhage history, haemorrhage date, no of vessels to be embolised,	To assess treatment outcome after combined embolisation with subsequent surgical therapy of brain AVMs and to analyse determinants of treatment-related neurologic deficits.	Unclear who assessed angioarchitecture For treatment: senior neuroradiologist senior neurosurgeons	none	Univariate logistic regression analyses multiple logistic regression model using backward elimination procedures

						Moyamoya-type changes, pial-to-pial collateralisation, intravascular pressure measurement				
Haw	J Neurosurg, 2006, Division of Neurosurgery, Vancouver General Hospital, University of British Columbia, Vancouver, Canada	306, 1984-2002	none	clinical presentations, BAVM haemorrhage, AVM location, eloquence, venous drainage, AVM size, SMG, fistula, feeding arteries	angiography	date of presentation, imaging source and date, lesion side, handedness, BAVM size, BAVM border with adjacent brain, haemorrhage location, size, periventricular drainage, number of draining veins leaving nidus, number of veins reaching sinus, venous stenosis/ occlusion, venous ectasia, venous reflux, sinus thrombosis arterial aneurysms, number of aneurysms, location, haemorrhage history,	To determine the rates of mortality and morbidity associated with the embolisation of AVMs of the brain and to analyse the factors related to embolisation-related complications.	Neurosurgeons, interventional neuroradiologists, radiosurgery specialists	none	GEE approach

						haemorrhage date, no of vessels to be embolised, Moyamoya-type changes, pial-to-pial collateralisation, intravascular pressure measurement				
Hernesniemi	Neurosurgery, 2008, Department of Neurosurgery, Helsinki University Central Hospital	238, 1942-2005	none	AVM rupture, AVM location, AVM size, venous drainage	DSA, CT, MRI	clinical presentations, date of presentation, imaging source and date, lesion side, handedness, BAVM eloquence, BAVM border with adjacent brain, haemorrhage location, size, periventricular drainage, number of draining veins leaving nidus, number of veins reaching sinus, venous stenosis/ occlusion, venous ectasia, venous reflux, sinus thrombosis	To perform a long-term follow-up study in an unselected, consecutive patient population with AVMs admitted to a single department between 1942 and 2005.	none	none	Univariate Cox regression analysis multivariate Cox regression analyses forward stepwise procedure to test

						feeding arteries, arterial aneurysms, number of aneurysms, location, haemorrhage history, haemorrhage date, no of vessels to be embolised, Moyamoya-type changes, pial-to-pial collateralisation, intravascular pressure measurement				
Hetts et al	AJNR, 2014, University of California, San Francisco	833, 2001 - 2013	none	Nidus morphology, nidus **location**, **draining veins**, **aneurysm**s	Angiogram, CT, MR	Clinical presentation, date of presentation, imaging source and date, lesion side, handedness, BAVM size, BAVM eloquence, BAVM border with adjacent brain, BAVM haemorrhage,	To determine whether clinical and angioarchitectural features of BAVM were different between children and adults	Neurointerventional radiologist Nil else	None	Univariable and multivariable Cox regression survival analyses, Kaplan-Meier survival analysis, log-rank test

						haemorrhage location, venous drainage, periventricular drainage, number of veins reaching sinus, venous stenosis/ occlusion, venous ectasia, venous reflux, sinus thrombosis, feeding arteries, haemorrhage history, haemorrhage date, no of vessels to be embolised, Moyamoya-type changes, pial-to-pial collateralisation, intravascular pressure measurement				
Hofmeister	Stroke, 2000, Berufsgenoss	1289,	SMG, deep venous	Deep venous drainage,	none	date of presentation,	To assess demographic, clinical, and	none	none	ANOVA

	enschaftliche Kliniken der Stadt Halle, Bergmannstrost, Halle/Saale, Germany	999 for age analysis Countries: Berlin, Paris, Middle and Far East, New York, and Toronto	drainage, eloquence	eloquence, AVM size, clinical presentation, SMG		imaging source and date, lesion side, handedness, BAVM location, BAVM border with adjacent brain, BAVM haemorrhage, haemorrhage location, size, periventricular drainage, number of draining veins leaving nidus, number of veins reaching sinus, venous stenosis/ occlusion, venous ectasia, venous reflux, sinus thrombosis feeding arteries, arterial aneurysms, number of aneurysms, location, haemorrhage history, haemorrhage date, no of vessels to be embolised, Moyamoya-type changes,	morphological characteristics of patients with brain AVMs in a multicentre study			contingency tables Bonferroni corrections log-linear models Chi^2 test of independence Post hoc analyses multivariate saturated hierarchical log-linear model

						pial-to-pial collateralisation, intravascular pressure measurement				
Hoh	Neurosurgery, 2002, Neurosurgical Service, Boston	424, 1991-1999	none	Sex, age, AVM size, AVM location, occurrence of ICH, seizure type, duration of seizures, treatment modality, AVM obliteration	None mentioned	clinical presentations, date of presentation, imaging source and date, lesion side, handedness, BAVM eloquence, BAVM border with adjacent brain, BAVM haemorrhage, haemorrhage location, size, venous drainage, periventricular drainage, number of draining veins leaving nidus, number of veins reaching sinus, venous stenosis/ occlusion, venous ectasia, venous reflux, sinus thrombosis feeding arteries,	To determine factors associated with cAVM seizure incidence & seizure outcomes	Neurosurgeons, interventional & diagnostic neuroradiologists, radiation oncologists, neurologists	none	Chi-square test, t test

						arterial aneurysms, number of aneurysms, location, haemorrhage history, haemorrhage date, no of vessels to be embolised, Moyamoya-type changes, pial-to-pial collateralisation, intravascular pressure measurement				
Hu	Neurosurgery, 2019, Department of Radiology, Taipei Veter-ans General Hospital, Taipei, Taiwan;	98, 2011-2017	Deep nidus location, arterial enlargement, perinidal neoangiogenesis, main drainage vein, focal venous pouch, venous rerouting, pseudophlebitic pattern, flow-related aneurysm, venous stenosis	clinical presentations, BAVM location, BAVM eloquence, BAVM size, arterial aneurysms: flow-related & intranidal, arterial enlargement, neoangiogenesis, number of draining veins leaving nidus, venous stenosis/ occlusion, focal venous pouch, venous rerouting,	DSA, MRI, QDSA	date of presentation, imaging source and date, lesion side, handedness, BAVM border with adjacent brain, BAVM haemorrhage, haemorrhage location, size, venous drainage, periventricular drainage, number of veins reaching sinus, venous ectasia, venous reflux,	To explore the impact of hemodynamics on GKRS outcomes	2 neuro-radiologists with 24 and 13 yr of experience in neuroimaging and radio-surgery,	Inter-observer agreement	Univariable and multivariable Cox regression analyses with hazard ratios (HRs) Kaplan–Meier analyses kappa statistic Youden index based on the receiver operating

				pseudophlebitic pattern		sinus thrombosis feeding arteries, number of aneurysms, location, haemorrhage history, haemorrhage date, no of vessels to be embolised, Moyamoya-type changes, pial-to-pial collateralisation, intravascular pressure measurement				characteristic curve analysis
Huang	Journal of Stroke and Cerebrovascular Diseases, 2018, Xiangya Hospital, Central South University, Changsha	173, 2014-2017	Location, venous drainage, number of draining veins, arterial aneurysm,	Epilepsy, location, aneurysms, nidus volume, venous drainage, number of draining veins, haematoma volume, AVM size	CT, MRI, DSA	clinical presentations, date of presentation, imaging source and date, lesion side, handedness, BAVM eloquence, BAVM border with adjacent brain, BAVM haemorrhage, haemorrhage location, periventricular drainage,	To Reanalyse Predictors for the Risk of Haemorrhage in Brain AVMs	neuroradiologists	nil	Fisher's exact test , Pearson $\chi 2$ test, independent samples t-test, linear regression analysis, logistic regres- sion analysis, receiver operating characteristic curve (ROC) and area

						number of veins reaching sinus, venous stenosis/ occlusion, venous ectasia, venous reflux, sinus thrombosis feeding arteries, number of aneurysms, location, haemorrhage history, haemorrhage date, no of vessels to be embolised, Moyamoya-type changes, pial-to-pial collateralisation, intravascular pressure measurement				under curve (AUC)
Hung 2019	Neurosurgery, 2019, Department of Neurosurgery, The Johns Hopkins University, School of Medicine,	526, 1990-2015	flow-related aneurysm	Clinical presentation, haemorrhage presentation, haemorrhage type, AVM location, flow-related aneurysm location,	DSA (though not specifically mentioned)	date of presentation, imaging source and date, lesion side, handedness, BAVM size, BAVM location, BAVM eloquence,	To characterise the risk of haemorrhage /AVM rupture (by observing the correlation between flow-related aneurysm and AVM-related haemorrhagic	none	none	Student's t-test χ^2 test Poisson rate-ratio test

	Baltimore, Maryland, USA			aneurysm size, multiple aneurysms, AVM size, SMG, eloquence, deep venous drainage		BAVM border with adjacent brain, BAVM haemorrhage, haemorrhage location, size, venous drainage, periventricular drainage, number of draining veins leaving nidus, number of veins reaching sinus, venous stenosis/ occlusion, venous ectasia, venous reflux, sinus thrombosis feeding arteries, arterial aneurysms, number of aneurysms, location, haemorrhage history, haemorrhage date, no of vessels to be embolised, Moyamoya-type changes, pial-to-pial collateralisatio n,	presentation and subsequent annual risk of rupture.)			

						intravascular pressure measurement				
Hung 2020	J Neurosurg, 2020, Department of Neurological Surgery, University of Virginia, Charlottesville, Virginia	267, 1989, 2012	revascularisation, collateral flow, neovascularisation, AVM obliteration	clinical presentations, BAVM size, SMG, BAVM haemorrhage, BAVM location, BAVM eloquence, venous drainage, flow-related aneurysm,	MRI/MRA, DSA	date of presentation, imaging source and date, lesion side, handedness, BAVM border with adjacent brain, haemorrhage location, size, periventricular drainage, number of draining veins leaving nidus, number of veins reaching sinus, venous stenosis/ occlusion, venous ectasia, venous reflux, sinus thrombosis feeding arteries, arterial aneurysms, number of aneurysms, location, haemorrhage history, haemorrhage date, no of vessels to be embolised,	To compare the long-term outcome of arteriovenous malformations (AVMs) treated with and without pre-SRS embolization.	neurosurgeon and a neuroradiologist	none	Pearson chi-square test, Fisher exact test, independent t-test, and Mann-Whitney U-test Kaplan-Meier method Univariate and multivariate analyses were performed using the Cox proportional hazards regression model univariate binary logistic

						Moyamoya-type changes, pial-to-pial collateralisation, intravascular pressure measurement				regression analysis
Huo	J Neurosurg, 2016, Department of Interventional Neuroradiology, Beijing Neurosurgical Institute and Beijing Tiantan Hospital, Beijing, China	404, 2002-2012	none	BAVM location, venous drainage, number of draining veins leaving nidus, BAVM size, SMG	MRI, DSA	clinical presentations, date of presentation, imaging source and date, lesion side, handedness, BAVM eloquence, BAVM border with adjacent brain, BAVM haemorrhage, haemorrhage location, size, periventricular drainage, number of veins reaching sinus, venous stenosis/ occlusion, venous ectasia, venous reflux, sinus thrombosis feeding arteries, arterial aneurysms,	To present the combined treatment experience with a large cohort of patients harbouring partially embolized AVMs followed by GKS and to assess the predictive factors for AVM obliteration and haemorrhage after GKS	attending neurosurgeon and neuroradiologist	none	t-test for continuous variables and the chi-square test for categorical variables log- rank (Mantel-Cox) test of the Kaplan-Meier univariate analysis logistic regression

						number of aneurysms, location, haemorrhage history, haemorrhage date, no of vessels to be embolised, Moyamoya-type changes, pial-to-pial collateralisation, intravascular pressure measurement				
Iancu-Gontard (from PubMed similar articles to Al Shahi)	AJNR, 2007, Centre Hospitalier de l'Universite de Montreal, Notre-Dame Hospital, Montreal	50, 1994-2005	none	SMG**: BAVM size**, **BAVM eloquence**, **venous drainage**, endovascular treatment results, collateral circulation/ **pial-to-pial collateralisation**, arterial **aneurysms**,	CT, MRI, DSA	clinical presentations, date of presentation, imaging source and date, lesion side, handedness, BAVM location, BAVM border with adjacent brain, BAVM haemorrhage, haemorrhage location, size, periventricular drainage,	To determine inter- and intraobserver agreement of various angioarchitectural characteristics of BAVM & endovascular treatment results.	Interventional neuroradiologists (2 experienced)	Yes	Kappa statistic

						number of draining veins leaving nidus, number of veins reaching sinus, venous stenosis/ occlusion, venous ectasia, venous reflux, sinus thrombosis number of aneurysms, location, haemorrhage history, haemorrhage date, no of vessels to be embolised, Moyamoya-type changes, intravascular pressure measurement				
Illies	Stroke, 2012, University Hospital Hamburg-Eppendorf	72, 2006-2011	none	Haemorrhage, nidus location, venous drainage, aneurysm presence,	DSA, 4D MRA, 3D TOF MRA	clinical presentations, date of presentation, imaging source and date,	To study if AVMs with anatomical properties associated with an increased	neuroradiologist	nil	Multiple normal regression model

				nidus size, venous stenosis, number of draining veins		lesion side, handedness, BAVM eloquence, BAVM border with adjacent brain, haemorrhage location, size, periventricular drainage, number of veins reaching sinus, venous ectasia, venous reflux, sinus thrombosis feeding arteries, arterial aneurysms, location, haemorrhage history, haemorrhage date, no of vessels to be embolised, Moyamoya-type changes, pial-to-pial collateralisation,	rupture risk exhibit different haemodynamic characteristics than those without these properties			

						intravascular pressure measurement				
Imbesi (from Al Shahi)	AJNR, 2002, University of California, San Diego Medical Center	11, ? duration	AVM nidus size	**AVM nidus size**	Angiograms	Everything else	To devise an improved method for measuring AVM nidus size that provides objective and reproducible results	Neuroradiologists (3 experienced)	Yes for inter-observer	Kendall coefficient of concordance
Iosif 2015	J Neurosurg, 2015, Dupuytrens University Hospital, Limoges	20, Jan 2008 – Jun 2013	none	**BAVM size**, **BAVM location**, SMG, **venous drainage**, **feeding arteries**, **number of draining veins leaving nidus**, GCS, mRS, no. of embolisation sessions	CT, MRA & DSA	clinical presentations, date of presentation, imaging source and date, lesion side, handedness, BAVM eloquence, BAVM border with adjacent brain, BAVM haemorrhage, haemorrhage location, size, periventricular drainage, number of veins reaching sinus, venous stenosis/ occlusion, venous ectasia, venous reflux,	To report outcomes of curative endovascular transvenous embolisation in a series of patients with untreatable lesions	Interventional neuroradiologists	none	Student t-test, de Agostino-Pearson test, chi-square test

						sinus thrombosis arterial aneurysms, number of aneurysms, location, haemorrhage history, haemorrhage date, no of vessels to be embolised, Moyamoya-type changes, pial-to-pial collateralisation, intravascular pressure measurement				
Iosif 2019	J NeuroInterve nt Surg, 2019, Department of interventional neuroradiolog y, "Dupuytren" University hospital, Limoges, France	73, 2008-2016	none	clinical presentations, BAVM location, BAVM size, SMG, arterial aneurysms, ve nous drainage, venous stenosis/ occlusion, venous ectasia,	MRI, angiography	date of presentation, imaging source and date, lesion side, handedness, BAVM eloquence, BAVM border with adjacent brain, BAVM haemorrhage, haemorrhage location, size, periventricular drainage, number of draining veins leaving nidus,	To achieve curative embolization, ideally in a single session, by dual microcatheteri zation techniques with arterial and/or venous access, according to the angioarchitect ure.	consultant interventional neuroradiologist s, senior neurosurgeon. Senior anaesthetist	none	chi^2 test, Student t-test d'Agostino-Pearson test

						number of veins reaching sinus, venous reflux, sinus thrombosis feeding arteries, number of aneurysms, location, haemorrhage history, haemorrhage date, no of vessels to be embolised, Moyamoya-type changes, pial-to-pial collateralisation, intravascular pressure measurement				
Iryo	J Comput Assist Tomogr, 2016, Department of Diagnostic Radiology, Kumamoto University, Japan	6, 2012-2013	none	BAVM size, feeding arteries, venous drainage,	4D ASL MRA, DSA	clinical presentations, date of presentation, imaging source and date, lesion side, handedness, BAVM location, BAVM eloquence, BAVM border with adjacent brain, BAVM haemorrhage,	to assess the usefulness of 3-T 4-dimensional (4D) arterial spin-labeling (ASL)–based magnetic resonance angiography (MRA) with color-coded time-of-arrival (TOA) maps for the evaluation of cerebral arteriovenous malformations (AVMs).	experienced neuroradiologist (19 & 20 years experience) and neurosurgeon	Interobserver, intermodality agreement	Kappa coefficient

						haemorrhage location, size, periventricular drainage, number of draining veins leaving nidus, number of veins reaching sinus, venous stenosis/ occlusion, venous ectasia, venous reflux, sinus thrombosis arterial aneurysms, number of aneurysms, location, haemorrhage history, haemorrhage date, no of vessels to be embolised, Moyamoya-type changes, pial-to-pial collateralisation, intravascular pressure measurement				
Jayaraman 2008	AJNR, 2008, Departments of Radiology, Stanford University	192, 1995-2005	none	clinical presentations, BAVM haemorrhage, BAVM eloquence,	angiography	date of presentation, imaging source and date, lesion side, handedness,	to examine the overall neurologic complication rate in patients	Neurology for assessing awake patients before & after	none	Univariate analysis

	Medical Centre, Stanford, California, USA			venous drainage, SMG, BAVM size,		BAVM location, BAVM border with adjacent brain, haemorrhage location, size, periventricular drainage, number of draining veins leaving nidus, number of veins reaching sinus, venous stenosis/ occlusion, venous ectasia, venous reflux, sinus thrombosis feeding arteries, arterial aneurysms, number of aneurysms, location, haemorrhage history, haemorrhage date, no of vessels to be embolised, Moyamoya-type changes, pial-to-pial collateralisation, intravascular pressure measurement	undergoing AVM embolization and analyse the factors that may determine increased risk.	provocative testing		

Jayaraman 2012	J NeuroInterve nt Surg 2012, Alpert Medical School at , Brown University, Providence, USA	2005-2009	none	clinical presentations, BAVM haemorrhage, lesion side, BAVM size, BAVM location, arterial aneurysms, venous drainage, venous stenosis/ occlusion, venous ectasia,	angiography	date of presentation, imaging source and date, handedness, BAVM eloquence, BAVM border with adjacent brain, haemorrhage location, size, periventricular drainage, number of draining veins leaving nidus, number of veins reaching sinus, venous reflux, sinus thrombosis feeding arteries, number of aneurysms, location, haemorrhage history, haemorrhage date, no of vessels to be embolised, Moyamoya-type changes, pial-to-pial collateralisatio n, intravascular pressure measurement	to provide consensus recommendati ons for reporting standards, terminology and written definitions when reporting on the radiological evaluation and endovascular treatment of cerebral arteriovenous malformations (AVMs).	Not specified	none	n/a

Jiang et al	The Neuroradiology Journal, 2011, Beijing Neurosurgical Institute, Beijing	302, 1999 - 2008	Varix, venous stenosis, BAVM location	**Clinical presentation**, **BAVM location**, **BAVM size**, **type of feeders**, **venous drainage**, **varices**, venous stenosis, **aneurysm location** (associated arterial, flow-related, intranidal) **aneurysm number**	DSA	date of presentation lesion side handedness BAVM eloquence BAVM border with adjacent brain BAVM haemorrhage haemorrhage location, size periventricular drainage number of draining veins leaving nidus number of veins reaching sinus venous reflux sinus thrombosis haemorrhage history haemorrhage date no of vessels to be embolised Moyamoya-type changes pial-to-pial collateralisation	To identify the characteristics of unruptured BAVMs presenting with seizures	none	none	Univariate tests, multivariate logistic regression model

						intravascular pressure measurement				
Jiao	J Neurosurg, 2018, Department of Neurosurgery, Beijing Tiantan Hospital	201, 2012-2015	Haemorrhagic presentation	AVM size, AVM side, diffuse AVM border, deep venous drainage, arterial feeders, haemorrhagic presentation, eloquence, SMG	CT, MRI, DSA	clinical presentations, date of presentation, imaging source and date, handedness, BAVM location, haemorrhage location, size, periventricular drainage, number of draining veins leaving nidus, number of veins reaching sinus, venous stenosis/ occlusion, venous ectasia, venous reflux, sinus thrombosis arterial aneurysms, number of aneurysms, location, haemorrhage history, haemorrhage date, no of vessels to be embolised, Moyamoya-type changes,	To construct a predictive grading system combining lesion-to-eloquence distance for selecting patients with BAVMs for surgery.	neurosurgeons	none	Univariable logistic regression analysis Multivariable logistic regression analyses

						pial-to-pial collateralisation, intravascular pressure measurement				
Jin	J Neurosurg, 2019, Division of Neuroradiology, Toronto Western Hospital, Toronto	353, 2000 - 2017	Nidus location, haemorrhage volume	Age, gender, **nidus location**, nidus volume, feeding artery, draining vein, venous drainage, SMG, type of haemorrhage, **haemorrhage volume**, mRS, EVD/ embolisation, F/U time, F/U MRS	CT, MRI, DSA	clinical presentations, date of presentation, imaging source and date, lesion side, handedness, BAVM border with adjacent brain, haemorrhage location, periventricular drainage, number of number of veins reaching sinus, venous stenosis/ occlusion, venous ectasia, venous reflux, sinus thrombosis arterial aneurysms, number of aneurysms, location, haemorrhage history, haemorrhage date,	To describe changes in the angioarchitecture of cAVMs between acute & delayed DSA obtained after haemorrhage, & to examine cAVM characteristics predicting change	Interventional neuroradiologists	none	Continuous variables: mean+/- SD, student t test (normal), Mann-Whitney U-test (non-normal distribution). Categorical variables: frequencies, Fisher exact test, Pearson chi-square test. Univariate/ multivariate logistic analyses done to assess predictors for angioarchitectural change.

						no of vessels to be embolised, Moyamoya-type changes, pial-to-pial collateralisation, intravascular pressure measurement				
Jordan	The Neuroradiology Journal, 2014, Interventional Neuroradiology Unit, CIMEQ, Institute of Neurology and Neurosurgery; La Habana, Cuba	71, 2006-2011	none	clinical presentations, BAVM haemorrhage, arterial aneurysms, BAVM size, BAVM location, BAVM eloquence, venous drainage, SMG,	angiography	date of presentation, imaging source and date, lesion side, handedness, BAVM border with adjacent brain, haemorrhage location, size, periventricular drainage, number of draining veins leaving nidus, number of veins reaching sinus, venous stenosis/ occlusion, venous ectasia, venous reflux, sinus thrombosis feeding arteries, number of aneurysms, location,	To determine the predictive factors of neurological deficit following endovascular procedures and to evaluate the functional repercussions of long-term complications prospectively in the endovascular treatment of AVMs.	none	none	univariate analysis multiple logistic regression model

						haemorrhage history, haemorrhage date, no of vessels to be embolised, Moyamoya-type changes, pial-to-pial collateralisation, intravascular pressure measurement				
Kakizawa	J Neurosurg, 2002, Department of Neurosurgery, Shinshu University School of Medicine, Matsumoto, Japan	3, ???	none	feeding arteries, number of draining veins leaving nidus,	3D DSA	clinical presentations, date of presentation, imaging source and date, lesion side, handedness, BAVM size, BAVM location, BAVM eloquence, BAVM border with adjacent brain, BAVM haemorrhage, haemorrhage location, size, venous drainage, periventricular drainage, number of veins reaching sinus,	to determine the presence of nidus compartments in clinical cases by using a new radiographic method.	none	none	none

						venous stenosis/ occlusion, venous ectasia, venous reflux, sinus thrombosis arterial aneurysms, number of aneurysms, location, haemorrhage history, haemorrhage date, no of vessels to be embolised, Moyamoya-type changes, pial-to-pial collateralisation, intravascular pressure measurement				
Kandai	Malaysian J Med Sci, 2010, Universiti Sains Malaysia, Kelantan	58, 2000-2007	BAVM size, BAVM location, BAVM haemorrhage	**BAVM size**, **venous drainage**, **arterial feeders**, **feeding-artery aneurysms**, **aneurysm location**, SMG, **BAVM location**, **BAVM haemorrhage**,	IADSA, CT, MRI	clinical presentations date of presentation imaging source and date lesion side handedness BAVM eloquence BAVM border with adjacent brain	To study BAVM angioarchitecture and determine risk factors for haemorrhage	None	None	Multiple logistic regression, Pearson's chi-square, Fisher's exact test

				haemorrhage pattern		haemorrhage location, size periventricular drainage number of draining veins leaving nidus number of veins reaching sinus venous stenosis/ occlusion venous ectasia venous reflux sinus thrombosis number of haemorrhage history haemorrhage date no of vessels to be embolised Moyamoya-type changes pial-to-pial collateralisation intravascular pressure measurement				

Kasliwal	J Neurosurg, 2009, Gamma Knife Unit, Department of Neurosurgery, All India Institute of Medical Sciences, New Delhi, India	489, 1997-2006	BAVM haemorrhage	BAVM haemorrhage, BAVM location, BAVM size, arterial aneurysms, venous drainage, SMG	DSA (if symptomatic, MRI or CT)	clinical presentations, date of presentation, imaging source and date, lesion side, handedness, BAVM eloquence, BAVM border with adjacent brain, haemorrhage location, size, periventricular drainage, number of draining veins leaving nidus, number of veins reaching sinus, venous stenosis/ occlusion, venous ectasia, venous reflux, sinus thrombosis feeding arteries, number of aneurysms, location, haemorrhage history, haemorrhage date, no of vessels to be embolised,	to analyse the outcome of patients sustaining haemorrhage after GKS;	none	none	chi-square test Kaplan-Meier curve

						Moyamoya-type changes, pial-to-pial collateralisation, intravascular pressure measurement				
Kellner et al	J Neurosurg Pediatrics, 2014, Columbia University, New York	85, 1991 - 2012	none	Supratentorial or infratentorial, **nidus side**, **venous drainage**, **nidus size**, **eloquence**, Spetzler-Martin grade, **BAVM haemorrhage**, **aneurysm**	angiography	Clinical presentation, date of presentation, imaging source and date, handedness, location, border with adjacent brain, haemorrhage location, size, periventricular drainage, number of draining veins leaving nidus number of veins reaching sinus venous stenosis/ occlusion venous ectasia venous reflux	To assess the association of draining vein anatomy with haemorrhage in paediatric BAVMs	Neurosurgeon, neuroradiologist Both consultants	None	Fisher's exact test, chi-square test, t-test, Wilcoxon signed-rank test, or Mann-Whitney test

						sinus thrombosis feeding arteries, haemorrhage history haemorrhage date no of vessels to be embolised Moyamoya-type changes pial-to-pial collateralisation intravascular pressure measurement				
Khaw	Stroke, 2004, Columbia University College of Physicians and Surgeons, New York	623, 1989-2002	Initial AVM presentation, haemorrhagic presentation, AVM location, AVM size, venous drainage, arterial aneurysms, feeding artery, AVM nidus, arterial ectasia	Initial AVM presentation, haemorrhagic presentation, AVM location, AVM size, venous drainage, arterial aneurysms and type, feeding artery, AVM nidus, arterial ectasia	CT, MRI, DSA	date of presentation, imaging source and date, lesion side, handedness, BAVM eloquence, BAVM border with adjacent brain, haemorrhage location, size, periventricular drainage, number of draining veins leaving nidus,	To analyse the association of haemorrhagic presentation with infratentorial brain AVMs	nil	nil	Univariate multivariate statistical models

						number of veins reaching sinus, venous stenosis/ occlusion, venous ectasia, venous reflux, sinus thrombosis number of aneurysms, location, haemorrhage history, haemorrhage date, no of vessels to be embolised, Moyamoya-type changes, pial-to-pial collateralisation, intravascular pressure measurement				
Kim 2014	Neurology, 2014, University of California, San Francisco	141, 1989-2003 and 2000-2010	Haemorrhagic presentation, associated arterial aneurysm, venous drainage	Haemorrhagic presentation, AVM size, venous drainage, AVM location, associated arterial aneurysm	CT, MRI, DSA	clinical presentations, date of presentation, imaging source and date, lesion side, handedness, BAVM eloquence, BAVM border with adjacent brain, haemorrhage location, size,	To identify risk factors for intracranial hemorrhage in the natural history course of brain AVMs using individual patient data meta-analysis of 4 existing cohorts.	neurosurgeons, neurointerventional radiologists, neurologists	nil	x^2 tests analysis of variance Kaplan–Meier survival curves and log-rank tests combined multivariable Cox regression analysis

						periventricular drainage, number of draining veins leaving nidus, number of veins reaching sinus, venous stenosis/ occlusion, venous ectasia, venous reflux, sinus thrombosis feeding arteries, number of aneurysms, location, haemorrhage history, haemorrhage date, no of vessels to be embolised, Moyamoya-type changes, pial-to-pial collateralisation, intravascular pressure measurement				Schoenfeld residuals, Harrell's C statistic
Kim 2004	Neurosurgery, 2004, University of California, San Francisco,	314, 1990-1999	Aneurysm, ICH location,	ICH and location, aneurysm, venous drainage, AVM size,	CT, MRI, DSA	clinical presentations, date of presentation, imaging source and date, lesion side, handedness,	To determine if coexisting extranidal arterial aneurysms would be associated	neuroradiologists	nil	univariate anal- ysis using Student's t test, Pear- son's □2 test,

						BAVM location, BAVM eloquence, BAVM border with adjacent brain, Haemorrhage size, periventricular drainage, number of draining veins leaving nidus, number of veins reaching sinus, venous stenosis/ occlusion, venous ectasia, venous reflux, sinus thrombosis feeding arteries, number of aneurysms, location, haemorrhage history, haemorrhage date, no of vessels to be embolised, Moyamoya-type changes, pial-to-pial collateralisation, intravascular pressure measurement	with an increased risk of incident intracranial hemorrhage (ICH) from BAVM rupture.			Fisher's exact test multivariate logistic regression model using backward stepwise regression involving the Wald statistic

Kim 2007	Stroke, 2007, Centre for Cerebrovascular Research, Department of Anaesthesia and Perioperative Care, University of California, San Francisco, USA	1464 (1028 KPMCP and 436 UCSF) 2000-2006	none	Clinical presentation, haemorrhage presentation, AVM size, eloquence, venous drainage, SMG	DSA but not clearly stated	date of presentation, imaging source and date, lesion side, handedness, BAVM location, BAVM border with adjacent brain, haemorrhage location, size, periventricular drainage, number of draining veins leaving nidus, number of veins reaching sinus, venous stenosis/ occlusion, venous ectasia, venous reflux, sinus thrombosis feeding arteries, arterial aneurysms, number of aneurysms, location, haemorrhage history, haemorrhage date, no of vessels to be embolised, Moyamoya-type changes,	To determine whether race/ethnicity was an independent risk factor for subsequent ICH in the natural course in a large, multiethnic cohort of patients with BAVM followed longitudinally.	For surveillance & BAVM management: neurology neurosurgery interventional neuroradiology Unclear for angio review	none	Kaplan-Meier survival curves log-rank test Multivariate Cox regression Univariate Cox regression analysis

						pial-to-pial collateralisation, intravascular pressure measurement				
Kocur	Pol J Radiol 2018, Medical University of Silesia, Department of Neurosurgery, Katowice, Poland	18, 2009-2014	none	clinical presentations, BAVM size, BAVM location, feeding arteries, SMG,	angiography	date of presentation, imaging source and date, lesion side, handedness, BAVM eloquence, BAVM border with adjacent brain, BAVM haemorrhage, haemorrhage location, size, venous drainage, periventricular drainage, number of draining veins leaving nidus, number of veins reaching sinus, venous stenosis/ occlusion, venous ectasia, venous reflux, sinus thrombosis arterial aneurysms, number of aneurysms,	To report our experience with the curative endovascular treatment of brain AVMs with special regard to radiographic and clinical outcomes and procedure-related complications.	none	none	none

						location, haemorrhage history, haemorrhage date, no of vessels to be embolised, Moyamoya-type changes, pial-to-pial collateralisation, intravascular pressure measurement				
Kouznetsov	Neurosurg Focus, 2014, Department of Radiology, CHUM, Montréal	233, 2001-2012	Haemorrhage from prenidal aneurysm rupture	AVM location, haemorrhage presentation, aneurysm size, aneurysm location	CT, angiography	clinical presentations, date of presentation, imaging source and date, lesion side, handedness, BAVM size, BAVM eloquence, BAVM border with adjacent brain, haemorrhage location, size, venous drainage, periventricular drainage, number of draining veins leaving nidus, number of veins reaching sinus,	To evaluate the relative proportions of cases of infra- and supratentorial AVMs in which patients presented with prenidal aneurysm rupture.	neuroradiologist		Z-test

						venous stenosis/ occlusion, venous ectasia, venous reflux, sinus thrombosis feeding arteries, number of aneurysms, location, haemorrhage date, no of vessels to be embolised, Moyamoya-type changes, pial-to-pial collateralisation, intravascular pressure measurement				
Kubalek et al	Acta Neurochir, 2003, University of Freiburg, Germany	171	Localisation, nidus size	Localisation, size, arterial supply, venous drainage	DSA, CT, MRI	Clinical presentation, date of presentation, imaging source and date, lesion side, handedness, BAVM eloquence, BAVM border with adjacent brain, BAVM haemorrhage including location and	To evaluate the angioarchitecture of cerebral arteriove-nous malformations (cAVMs) with special regard to its influence on the risk of intracranial	None	None	χ2

						size, periventricular drainage, number of draining veins leaving nidus, number of veins reaching sinus, venous stenosis, venous ectasia, venous reflux, sinus thrombosis, feeding arteries, aneurysms, number of vessels to be embolised, Moyamoya-type changes, pial-to-pial collaterals, intravascular pressure measurements	haemorrhage			
Kurita	Acta Neurochir (Wien), 2001, Department of Neurosurgery, Graduate School of Medicine, University of Tokyo, Japan	Two, ???	none	clinical presentations, BAVM location, feeding arteries, number of draining veins leaving nidus,	CT, MRI, angiography	date of presentation, imaging source and date, lesion side, handedness, BAVM size, BAVM eloquence,	To describe two patients with an unruptured pial AVM accompanied by significant brain oedema	none	none	none

				number of veins reaching sinus, venous ectasia,		BAVM border with adjacent brain, BAVM haemorrhage, haemorrhage location, size, venous drainage, periventricular drainage, venous stenosis/ occlusion, venous reflux, sinus thrombosis arterial aneurysms, number of aneurysms, location, haemorrhage history, haemorrhage date, no of vessels to be embolised, Moyamoya-type changes, pial-to-pial collateralisation, intravascular pressure measurement	at initial presentation			
Lai	Clin Neuroradiol, 2018, Department of	63, 1999-2013	Eloquence, aneurysm, venous ectasia	clinical presentations, BAVM haemorrhage, BAVM location, BAVM size,	angiography	date of presentation, imaging source and date, lesion side, handedness,	To identify risk factors associated with haemorrhage in posterior	senior staff neuroradiologists	none	Fisher's exact test or the χ^2-test

	Neurosurgery, Zhujiang Hospital, Guangzhou, China			venous drainage, venous ectasia, arterial aneurysms, SMG, eloquence		BAVM border with adjacent brain, haemorrhage location, size, periventricular drainage, number of draining veins leaving nidus, number of veins reaching sinus, venous stenosis/ occlusion, venous reflux, sinus thrombosis feeding arteries, number of aneurysms, location, haemorrhage history, haemorrhage date, no of vessels to be embolised, Moyamoya-type changes, pial-to-pial collateralisation, intravascular pressure measurement	fossa bAVM and to assess clinical outcomes in patients receiving initial endovascular embolization.			Student's *t*-test or the Wilcoxon rank sum test multivariate logistic regression analysis McNemar's test
Lang	J Neurosurg Pediatr, 2012, Department of Neurosurgery,	48, 2005-2010	recurrent AVM	clinical presentations, BAVM size, BAVM location,	DSA, MRI/MRA, CTA	date of presentation, imaging source and date,	To describe the timing of AVM recurrences	Board-certified pediatric neuroradiologist	nil	Wilcoxon rank-sum test

	University of Pennsylvania Medical Center, Philadelphia			BAVM eloquence, venous drainage, SMG		lesion side, handedness, BAVM border with adjacent brain, BAVM haemorrhage, haemorrhage location, size, periventricular drainage, number of draining veins leaving nidus, number of veins reaching sinus, venous stenosis/ occlusion, venous ectasia, venous reflux, sinus thrombosis feeding arteries, arterial aneurysms, number of aneurysms, location, haemorrhage history, haemorrhage date, no of vessels to be embolised, Moyamoya-type changes, pial-to-pial collateralisatio n,	after resection and the modalities on which the recurrences were detected.			Fisher's exact test survival analysis

						intravascular pressure measurement				
Ledezma	Neurosurger, 2006, Department of Neurological Surgery, University of Southern California, Los Angeles, California	168, 1993-2004	none	clinical presentations, BAVM haemorrhage, SMG, venous drainage, BAVM size, BAVM eloquence, arterial aneurysms, BAVM location,	MRI, CT, DSA	date of presentation, imaging source and date, lesion side, handedness, BAVM border with adjacent brain, haemorrhage location, size, periventricular drainage, number of draining veins leaving nidus, number of veins reaching sinus, venous stenosis/ occlusion, venous ectasia, venous reflux, sinus thrombosis feeding arteries, number of aneurysms, location, haemorrhage history, haemorrhage date, no of vessels to be embolised, Moyamoya-type changes,	To review our combined neurovascular unit's experience with embolization for brain AVMs over an 11 year period to determine the incidence of complications and associated morbidity, mortality, and clinical outcome.	cerebrovascular neurosurgeons, endovascular neurosurgeons, interventional neuro-radiologists, and radiosurgeons	none	Univariate tests (chi^2 test or Fisher's exact test) and a multivariate logistic regression model

						pial-to-pial collateralisation, intravascular pressure measurement				
Lee	Neuroradiology, 2002, Department of Medical Imaging, Toronto Western Hospital	4 live cases, 29 cases from literature	AVM size	Clinical presentation, AVM size, AVM location, arterial feeder, number of draining veins, venous drainage, SMG	CT, MRI, DSA	date of presentation, imaging source and date, lesion side, handedness, BAVM eloquence, BAVM border with adjacent brain, BAVM haemorrhage, haemorrhage location, size, periventricular drainage, number of veins reaching sinus, venous stenosis/ occlusion, venous ectasia, venous reflux, sinus thrombosis arterial aneurysms, number of aneurysms, location, haemorrhage history, haemorrhage date,	nil	nil	nil	

						no of vessels to be embolised, Moyamoya-type changes, pial-to-pial collateralisation, intravascular pressure measurement				
Liew	Neurosurgery, 2020, Department of Neurosurgery, Johns Hopkins University School of Medicine, Baltimore, Maryland	763, 1990 - 2015	nidus size, spontaneous obliteration, time to obliteration, intervention, incidence of spontaneous obliteration	clinical presentations, BAVM size, BAVM location, BAVM haemorrhage, venous drainage, feeding arteries, number of draining veins leaving nidus, venous stenosis/ occlusion, SMG, arterial aneurysms: nidus aneurysm, unrelated aneurysm	DSA	date of presentation, imaging source and date, lesion side, handedness, BAVM eloquence, BAVM border with adjacent brain, haemorrhage location, size, periventricular drainage, number of veins reaching sinus, venous ectasia, venous reflux, sinus thrombosis number of aneurysms, location, haemorrhage history, haemorrhage date, no of vessels to be embolised,	To determine the incidence rate and predisposing factors of SpO in a North American cohort.	board-certified neuroradiologist	nil	Student's *t*-test and Fisher's exact test

						Moyamoya-type changes, pial-to-pial collateralisation, intravascular pressure measurement				
Lin	J Neurosurg 2020 Department of Radiology and Neurological Institute, Department of Neurosurgery, Taipei Veterans General Hospital, Taiwan	119, 2011-2017	Deep location, deep venous drainage, flow related aneurysm, main drainage vein, venous stenosis, venous sac	clinical presentations, BAVM haemorrhage, SMG, venous drainage, BAVM location, arterial aneurysms, venous stenosis/ occlusion, venous ectasia	DSA, MRI, CT	date of presentation, imaging source and date, lesion side, handedness, BAVM size, BAVM eloquence, BAVM border with adjacent brain, haemorrhage location, size, periventricular drainage, number of draining veins leaving nidus, number of veins reaching sinus, , venous reflux, sinus thrombosis feeding arteries, number of aneurysms, location, haemorrhage history,	To examine whether cerebral hemodynamic analysis using quantitative digital subtraction angiography (QDSA) can outperform conventional DSA angioarchitecture analysis in evaluating the risk of haemorrhage associated with supratentorial arteriovenous malformations (AVMs).	neuroradiologist with 12 years of experience in radiosurgery and endovascular treatment.	none	Pearson's chi-square test Student t-test univariate & multivariate logistic regression Receiver operating characteristic (ROC) curve analysis

						haemorrhage date, no of vessels to be embolised, Moyamoya-type changes, pial-to-pial collateralisation, intravascular pressure measurement				
Liu 2014	*Interventional Neuroradiology* 2014 Interventional Neuroradiology Department, Beijing Neurosurgical Institute and Beijing Tiantan Hospital, China	31, 2011-2013	none	clinical presentations, BAVM haemorrhage, arterial aneurysms, SMG, BAVM size, BAVM location,	CT, DSA	date of presentation, imaging source and date, lesion side, handedness, BAVM eloquence, BAVM border with adjacent brain, haemorrhage location, size, venous drainage, periventricular drainage, number of draining veins leaving nidus, number of veins reaching sinus, venous stenosis/ occlusion, venous ectasia, venous reflux, sinus thrombosis	To report our results of cerebral AVMs treated with Glubran 2 targeting for curative embolization	none	none	none

						feeding arteries, , number of aneurysms, location, haemorrhage history, haemorrhage date, no of vessels to be embolised, Moyamoya-type changes, pial-to-pial collateralisation, intravascular pressure measurement				
Liu 2013	Neurosurg Rev, 2013, Department of Neurosurgery, Beijing Tiantan Hospital	41, 2009-2011	none	Clinical presentation, Previous haemorrhage, venous drainage, eloquence, AVM size, SMG, AVM side	DSA, CT, MRI	date of presentation, imaging source and date, handedness, BAVM location, BAVM border with adjacent brain, BAVM haemorrhage, haemorrhage location, size, periventricular drainage, number of draining veins leaving nidus, number of veins reaching sinus,	To evaluate the risk factors associated with long-term prognosis of sylvian AVMs treated microsurgically	neurosurgeon	none	Chi-square rank-sum test multivariate logistic regression Odds ratios (ORs)

						venous stenosis/ occlusion, venous ectasia, venous reflux, sinus thrombosis feeding arteries, arterial aneurysms, number of aneurysms, location, haemorrhage date, no of vessels to be embolised, Moyamoya-type changes, pial-to-pial collateralisation, intravascular pressure measurement				
Liu 2015	BMC Neurology, 2015, West China hospital of Sichuan University, Chengdu	89, Mar 2008 – Dec 2013	none	**clinical presentations**, **BAVM size**, **venous drainage**, **BAVM eloquence**, **BAVM location**, SMG, treatment	DSA/ CT angiography	date of presentation, imaging source and date, lesion side, handedness, BAVM border with adjacent brain, BAVM haemorrhage, haemorrhage location, size, , periventricular drainage,	To identify factors associated with seizure occurrence and long-term seizure control in paediatric cAVMs	nil	none	Chi-squared test, student's t-test, multivariate logistic regression, 2-tailed

						number of draining veins leaving nidus, number of veins reaching sinus, venous stenosis/ occlusion, venous ectasia, venous reflux, sinus thrombosis feeding arteries, arterial aneurysms, number of aneurysms, location, haemorrhage history, haemorrhage date, no of vessels to be embolised, Moyamoya-type changes, pial-to-pial collateralisation, intravascular pressure measurement				
Lockwood	World Neurosurg, 2018, Department of Neurosurgery, New Orleans,	One ???	none	clinical presentations, arterial aneurysms, BAVM location, feeding arteries, BAVM size,	CT, angiography	date of presentation, imaging source and date, lesion side, handedness, BAVM eloquence,	To present a 75-year-old female who presented with a sub-arachnoid hemorrhage	none	none	none

	Louisiana, USA			venous drainage,		BAVM border with adjacent brain, BAVM haemorrhage, haemorrhage location, size, periventricular drainage, number of draining veins leaving nidus, number of veins reaching sinus, venous stenosis/ occlusion, venous ectasia, venous reflux, sinus thrombosis number of aneurysms, location, haemorrhage history, haemorrhage date, no of vessels to be embolised, Moyamoya-type changes, pial-to-pial collateralisation, intravascular pressure measurement	secondary to a ruptured aneurysm arising from a flow- related basilar perforator artery feeder of an anterior pontine AVM. Also to report the successful treatment of the aneurysm with coil embolisation.			
Luo 2012	European Journal of Radiology,	302, 1999-2008	AVM nidus size, AVM location, type	Sex, haemorrhage presentation,	angiography	clinical presentations,	To explore angioarchitectural features	nil	none	Chi squared test

	2012, Beijing Neurosurgical Institute		of feeders, varices, venous stenoses, aneurysm type	deep and infratentorial, AVM size (>3cm), AVM location, type of feeders, deep/superficial venous drainage, number of arterial feeders (>3), number of draining veins, venous varices, venous stenoses, perforating feeders, location and number of aneurysms, aneurysm type		date of presentation, imaging source and date, lesion side, handedness, BAVM eloquence, BAVM border with adjacent brain, size, periventricular drainage, number of veins reaching sinus, venous ectasia, venous reflux, sinus thrombosis. haemorrhage date, no of vessels to be embolised, Moyamoya-type changes, pial-to-pial collateralisation, intravascular pressure measurement	of BAVMs in different ages.			
Luo 2014	Acta Neurochir, 2014, Department of Radiology, Taipei Veterans General	523, 2002-2012	none	clinical presentations, SMG, fistula, feeding arteries, number of draining veins leaving nidus, BAVM location,	MRI, DSA, TOF MRA	date of presentation, imaging source and date, lesion side, handedness, BAVM size, BAVM eloquence,	To report the angiographic change of AVF components of CAVMs after SRS and outcomes of	interventional neuroradiology, neurosurgery	none	none

	Hospital, Taiwan, Republic of China			venous ectasia,		BAVM border with adjacent brain, BAVM haemorrhage, haemorrhage location, size, venous drainage, periventricular drainage, number of veins reaching sinus, venous stenosis/ occlusion, venous reflux, sinus thrombosis arterial aneurysms, number of aneurysms, location, haemorrhage history, haemorrhage date, no of vessels to be embolised, Moyamoya-type changes, pial-to-pial collateralisation, intravascular pressure measurement	endovascular embolisation.			
Lv 2010	Interventional Neuroradiology, 2010,	144, 1998-2003	BAVM haemorrhage,	clinical presentations,	DSA	date of presentation,	To estimate the risk and rates of ICH	none	none	Kaplan-Meier survival analysis

	Beijing Neurosurgical Institute and Beijing Tiantan Hospital, China			BAVM haemorrhage, BAVM size, BAVM location, venous drainage, arterial aneurysms,		imaging source and date, lesion side, handedness, BAVM eloquence, BAVM border with adjacent brain, haemorrhage location, size, periventricular drainage, number of draining veins leaving nidus, number of veins reaching sinus, venous stenosis/ occlusion, venous ectasia, venous reflux, sinus thrombosis feeding arteries, number of aneurysms, location, haemorrhage history, haemorrhage date, no of vessels to be embolised, Moyamoya-type changes, pial-to-pial collateralisatio n,	in patients harboring BAVM after endovascular embolisation			log rank test multivariate proportional-hazards regression model

						intravascular pressure measurement				
Lv Nov 2011	World Neurosurgery, 2011, Beijing Neurosurgical Institute	302, 1999-2008	unrelated aneurysms, Willis circle aneurysms, intranidal aneurysms	**BAVM size**, **BAVM location**, **venous drainage**, BAVM haemorrhage, multiple arterial aneurysms	CT, MRI, DSA	clinical presentations date of presentation imaging source and date lesion side handedness BAVM eloquence BAVM border with adjacent brain haemorrhage location & size periventricular drainage **number of draining veins**, **venous stenosis**, number of veins reaching sinus, venous ectasia venous reflux sinus thrombosis **feeders**, haemorrhage history	**To evaluate the characteristics of brain arteriovenous mal-formations (AVMs) with coexisting flow-related and Willis circle aneurysms.**	None	None	Univariate tests (χ2, t test) and multivariate logistic regression model , Fisher exact test

						haemorrhage date no of vessels to be embolised Moyamoya-type changes pial-to-pial collateralisation intravascular pressure measurement				
Lv Sept 2011	World Neurosurgery, 2011, Beijing Neurosurgical Institute	302, 1999-2008	Initial AVM presentations, Haemorrhagic presentation, **BAVM location**, **BAVM size**, **venous drainage**, Willis circle aneurysms, intranidal aneurysms	**BAVM size**, **BAVM location**, **venous drainage**, BAVM haemorrhage,	CT, MRI, DSA	clinical presentations, date of presentation, imaging source and date, lesion side, handedness, BAVM eloquence, BAVM border with adjacent brain, haemorrhage location, size, periventricular drainage, number of draining veins leaving nidus, number of veins reaching sinus, venous stenosis/ occlusion, venous ectasia,	**To analyze the characteristics of brain arteriovenous malforma-tions (AVMs) associated with cerebral aneurysms.**	nil	nil	Univariate tests (χ2, t test) and multivariate logistic regression model

						venous reflux, sinus thrombosis feeding arteries, arterial aneurysms, number of aneurysms, location, haemorrhage history, haemorrhage date, no of vessels to be embolised, Moyamoya-type changes, pial-to-pial collateralisation, intravascular pressure measurement				
Lv 2013	World Neurosurg, 2013, Beijing Neurosurgical Institute and Beijing Tiantan Hospital,	302, 1999-2008	AVM size, AVM location, arterial feeders, varix, venous stenosis, aneurysms	AVM location, AVM size, arterial feeders, number of draining veins, varices, venous stenosis, SMG, eloquence, venous drainage, coexisting aneurysms	DSA	clinical presentations, date of presentation, imaging source and date, lesion side, handedness, BAVM border with adjacent brain, BAVM haemorrhage, haemorrhage location, size, periventricular drainage,	To identify the specific angioarchitectural characteristics of AVMs that are associated with a clinical presentation of non-haemorrhagic neurologic deficits.	nil	nil	Univariate tests and multivariate logistic analysis (chi square test, *t*-test)

						number of veins reaching sinus, venous ectasia, venous reflux, sinus thrombosis number of aneurysms, location, haemorrhage history, haemorrhage date, no of vessels to be embolised, Moyamoya-type changes, pial-to-pial collateralisation, intravascular pressure measurement				
Lv 2015	World Neurosurg, 2015, Beijing Neurosurgical Institute and Beijing Tiantan Hospital,	267, 2004 - 2013	BAVM location	BAVM haemorrhage, BAVM location, SMG, haemorrhage pattern	CT, MRI, DSA	clinical presentations, date of presentation, imaging source and date, lesion side, handedness, BAVM size, BAVM eloquence, BAVM border with adjacent brain, haemorrhage location, size, venous drainage,	to determine the influence of patient age at diagnosis on haemorrhage patterns and outcomes.	nil	nil	t-test univariate analysis

						periventricular drainage, number of draining veins leaving nidus, number of veins reaching sinus, venous stenosis/ occlusion, venous ectasia, venous reflux, sinus thrombosis feeding arteries, arterial aneurysms, number of aneurysms, location, haemorrhage history, haemorrhage date, no of vessels to be embolised, Moyamoya-type changes, pial-to-pial collateralisation, intravascular pressure measurement				
Ma 2017a	Eur Radiol, 2017, Beijing Tiantan	110, 2009-2015	Nidus size, venous ectasia, venous	**Nidus size**, **venous drainage**, **venous**	Biplanar DSA, CT, MRI	clinical presentations date of presentation	To identify bAVM angiographic features	2 blinded neuroradiologists, nil else	none	kappa coefficient, Cox proportional

	Hospital, Beijing		drainage, AV shunt, aneurysm, haemorrhage	**ectasia**, AV shunt, **aneurysm**, **haemorrhage**		imaging source and date lesion side handedness, BAVM location BAVM eloquence BAVM border with adjacent brain BAVM haemorrhage haemorrhage location, size, periventricular drainage number of draining veins leaving nidus number of veins reaching sinus venous stenosis/ occlusion, venous reflux sinus thrombosis, feeding arteries, haemorrhage history, haemorrhage date,	suggesting unbalanced inflow and outflow to detect children at higher risk for future haemorrhage.			hazards analysis, Kaplan-Meier survival curves and log-rank tests

						no of vessels to be embolised Moyamoya-type changes pial-to-pial collateralisation, intravascular pressure measurement				
Ma 2017b	Cerebrovasc Dis, 2017, Beijing Tiantan Hodpital, Capital Medical University, Beijing	134, Jul 2009 – Dec 2014	none	**clinical presentations**, **venous drainage**, long draining vein, **venous ectasia**, **BAVM location**, **BAVM eloquence**, **arterial aneurysms**, **number of aneurysms**, **BAVM size**, SMG, treatment-free follow up	MRI, CT, DSA	date of presentation, imaging source and date, lesion side, handedness, BAVM border with adjacent brain, BAVM haemorrhage, haemorrhage location, size, periventricular drainage, number of draining veins leaving nidus, number of veins reaching sinus, venous stenosis/ occlusion, venous reflux, sinus thrombosis feeding arteries,	To assess the clinical outcome after cAVM rupture and identify features to predict severe haemorrhage in children	2 experienced neuroradiologists	none	t test, Wilcoxon rank-sum test, chi-square, Fisher's exact test, univariate & multivariate logistic regression, multi-collinearity and model fit, calibration curve, C-statistic

						location, haemorrhage history, haemorrhage date, no of vessels to be embolised, Moyamoya-type changes, pial-to-pial collateralisation, intravascular pressure measurement				
Ma 2015	Am J Neuroradiol, 2015, Beijing Tiantan Hospital	108, 2009 - 2014	BAVM location, periventricular location, haematoma volume, deep haematoma, venous drainage, aneurysm, BAVM nidus	Haemorrhage presentation, venous drainage, deep location, periventricular location, posterior fossa location, associated aneurysm, BAVM nidus size	CT, MRI, DSA	date of presentation, imaging source and date, lesion side, handedness, BAVM eloquence, BAVM border with adjacent brain, haemorrhage location, size, periventricular drainage, number of draining veins leaving nidus, number of veins reaching sinus, venous stenosis/ occlusion, venous ectasia, venous reflux,	To analyse various features of brain AVMs to assess the risk of haemorrhage in children.	neuroradiologists	Yes for interobserver	t tests, chi-square tests, the kappa coefficient Cox proportional hazards analysis Kaplan-Meier survival curves and log-rank tests univariate and multivariable logistic regression analyses proportional-odds regres-sion model

						sinus thrombosis feeding arteries, number of aneurysms, location, haemorrhage history, haemorrhage date, no of vessels to be embolised, Moyamoya-type changes, pial-to-pial collateralisation, intravascular pressure measurement				
Machnowska	Can J Neurol Sci, 2013, Division of Neuroradiology, Toronto Western Hospital, Canada.	211, 2000 - 2009	none	clinical presentations, BAVM haemorrhage, BAVM size, BAVM border with adjacent brain, venous drainage, number of draining veins leaving nidus, venous ectasia, feeding arteries, BAVM eloquence,	DSA	date of presentation, imaging source and date, lesion side, handedness, BAVM location, haemorrhage location, size, periventricular drainage, number of veins reaching sinus, venous stenosis/ occlusion, venous reflux, sinus thrombosis	To correlate the occurrence of symptomatic complications with pre-radio-therapeutical angioarchitectural features.	senior neurosurgeon with neuroradiology, radiation oncology and a physicist.	none	two-sided t-tests Chi-squared and Fisher's exact tests multivariable logistic regression model

						arterial aneurysms, number of aneurysms, location, haemorrhage history, haemorrhage date, no of vessels to be embolised, Moyamoya-type changes, pial-to-pial collateralisation, intravascular pressure measurement				
Maher	J Neurosurg Paediatrics, 2009, Department of Neurosurgery, University of Michigan, Ann Arbor, Michigan;	67, 1990-2005	none	Clinical presentation, draining veins, AVM location, venous drainage, SMG	MRI, DSA	date of presentation, imaging source and date, lesion side, handedness, BAVM size, BAVM location, BAVM eloquence, BAVM border with adjacent brain, BAVM haemorrhage, haemorrhage location, size, venous drainage, periventricular drainage,	To review the experience of a single surgeon in the surgical treatment of AVMs in children, with specific attention to the angioarchitectural appearance of these lesions.	none	none	N/a

						number of draining veins leaving nidus, number of veins reaching sinus, venous stenosis/ occlusion, venous ectasia, venous reflux, sinus thrombosis feeding arteries, arterial aneurysms, number of aneurysms, location, haemorrhage history, haemorrhage date, no of vessels to be embolised, Moyamoya-type changes, pial-to-pial collateralisation, intravascular pressure measurement				
Majumdar	J NeuroInterve nt Surg, 2016, Rush Medical College, Chicago	51, 2008-2013	AVM, midline shift, haemorrhage location, deep venous drainage,	AVM size, deep venous drainage, associated aneurysm, haemorrhage location,	MRI, CT, DSA	clinical presentations, date of presentation, imaging source and date, lesion side, handedness,	To perform a detailed critical assessment of the morbidity associated	Neurosurgeon, neurologist		ANOVA F-test, Student t test, and chi-square tests

			haematoma evacuation	haematoma diameter, AVM infratentorial location		BAVM eloquence, BAVM border with adjacent brain, BAVM haemorrhage, periventricular drainage, number of draining veins leaving nidus, number of veins reaching sinus, venous stenosis/ occlusion, venous ectasia, venous reflux, sinus thrombosis feeding arteries, number of aneurysms, location, haemorrhage history, haemorrhage date, no of vessels to be embolised, Moyamoya-type changes, pial-to-pial collateralisation, intravascular pressure measurement	with ruptured brain AVMs.			

Mangiafico	Interventional Neuroradiology, 2001, Neuroradiology Unit, Careggi Hospital, Florence, Italy	One ???	none	clinical presentations, BAVM location, feeding arteries, number of draining veins leaving nidus, SMG,	CT, MRI, DSA	date of presentation, imaging source and date, lesion side, handedness, BAVM size, BAVM eloquence, BAVM border with adjacent brain, BAVM haemorrhage, haemorrhage location, size, venous drainage, periventricular drainage, number of veins reaching sinus, venous stenosis/ occlusion, venous ectasia, venous reflux, sinus thrombosis arterial aneurysms, number of aneurysms, location, haemorrhage history, haemorrhage date, no of vessels to be embolised,	To report the observation of a patient with a Spetzler-Martin grade 3, sympto-matic, cAVM uncomplicated, endovascular embolisation disappeared at follow-up.	none	none	none

						Moyamoya-type changes, pial-to-pial collateralisation, intravascular pressure measurement				
Miyasaka	Acta Neurochir Wien, 2000, Department of Neurosurgery, Kitasato University School of Medicine	30, ???	none	Haemorrhage, AVM size, number of draining veins	DSA	clinical presentations, date of presentation, imaging source and date, lesion side, handedness, BAVM location, BAVM eloquence, BAVM border with adjacent brain, BAVM haemorrhage, haemorrhage location, size, venous drainage, periventricular drainage, number of veins reaching sinus, venous stenosis/ occlusion, venous ectasia, venous reflux, sinus thrombosis feeding arteries,	To determine whether there is a physiological explanation for the predisposition of patients with certain angiographic characteristics to haemorrhage from cerebral AVMs	nil	nil	two-tailed t test Mann-Whitney U test

						arterial aneurysms, number of aneurysms, location, haemorrhage date, no of vessels to be embolised, Moyamoya-type changes, pial-to-pial collateralisation, intravascular pressure measurement				
Mohr	Curr Neurol Neurosci Rep, 2013, Neurological Institute, Doris and Stanley Tananbaum Stroke Center, Columbia University Medical Center	n/a	nil	clinical presentations, nidus, feeder, draining vein, arterial aneurysm, BAVM size, venous drainage, venous stenosis/ occlusion,	DSA	date of presentation, imaging source and date, lesion side, handedness, BAVM location, BAVM eloquence, BAVM border with adjacent brain, BAVM haemorrhage, haemorrhage location, size, periventricular drainage, number of veins reaching sinus, venous ectasia, venous reflux, sinus thrombosis	Educational article on diagnosis and treatment of AVMs	None	None	None

						number of aneurysms, location, haemorrhage history, haemorrhage date, no of vessels to be embolised, Moyamoya-type changes, pial-to-pial collateralisation, intravascular pressure measurement				
Morgan 2012	J Neurosurg 2012, Australian School of Advanced Medicine, Macquarie University Library, Sydney, New South Wales, Australia	427, 1989-2012	none	clinical presentations, BAVM size, BAVM location, SMG, venous drainage,	CT, MRI, DSA	date of presentation, imaging source and date, lesion side, handedness, BAVM eloquence, BAVM border with adjacent brain, BAVM haemorrhage, haemorrhage location, size, periventricular drainage, number of draining veins leaving nidus, number of veins reaching sinus,	to ascertain the risk and risk factors of recurrence after resection of AVMs of the brain.	none	none	Kaplan-Meier survival curves log-rank (Mantel-Cox) test Cox regression Fisher exact test 2-tailed Student unpaired t-test

						venous stenosis/ occlusion, venous ectasia, venous reflux, sinus thrombosis feeding arteries, arterial aneurysms, number of aneurysms, location, haemorrhage history, haemorrhage date, no of vessels to be embolised, Moyamoya-type changes, pial-to-pial collateralisation, intravascular pressure measurement				
Morgan 2016	Neurosurgery, 2016, Department of Clinical Medicine, Macquarie University, New South Wales	753, 1989-2014	SMG, Spetzler Ponce Category (SPC)	Haemorrhage presentation, BAVM haemorrhage, SAH haemorrhage presentation, BAVM size, Arterial aneurysm, aneurysm location,	DSA, CT, MRI	clinical presentations, date of presentation, imaging source and date, lesion side, handedness, BAVM size, BAVM location, BAVM eloquence,	To identify patient- and bAVM-specific factors associated with associated proximal intracranial aneurysm.	none	none	x^2, Fisher exact, t test, or Mann-Whitney U test multiple logistic regression analyses (forward stepwise)

				aneurysm size, venous drainage, BAVM location, SMG, SPC		BAVM border with adjacent brain, BAVM haemorrhage, haemorrhage location, size, venous drainage, periventricular drainage, number of draining veins leaving nidus, number of veins reaching sinus, venous stenosis/ occlusion, venous ectasia, venous reflux, sinus thrombosis feeding arteries, arterial aneurysms, number of aneurysms, location, haemorrhage history, haemorrhage date, no of vessels to be embolised, Moyamoya-type changes, pial-to-pial collateralisation,				

						intravascular pressure measurement				
Morgan 2017	J Neurosurg, 2017, Departments of Clinical Medicine and Statistics, Macquarie University, Sydney, New South Wales, Australia	778, 1989-2014	none	clinical presentations, BAVM haemorrhage, arterial aneurysms, BAVM size, venous drainage, BAVM eloquence,	MRI, CTA DSA	date of presentation, imaging source and date, lesion side, handedness, BAVM location, BAVM border with adjacent brain, haemorrhage location, size, periventricular drainage, number of draining veins leaving nidus, number of veins reaching sinus, venous stenosis/ occlusion, venous ectasia, venous reflux, sinus thrombosis feeding arteries, number of aneurysms, location, haemorrhage history, haemorrhage date, no of vessels to be embolised,	To adapt and apply the extended definition of favourable outcome established for Gamma Knife radiosurgery (GKRS) to surgery for (bAVMs).	neurosurgeon	none	chi-square, Fisher exact test, Student t-test, multiple logistic regression analyses (backward Wald) modified Wald method

						Moyamoya-type changes, pial-to-pial collateralisation, intravascular pressure measurement				
Motebejane	Interdisciplinary Neurosurgery, 2018, Inkosi Albert Luthuli Central Hospital, Durban	158, 2005-2015	BAVM location	**BAVM size**, **BAVM location**, SMG, **BAVM side**, **venous drainage**, **aneurysms** present and type	CT, MRI, DSA	clinical presentations date of presentation imaging source and date handedness BAVM eloquence BAVM border with adjacent brain BAVM haemorrhage haemorrhage location, size periventricular drainage number of draining veins leaving nidus number of veins reaching sinus venous stenosis/ occlusion	To determine the demographic and angioarchitectural features associated with clinical presentation of seizures in BAVM patients	Interventional neuroradiologist (>20 years experience)	none	

						venous ectasia venous reflux sinus thrombosis feeding arteries number of aneurysms location haemorrhage history haemorrhage date no of vessels to be embolised Moyamoya-type changes pial-to-pial collateralisation intravascular pressure measurement				
Nagaraja	Neuroradiology, 2006, Section of Academic Radiology, University of Sheffield, UK	40, ???	none	BAVM size, BAVM location, BAVM border with adjacent brain, venous drainage, Flow-related changes	Angiograms, MRA	clinical presentations, date of presentation, imaging source and date, lesion side, handedness, BAVM eloquence, BAVM haemorrhage,	To investigate the role of magnetic resonance angiography (MRA) in the early follow-up of patients after stereotactic radiosurgery	radiologists	none	Fisher's test

						haemorrhage location, size, periventricular drainage, number of draining veins leaving nidus, number of veins reaching sinus, venous stenosis/ occlusion, venous ectasia, venous reflux, sinus thrombosis feeding arteries, arterial aneurysms, number of aneurysms, location, haemorrhage history, haemorrhage date, no of vessels to be embolised, Moyamoya-type changes, pial-to-pial collateralisation, intravascular pressure measurement	(STRS) for cerebral arteriovenous malformations (AVMs) and to determine the influence of individual morphological factors of AVMs in early response to treatment.			
Neidert	World Neurosurg, 2016, Departments	67, 2006-2013	none	AVM location, intraventricular haemorrhage,	CTA	clinical presentations, date of presentation,	To establish an AVM grading score for patients	none	none	Mann-Whitney test

	of Neurosurgery Neuroradiology, University Hospital Zurich			intracerebral haemorrhage volume, spot sign on CTA, AVM size, deep venous drainage, eloquence, diffuse nidus, SMG	Unclear if other imaging used	imaging source and date, lesion side, handedness, haemorrhage location, periventricular drainage, number of draining veins leaving nidus, number of veins reaching sinus, venous stenosis/ occlusion, venous ectasia, venous reflux, sinus thrombosis feeding arteries, arterial aneurysms, number of aneurysms, location, haemorrhage history, haemorrhage date, no of vessels to be embolised, Moyamoya-type changes, pial-to-pial collateralisation, intravascular pressure measurement	with ruptured AVM and associated ICH to predict clinical outcome.			chi2 test or Fisher exact test areas under the receiver-operating characteristic curves

Nishino	J Neurosurg, 2017, Department of Neurosurgery, Brain Research Institute, Niigata University	10, 1999-2014	none	Clinical presentation, AVM location, arterial supply, draining veins, aneurysms, nidus volume, venous ectasia, varix	MRI, MR, DSA	date of presentation, imaging source and date, lesion side, handedness, BAVM eloquence, BAVM border with adjacent brain, BAVM haemorrhage, haemorrhage location, size, venous drainage, periventricular drainage, number of veins reaching sinus, venous stenosis/ occlusion, venous reflux, sinus thrombosis number of aneurysms, location, haemorrhage history, haemorrhage date, no of vessels to be embolised, Moyamoya-type changes, pial-to-pial collateralisation,	To evaluate the clinical and radiographic features of cerebellopontine angle AVMs as well as the treatment options.	none	none	nil

						intravascular pressure measurement				
Nisson 2018	World Neurosurg, 2018, University of Arizona, College of Medicine, Tucson, Arizona, USA	120, 1999-2015	none	BAVM haemorrhage, BAVM eloquence, arterial aneurysms, venous drainage, BAVM location, BAVM size, SMG	angiography	clinical presentations, date of presentation, imaging source and date, lesion side, handedness, BAVM border with adjacent brain, haemorrhage location, size, periventricular drainage, number of draining veins leaving nidus, number of veins reaching sinus, venous stenosis/ occlusion, venous ectasia, venous reflux, sinus thrombosis feeding arteries, number of aneurysms, location, haemorrhage history, haemorrhage date, no of vessels to be embolised,	to describe and characterize the features of microsurgically resected cerebellar lesions.			independent t test Wilcoxon rank sum test chi^2 test Fisher exact test Univariate and multivariate logistic regression analyses area under the receiver operating characteristic (ROC) curves

						Moyamoya-type changes, pial-to-pial collateralisation, intravascular pressure measurement				
Nisson 2020	**J Neurosurg, 2020,** College of Medicine, University of Arizona, Tucson, Arizona	120, 1999 - 2013	Eloquence, haemorrhage presentation	BAVM haemorrhage, BAVM eloquence, arterial aneurysms, venous drainage, BAVM location, BAVM size, **SMG**	DSA	clinical presentations, date of presentation, imaging source and date, lesion side, handedness, BAVM border with adjacent brain, BAVM haemorrhage, haemorrhage location, size, periventricular drainage, number of draining veins leaving nidus, number of veins reaching sinus, venous stenosis/ occlusion, venous ectasia, venous reflux, sinus thrombosis feeding arteries, number of aneurysms,	To evaluate the existing Spetzler-Martin (SM), Spetzler-Ponce (SP), and Lawton-Young (LY) grading systems for cerebellar arteriovenous malformations (AVMs) and to propose a new grading system to estimate the risks associated with these lesions.	nil	nil	t-test Wilcoxon rank-sum test chi-square test Fisher exact test univariate and multivariate logistic regression area under the receiver operating characteristic curve (AUROC)

						location, haemorrhage history, haemorrhage date, no of vessels to be embolised, Moyamoya-type changes, pial-to-pial collateralisation, intravascular pressure measurement				Hosmer-Lemeshow test
Niu	Neurosci Bull, 2012, Beijing Tiantan Hospital & Capital Medical University, Beijing	31, 2009 – 2010 (and brain specimens from 6 trauma and 6 epilepsy patients as controls)	location	**BAVM size**, **BAVM location**, shunt vessels, **venous drainage**	DSA	clinical presentations date of presentation imaging source and date lesion side handedness BAVM eloquence BAVM border with adjacent brain BAVM haemorrhage haemorrhage location, size periventricular drainage	To assess the relationship between haemorrhage, angioarchitectural factors and collagen of AVMs	none	none	Unpaired t-test, chi-squared test, multivariate linear stepwise regression, ANOVA

						number of draining veins leaving nidus number of veins reaching sinus venous stenosis/ occlusion venous ectasia venous reflux sinus thrombosis feeding arteries arterial aneurysms number of aneurysms location haemorrhage history haemorrhage date no of vessels to be embolised Moyamoya-type changes pial-to-pial collateralisation intravascular pressure measurement				

Ognard	Journal of Neuroradiology, 2017, CHU de la Cavale-Blanche, Brest	10, July 2015-July 2016	none	**BAVM size**, **BAVM location**, **venous drainage**, SMG	4D DSA, 2D DSA	clinical presentations, date of presentation, imaging source and date, lesion side, handedness, BAVM eloquence, BAVM border with adjacent brain, BAVM haemorrhage, haemorrhage location, size, periventricular drainage, number of draining veins leaving nidus, number of veins reaching sinus, venous stenosis/ occlusion, venous ectasia, venous reflux, sinus thrombosis feeding arteries,	To study agreement on a new method of 4D DSA compared to 2D DSA in AVM grading using SMG	Interventional neuroradiology resident (2 years), Interventional neuroradiology consultant (>5 years), vascular neurosurgeon (>5 years)	Yes	Wilcoxon-Mann-Whitney's U-test, kappa coefficient, Cochran Q, Wilcoxon signed rank test

						arterial aneurysms, number of aneurysms, location, haemorrhage history, haemorrhage date, no of vessels to be embolised, Moyamoya-type changes, pial-to-pial collateralisation, intravascular pressure measurement				
Orning	J NeuroInterve nt Surg, 2016, Department of Neurosurgery, University of Illinois at Chicago	571, 1995-2015	none	Location, aneurysms	CT, CTA, DSA	clinical presentations, date of presentation, imaging source and date, lesion side, handedness, BAVM size, BAVM eloquence, BAVM border with adjacent brain, BAVM haemorrhage, haemorrhage location, size,	To examine the prevalence and haemorrhagic risk of posterior fossa AVM-associated feeder vessel aneurysms.	endovascular neurosurgeons	none	χ square test.

						venous drainage, periventricular drainage, number of draining veins leaving nidus, number of veins reaching sinus, venous stenosis/ occlusion, venous ectasia, venous reflux, sinus thrombosis feeding arteries, number of aneurysms, location, haemorrhage history, haemorrhage date, no of vessels to be embolised, Moyamoya-type changes, pial-to-pial collateralisation, intravascular pressure measurement				
Oulasvirta	Neurosurgery, 2019, Department of Neurosurgery,	805, 1942-2014	AVM location, haemorrhage presentation,	AVM size, venous drainage, AVM location, SMG,	CT, MRI, DSA	clinical presentations, date of presentation, imaging source and date,	To clarify the characteristics and long-term outcome of	none	none	Pearson chi-square test multivariate analysis performed

	Helsinki University Hospital			associated aneurysm		lesion side, handedness, BAVM eloquence, BAVM border with adjacent brain, BAVM haemorrhage, haemorrhage location, size, periventricular drainage, number of draining veins leaving nidus, number of veins reaching sinus, venous stenosis/ occlusion, venous ectasia, venous reflux, sinus thrombosis feeding arteries, number of aneurysms, location, haemorrhage history, haemorrhage date, no of vessels to be embolised, Moyamoya-type changes, pial-to-pial collateralisatio n,	paediatric patients with AVM.			using binary logistic regression with the backward Wald method

						intravascular pressure measurement				
Ozyurt	J Magn Reson Imaging, 2017, Bogazici University, Istanbul	10, ?duration	Nidus volume (distance between the centres of volumes) and Jaccard Index (measure of spatial overlap between two nidus definitions and is equal to the ratio of overlapping volume to encompassing volume)	**BAVM size**,	DSA, MRI, MRA	clinical presentations, date of presentation, imaging source and date, lesion side, handedness, BAVM location, BAVM eloquence, BAVM border with adjacent brain, BAVM haemorrhage, haemorrhage location, size, venous drainage, periventricular drainage, number of draining veins leaving nidus, number of veins reaching sinus, venous stenosis/ occlusion,	To test whether the combined use of 4D arterial spin labelling angiography and contrast-enhanced MRA can work as a prospective alternative to DSA for the delineation of the AVM nidus in SRS planning	Neuroradiologist (24 years experience), Neuroradiologist (14 years)	Yes	Spearman rho test, intraclass correlation coefficient, Bland-Altman plot, Friedman test

						venous ectasia, venous reflux, sinus thrombosis feeding arteries, arterial aneurysms, number of aneurysms, location, haemorrhage history, haemorrhage date, no of vessels to be embolised, Moyamoya-type changes, pial-to-pial collateralisation, intravascular pressure measurement				
Pai	Turk Neurosurg, 2019, Bangalore Medical College and Research Institute, Department	14, 2015-2017	none	clinical presentations, BAVM haemorrhage, BAVM location, SMG, BAVM eloquence, BAVM size, feeding arteries,	DSA, CT, MRA/MRI	date of presentation, imaging source and date, lesion side, handedness, haemorrhage location, size, periventricular drainage,	To describe the authors' experiences with surgical excision of cerebral arteriovenous malformations (AVMs) using temporary	None	None	none

	of Neurosurgery, Bangalore, India			BAVM border with adjacent brain, venous drainage,		number of draining veins leaving nidus, number of veins reaching sinus, venous stenosis/ occlusion, venous ectasia, venous reflux, sinus thrombosis arterial aneurysms, number of aneurysms, location, haemorrhage history, haemorrhage date, no of vessels to be embolised, Moyamoya-type changes, pial-to-pial collateralisation, intravascular pressure measurement	proximal artery clipping to reduce intraoperative bleeding and excision time.			
Pan 2013 et al	European Journal of Radiology, 2013, The First Affiliated Hospital, Hangzhou, China	152, 2005-2008	Terminal feeding arteries, perforating feeders, venous ectasia, venous	**Location**, **size**, **number of arterial feeders**, **aneurysms**, **number of draining veins**, **venous drainage**,	angiography	clinical presentations date of presentation imaging source and date lesion side handedness	To identify angioarchitectural characteristic associated with the initial haemorrhagic event of	Neurosurgeon & neuroradiologist Nil else	none	Multivariate analysis (backward conditional logistic regression)

			stenosis, location	varix, **venous stenosis, clinical presentations**		BAVM eloquence BAVM border with adjacent brain BAVM haemorrhage haemorrhage location, size periventricular drainage number of veins reaching sinus venous ectasia venous reflux sinus thrombosis feeding arteries number of aneurysms location haemorrhage history haemorrhage date no of vessels to be embolised Moyamoya-type changes pial-to-pial collateralisation	supratentorial AVMs			

						intravascular pressure measurement				
Pan 2014	Am J Neuroradiol, 2014, The First Affiliated Hospital, Hangzhou, China	130, 2005-2008	Terminal feeding arteries, perforating feeders, venous ectasia, venous stenosis, location	**Presentation**, **location**, **size**, **arterial feeders**, **arterial aneurysms** (perinidal & intranidal), **venous drainage**, SMG, **venous ectasia**, **venous stenosis**, embolisation degree, neurological deficits NIHSS,	CT, MRI	date of presentation imaging source and date lesion side handedness BAVM eloquence BAVM border with adjacent brain BAVM haemorrhage haemorrhage location, size periventricular drainage number of draining veins leaving nidus number of veins reaching sinus venous reflux sinus thrombosis number of aneurysms location haemorrhage history	To assess the angioarchitectural characteristics associated with complications of embolisation in supratentorial AVMs	none	none	Multivariate analysis (backward conditional logistic regression), univariate analysis

						haemorrhage date no of vessels to be embolised Moyamoya-type changes pial-to-pial collateralisation intravascular pressure measurement				
Panni	Acta Neurochirurgica, 2020, Department of Neurosurgery and Gamma Knife Radiosurgery, San Raffaele Scientific Institute, Vita-Salute University, Milan	191, 2004-2014	Feeding artery enlargement, venous dilation, flow	clinical presentations, **Nidus,** feeding arteries, BAVM location, BAVM eloquence, BAVM size, Flow, BAVM border with adjacent brain, AVF, venous ectasia, arterial aneurysms, venous drainage, SMG, number of feeders, feeder dilation, feeder territory, venous stenosis/ occlusion, venous varices,	DSA, MRI	date of presentation, imaging source and date, lesion side, handedness, BAVM size, BAVM haemorrhage, haemorrhage location, size, periventricular drainage, number of draining veins leaving nidus, number of veins reaching sinus, venous reflux, sinus thrombosis number of aneurysms, location, haemorrhage history,	to identify angioarchitectural features predictive of post-radiosurgical bAVM obliteration.	neurointerventionists one had at least 10 years of experience	nil	Univariate logistic regression backward stepwise multiple logistic regression receiver operating characteristic (ROC) curve analyses

						haemorrhage date, no of vessels to be embolised, Moyamoya-type changes, pial-to-pial collateralisation, intravascular pressure measurement				
Parkhutik	Stroke, 2012, Department of Neurology, Neuroradiology, Hospital Universitario la Fe, Valencia, Spain	108, ???	BAVM haemorrhage, arterial hypertension	clinical presentations, BAVM size, BAVM location, venous drainage, BAVM eloquence, arterial aneurysms, BAVM haemorrhage, number of draining veins leaving nidus, SMG	DSA, MRI, CT	date of presentation, imaging source and date, lesion side, handedness, BAVM border with adjacent brain, haemorrhage location, size, periventricular drainage, number of veins reaching sinus, venous stenosis/ occlusion, venous ectasia, venous reflux, sinus thrombosis feeding arteries, number of aneurysms, location, haemorrhage history,	To evaluate the usefulness of radiosurgery in preventing cerebral bleeds in both ruptured and nonruptured brain AVM.	none	none	Univariate tests (chi^2, *t* test) multivariate logistic regression analysis Kaplan-Meier survival curves, log-rank tests Univariate and multivariate Cox regression hazard models

						haemorrhage date, no of vessels to be embolised, Moyamoya-type changes, pial-to-pial collateralisation, intravascular pressure measurement				
Patel	Am J Neuroradiol, 2001, Department of Neuroradiology, Royal Hallamshire Hospital, Sheffield	27, 1985-1998	none	AVM size, AVM location, number and source of feeding arteries, number& direction of draining veins, clinical presentation	DSA	date of presentation, imaging source and date, lesion side, handedness, BAVM eloquence, BAVM border with adjacent brain, BAVM haemorrhage, haemorrhage location, size, venous drainage, periventricular drainage, venous stenosis/ occlusion, venous ectasia, venous reflux, sinus thrombosis arterial aneurysms, number of aneurysms,	To determine whether spontaneous obliteration can be predicted and, once it occurs, whether it is likely to be permanent.	Neurosurgeon, neurologist	nil	nil

						location, haemorrhage history, haemorrhage date, no of vessels to be embolised, Moyamoya-type changes, pial-to-pial collateralisation, intravascular pressure measurement				
Paul	Neurosurgery, 2014, Interventional Neuroradiology, Neurosurgery and Radiosurgery Department, Ruber International Hospital, Madrid, Spain	662, 1993-2005	none	clinical presentations, BAVM border with adjacent brain, venous drainage, number of draining veins leaving nidus, venous stenosis/ occlusion, venous ectasia, BAVM location, Flow velocity, Fistulous or Plexiform Angioarchitecture, BAVM size,	angiography	date of presentation, imaging source and date, lesion side, handedness, BAVM eloquence, BAVM haemorrhage, haemorrhage location, size, periventricular drainage, number of veins reaching sinus, venous reflux, sinus thrombosis feeding arteries, arterial aneurysms, number of aneurysms, location,	To report the long-term outcomes of Gamma Knife RS (GKRS) in brain AVMs, focusing on how the angioarchitectural and hemodynamic parameters of AVMs affect the post-RS results.	interventional neuroradiologist	none	Pearson x^2 test nonparametric Mann-Whitney U test Binary logistic regression Hosmer-Lemeshow goodness- of-fit test.

						haemorrhage history, haemorrhage date, no of vessels to be embolised, Moyamoya-type changes, pial-to-pial collateralisation, intravascular pressure measurement				
Pawlikowska	Stroke, 2004, Cardiovascular Research Institute University of California, San Francisco	180, 2000 -	haemorrhage	BAVM size, venous drainage, BAVM haemorrhage,	DSA, CT, MRI	clinical presentations, date of presentation, imaging source and date, lesion side, handedness, BAVM location, BAVM eloquence, BAVM border with adjacent brain, BAVM haemorrhage, haemorrhage location, size, periventricular drainage, number of draining veins leaving nidus, number of veins reaching sinus,	To determine whether identification of genetic polymorphisms associated with ICH would facilitate risk stratification in BAVM patients.	nil	nil	Chi-square, Bonferroni correction logistic regression

						venous stenosis/ occlusion, venous ectasia, venous reflux, sinus thrombosis feeding arteries, arterial aneurysms, number of aneurysms, location, haemorrhage history, haemorrhage date, no of vessels to be embolised, Moyamoya-type changes, pial-to-pial collateralisation, intravascular pressure measurement				
Pekmezci	Clinical Neuropathology, 2016, University of California, San Francisco	1989-2014	none	Haemorrhage presentation, deep venous drainage, AVM size, deep location, associated aneurysm	Not mentioned	clinical presentations, date of presentation, imaging source and date, lesion side, handedness, BAVM eloquence, BAVM border with adjacent brain,	To determine critical histological features that can be correlated with preoperative radioimaging findings and allow better identification	nil	nil	Non-parametric correlation analysis noting Spearman's rho Univariable and multivariable

						haemorrhage location, size, periventricular drainage, number of draining veins leaving nidus, number of veins reaching sinus, venous stenosis/ occlusion, venous ectasia, venous reflux, sinus thrombosis feeding arteries, number of aneurysms, location, haemorrhage history, haemorrhage date, no of vessels to be embolised, Moyamoya-type changes, pial-to-pial collateralisation, intravascular pressure measurement	of patients with greater risk of adverse outcome			logistic regression analyses Bonferroni-corrected significance level
Pohjola	World Neurosurg, 2018, Department of	38, 1990-2014	AVM location, venous drainage	AVM location, AVM size, venous drainage, associated	DSA, CTA, CT, MRI, MRA	clinical presentations, date of presentation, imaging source and date,	To analyse the preoperative features influencing clinical outcomes	nil	nil	Fisher exact test

	Neurosurgery, Helsinki University Hospital and Clinical Neurosciences			aneurysms, haemorrhage, eloquence, SMG		lesion side, handedness, BAVM border with adjacent brain, haemorrhage location, size, periventricular drainage, number of draining veins leaving nidus, number of veins reaching sinus, venous stenosis/ occlusion, venous ectasia, venous reflux, sinus thrombosis feeding arteries, number of aneurysms, location, haemorrhage history, haemorrhage date, no of vessels to be embolised, Moyamoya-type changes, pial-to-pial collateralisation, intravascular pressure measurement	after surgery at the early recovery stage and at last follow-up.			Mann-Whitney U test logistic regression models

Potts	Neurosurgery, 2013, Department of Neurological Surgery, Department of Anaesthesia and Perio-perative Care, Centre for Cerebro-vascular Research, University of California, San Francisco, USA	514, 1997-2011	none	clinical presentations, BAVM haemorrhage, BAVM border with adjacent brain, BAVM size, BAVM location, venous drainage, BAVM eloquence, SMG,	Angiography	date of presentation, imaging source and date, lesion side, handedness, haemorrhage location, size, periventricular drainage, number of draining veins leaving nidus, number of veins reaching sinus, venous stenosis/ occlusion, venous ectasia, venous reflux, sinus thrombosis feeding arteries, arterial aneurysms, number of aneurysms, location, haemorrhage history, haemorrhage date, no of vessels to be embolised, Moyamoya-type changes, pial-to-pial collateralisatio n,	To describe and discuss the technical considerations of microsurgical resection for deep-seated AVMs.	neurosurgeons, neurologists, interventional neuroradiologist s, and radiation oncologists	none	x^2 tests t test Univariate and multivariate analyses stepwise logistic regression model mixed-direction stepwise regression analysis

						intravascular pressure measurement				
Ravindra	J Neurosurg Paediatr, 2019, Division of Paediatric Neurosurgery, University of Utah, Salt Lake City	97, 1996-2017	none	Clinical presentation, AVM location, SMG, AVM size, eloquence, venous drainage, aneurysm	Angiography, MRI	date of presentation, imaging source and date, lesion side, handedness, BAVM border with adjacent brain, BAVM haemorrhage, haemorrhage location, size, periventricular drainage, number of draining veins leaving nidus, number of veins reaching sinus, venous stenosis/ occlusion, venous ectasia, venous reflux, sinus thrombosis feeding arteries, number of aneurysms, location, haemorrhage history, haemorrhage date, no of vessels to be embolised,	To describe the long-term functional outcomes of paediatric patients who undergo AVM surgery and to identify predictors of sustained neurological deficits.	none	none	Multivariate analysis Univariate statistical analysis Mann-Whitney U-test) Fisher exact test Multivariate logistic regression analysis Hosmer-Lemeshow goodness-of-fit test

						Moyamoya-type changes, pial-to-pial collateralisation, intravascular pressure measurement				
Reitz et al	World Neurosurgery, 2016, University Hospital Hamburg Eppendorf, Hamburg	24, nil	None, location	**Clinical presentation**, **haemorrhage**, SMG, **size**, **location**, nidus size, **venous drainage**, **aneurysms** (flow-associated/intranidal), **arterial** territorial blood supply, **number of feeders**, treatment and timing, outcomes	angiography	date of presentation imaging date lesion side handedness BAVM eloquence BAVM border with adjacent brain haemorrhage location, size periventricular drainage number of draining veins leaving nidus number of veins reaching sinus venous stenosis/ occlusion venous ectasia venous reflux sinus thrombosis	To study angioarchitectural risk factors for haemorrhage and clinical long-term outcome in paediatric patients with BAVMs	none	none	Student's t-test, likelihood-ratio chi squared test, univariate logistic regression analysis, multivariate regression, Firth's method for exact logistic regression

						number of aneurysms location haemorrhage date no of vessels to be embolised Moyamoya-type changes pial-to-pial collateralisation intravascular pressure measurement				
Riordan	J Neurosurg Pediatr, 2018, Departments of Neurosurgery and Neurointervention al Radiology, Boston Children's Hospital	57, 2006-2017	none	AVM location, clinical presentation	CTA, MRI, DSA	date of presentation, imaging source and date, lesion side, handedness, BAVM size, BAVM eloquence, BAVM border with adjacent brain, BAVM haemorrhage, haemorrhage location, size, venous drainage, periventricular drainage, number of draining veins leaving nidus,	To quantify the incidence and characterise clinical and radiographic factors associated with sudden death from the haemorrhage of previously undiagnosed AVMs in children.	paediatric neuroradiologist	none	n/a

						number of veins reaching sinus, venous stenosis/ occlusion, venous ectasia, venous reflux, sinus thrombosis feeding arteries, arterial aneurysms, number of aneurysms, location, haemorrhage history, haemorrhage date, no of vessels to be embolised, Moyamoya-type changes, pial-to-pial collateralisation, intravascular pressure measurement				
Robert 2014	BMJ, 2014, Rothschild Foundation Hospital, Paris	38, 1995-2013	Location	Location, nidus size, **nidus border**, venous drainage, arterial feeders, aneurysms, number of draining	angiography	Clinical presentation, date of presentation, imaging source and date, lesion side, handedness, BAVM eloquence,	To identify angiographic factors influencing the success of endovascular treatment of arteriovenous malformations involving the	None	None	Fisher's exact test

				veins, venous stenosis, sinus occlusion, venous ectasia, venous reflux, pseudophlebitic pattern		BAVM border with adjacent brain, BAVM haemorrhage including location and size, periventricular drainage, number of veins reaching sinus, Moyamoya-type changes, pial-to-pial collaterals, intravascular pressure measurements	corpus callosum			
Robert 2015	Journal of the Neurological Sciences, 2015, Rothschild Foundation Hospital, Paris	59, 1995-2013	none	Arterial supply, aneurysms, venous drainage, number of draining veins, venous stenosis, venous occlusion, venous ectasia, venous reflux, sinus thrombosis	CT, MRI, DSA	clinical presentations, date of presentation, imaging source and date, lesion side, handedness, BAVM size, BAVM location, BAVM eloquence, BAVM border with adjacent brain, BAVM haemorrhage,	To describe anatomic and angiographic features of our series of cerebellar AVMs	none	none	none

						haemorrhage location, size, periventricular drainage, number of veins reaching sinus, number of aneurysms, location, haemorrhage history, haemorrhage date, no of vessels to be embolised, Moyamoya-type changes, pial-to-pial collateralisation, intravascular pressure measurement				
Robert 2016	Journal of Clinical Neuroscience, 2016, Department of Interventional Neuroradiology, Rothschild Foundation Hospital, Paris, France	69, 1995-2013	none	clinical presentations, BAVM haemorrhage, BAVM size, BAVM location, BAVM eloquence, SMG, feeding arteries, BAVM border with adjacent brain, arterial aneurysms, venous drainage,	CT, MRI, DSA	date of presentation, imaging source and date, lesion side, handedness, haemorrhage location, size, periventricular drainage, number of veins reaching sinus, venous stenosis/ occlusion, venous reflux,	To present our clinical and angiographic results of the management of posterior fossa AVM treated with an endovascular technique, combined with microsurgery or radiosurgery when necessary.	neurosurgeons interventional neuroradiologists	none	none

				number of draining veins leaving nidus, venous ectasia,		sinus thrombosis number of aneurysms, location, haemorrhage history, haemorrhage date, no of vessels to be embolised, Moyamoya-type changes, pial-to-pial collateralisation, intravascular pressure measurement				
Robert 2017	Journal of the Neurological Sciences, 2017, Department of Interventional Neuroradiology, Rothschild Foundation Hospital, Paris	134 1995 to 2013	none	Clinical presentation, SMG, AVM location, AVM side, AVM border, eloquence, arterial supply, associated aneurysm, venous drainage, venous stenosis, venous ectasia, venous reflux	DSA	date of presentation, imaging source and date, handedness, BAVM haemorrhage, haemorrhage location, size, periventricular drainage, number of draining veins leaving nidus, number of veins reaching sinus, sinus thrombosis number of aneurysms, location,	To propose a more comprehensive grading system than the Spetzler-Martin to evaluate the endovascular curability of an AVM.	vascular neurosurgeons, interventional neuroradiologists	none	Fisher's exact test Univariate linear regressions

						haemorrhage history, haemorrhage date, no of vessels to be embolised, Moyamoya-type changes, pial-to-pial collateralisation, intravascular pressure measurement				
Sahlein et al.	Stroke, 2014, NYU Langone Medical Center, New York	122, 1996-2006	Location, nidus size, bAVM eloquence, bAVM border	**location**, **depth**, **nidus size**, bAVM flow physiology, **arterial supply** (organized by major feeding territory), **aneurysms** (**number and location**, **pial collaterals**, **bAVM border morphology**, presence of **moya moya–type changes**, venous characteristics (**number of draining veins**,	angiography	Clinical presentation, date of presentation, imaging source and date, lesion side, handedness, BAVM haemorrhage including location and size, no. of veins reaching sinus, venous reflux, sinus thrombosis, no. of vessels to be embolised, intravascular pressure	Predict a BAVM haemorrhage, & extrapolate to a physiological model	3 neuroradiologists, nil else	none	$\chi 2$, Fisher exact test, Student t test, 1-way ANOVA, and Wilcoxon rank-sum

				superficial versus deep drainage, presence of venous angiopathy), **bAVM eloquence** as defined by SMG, BAVM haemorrhage		measurements				
Sandalcioglu	Cerebrovasc Dis, 2010, Department of Neurosurgery, University Hospital Essen, Essen, Germany	145, 13 year period	AVM	clinical presentations, BAVM haemorrhage, BAVM size, BAVM location, BAVM eloquence, venous drainage, SMG	Angiography, MRI	date of presentation, imaging source and date, lesion side, handedness, BAVM border with adjacent brain, haemorrhage location, size, periventricular drainage, number of draining veins leaving nidus, number of veins reaching sinus, venous stenosis/ occlusion, venous ectasia, venous reflux, sinus thrombosis feeding arteries,	to investigate the expression of angiogenic and proliferative factors in relation to different clinical conditions and treatment modalities.	none	none	chi^2 test Bonferroni method

						arterial aneurysms, number of aneurysms, location, haemorrhage history, haemorrhage date, no of vessels to be embolised, Moyamoya-type changes, pial-to-pial collateralisation, intravascular pressure measurement				
Schmidt	Trends in Neurovascular Surgery, 2011 , Department of Neurosurgery, University Medical Center Hamburg-Eppendorf, Germany	474, 1990-2010	arterial aneurysms, BAVM haemorrhage,	clinical presentations, BAVM location, SMG, BAVM haemorrhage, arterial aneurysms, venous stenosis/ occlusion, fistula, BAVM size, BAVM eloquence, venous drainage,	angiography	date of presentation, imaging source and date, lesion side, handedness, BAVM border with adjacent brain, haemorrhage location, size, periventricular drainage, number of draining veins leaving nidus, number of veins reaching sinus, venous ectasia, venous reflux, sinus thrombosis	to determine the frequency of aneurysms associated with (AVMs) of the posterior fossa and their relation to haemorrhagic presentation in comparison to supratento-rial AVMs.	Neurosurgeon neuroradiologist	none	univariate and multivariate analyses

						feeding arteries, number of aneurysms, location, haemorrhage history, haemorrhage date, no of vessels to be embolised, Moyamoya-type changes, pial-to-pial collateralisation, intravascular pressure measurement				
Schwartz	Surg Neurol 2002, Department of Neuroradiology, Department of Neurosurgery Hospital of the University of Pennsylvania, Philadelphia, Pennsylvania	3, 1985 - 2000	nil	feeding arteries, venous drainage, number of draining veins leaving nidus, arterial aneurysms, clinical presentations,	DSA, MRI, ct	date of presentation, imaging source and date, lesion side, handedness, BAVM size, BAVM location, BAVM eloquence, BAVM border with adjacent brain, BAVM haemorrhage, haemorrhage location, size, periventricular drainage, number of veins reaching sinus,	to determine possible mech-anisms underlying this unusual phenomenon.	nil	nil	nil

						venous stenosis/ occlusion, venous ectasia, venous reflux, sinus thrombosis number of aneurysms, location, haemorrhage history, haemorrhage date, no of vessels to be embolised, Moyamoya-type changes, pial-to-pial collateralisation, intravascular pressure measurement				
Shakur a 2016	Journal of Clinical Neuroscience, 2016, Department of Neurosurgery, University of Illinois at Chicago	75, 2007-2014	none	Haemorrhagic presentation, Venous stenosis, deep venous drainage, single draining vein, AVM location, AVM size, SMG	QMRA, MRA, DSA	clinical presentations, date of presentation, imaging source and date, lesion side, handedness, BAVM eloquence, BAVM border with adjacent brain, haemorrhage location, size, periventricular drainage,	To examine the relationship of pulsatility and resistance indices to AVM angioarchitectural features and haemorrhage	Neuroendovascular surgeons	nil	paired 2-tailed student's t-test Univariate linear regression analysis independent 2-tailed student's t-test

						number of veins reaching sinus, venous ectasia, venous reflux, sinus thrombosis feeding arteries, arterial aneurysms, number of aneurysms, location, haemorrhage history, haemorrhage date, no of vessels to be embolised, Moyamoya-type changes, pial-to-pial collateralisation, intravascular pressure measurement				
Shakur 2018	World Neurosurg, 2018, Departments of Neurosurgery /Neurology, University of Illinois, Chicago, USA	281, 1990 and 2016	venous stenosis	Haemorrhage presentation, SMG, AVM size, venous drainage, venous stenosis, venous ectasia	angiogram	clinical presentations, date of presentation, imaging source and date, lesion side, handedness, BAVM size, BAVM location, BAVM eloquence,	To determine the relationship between venous stenosis and age.	neurosurgery research fellows trained in DSA (with work verified by senior author)	none	chi-square test linear regression analysis independent 2-tailed Student's t-test.

						BAVM border with adjacent brain, BAVM haemorrhage, haemorrhage location, size, venous drainage, periventricular drainage, number of draining veins leaving nidus, number of veins reaching sinus, venous stenosis/ occlusion, venous ectasia, venous reflux, sinus thrombosis feeding arteries, arterial aneurysms, number of aneurysms, location, haemorrhage history, haemorrhage date, no of vessels to be embolised, Moyamoya-type changes, pial-to-pial collateralisatio n,				

						intravascular pressure measurement				
Shakur c 2016	www.neurosurgery-online.com, 2016, Department of Neurosurgery, University of Illinois at Chicago	64, 2007 - 2014	none	Clinical presentation, venous stenosis, intranidal fistula, venous ectasia, arterial ectasia, venous varix, arterial steal, AVM size, AVM flow, feeder arteries, feeder/ intranidal aneurysms, venous drainage, number of draining veins	QMRA, 3D-MRA Angiography not mentioned	date of presentation, imaging source and date, lesion side, handedness, BAVM location, BAVM eloquence, BAVM border with adjacent brain, BAVM haemorrhage, haemorrhage location, size, periventricular drainage, number of veins reaching sinus, venous reflux, sinus thrombosis number of aneurysms, location, haemorrhage history, haemorrhage date, no of vessels to be embolised, Moyamoya-type changes, pial-to-pial collateralisation,	To measure flow volume rate in AVM feeders using quantitative magnetic resonance angiography and analyse the impact of AVM clinical and anatomical characteristics on flow	none	none	χ^2 test

						intravascular pressure measurement				
Shakur d 2015	Journal of Clinical Neuroscience, 2016, Department of Neurosurgery, University of Illinois at Chicago, USA	29, 2007-2013	none	Haemorrhagic presentation, SMG, venous drainage	QMRA, MRI, DSA	clinical presentations, date of presentation, imaging source and date, lesion side, handedness, BAVM size, BAVM location, BAVM eloquence, BAVM border with adjacent brain, haemorrhage location, size, periventricular drainage, number of draining veins leaving nidus, number of veins reaching sinus, venous stenosis/ occlusion, venous ectasia, venous reflux, sinus thrombosis feeding arteries, arterial aneurysms, number of aneurysms, location,	To examine the relationship between intranidal vessel characteristics and AVM flow.	none	none	Univariate analysis linear or exponential regression

						haemorrhage history, haemorrhage date, no of vessels to be embolised, Moyamoya-type changes, pial-to-pial collateralisation, intravascular pressure measurement				
Shankar et al	American Journal of Neuroradiology, 2013, Toronto Western Hospital, Toronto	78, 2000-2009	Arterial dilation, fistula, perinidal angiogenesis, pseudophlebitic pattern, venous stenosis, venous ectasia, long course of draining vein, BAVM location	Arterial dilation, fistula, perinidal angiogenesis, intranidal aneurysm, pseudophlebitic pattern, **venous stenosis**, **venous ectasia**, long course of draining vein, **BAVM size & location**, **feeding arteries**,	bilateral internal carotid arteries, at least 1 vertebral artery, and at least the ipsilateral external carotid artery biplane DSA Nil else	Clinical presentation, date of presentation, imaging source and date, lesion side, handedness, eloquence, nidus border, BAVM haemorrhage including location and size, no. of veins reaching sinus, no. of draining veins, venous reflux, sinus thrombosis, aneurysms, no. of vessels	Propose a scoring system to predict seizures in patients with BAVMs.	neuroradiologists and neurosurgeons, nil else	none	Chi squared and Fisher exact tests

						to be embolised, Moyamoya-type changes, pial-to-pial collaterals, intravascular pressure measurements				
Sheng	J NeuroInterven t Surg 2014 Department of Neurosurgery, Wuhan General Hospital of Guangzhou Military Commend, Wuhan, China	10, nil	nil	clinical presentations, BAVM location, feeding arteries, number of draining veins leaving nidus, arterial aneurysms,	DSA	date of presentation, imaging source and date, lesion side, handedness, BAVM size, BAVM eloquence, BAVM border with adjacent brain, BAVM haemorrhage, haemorrhage location, size, venous drainage, periventricular drainage, number of veins reaching sinus, venous stenosis/ occlusion, venous ectasia, venous reflux, sinus thrombosis	To assess feasibility of using the vessel fusion technique for assisting AVM diagnosis was investigated	radiologist	nil	nil

						number of aneurysms, location, haemorrhage history, haemorrhage date, no of vessels to be embolised, Moyamoya-type changes, pial-to-pial collateralisation, intravascular pressure measurement				
Shotar	J Neurosurg, 2018, Pitié-Salpêtrière Hospital; and Paris VI University,	135, 2003-2014	none	AVM location, venous drainage, number of draining veins, AVM diameter, AVM volume, SMG	DSA, CT, MRI	clinical presentations, date of presentation, imaging source and date, lesion side, handedness, BAVM eloquence, BAVM border with adjacent brain, BAVM haemorrhage, haemorrhage location, size, periventricular drainage, number of veins reaching sinus,	To design a score for stratifying patients with BAVM rupture, based on the likelihood of a poor long-term neurological outcome.	Neurosurgeon, neuroradiologist	none	Univariate and multivariate Cox proportional-hazards logistic regression analyses Kaplan-Meier analysis. log-rank test

						venous stenosis/ occlusion, venous ectasia, venous reflux, sinus thrombosis feeding arteries, arterial aneurysms, number of aneurysms, location, haemorrhage history, haemorrhage date, no of vessels to be embolised, Moyamoya-type changes, pial-to-pial collateralisation, intravascular pressure measurement				chi-square test Fisher's exact test
Singh	The Neuroradiology Journal, 2018, Department of Neuroradiology, Sri Bala Ji Medical Institute, India	21	none	BAVM location, feeding arteries, venous drainage, nidus flow characteristics, venous stenosis/ occlusion, feeder enlargement, ECA feeder,	Angiography, CTA	clinical presentations, date of presentation, imaging source and date, lesion side, handedness, BAVM size, BAVM eloquence, BAVM border with adjacent brain,	to compare results of Time Resolved-CTA and DSA evaluations of cranial AVMs to determine if the two methods identify the same crucial	3 experienced neuroradiologists	none	nonparametric tests of significance. The Wilcoxon signed-rank test Fisher's exact probability test

				arterial aneurysms, angiogenesis, pseudophlebitic pattern		BAVM haemorrhage, haemorrhage location, size, periventricular drainage, number of draining veins leaving nidus, number of veins reaching sinus, venous ectasia, venous reflux, sinus thrombosis number of aneurysms, location, haemorrhage history, haemorrhage date, no of vessels to be embolised, Moyamoya-type changes, pial-to-pial collateralisation, intravascular pressure measurement	features of AVMs required in patient management.			
Han	J Neurosurg Pediatr, 2015, Department of Neurological Surgery, Boston's Children's	15, 1982-2006	none	AVM location	CTA, DSA	clinical presentations, date of presentation, imaging source and date, lesion side, handedness, BAVM size,	To report the largest series of brainstem AVMs to define 6 subtypes, assess this "occlusion in	none	none	n/a

	Hospital and Harvard Medical School					BAVM location, BAVM eloquence, BAVM border with adjacent brain, size, venous drainage, periventricular drainage, number of draining veins leaving nidus, number of veins reaching sinus, venous stenosis/ occlusion, venous ectasia, venous reflux, sinus thrombosis feeding arteries, arterial aneurysms, number of aneurysms, location, haemorrhage date, no of vessels to be embolised, Moyamoya-type changes, pial-to-pial collateralisatio n,	situ" technique, and analyze the microsurgical results.			

						intravascular pressure measurement				
Soltanolkotabi	J Neurosurg, 2013, Department of Radiology, Northwestern University Feinberg School of Medicine, Chicago, Illinois, USA	25, 2005-2011	BAVM eloquence,	clinical presentations, BAVM haemorrhage, BAVM location, SMG, BAVM size, BAVM eloquence, BAVM border with adjacent brain, venous drainage, feeding arteries,	angiography	date of presentation, imaging source and date, lesion side, handedness, haemorrhage location, size, periventricular drainage, number of draining veins leaving nidus, number of veins reaching sinus, venous stenosis/ occlusion, venous ectasia, venous reflux, sinus thrombosis arterial aneurysms, number of aneurysms, location, haemorrhage history, haemorrhage date, no of vessels to be embolised, Moyamoya-type changes, pial-to-pial collateralisation,	to assess the safety and efficacy of Onyx embolization in the treatment of intracranial arteriovenous malformations (AVMs) in pediatric patients.	interventional neuroradiologist	none	Univariate tests (χ^2 test)

						intravascular pressure measurement				
Sorenson	Journal of Clinical Neuroscience, 2019, School of Medicine, University of Minnesota, Minneapolis, USA	14, 2000-2018	none	BAVM size, BAVM location, feeding arteries, BAVM haemorrhage, haemorrhage location, arterial aneurysms, venous ectasia, number of draining veins leaving nidus, visibility on MRI, involved lesion tissue, terminal or en passage nidus, arterial dilatation, fistula, venous stenosis/ occlusion,	angiography , MRI	clinical presentations, date of presentation, imaging source and date, lesion side, handedness, BAVM eloquence, BAVM border with adjacent brain, size, venous drainage, periventricular drainage, number of veins reaching sinus, venous reflux, sinus thrombosis number of aneurysms, location, haemorrhage history, haemorrhage date, no of vessels to be embolised, Moyamoya-type changes, pial-to-pial collateralisatio n,	to investigate the natural history of brainstem AVMs with incomplete nidus obliteration after initial treatment	senior board-certified neuroradiologist	none	Fisher's exact test.

						intravascular pressure measurement				
Stapf 2002a	J Neurol Neurosurg Psychiatry, 2002, Stroke Center, The Neurological Institute, New York,	463, 1989-???	Clinical presentation, AVM size, venous drainage, Arterial aneurysms, feeding artery, AVM nidus	Clinical presentation, AVM size, venous drainage pattern, aneurysms	CT, MRI, DSA	date of presentation, imaging source and date, lesion side, handedness, BAVM location, BAVM eloquence, BAVM border with adjacent brain, haemorrhage location, size, periventricular drainage, number of draining veins leaving nidus, number of veins reaching sinus, venous stenosis/ occlusion, venous ectasia, venous reflux, sinus thrombosis feeding arteries, number of aneurysms, location, haemorrhage history, haemorrhage date,	To assess the effect of concurrent arterial aneurysms on the risk of incident haemorrhage from AVMs	neuroradiologists	nil	univariate tests (χ^2 test, *t* test) attributable risk determined by Fleiss

						no of vessels to be embolised, Moyamoya-type changes, pial-to-pial collateralisation, intravascular pressure measurement				
Stapf 2002 b	Stroke 2002, Stroke Center, Columbia University College of Physicians and Surgeons, New York, USA	240, 1989-2000	BAVM haemorrhage,	clinical presentations, BAVM haemorrhage, BAVM size, BAVM location,	DSA	date of presentation, imaging source and date, lesion side, handedness, BAVM eloquence, BAVM border with adjacent brain, haemorrhage location, size, venous drainage, periventricular drainage, number of draining veins leaving nidus, number of veins reaching sinus, venous stenosis/ occlusion, venous ectasia, venous reflux, sinus thrombosis feeding arteries,	to determine the frequency and predictors of residual dysplastic vessels on cerebral angiography after AVM surgery.	senior radiology house staff	none	Univariate (chi^2 test, *t* test, Spearman correlation) multivariate (logistic regression) Bonferroni correction

						arterial aneurysms, number of aneurysms, location, haemorrhage history, haemorrhage date, no of vessels to be embolised, Moyamoya-type changes, pial-to-pial collateralisation, intravascular pressure measurement				
Stapf, 2003	Stroke, 2003, Columbia University College of Physicians and Surgeons, New York	542, none	Initial AVM presentation, incident AVM haemorrhage, arterial aneurysms, feeding artery, AVM nidus size, location	Clinical presentation, AVM size, AVM location, venous drainage, arterial aneurysms	CT, MRI, angiography	date of presentation, imaging date, lesion side, handedness, BAVM eloquence, BAVM border with adjacent brain, haemorrhage location, size, periventricular drainage, number of draining veins leaving nidus, number of veins reaching sinus,	To determine the effect of age on clinical and morphological characteristics of cAVM patients	Neurosurgeons, neuroradiologists, neurologists nil	none	Chi squared test, ANOVA, Tukey's HSD, Spearman's rank correlation, nonlinear correlations,

						venous stenosis/ occlusion, venous ectasia, venous reflux, sinus thrombosis feeding arteries, number of aneurysms, location, haemorrhage history, haemorrhage date, no of vessels to be embolised, Moyamoya-type changes, pial-to-pial collateralisation, intravascular pressure measurement				
Stapf 2006	Neurology, 2006, Stroke Center/Neurological Institute, Columbia University, New York	622, 1989-???	Clinical presentation, initial haemorrhagic AVM presentation, AVM size, venous	Clinical presentation, initial haemorrhagic AVM presentation AVM size, anatomic	CT, MRI, DSA	date of presentation, imaging source and date, lesion side, handedness, BAVM eloquence,	To analyse the effect of certain factors on the risk of intracranial haemorrhage from untreated BAVMs at	neurosurgeons, neuroradiologists, and neurologists	nil	Univariate and multivariate logistic regression, Cox proportional

			drainage, anatomic location, borderzone location, arterial aneurysms, feeding artery, AVM nidus	location, venous drainage pattern, and associated arterial aneurysms, borderzone location, feeding artery,		BAVM border with adjacent brain, haemorrhage location, size, periventricular drainage, number of draining veins leaving nidus, number of veins reaching sinus, venous stenosis/ occlusion, venous ectasia, venous reflux, sinus thrombosis number of aneurysms, location, haemorrhage history, haemorrhage date, no of vessels to be embolised, Moyamoya-type changes, pial-to-pial collateralisation, intravascular pressure measurement	initial presentation and during follow-up.			hazard models
Stefani 2001	Stroke, 2001, University of Toronto, Toronto	390, 1989 - 1997	venous ectasia, venous	**Location**, **size**, **venous drainage**, **venous**	none	clinical presentations date of presentation	To study angioarchitectural factors of BAVMs	none	none	Logistic regression, univariate and

			stenosis, Location	**ectasia**, **venous stenosis**, **aneurysms**, **arterial feeders**		imaging source and date lesion side handedness BAVM eloquence BAVM border with adjacent brain BAVM haemorrhage haemorrhage location, size periventricular drainage number of veins reaching sinus venous reflux sinus thrombosis number of aneurysms location haemorrhage history haemorrhage date no of vessels to be embolised Moyamoya-type changes	associated with haemorrhage			multivariate analysis,

						pial-to-pial collateralisation intravascular pressure measurement				
Stefani 2002	Stroke, 2002, University of Toronto	390, 1989-???	AVM size, AVM location, arterial feeders, venous drainage, number of draining veins, venous ectasia, venous stenosis,	AVM size, AVM location, arterial feeders, venous drainage, number of draining veins, venous ectasia, venous stenosis, arterial aneurysms	DSA	clinical presentations, date of presentation, imaging source and date, lesion side, handedness, BAVM eloquence, BAVM border with adjacent brain, BAVM haemorrhage, haemorrhage location, size, periventricular drainage, number of veins reaching sinus, venous reflux, sinus thrombosis, number of aneurysms, location, haemorrhage history, haemorrhage date, no of vessels to be embolised,	To investigate the association between angiographic features of brain AVMs and the risk of future haemorrhagic events.	neurosurgeons, neuroradiologists, radiotherapists	nil	survival analyses, Cox regression, Univariate analyses, correlational analysis (Pearson's correlation), Multivariate stepwise analyses

						Moyamoya-type changes, pial-to-pial collateralisation, intravascular pressure measurement				
Stein 2018	Clinical Neurology and Neurosurgery, 2018, University Hospital Essen, Essen	46, 1990-2015	none	**Clinical presentation**, **haemorrhage**, **location**, **eloquence**, nidus size, **venous drainage**, fistulous or high flow nidal pattern, **aneurysm** (flow-related)	CT, MRI, DSA	date of presentation imaging date lesion side handedness BAVM size BAVM border with adjacent brain haemorrhage location, size periventricular drainage number of draining veins leaving nidus number of veins reaching sinus venous stenosis/ occlusion venous ectasia venous reflux sinus thrombosis feeding arteries	To evaluate characteristic clinical and angiographic features of AVMs in paediatric patients, and their correlation with presentation age	none	none	t-test, Levene test for homogeneity of variances, non-parametric Hodges-Lehmann test, non-parametric Wilcoxon-Mann-Whitney test

						arterial aneurysms number of haemorrhage history haemorrhage date no of vessels to be embolised Moyamoya-type changes pial-to-pial collateralisation intravascular pressure measurement				
Stein 2016 a	Acta Neurochir, 2016, Department of Neurosurgery, University Hospital Essen, Germany	Six, 1990-2015	none	clinical presentations, BAVM haemorrhage, BAVM size, BAVM location, number of draining veins leaving nidus, feeding arteries, SMG	CT, MRI, DSA	date of presentation, imaging source and date, lesion side, handedness, BAVM eloquence, BAVM border with adjacent brain, haemorrhage location, size, venous drainage, periventricular drainage, number of veins reaching sinus,	To present clinical, angiographic, and therapeutic characteristics of patients harbouring sporadic multiple AVMs.	experienced neurosurgeons, neuroradiologists, and radiosurgeons	none	none

						venous stenosis/ occlusion, venous ectasia, venous reflux, sinus thrombosis arterial aneurysms, number of aneurysms, location, haemorrhage history, haemorrhage date, no of vessels to be embolised, Moyamoya-type changes, pial-to-pial collateralisation, intravascular pressure measurement				
Stein 2016 b	Cerebrovasc Dis 2016, Department of Neurosurgery, University Hospital Essen, Germany	485, 1990 - 2013	nil	clinical presentations, arterial aneurysms, BAVM haemorrhage, Aneurysm location,	DSA	date of presentation, imaging source and date, lesion side, handedness, BAVM size, BAVM location, BAVM eloquence, BAVM border with adjacent brain, haemorrhage location, size,	to determine Associated aneurysm characteristics in posterior fossa AVMs and to compare with AAs accompanying supra-tentorial AVMs, with special focus	neurosurgeons and neuroradi-ologists	nil	T test Levene test, the homogeneity of variances non-parametric statistical procedure

						venous drainage, periventricular drainage, number of draining veins leaving nidus, number of veins reaching sinus, venous stenosis/ occlusion, venous ectasia, venous reflux, sinus thrombosis feeding arteries, number of aneurysms, haemorrhage history, haemorrhage date, no of vessels to be embolised, Moyamoya-type changes, pial-to-pial collateralisation, intravascular pressure measurement	on aneurysm size.			Wilcoxon Mann–Whitney test
Stein 2015	Cerebrovasc Dis, 2015, Department of Neurosurgery	409, 1990-2013	Haemorrhagic presentation, ruptured aneurysms	Haemorrhagic presentation, Aneurysm location, number of	CT, MRI, DSA	clinical presentations, date of presentation, imaging source and date,	To determine the angiographic and clinical characteristics of AAs with	experienced neurosurgeons neuroradiologists	none	Normal Scores Test, Kolmogorov-Smirnov Two-Sample Test

	& Radiology, University Hospital Essen, Germany			aneurysms, aneurysm size, number of ruptured aneurysms		lesion side, handedness, BAVM size, BAVM location, BAVM eloquence, BAVM border with adjacent brain, size, venous drainage, periventricular drainage, number of draining veins leaving nidus, number of veins reaching sinus, venous stenosis/ occlusion, venous ectasia, venous reflux, sinus thrombosis feeding arteries, haemorrhage date, no of vessels to be embolised, Moyamoya-type changes, pial-to-pial collateralisation, intravascular pressure measurement	special focus on aneurysm size and their consequences for treatment.			

Stiefel	Surgical Neurology, 2007, Department of Neurosurgery, and Division of Interventional Neuroradiology, University of Pennsylvania Medical Center, Philadelphia, USA	One, ???	none	clinical presentations, BAVM location, feeding arteries,	angiography	date of presentation, imaging source and date, lesion side, handedness, BAVM size, BAVM eloquence, BAVM border with adjacent brain, BAVM haemorrhage, haemorrhage location, size, venous drainage, periventricular drainage, number of draining veins leaving nidus, number of veins reaching sinus, venous stenosis/ occlusion, venous ectasia, venous reflux, sinus thrombosis arterial aneurysms, number of aneurysms, location, haemorrhage history, haemorrhage date,	To present a case report of de novo aneurysm formation and regression after BAVM embolisation	none	none	none

						no of vessels to be embolised, Moyamoya-type changes, pial-to-pial collateralisation, intravascular pressure measurement				
Sturiale	Journal of the Neurological Sciences, 2013, Institute of Neurosurgery, Catholic University School of Medicine, Rome	30, 2007-2011	none	AVM location, venous drainage, AVM size, AVM volume, coexisting aneurysms, perforating feeders, haematoma diameter, haematoma volume	CT, DSA	clinical presentations, date of presentation, imaging source and date, lesion side, handedness, BAVM eloquence, BAVM border with adjacent brain, BAVM haemorrhage, haemorrhage location, periventricular drainage, number of draining veins leaving nidus, number of veins reaching sinus, venous stenosis/ occlusion, venous ectasia, venous reflux, sinus thrombosis	To evaluate the influence on clinical appearance and outcome of the parenchymal and non-parenchymal bleedings associated with ruptured AVMs.	none	none	t-Student test Fisher's exact test logistic regression models

						number of aneurysms, location, haemorrhage history, haemorrhage date, no of vessels to be embolised, Moyamoya-type changes, pial-to-pial collateralisation, intravascular pressure measurement				
Suzuki	Turkish Neurosurgery 2012, Mie University, Graduate School of Medicine, Department of Neurosurgery, Tsu/Mie, Japan	7, ???	none	BAVM location, SMG	2D DSA, MRI, DSA-MR fusion	clinical presentations, date of presentation, imaging source and date, lesion side, handedness, BAVM size, BAVM eloquence, BAVM border with adjacent brain, BAVM haemorrhage, haemorrhage location, size, venous drainage, periventricular drainage, number of draining veins leaving nidus,	To assess the usefulness of DSA-MR fusion images concerning the pretreatment evaluation for cerebral (AVM)	Two experienced neurosurgeons who were experienced in performing microsurgical, endovascular and radiosurgical treatments	none	none

						number of veins reaching sinus, venous stenosis/ occlusion, venous ectasia, venous reflux, sinus thrombosis feeding arteries, arterial aneurysms, number of aneurysms, location, haemorrhage history, haemorrhage date, no of vessels to be embolised, Moyamoya-type changes, pial-to-pial collateralisation, intravascular pressure measurement				
Taeshineetanakul et al	Neurosurgery, 2012, Toronto Western Hospital, Toronto	139, 2000-2009	Angiogenesis, flow pattern, pseudophlebitic pattern, nidus type/ border	Feeding artery enlargement, **aneurysms**, angiogenesis, **nidus size**, **location**/ **eloquence**, nidus type/ **border**, flow	Biplanar DSA	Clinical presentation, date of presentation, imaging source and date, lesion side, handedness, BAVM	To determine if angioarchitecture affects the obliteration rate after radiosurgery in BAVMs	2 neuroradiologists, with 6 and 12 years experience	none	$\chi 2$, Spearman, and φ correlations and the Mann-Whitney test

				pattern, **venous ectasia**, venous pouches, **drainage pattern**, **number of draining veins**, venous rerouting, pseudophlebitic pattern		haemorrhage including location and size, no. of veins reaching sinus, venous reflux, sinus thrombosis, no. of vessels to be embolised, intravascular pressure measurements				
Tanaka	Radiology Case Reports, 2018, Department of Neurology, Neurological Institute, Graduate School of Medical Sciences, Kyushu University, Fukuoka, Japan	2, ???	none	SMG, feeding arteries, venous drainage, BAVM location, clinical presentations, BAVM haemorrhage,	DSA, CT, carotid US	date of presentation, imaging source and date, lesion side, handedness, BAVM size, BAVM eloquence, BAVM border with adjacent brain, haemorrhage location, size, periventricular drainage, number of draining veins leaving nidus, number of veins reaching sinus, venous stenosis/ occlusion,	To report 2 cases of cerebral arteriovenous malformation (AVM) showing an elevated ED ratio of the CCA, which decreased after surgery.	none	none	none

						venous ectasia, venous reflux, sinus thrombosis arterial aneurysms, number of aneurysms, location, haemorrhage history, haemorrhage date, no of vessels to be embolised, Moyamoya-type changes, pial-to-pial collateralisation, intravascular pressure measurement				
Taschner	Radiology, 2008, Departments of Neuroradiology and Neurosurgery, Hopital Roger Salengro, University Hospital Lille, France;	28, 2005-2006	venous drainage, feeding arteries,	clinical presentations, BAVM haemorrhage, BAVM location, BAVM size, venous drainage, feeding arteries,	DSA, MRA	date of presentation, imaging source and date, lesion side, handedness, BAVM eloquence, BAVM border with adjacent brain, haemorrhage location, size, periventricular drainage, number of draining veins leaving nidus,	To prospectively compare the agreement between digital sub-traction angiography (DSA) and time-resolved magnetic reso-nance (MR) angiography with sensitivity encoding (SENSE) in combination with keyhole	Two neuroradiologists (with 7 and 20 years of experience per-forming DSA) Two other raters (with 9 and 12 years of experience in neuro MR imaging)	interobserver agreement intermodality agreement K coefficient	

						number of veins reaching sinus, venous stenosis/ occlusion, venous ectasia, venous reflux, sinus thrombosis arterial aneurysms, number of aneurysms, location, haemorrhage history, haemorrhage date, no of vessels to be embolised, Moyamoya-type changes, pial-to-pial collateralisation, intravascular pressure measurement	acquisition and contrast material–enhanced robust-timing angiography (CENTRA) k-space sam-pling techniques for the characterization of intracranial arterio-venous malformations (AVMs).			
Tasic	Turkish Neurosurgery 2011, Clinical Centre of Serbia, Institute for Neurosurgery, Belgrade, Serbia, Yugoslavia	39, 1995-2004	AVM	BAVM haemorrhage, BAVM size, BAVM location, venous drainage, feeding arteries,	angiography	clinical presentations, date of presentation, imaging source and date, lesion side, handedness, BAVM eloquence, BAVM border with adjacent brain,	To define those variables that contribute to frequency of haemorrhage	neurosurgeons neuroradiologists	none	Mann-Whitney U-test multivariant logistic regression

						haemorrhage location, size, periventricular drainage, number of draining veins leaving nidus, number of veins reaching sinus, venous stenosis/ occlusion, venous ectasia, venous reflux, sinus thrombosis arterial aneurysms, number of aneurysms, location, haemorrhage history, haemorrhage date, no of vessels to be embolised, Moyamoya-type changes, pial-to-pial collateralisation, intravascular pressure measurement				
Todaka	Stroke, 2003, Department of Neurosurgery, Kumamoto	30, 2000-2002	nil	Haemorrhage, AVM size, number of draining veins,	DSA, MRI	clinical presentations, date of presentation,	To clarify haemodynamic risk factors for haemorrhage in AVMs	nil	nil	Student's *t* test Welch's *t* test F test

	University School of Medicine			diameter of feeding artery, diameter of draining vein		imaging source and date, lesion side, handedness, BAVM location, BAVM eloquence, BAVM border with adjacent brain, haemorrhage location, size, venous drainage, periventricular drainage, number of veins reaching sinus, venous stenosis/ occlusion, venous ectasia, venous reflux, sinus thrombosis feeding arteries, arterial aneurysms, number of aneurysms, location,	using the mean transit time (MTT) of feeding arteries and draining veins in AVMs with and without haemorrhage			

						haemorrhage history, haemorrhage date, no of vessels to be embolised, Moyamoya-type changes, pial-to-pial collateralisation, intravascular pressure measurement				
Togao 2019	Neuroradiology, 2019, Department of Clinical Radiology, Kyushu University, Fukuoka, Japan	21, 2014 - 2017	nil	clinical presentations, number of draining veins leaving nidus, feeding arteries, BAVM size, BAVM eloquence, venous drainage, SMG, BAVM location, BAVM haemorrhage, haemorrhage history,	DSA, MRA	date of presentation, imaging source and date, lesion side, handedness, BAVM border with adjacent brain, haemorrhage location, size, periventricular drainage, number of veins reaching sinus, venous stenosis/ occlusion, venous ectasia, venous reflux, sinus thrombosis arterial aneurysms,	To evaluate the performance of acceleration-selective arterial spin labeling (AccASL) MR angiography in the visual-ization of brain arteriovenous malformations (AVMs) in comparison with digital subtraction angiography (DSA) and	Four neuroradiologists: board-certified radiologist with 15 years of experience resident with 4 years of experience two board-certified neuroradiologists (O.T., 17 years of experience,	Inter-rater agreements	kappa statistic repeated measures analysis of variance with post hoc Tukey's test Wilcoxon matched pairs test paired t test

						number of aneurysms, location, haemorrhage date, no of vessels to be embolised, Moyamoya-type changes, pial-to-pial collateralisation, intravascular pressure measurement	time-of-flight (TOF) MR angiography	A.H., 19 years of experience)		
Togao 2020	European Radiology, 2020 Department of Clinical Radiology, Kyushu University, Fukuoka, Japan	15, 2016 - 2019	BAVM size,	clinical presentations, BAVM location, feeding arteries, BAVM size, number of draining veins leaving nidus, venous drainage,	DSA, MRA, TOF MRA	date of presentation, imaging source and date, lesion side, handedness, BAVM eloquence, BAVM border with adjacent brain, BAVM haemorrhage, haemorrhage location, size, periventricular drainage, number of veins reaching sinus, venous stenosis/ occlusion, venous ectasia, venous reflux,	To evaluate the usefulness of 4D-MR angiography based on super-selective pseudo-continuous ASL combined with keyhole and view-sharing (4D-S-PACK) for vessel-selective visualization and to examine the ability of this technique to	3 board-certified neuroradiologists (observer 1 with 11 years of experience and observer 2 with 5 years of experi- ence, another with 19 years of experience	Inter-rater agreements	intraclass correlation coefficient paired t test chi-square test Wilcoxon matched-pairs signed-rank test.

						sinus thrombosis arterial aneurysms, number of aneurysms, location, haemorrhage history, haemorrhage date, no of vessels to be embolised, Moyamoya-type changes, pial-to-pial collateralisation, intravascular pressure measurement	visualize brain arteriovenous malformations (AVMs).			
Tong 2015	Acta Neurochir, 2015, Department of Neurosurgery, Beijing Tiantan Hospital	98, 1990-2012	none	Clinical presentation, SMG, AVM size, AVM location, eloquence, venous drainage, arterial supply, associated aneurysms	CTA, DSA	date of presentation, imaging source and date, lesion side, handedness, BAVM border with adjacent brain, BAVM haemorrhage, haemorrhage location, size, periventricular drainage, number of draining veins leaving nidus,	To describe a single institution's experience treating arteriovenous malformations (AVMs) in elderly patients in terms of clinical features, haemorrhage risk, treatment modality and	none	none	Univariate and multivariate logistic regression analyses chi-square test

						number of veins reaching sinus, venous stenosis/ occlusion, venous ectasia, venous reflux, sinus thrombosis number of aneurysms, location, haemorrhage history, haemorrhage date, no of vessels to be embolised, Moyamoya-type changes, pial-to-pial collateralisation, intravascular pressure measurement	functional outcome			
Tong a 2016	World Neurosurg, 2016, Department of Neurosurgery, Beijing Tiantan Hospital	225, 2000-2015	eloquence	AVM size, AVM location, eloquence, feeding artery, venous drainage, associated aneurysm	CT, MRI, DSA	clinical presentations, date of presentation, imaging source and date, lesion side, handedness, BAVM border with adjacent brain, BAVM haemorrhage, haemorrhage location, size,	To summarize the clinical presentation, risk of haemorrhage, and predictors of post-haemorrhage outcome in patients with cerebellar AVMs	nil	nil	Student's t-tests chi-square test uni- variate and multivariate logistic regression analyses area under the receiver

						periventricular drainage, number of draining veins leaving nidus, number of veins reaching sinus, venous stenosis/ occlusion, venous ectasia, venous reflux, sinus thrombosis number of aneurysms, location, haemorrhage history, haemorrhage date, no of vessels to be embolised, Moyamoya-type changes, pial-to-pial collateralisation, intravascular pressure measurement				operating characteristic (AUROC) curve
Tong 2016 b	World Neurosurg, 2016, Department of Neurosurgery, Beijing Tiantan Hospital	149, 2000-2015	AVM haemorrhage	AVM haemorrhage, AVM size, AVM location, venous drainage, feeding artery,	DSA, CT, MRI	clinical presentations, date of presentation, imaging source and date, lesion side, handedness, BAVM eloquence,	To identify the risk factors for subsequent haemorrhage in patients with un-treated	nil	nil	Pearson chi^2 test Mann-Whitney U test

				associated aneurysm		BAVM border with adjacent brain, BAVM haemorrhage, haemorrhage location, size, periventricular drainage, number of draining veins leaving nidus, number of veins reaching sinus, venous stenosis/ occlusion, venous ectasia, venous reflux, sinus thrombosis number of aneurysms, location, haemorrhage date, no of vessels to be embolised, Moyamoya-type changes, pial-to-pial collateralisation, intravascular pressure measurement	cerebellar AVMs			Kaplan-Meier product-limit method, log-rank test Univariate Cox regression analysis multivariate Cox proportional hazards model with a forward stepwise regression procedure
Tong 2016 c	World Neurosurg, 2016, Department	3299, 1980-2015	Clinical presentation, haemorrhage presentation,	Clinical presentation, haemorrhage, AVM size,	DSA, CT, MRI	date of presentation, imaging source and date, handedness,	To identify whether age, sex, and lesion location are associated	none	none	Chi square test, independent sample t test

	of Neurosurgery, Beijing Tiantan Hospital		AVM side, AVM location	AVM side, location, associated aneurysms, SMG, venous drainage, arterial supply		BAVM eloquence, BAVM border with adjacent brain, haemorrhage location, size, venous drainage, periventricular drainage, number of draining veins leaving nidus, number of veins reaching sinus, venous stenosis/ occlusion, venous ectasia, venous reflux, sinus thrombosis feeding arteries, number of aneurysms, location, haemorrhage history, haemorrhage date, no of vessels to be embolised, Moyamoya-type changes, pial-to-pial collateralisation,	with initial presentation in patients with brain (AVMs).			

						intravascular pressure measurement				
Tong 2017	World Neurosurg, 2017, Department of Neurosurgery, Beijing Tiantan Hospital, China	282, 2008-2015	none	clinical presentations, lesion side, handedness, BAVM size, BAVM location, BAVM eloquence, venous drainage, feeding arteries, SMG, arterial aneurysms,	DSA, CTA	date of presentation, imaging source and date, BAVM border with adjacent brain, BAVM haemorrhage, haemorrhage location, size, periventricular drainage, number of draining veins leaving nidus, number of veins reaching sinus, venous stenosis/ occlusion, venous ectasia, venous reflux, sinus thrombosis number of aneurysms, location, haemorrhage history, haemorrhage date, no of vessels to be embolised, Moyamoya-type changes,	To describe our single-center experience treating unruptured brain arteriovenous malformations (uBAVMs) with microsurgical treatment.	neurosurgeons	none	Univariate and multivariate logistic analyses

						pial-to-pial collateralisation, intravascular pressure measurement				
Tritt	Clin Neuroradiol 2017, institute of neuroradiology, hospital of Goethe university, Frankfurt, Germany	20 ???	none	clinical presentations, BAVM haemorrhage, BAVM size, BAVM location, venous drainage, arterial aneurysms, SMG, feeding arteries,	DSA, MRI/MRA	date of presentation, imaging source and date, lesion side, handedness, BAVM eloquence, BAVM border with adjacent brain, haemorrhage location, size, periventricular drainage, number of draining veins leaving nidus, number of veins reaching sinus, venous stenosis/ occlusion, venous ectasia, venous reflux, sinus thrombosis number of aneurysms, location, haemorrhage history, haemorrhage date,	to prove the technical feasibility of creating fused images of time-resolved 3D reconstructions and MPRAGE MRI data sets and to check the reliability of the correct anatomical display of the angioma nidus and the venous drainage in the fused images of patients with intracranial arteriovenous malformations (AVM)	experienced one neuroradiologist and one neurosurgeon	inter-rater variability	Pearson-R

						no of vessels to be embolised, Moyamoya-type changes, pial-to-pial collateralisation, intravascular pressure measurement				
Tsuchiya	Eur Radiol, 2002, Department of Radiology, Kyorin University School of Medicine, Tokyo, Japan	15 ???	none	feeding arteries, venous drainage, number of draining veins leaving nidus, BAVM size, BAVM location,	MRA, DSA	clinical presentations, date of presentation, imaging source and date, lesion side, handedness, BAVM eloquence, BAVM border with adjacent brain, BAVM haemorrhage, haemorrhage location, size, periventricular drainage, number of veins reaching sinus, venous stenosis/ occlusion, venous ectasia, venous reflux, sinus thrombosis arterial aneurysms,	To evaluate the utility of surface anatomy scanning (SAS) of the brain with superimposition of MR angiograms in the diagnosis and presurgical planning of superficial cAVMs	neurosurgeon Radiologists	Interobserver	none

						number of aneurysms, location, haemorrhage history, haemorrhage date, no of vessels to be embolised, Moyamoya-type changes, pial-to-pial collateralisation, intravascular pressure measurement				
Unlu	European Journal of Radiology 60, 2006, Department of Radiology, Trakya University Medicine School, Edirne, Turkey	20, 2001-2005	none	clinical presentations, BAVM haemorrhage, feeding arteries, venous drainage,	MRA, DSA	date of presentation, imaging source and date, lesion side, handedness, BAVM size, BAVM location, BAVM eloquence, BAVM border with adjacent brain, haemorrhage location, size, periventricular drainage, number of draining veins leaving nidus, number of veins reaching sinus,	to compare the diagnostic utility of three-dimensional (3D) time-of-flight (TOF) magnetic resonance angiography (MRA) and contrast-enhanced 3D MRA in patients with intracranial arteriovenous malformations (AVMs) in different sizes and locations.	Two radiologists, experienced on neurovascular imaging	interobserver	non-parametric method eg Wilcoxon signed-rank's test Spearman rank correlation test.

						venous stenosis/ occlusion, venous ectasia, venous reflux, sinus thrombosis arterial aneurysms, number of aneurysms, location, haemorrhage history, haemorrhage date, no of vessels to be embolised, Moyamoya-type changes, pial-to-pial collateralisation, intravascular pressure measurement				
Valavanis	Schweiz Arch Neurol Psychiatr, 2004, University Hospital of Zurich, Zurich	None	angiogenesis	**Nidus size**, **clinical presentation**, **eloquence**, **nidus border**, angiogenesis, mono or multicompartmental, intercompartmental communications, fistula, **feeding artery**	DSA, multiplanar MRI, DTI MR, 3D-tractography, functional MR, MRA Nil else	date of presentation, imaging source and date, lesion side, handedness, BAVM location, BAVM haemorrhage including location and size, no. of	Endovascular BAVM treatment with emphasis on cure	None	None	None

				types, modes of supply, **types & patterns of venous drainage** & **relation to normal brain drainage**		veins reaching sinus, venous reflux, venous ectasia, stenosis, sinus thrombosis, aneurysms, no. of vessels to be embolised, Moyamoya-type changes, pial-to-pial collaterals, intravascular pressure measurements				
Van den Berg	Neurosurgery 2008 Department of Radiology, Free University Medical Center and Academic Medical Center, Amsterdam, The Netherlands	30, 1998-2006	none	BAVM size, SMG, venous drainage, venous stenosis/ occlusion, number of draining veins leaving nidus,	MRI, DSA	clinical presentations, date of presentation, imaging source and date, lesion side, handedness, BAVM location, BAVM eloquence, BAVM border with adjacent brain, BAVM haemorrhage, haemorrhage location, size, periventricular drainage,	to analyse the cause of extensive perinidal white matter changes seen surrounding radiosurgically treated BAVMs	experienced interventional neuroradiologist	none	Pearson's χ^2 test Fisher's exact test linear-by-linear association Student's *t* test

						number of veins reaching sinus, venous ectasia, venous reflux, sinus thrombosis feeding arteries, arterial aneurysms, number of aneurysms, location, haemorrhage history, haemorrhage date, no of vessels to be embolised, Moyamoya-type changes, pial-to-pial collateralisation, intravascular pressure measurement				
Van Rooij	Am J Neuroradiol, 2012, Departments of Radiology and Neurosurgery, St. Elisabeth Ziekenhuis, Tilburg, the Netherlands	24, 2008-2011	none	clinical presentations, BAVM haemorrhage, BAVM size, BAVM location, SMG, number of draining veins leaving nidus, feeding arteries,	MR, CT, angiography	date of presentation, imaging source and date, lesion side, handedness, BAVM eloquence, BAVM border with adjacent brain, haemorrhage location, size,	To report experience with curative embolisation of selected brain AVMs with Onyx.	neuroradiologists, neurologists, neurosurgeons	none	none

						venous drainage, periventricular drainage, number of veins reaching sinus, venous stenosis/ occlusion, venous ectasia, venous reflux, sinus thrombosis arterial aneurysms, number of aneurysms, location, haemorrhage history, haemorrhage date, no of vessels to be embolised, Moyamoya-type changes, pial-to-pial collateralisation, intravascular pressure measurement				
Viana	J NeuroInterve nt Surg, 2017, Division of interventional Neuroradiolo gy, Department	12, 2011-2016	none	SMG, BAVM haemorrhage, BAVM location, BAVM size, venous drainage, feeding arteries,	DSA	clinical presentations, date of presentation, imaging source and date, lesion side, handedness,	to assess the safety and efficacy of the transvenous approach for embolising	neurologist	none	χ^2 or Fisher's exact tests, Mann–Whitney test or Student's *t*-test

	of internal Medicine, University of São Paulo, Ribeira, Brazil			arterial aneurysms,		BAVM eloquence, BAVM border with adjacent brain, haemorrhage location, size, periventricular drainage, number of draining veins leaving nidus, number of veins reaching sinus, venous stenosis/ occlusion, venous ectasia, venous reflux, sinus thrombosis number of aneurysms, location, haemorrhage history, haemorrhage date, no of vessels to be embolised, Moyamoya-type changes, pial-to-pial collateralisation, intravascular pressure measurement	superficial AVMs.			
Weber	Am J Neuroradiol, 2007,	93, 2001-2004	none	clinical presentations,	angiography	date of presentation,	To report our experiences in the	neuroradiologist	none	none

	Department of Radiology and Neuroradiology, Alfried Krupp Krankenhaus, Essen, Germany			BAVM haemorrhage, BAVM location, number of draining veins leaving nidus, feeding arteries, BAVM border with adjacent brain, shunt,		imaging source and date, lesion side, handedness, BAVM size, BAVM eloquence, haemorrhage location, size, venous drainage, periventricular drainage, number of veins reaching sinus, venous stenosis/ occlusion, venous ectasia, venous reflux, sinus thrombosis arterial aneurysms, number of aneurysms, location, haemorrhage history, haemorrhage date, no of vessels to be embolised, Moyamoya-type changes, pial-to-pial collateralisation, intravascular pressure measurement	treatment of intracranial AVMs with Onyx embolization before neuro- or radiosurgery.	neurologist		

Willinsky	Interventional Neuroradiology, 2001, The Toronto Western Hospital, Toronto	80, 1984-1999	none	**BAVM location**, pure AV fistula, **feeding arteries number & type**, **number of draining veins leaving nidus**, **BAVM size,** SMG.	DSA	clinical presentations, date of presentation, imaging source and date, lesion side, handedness, BAVM eloquence, BAVM border with adjacent brain, BAVM haemorrhage, haemorrhage location, size, venous drainage, periventricular drainage, number of veins reaching sinus, venous stenosis/ occlusion, venous ectasia, venous reflux, sinus thrombosis, arterial aneurysms,	To correlate a proposed grading system based on the angioarchitecture to the percentage obliteration achieved by embolisation	None mentioned	no	Fisher's exact test (2-tailed)

						number of aneurysms, location, haemorrhage history, haemorrhage date, no of vessels to be embolised, Moyamoya-type changes, pial-to-pial collateralisation, intravascular pressure measurement				
Wrede	Eur Radiol, 2016, Erwin L. Hahn Institute for Magnetic Resonance Imaging, University Duisburg-Essen, Germany	20,	none	lesion side, BAVM location, feeding arteries, number of draining veins leaving nidus, arterial aneurysms, BAVM size, SMG, venous drainage,	MRI, DSA	clinical presentations, date of presentation, imaging source and date, handedness, BAVM eloquence, BAVM border with adjacent brain, BAVM haemorrhage, haemorrhage location, size, periventricular drainage, number of veins reaching sinus,	To evaluate prospectively 7 Tesla time-of-flight (TOF) magnetic resonance angiography (MRA) and 7 Tesla non-contrast-enhanced magnetization-prepared rapid acquisition gradient-echo (MPRAGE) for delineation of	senior interventional neuro-radiologists	Inter-observer	kappa coefficient Wilcoxon matched-pairs two-sided signed-ranks test Bonferroni correction Skillings Mack test

						venous stenosis/ occlusion, venous ectasia, venous reflux, sinus thrombosis number of aneurysms, location, haemorrhage history, haemorrhage date, no of vessels to be embolised, Moyamoya-type changes, pial-to-pial collateralisation, intravascular pressure measurement	intracerebral arteriovenous malformations (AVMs) in comparison to 1.5 Tesla TOF MRA and DSA			generalized Friedman test
Wu	World Neurosurg, 2016, Neurological Institute, Taipei Veterans General Hospital and National Yang-Ming University, Taipei,	220, 2007-2010	arterial dilation, fistulous component, venous stenosis, long course drainage veins	Nidus diameter, arterial borderzone location, arterial dilation, fistulous components, venous ectasia, venous stenosis, long course drainage veins,	DSA, MRI	clinical presentations, date of presentation, imaging source and date, lesion side, handedness, BAVM location, BAVM eloquence, BAVM border with adjacent brain,	To corroborate which pretreatment angioarchicte ctural characteristics and posttreatmen t MRI features were associated with better seizure and AED outcomes in	Neuroradiologis ts, neurosurgeons	nil	Mann-Whitney U-test (2-tailed), chi2 test or Fisher exact test (2-tailed), multivariate logistic regression analysis, Kaplan-Meier survival analysis, log-rank test

				retrograde cortical veins		BAVM haemorrhage, haemorrhage location, size, venous drainage, periventricular drainage, number of draining veins leaving nidus, number of veins reaching sinus, sinus thrombosis feeding arteries, arterial aneurysms, number of aneurysms, location, haemorrhage history, haemorrhage date, no of vessels to be embolised, Moyamoya-type changes, pial-to-pial collateralisation,	BAVM patients treated by Gamma Knife SRS.			

						intravascular pressure measurement				
Yamada	J Neurosurg, 2007, Department of Neurosurgery, Kyoto University Graduate School of Medicine,	305, 1983-2005	AVM size, AVM location, venous drainage	AVM size, AVM location, venous drainage	DSA, CT, MRI	clinical presentations, date of presentation, imaging source and date, lesion side, handedness, BAVM eloquence, BAVM border with adjacent brain, BAVM haemorrhage, haemorrhage location, size, periventricular drainage, number of draining veins leaving nidus, number of veins reaching sinus, venous stenosis/ occlusion, venous ectasia, venous reflux,	To identify the natural history of untreated cerebral AVMs and the risk factors for subsequent haemorrhage after an initial AVM diagnosis	nil	nil	Cox proportional hazards regression model, log-rank test of the Kaplan–Meier life tables, univariate analyses, multivariate analyses

						sinus thrombosis feeding arteries, arterial aneurysms, number of aneurysms, location, haemorrhage history, haemorrhage date, no of vessels to be embolised, Moyamoya-type changes, pial-to-pial collateralisation, intravascular pressure measurement				
Yang 2015 a	World Neurosurg, 2015, Department of Neurosurgery, Johns Hopkins University School of Medicine, Baltimore	194, 1993-2010	AVM size, feeding arteries, AVM location	AVM size, AVM location, AVM side, venous drainage, number of feeding arteries, number of draining veins, SMG, location of	DSA, MRI	clinical presentations, date of presentation, imaging source and date, handedness, BAVM eloquence, BAVM border with adjacent brain, BAVM haemorrhage,	To examine the association of patient demographics and angiographic features with haemorrhagic presentation of AVMs	diagnostic and interventional neuroradiologists	none	univariate analysis, chi^2 test and Student t test Univariate logistic regression analysis multivariate logistic

				feeding arteries, intranidal aneurysms, venous stenosis, varix		haemorrhage location, size, periventricular drainage, number of veins reaching sinus, venous ectasia, venous reflux, sinus thrombosis arterial aneurysms, number of aneurysms, haemorrhage history, haemorrhage date, no of vessels to be embolised, Moyamoya-type changes, pial-to-pial collateralisation, intravascular pressure measurement				regression model Collinearity was checked for the final model using variance inflation factor (VIF) analysis;
Yang 2015 b	World Neurosurg, 2015, Department of Neurosurgery, Johns Hopkins University School of Medicine, Baltimore	194, 1993-2010	AVM size, feeding arteries, number of feeding arteries, number of draining veins	Clinical presentation, AVM size, AVM location, side of AVM, venous drainage pattern, number of feeding arteries,	DSA, MRI	date of presentation, imaging source and date, handedness, BAVM eloquence, BAVM border with adjacent brain, BAVM haemorrhage,	To determine racial associations with haemorrhagic presentation in cAVMs	neuroradiologists – not for study but for clinical care	nil	Chi square test, student t test, Univariate logistic regression analysis, multivariate logistic

				number of draining veins, Spetzler-Martin grade, location of feeding arteries, presence of intranidal aneurysms, venous stenosis, varix		haemorrhage location, size, periventricular drainage, number of veins reaching sinus, venous ectasia, venous reflux, sinus thrombosis number of aneurysms, location, haemorrhage history, haemorrhage date, no of vessels to be embolised, Moyamoya-type changes, pial-to-pial collateralisation, intravascular pressure measurement				regression analysis. Collinearity was checked for the final model using variance inflation factor analysis
Yang 2016 a	Neurosurgery, 2016, Department of Neurosurgery, Johns Hopkins University School of Medicine, Baltimore	12, 1990-2013	NONE	Haemorrhage presentation, clinical presentation, AVM size, eloquence, deep venous drainage, SMG, location	CT, DSA	date of presentation, imaging source and date, lesion side, handedness, BAVM border with adjacent brain, haemorrhage location, size, periventricular drainage,	To clarify the clinical characteristics and haemorrhagic risk in HHT-related AVMs.	nil	nil	Student's t test Wilcoxon rank-sum test Uncorrected x2 test or Fisher's exact test

						number of draining veins leaving nidus, number of veins reaching sinus, venous stenosis/ occlusion, venous ectasia, venous reflux, sinus thrombosis feeding arteries, arterial aneurysms, number of aneurysms, location, haemorrhage history, haemorrhage date, no of vessels to be embolised, Moyamoya-type changes, pial-to-pial collateralisation, intravascular pressure measurement				Poisson rate ratio test
Yang 2016 b	J Neurosurg Pediatr, 2016, John Hopkins University School of Medicine, Baltimore	124, 1990-2013	none	Clinical presentation, AVM size, eloquence, deep venous drainage, SMG, location	DSA	date of presentation, imaging source and date, lesion side, handedness,	To determine long-term haemorrhagic risk in paediatric patients with AVMs	nil	nil	Student t-test, Wilcoxon rank-sum test. Fisher's exact test, chi-square test, Kaplan-Meier

						BAVM border with adjacent brain, BAVM haemorrhage, haemorrhage location, size, periventricular drainage, number of draining veins leaving nidus, number of veins reaching sinus, venous stenosis/ occlusion, venous ectasia, venous reflux, sinus thrombosis feeding arteries, arterial aneurysms, number of aneurysms, location, haemorrhage history, haemorrhage date, no of vessels to be embolised, Moyamoya-type changes, pial-to-pial collateralisation,				curve, log-rank test, Cox proportional hazard re-gression analysis

						intravascular pressure measurement				
Yang 2017	Neurosurgery, 2017, Department of Neurosurgery, Hopkins University School of Medicine, Baltimore, Maryland, USA	90, 1990-2013	BAVM size, BAVM location, Deep venous drainage,	clinical presentations, BAVM haemorrhage, BAVM size, BAVM location, BAVM eloquence, venous drainage, SMG,	angiography	date of presentation, imaging source and date, lesion side, handedness, BAVM border with adjacent brain, haemorrhage location, size, periventricular drainage, number of draining veins leaving nidus, number of veins reaching sinus, venous stenosis/ occlusion, venous ectasia, venous reflux, sinus thrombosis feeding arteries, arterial aneurysms, number of aneurysms, location, haemorrhage history, haemorrhage date, no of vessels to be embolised,	To describe the progression and risk factors of post-treatment seizure in children with AVMs.	none	none	univariate and multivariate Cox proportional hazard models Kaplan–Meier survival curve Log-rank test.

						Moyamoya-type changes, pial-to-pial collateralisation, intravascular pressure measurement				
Ye	Medicine, 2017, Department of Neurosurgery, West China Hospital of Sichuan University, Chengdu	89, 2010-2016	none	Haemorrhage, aneurysm, AVM location	CT, CTA, DSA, MRA	clinical presentations, date of presentation, imaging source and date, lesion side, handedness, BAVM size, BAVM eloquence, BAVM border with adjacent brain, haemorrhage location, size, venous drainage, periventricular drainage, number of draining veins leaving nidus, number of veins reaching sinus, venous stenosis/ occlusion, venous ectasia, venous reflux, sinus thrombosis	To discuss the clinical features and prognostic factors of outcomes in the patients with AVM-related IVH.	none	none	univariate logistic regression multivariate logistic regression Student t test Pearson chi-squared test

						feeding arteries, number of aneurysms, location, haemorrhage history, haemorrhage date, no of vessels to be embolised, Moyamoya-type changes, pial-to-pial collateralisation, intravascular pressure measurement				
Yen	Prog Neurol Surg, 2013, Department of Neurological Surgery, University of Virginia, Charlottesville, USA	1400, 1989-2009	none	BAVM haemorrhage, number of draining veins leaving nidus, venous drainage, feeding arteries, BAVM location, arterial aneurysms, BAVM size,	Assumed angiography	clinical presentations, date of presentation, imaging source and date, lesion side, handedness, BAVM eloquence, BAVM border with adjacent brain, haemorrhage location, size, periventricular drainage, number of veins reaching sinus, venous stenosis/ occlusion,	To describe the natural history of AVMs and the risk factors associated with haemorrhage, to focus on the haemorrhage rate following radiosurgery	neurosurgeon	none	Univariate and multivariate logistic regressions Univariate and multivariate proportional hazard models

						venous ectasia, venous reflux, sinus thrombosis number of aneurysms, location, haemorrhage history, haemorrhage date, no of vessels to be embolised, Moyamoya-type changes, pial-to-pial collateralisation, intravascular pressure measurement				
Yi et al	Neurosurg Q, 2016, Hallym Sacred Heart Hospital, Korea	50, 2004-2010	Nidus size, venous stenosis, venous kinking, venous recruitment, venous drainage pattern, venous reflux, venous obstacles	**Nidus size**, **number of draining veins**, **venous stenosis**, venous kinking, venous recruitment, **venous drainage pattern**, **venous reflux**, venous obstacles	DSA, CT, MRI	Clinical presentation, date of presentation, imaging date, lesion side, handedness, BAVM location, BAVM eloquence, BAVM border with adjacent brain, BAVM haemorrhage including location and size, periventricular drainage,	To identify angioarchitectural characteristics associated with the risk of hemorrhage in cerebral AVMs	2 readers, unclear specialty	none	χ2 Fisher exact test, Stepwise logistic regressionprocedure

						number of veins reaching sinus, venous ectasia, sinus thrombosis, feeding arteries, number of vessels to be embolised, Moyamoya-type changes, pial-to-pial collaterals, intravascular pressure measurements				
Yu	Interv Neuroradiol, 2018, University of California, San Francisco	169, 2000 to 2015	none	Haemorrhage volume, presence of intraventricular haemorrhage, associated aneurysms, AVM size, diffuse AVM border, eloquent location, Deep venous drainage, lobar location, multiple feeding arteries,	CT, DSA	clinical presentations, date of presentation, imaging source and date, lesion side, handedness, BAVM haemorrhage, haemorrhage location, periventricular drainage, number of draining veins leaving nidus, number of veins reaching sinus, venous reflux,	To identify the demographical, clinical, and bAVM anatomical variables associated with ICH volume and the presence of intraventricular hemorrhage (IVH) of ruptured bAVMs to help better predict outcome for	neurointerventional radiologists	nil	univariable linear regression analysis multivariable regression analysis logistic regression analysis

				venous ectasia, venous stenosis		sinus thrombosis arterial aneurysms, number of aneurysms, location, haemorrhage history, haemorrhage date, no of vessels to be embolised, Moyamoya-type changes, pial-to-pial collateralisation, intravascular pressure measurement	unruptured bAVMs.			
Zhao	Surgical Neurology, 2005, Department of Neurosurgery, Beijing Tiantan Hospital, Beijing	2086, 1956 - 2001	none	Age, sex, SMG, clinical presentation	CT, DSA, MRI	date of presentation, imaging source and date, lesion side, handedness, BAVM location, BAVM border with adjacent brain, BAVM haemorrhage, haemorrhage location, size, periventricular drainage, number of draining veins leaving nidus,	To assess the clinical characteristics and surgical results of cAVMs	nil	none	Chi squared test

						number of veins reaching sinus, venous stenosis/ occlusion, venous ectasia, venous reflux, sinus thrombosis feeding arteries, arterial aneurysms, number of aneurysms, location, haemorrhage history, haemorrhage date, no of vessels to be embolised, Moyamoya-type changes, pial-to-pial collateralisation, intravascular pressure measurement				
Zheng	Childs Nerv Syst 2014, Department of Neurosurgery, Zhujiang Hospital, Guangzhou China	127, 2000-2012	none	clinical presentations, BAVM location, BAVM haemorrhage, venous drainage, BAVM size, arterial aneurysms, SMG	CT, angiography	date of presentation, imaging source and date, lesion side, handedness, BAVM eloquence, BAVM border with adjacent brain,	to characterize clinical features and evaluate the clinical outcome of endovascular embolization treatment of	single interventional neuro-radiologist	none	Fisher's exact test chi-squared test Student's t test.

						haemorrhage location, size, periventricular drainage, number of draining veins leaving nidus, number of veins reaching sinus, venous stenosis/ occlusion, venous ectasia, venous reflux, sinus thrombosis feeding arteries, number of aneurysms, location, haemorrhage history, haemorrhage date, no of vessels to be embolised, Moyamoya-type changes, pial-to-pial collateralisation, intravascular pressure measurement	intracranial arteriovenous malformations in pediatric patients.			
Zhu	Neurol Sci (2016), Department of Neurosurgery,	142, 1997-2014	Haemorrhage, prenidal aneurysm, intranidal aneurysm	lesion side, BAVM size, BAVM location, arterial aneurysms,	Angiography, CTA, MRA	clinical presentations, date of presentation, imaging source and date,	To determine the safety and effectiveness of cerebellar	none	none	chi^2 test, Fisher's exact test, Student's t test, or

	Zhujiang Hospital, Southern Medical University, Guangzhou China			venous drainage, SMG		handedness, BAVM eloquence, BAVM border with adjacent brain, BAVM haemorrhage, haemorrhage location, size, periventricular drainage, number of draining veins leaving nidus, number of veins reaching sinus, venous stenosis/ occlusion, venous ectasia, venous reflux, sinus thrombosis feeding arteries, number of aneurysms, location, haemorrhage history, haemorrhage date, no of vessels to be embolised, Moyamoya-type changes, pial-to-pial collateralisatio n,	(AVMs) embolization and find out the suitable methods to manage associated aneurysms.			Wilcoxon's two-sample test multivariable Logistic regression model

						intravascular pressure measurement				
Zipfel	J Neurosurg 2004 Department of Neurosurgery, University of Miami, Florida, USA	268 ???	none	clinical presentations, BAVM location, BAVM size, SMG, BAVM eloquence, BAVM haemorrhage, BAVM border with adjacent brain, number of draining veins leaving nidus, venous stenosis/ occlusion, venous ectasia, arterial aneurysms, feeding arteries,	CT, DSA	date of presentation, imaging source and date, lesion side, handedness, haemorrhage location, size, venous drainage, periventricular drainage, number of veins reaching sinus, venous reflux, sinus thrombosis number of aneurysms, location, haemorrhage history, haemorrhage date, no of vessels to be embolised, Moyamoya-type changes, pial-to-pial collateralisation, intravascular pressure measurement	to determine which morphological features of (AVMs) are statistically predictive of preradiosurgical haemorrhage, postradiosurgical haemorrhage, and neuroimaging-defined failure of radiosurgical treatment.	none	none	univariate & Multivariate logistic regression analysis
Zwanzger	Radiología. 2020 Neurorradiolo	22, 2007-2012	nil	BAVM haemorrhage, BAVM location,	CTA, DSA	clinical presentations, date of presentation,	To compare the usefulness of CT angiography against the gold standard, digital	Four radiologists Two neuroradiologist	Inter observer agreement	Sens spec PPV

	gía intervencionista, Departamento de Radiología, Universidad de Barcelona			SMG, BAVM size, BAVM eloquence, venous drainage, arterial aneurysms, number of veins reaching sinus, venous stenosis/ occlusion, venous ectasia, perforating arteries		imaging source and date, lesion side, handedness, BAVM border with adjacent brain, haemorrhage location, size, periventricular drainage, number of draining veins leaving nidus, venous reflux, sinus thrombosis feeding arteries, number of aneurysms, location, haemorrhage history, haemorrhage date, no of vessels to be embolised, Moyamoya-type changes, pial-to-pial collateralisation, intravascular pressure measurement	sub- traction angiography (DSA), in the characterisation of cerebral arteriovenous malformations (AVM) that present with bleeding.	s (one with more than 10 years' experience and the other with four years' experience in neuroimaging) two neuroradiologists (one with more than 10 years' experience and the other with five years' experience in neuroimaging)		diagnostic precision and consistency between readers